PB 273 507

REPORT NO.
UCB/EERC-77/11
MAY 1977

EARTHQUAKE ENGINEERING RESEARCH AT BERKELEY – 1976

Papers presented by faculty participants and research personnel associated with the Earthquake Engineering Research Center at the Sixth World Conference on Earthquake Engineering, New Delhi, India, January 1977.

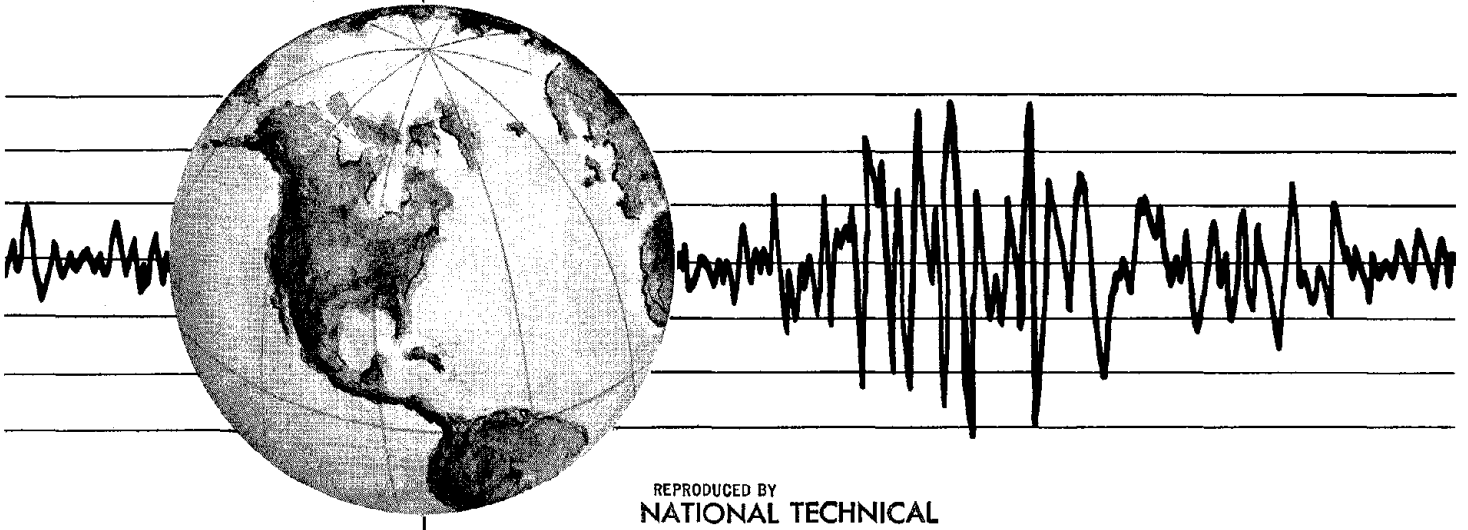

EARTHQUAKE ENGINEERING RESEARCH CENTER

EARTHQUAKE ENGINEERING RESEARCH AT BERKELEY - 1976

Papers presented by faculty participants and research personnel associated with the Earthquake Engineering Research Center at the Sixth World Conference on Earthquake Engineering
New Delhi, India
January 1977

EERC Report No. UCB/EERC-77/11
College of Engineering
University of California
Berkeley, California

May 1977

FOREWORD

At the Sixth World Conference on Earthquake Engineering held in New Delhi, India, January 10-14, 1977, twenty five papers were presented by faculty participants and research personnel associated with the Earthquake Engineering Research Center, University of California, Berkeley. The papers have been compiled in this report to illustrate some of the research work in earthquake engineering being conducted at the University of California, Berkeley. The research work described in the papers has been sponsored by several agencies including the following: National Science Foundation; National Bureau of Standards; Alyeska Pipeline Service Company.

TABLE OF CONTENTS

TABLE OF CONTENTS (cont'd)

CHARACTERISTICS OF THREE-DIMENSIONAL GROUND MOTIONS ALONG PRINCIPAL AXES, SAN FERNANDO EARTHQUAKE

Tetsuo Kubo[I] and Joseph Penzien[II]

SYNOPSIS

Using the concept of an orthogonal set of principal axes and applying both the time and the frequency domain moving-window technique to the accelerograms recorded during the San Fernando earthquake of February 9, 1971, characteristics of three-dimensional ground motions along principal axes are determined. It is concluded from the resulting intensity functions and the time dependent frequency contents that realistic three components of ground motion can be generated stochastically as nonstationary random processes along their corresponding principal axes without cross correlation with one another in a statistical sense.

INTRODUCTION

It is becoming increasingly evident that responses of some important structural systems such as three-dimensional piping systems, nuclear power plants, highway structures and earthfill dams are significantly affected by more than one component of ground motion excitation. Because of this awareness, there will be an increasing demand, in the future, for dynamic analyses of such structural systems using multi-dimensional ground motions.

A number of stochastic models for earthquake ground motions have been employed in the one-dimensional form; however, when extending the use of such models to the two- or three-dimensional form, the question "Should the components of motion be cross correlated statistically?" immediately arises. If correlated, one must establish appropriate cross-spectral density functions in addition to realistic power spectral density functions.

Similar to the stress state problem, an orthogonal set of principal axes exists for ground motions along which the components of motion have maximum, minimum and intermediate values of variance and have zero values of covariance. This property suggests that components of motion need not be cross correlated statistically provided they are directed along principal axes.

METHOD OF ANALYSIS

Principal Axes of Ground Motions [1,2] Suppose three translational components of ground motion at point 0 along an arbitrary set of orthogonal axes x, y and z are represented by the relation

$$a_i(t) = \zeta_i(t)\, b_i(t) \qquad i = x,y,z \tag{1}$$

where $b_i(t)$ and $\zeta_i(t)$ $(i = x,y,z)$ are stationary random processes and deterministic intensity functions, respectively. If the processes are considered to be Gaussian, covariance functions defined by

[I] Graduate Student, University of Tokyo, Tokyo, Japan and formerly Assistant Specialist, Earthquake Engineering Research Center, University of California, Berkeley

[II] Professor of Structural Engineering, University of California, Berkeley, California, U.S.A.

$$E[a_i(t)\ a_j(t+\tau)] = \zeta_i(t)\ \zeta_j(t+\tau)\ E[b_i(t)\ b_j(t+\tau)] \quad i,j = x,y,z \quad (2)$$

characterize completely the processes in a probabilistic sense [3]. Since real earthquake accelerograms demonstrate a very rapid loss in correlation with increasing values of $|\tau|$, the influence of coordinate directions on the covariance functions can be investigated substituting $\tau=0$ in Eqs. (2). Principal variances and the directions of principal axes can be obtained respectively as eigenvalues and corresponding eigenvectors of the covariance matrix defined by Eqs. (2).

Moving-Window Procedure Variances and covariances (μ_{ij} i,j = x,y,z) are obtained as continuous functions of time t_o using the so-called "moving-window" technique, i.e. using the relation [4]

$$\mu_{ij}(t_o,\Delta T) = < [a_i(t)-\bar{a}_i][a_j(t)-\bar{a}_j] >_{t_o - \frac{\Delta T}{2}}^{t_o + \frac{\Delta T}{2}} \qquad i,j = x,y,z \qquad (3)$$

where the time averages are taken over the interval ΔT centered at time t_o but where the mean values $\bar{a}_i$ and $\bar{a}_j$ are found by averaging $a_i(t)$ and $a_j(t)$ over the entire duration of motion. The values of time window length ΔT in Eqs. (3) should be taken sufficiently long so that the higher frequency fluctuations are essentially removed but the slower time dependent characteristics are retained, i.e. the time average over duration ΔT will be essentially equal to the average taken across the ensemble. This formulation allows one to obtain the time dependency of principal variances and their corresponding directions of principal axes.

Using the Fourier transformation, the moving-window technique, as applied in the time domain above, can be applied in the frequency domain as well. In this case, however, variances and covariances are evaluated as continuous functions of frequency f_o. In the frequency domain formulation, one can investigate principal variances, directions of principal axes, etc. associated with those frequencies of ground motion in the range $(f_o-\Delta f/2) < f < (f_o+\Delta f/2)$. Hopefully, this approach can be used to reveal certain characteristic features of the various types of seismic waves associated with strong ground motions.

Time Dependent Frequency Content Variation of frequency content of ground motions with time is examined by Fourier amplitude spectra generated by the moving-window technique as follows

$$A(\omega,t_o,\Delta T) = \left| \int_{t_o - \frac{\Delta T}{2}}^{t_o + \frac{\Delta T}{2}} a(t)\ e^{-i\omega t} dt \right| \qquad (4)$$

Since intensity of ground motion can be expressed in terms of variances [5], the moving-window Fourier amplitude spectra can be normalized with respect to the maximum values generated for time t_o when determining frequency variations with time.

RESULTS OF ANALYSIS

Principal Variances and Directions of Principal Axes Both the time domain and frequency domain moving-window analysis described above has been applied to the ground motions recorded during the San Fernando

earthquake of February 9, 1971. The time- and frequency-dependent principal variances and directions of principal axes have been evaluated for acceleration records at 99 stations. The direction of a principal axis is represented by direction angles ϕ and θ in three-dimensional space as shown in Fig. 1.

In this paper, the results for station No. 264, basement of the Millikan Library, CALTECH, are presented. Figure 2 shows the time-dependent principal variances and directions of principal axes as determined using discrete values of t_o one-half second apart and using 5 seconds for ΔT in Eqs. (3). Similarly, Fig. 3 shows the results of frequency-dependency using a frequency bandwidth Δf nearly equal to 0.98 Hz placed at uniform frequency intervals of 0.49 Hz. The solid, short-dashed and intermediate-dashed curves in these figures represent the major, minor and intermediate principal axes, respectively and the horizontal long-dashed straight line represents the direction θ_E to the reported epicenter. Although, the functions of principal transformation shown in Figs. 2 and 3 have numerous unexplainable features, certain correlations in the time domain moving-window formulation should be noted as follows:

(1) Usually during the early periods of low intensity motion, either the major or the intermediate principal axis is nearly vertical, i.e. the vertical component represents a large amount of energy in comparison with the horizontal components.
(2) Later, the major and intermediate principal axes shift towards horizontal positions with the minor axis taking the nearly vertical position.
(3) Following the shift of the major principal axis towards a horizontal position, the horizontal directions of the major and intermediate axes can suddenly interchange. This interchange which occurs after the period of high intensity motion is due to a corresponding change in the direction along which the seismic waves have maximum energy.
(4) Usually during the period of high intensity motion, the horizontal direction of either the major or the intermediate principal axis is towards the fault slip zone. This characteristic suggests that the direction along which seismic waves contain maximum energy either coincides with the direction to the fault slip zone or is at right angle to it.

Figure 4 shows the horizontal directions (θ) of the major and intermediate principal axes for stations in the extended Los Angeles area at the period when the motions are of highest intensity. While the correlation is not strong, there is a tendency of the directions of the major principal axis or, in some cases, the intermediate principal axis to point in the general direction of the fault slip zone [6] which is also the general direction towards the previously reported locations of surface fault traces south of the epicenter [7]. Since the concept of intensity defined here is identical to that defined by Arias [8], one can speculate that the direction of the major principal axis coincides with the direction to maximum energy release in the fault slip zone.

Time Dependent Frequency Content along Principal Axes Applying the moving-window technique, the Fourier spectral amplitude analysis has been employed to evaluate variations of frequency content for the principal components of motion with time. Spectral amplitudes have been evaluated using a time window length of 5 seconds which is identically the same as that used in the time domain formulation of principal axes. To determine the general characteristics, the amplitude spectra are smoothed by weighed convolutions. In Fig. 5, the time dependencies of frequency content for

station No. 264 are shown using a three-dimensional spectral diagram in which the contour lines represent levels of the normalized Fourier amplitude. The shaded zones in the diagram represent the highest range of spectral magnitude; thus, indicating the corresponding range of dominant frequencies at time t_o. The characteristic features of these diagrams representing variation of frequency content with time can be summarized as follows:

(1) The dominant frequency is found to have decreasing values with time. This tendency coincides with the results reported in the literature [9].

(2) In some cases, the dominant frequency changes its value suddenly at a fixed time which may indicate the arrival of different types of seismic waves.

(3) Generally, it is observed that spectral density functions derived from the three-dimensional diagrams are less sharply peaked for motions along the minor axis than for motions along the major and intermediate axes. This tendency agrees with the results of the moving-window analysis in the frequency domain which show that principal variances along the minor principal axis are more uniform than those along the major and intermediate principal axes.

SIMULATION OF THREE-DIMENSIONAL GROUND MOTIONS

It was concluded previously that three components of ground motion are independent of one another, provided they are directed along a set of principal axes. Therefore, one can simulate the three components by generating independent motions having appropriate intensity and frequency content and directing them along principal axes.

Sample accelerograms, having properties of spectral density and deterministic intensity function as shown in Fig. 6, have been simulated using Toki's method [10] along a set of principal axes. Assuming the horizontal and vertical direction angles (θ,ϕ) of principal axes to be time dependent as shown in Fig. 6, the simulated components are transformed to three components along the principal axes of the structural system for use in dynamic analysis. The resulting components of motion are shown in Fig. 7. Assuming that these motions were recorded by an accelerograph installed in the structural system, principal variances, directions of principal axes and frequency content of motion along the principal axes have been evaluated. The resulting properties of principal variances and directions of principal axes are presented in Fig. 8 and those of the corresponding time dependency of frequency content are represented in Fig. 9. The properties of the simulated motions generally coincide well with the prescribed properties.

CONCLUDING STATEMENT

The objective of the study described herein is to establish an appropriate stochastic model for three-dimensional ground motions which reflect the significant statistical properties of the motions of the San Fernando earthquake.

The resulting model is represented by the product of a deterministic intensity function and a constant intensity process having a variable frequency content with time. The properties of the simulated motion reveal complexities similar to the characteristics of the motions recorded during the San Fernando earthquake. Therefore, this simple model as prescribed appears to be adequate.

ACKNOWLEDGEMENT

The results presented in this paper have been taken from reference No. 2 which contains similar data for many stations and presents much more detailed observations and analyses.

The financial support provided by the National Science Foundation under Grant No. GI-36387 is acknowledged with sincere thanks and appreciation.

BIBLIOGRAPHY

1. Penzien, J. and M. Watabe, "Characteristics of 3-Dimensional Earthquake Ground Motions", Earthquake Engineering and Structural Dynamics, Vol. 3, No. 4, April-June 1975.
2. Kubo, T. and J. Penzien, "Time and Frequency Domain Analysis of Three-Dimensional Ground Motions, San Fernando Earthquake", EERC 76-6, University of California, Berkeley, California, March 1976.
3. Bendat, J. S. and A. G. Piersol, "Random Data : Analysis and Measurement Procedures", Wiley-Interscience, 1971.
4. Båth, M., "Spectral Analysis in Geophysics", Elsevier, 1974.
5. Iyengar, R. N. and K. T. S. R. Iyengar, "A Nonstationary Random Model for Earthquake Accelerograms", Bull. Seis. Soc. Amer., Vol. 69, No. 3, June 1969.
6. Housner, G. W., "General Features of the San Fernando Earthquake", in "Engineering Features of the San Fernando Earthquake, February 9, 1971", edited by P. C. Jennings, EERL 71-02, California Institute of Technology, Pasadena, California, June 1971.
7. Duke, C. M. et al., "Subsurface Site Conditions and Geology in the San Fernando Earthquake Area", UCLA-ENG-7206, University of California, Los Angeles, California, December 1971.
8. Arias, A., "A Measure of Earthquake Intensity", in "Seismic Design for Nuclear Power Plants", edited by R. J. Hansen, MIT Press, 1970.
9. Saragoni, G. R. and G. C. Hart, "Nonstationary Analysis and Simulation of Earthquake Ground Motions", UCLA-ENG-7238, University of California, Los Angeles, California, June 1972.
10. Toki, K., "Simulation of Earthquake Motion and its Application", Bull. Disas. Prev. Res. Insti., Kyoto University, Kyoto, March 1968. (in Japanese)

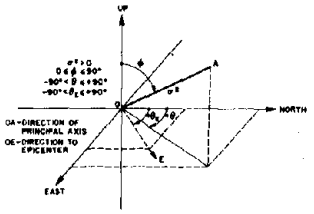

Fig. 1 Directions of principal axes in three-dimensional space.

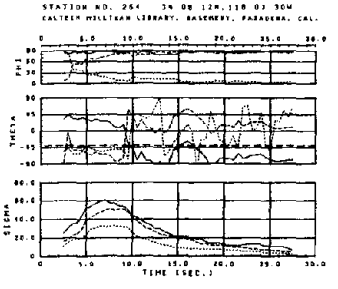

Fig. 2 Time dependent directions of principal axes and square roots of principal variances.

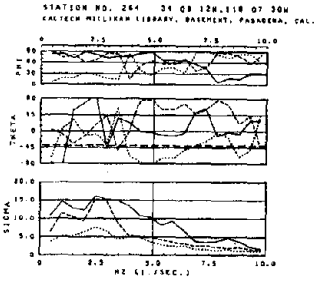

Fig. 3 Frequency dependent directions of principal axes and square roots of principal variances.

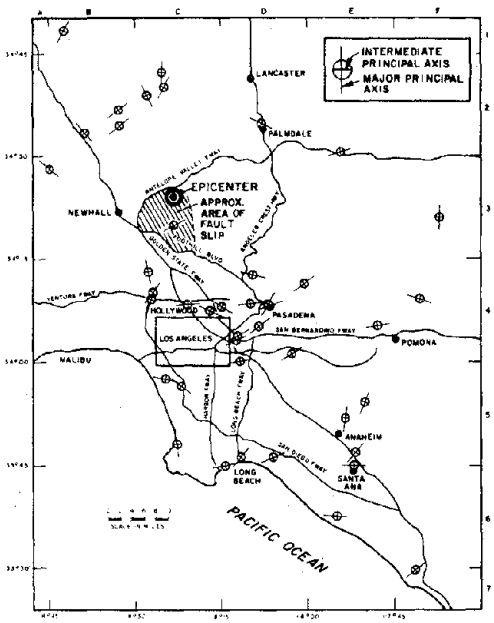

Fig. 4 Directions of major and intermediate principal axes of stations in the extended Los Angeles area.

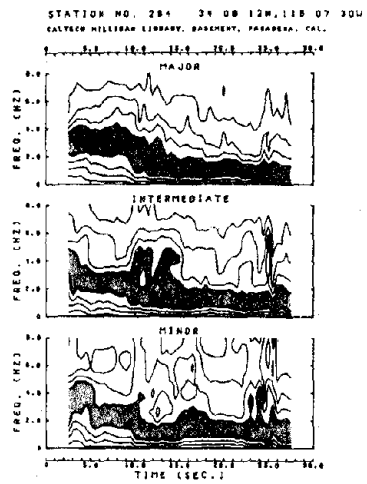

Fig. 5 Time dependent frequency distribution.

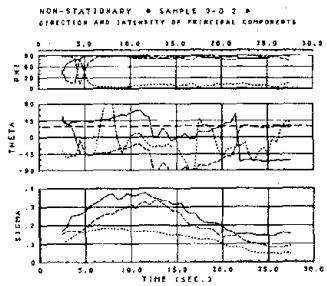

Fig. 8 Time dependent directions of principal axes and square roots of principal variances for simulated motion.

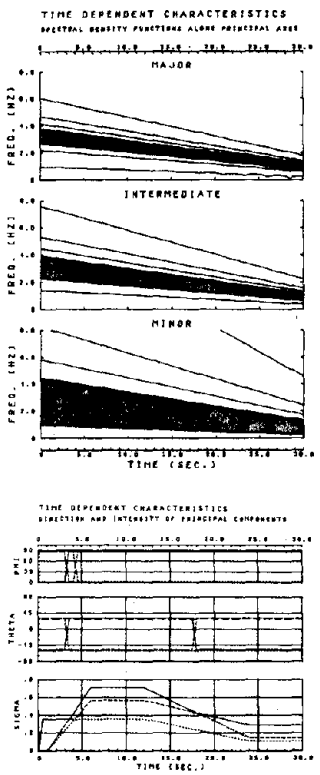

Fig. 6 Prescribed intensity and spectral density function.

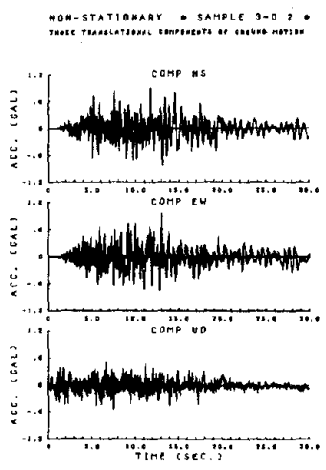

Fig. 7 Time histories of simulated motion.

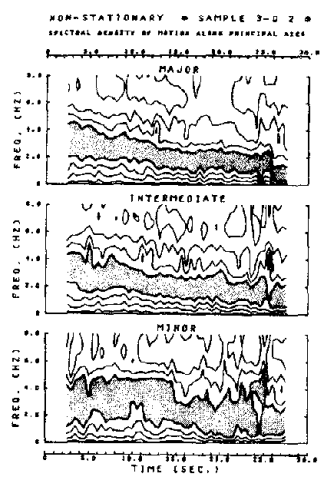

Fig. 9 Time dependent frequency distribution for simulated motion.

EARTHQUAKE LOSSES AS A FUNCTION OF CONSTRUCTION TYPES

by

Karl V. Steinbrugge[I], Henry J. Lagorio[II], and S. T. Algermissen[III]

SYNOPSIS

Government agencies and insurance companies must realistically estimate life hazard and potential aggregate property damage along with their geographic distributions for destructive earthquakes in any relevant region. Often it is necessary to accomplish the foregoing by a rapid and economical methodology in order to quickly resolve specific planning problems. In this regard, recent studies have produced several practical procedures which have suited a few of these needs.

Specifically, this paper discusses some of these developments regarding aggregate property damage. Government sponsored studies have improved methods for establishing aggregate total losses for maximum credible events and percentage losses as a function of construction types. Methodology and typical results are given.

INTRODUCTION

Any study of insurance relationships among potential monetary losses, earthquake intensity-frequency parameters (or equivalent parameters), and building construction classes should be directed to at least two fundamental questions:

A. What is the expected total monetary loss or, as often stated, the aggregate probable maximum loss for all insured construction in the event of the maximum probable earthquake in the underwriting area under consideration?

B. What is the average annual loss over long periods of time in a given region for each particular construction class?

Question A is important for several reasons. For the individual insurance company, an improper evaluation could result in company insolvency. Secondly, for the insurance industry as a whole, it involves the financial capacity of the private sector to accommodate a very large increased demand for earthquake insurance should this coverage be mandated for one or more classes of construction or types of occupancy. Thirdly, for government at Federal and state levels, it involves one factor in policy decisions regarding government's role in reinsurance should the private sector be unable to absorb the demands resulting from mandation.

I Manager, Earthquake Department, Insurance Services Office (San Francisco, California).

II Program Manager, National Science Foundation, Washington, D. C. (on leave, Professor of Architecture, University of California, Berkeley, California).

III Geophysicist, U. S. Geological Survey (Denver Federal Center, Denver, Colorado).

The second of the aforementioned questions addressed in this paper is based on a detailed study by the authors prepared by the U. S. Geological Survey for the U. S. Department of Housing and Urban Development (in press at this writing) using the metropolitan San Francisco, California area as a case history. The computational efforts of M. McGrath and S. Hansen of the U. S. Geological Survey are gratefully acknowledged. Additionally, the advice and guidance of Theodore H. Levin of the Department of Housing and Urban Development was most helpful during the more difficult stages of this study.

SIMULATED LOSS TECHNIQUES

Simulated loss estimation techniques have been developed in recent years. These techniques show substantial promise in reducing the large uncertainties currently present in estimating total potential loss for any event and in establishing earthquake insurance rates. In a region such as San Francisco, earthquakes have damage patterns that are related to their magnitude and the associated distribution of shaking, to length of faulting and displacement along the fault, to the geographic distribution of buildings together with the type of construction and materials used and to other measurable characteristics. Using the historical seismic record, or some other estimate of the seismicity of the area, it is possible to estimate, by class of construction, the damage and associated losses likely to occur in the future for any postulated distribution of buildings.

BUILDING CLASSIFICATION

Classification of buildings and other structures for earthquake insurance research purposes requires a knowledge of the relative damageabilities among building types. Additionally, the number of building classes becomes a practical matter involving the levels of insurance rates. In this latter context, it is obvious that a low seismicity will produce a relatively low level of rates and it follows that the rate differential among building classes tends to be small if the overall rate levels are low. Very small rate differentials, say one mill per $100 of insured value, simply are inadequate to pay for the field inspection costs for identifying the appropriate building classes for all but the very largest valued risks. As one result, in areas where the seismicity is low, building classification systems should be simple in order to keep overhead costs within reasonable bounds. Secondly, a country having a relatively few number of construction types for most of their buildings probably will require a simplistic building classification system, even though the rates may be high due to a high seismicity.

The basic key to a successful building classification system is identifying the degree of damage control exercised by the structural system and the ease in recognizing this damage control. Damage control may exist by design on the part of the architect/engineer, or by accident of design, or by being inherent in the construction material. For example, an all-steel gasoline service station falls into the last category. It follows, then, that an appropriately written set of building classification rules will identify the damage control features and reflect them in the classes.

The following is a listing of the six basic building classes for earthquake insurance purposes in common use in United States and also used for this study. Approximately 20 building sub-classes exist within this set, but sub-classes have not been repeated below for clarity.

Class I: Wood frame construction.
Class II: All metal construction.
Class III: Steel frame construction.
Class IV: Reinforced concrete construction.
Class V: Mixed construction.
Class VI: Earthquake resistive construction having damage control features.

Classes I through V are readily identifiable by their materials of construction. Some of the sub-classes of III through V require sub-professional or professional assistance. Class VI buildings require special attention by professional structural engineers for accurate application.

EXISTING BUILDING INVENTORY

A detailed examination was made of 20 of the most promising sources of existing building inventories in the context of one specific objective, namely, the geographic distribution of property values by specific construction class and by census tract. Data sources included land-use planning maps, property tax records, building department archives, disaster office records, and insurance sources. While insurance company files were potentially the most useful, data conversion costs would have been prohibitive.

The following methodology for building inventory was adopted since the usefulness of readily available data sources and their adaptation were impractical for purposes of this study:

First, mapping: Geographically determine the distribution of inventory of each building class on suitable maps, with the distribution relatable to census tracts.

Second, quantification: Determine the extent of the total inventory of each building class for each census tract.

Third, tabulation: Tabulate the percentages by census tract.

MONETARY LOSS CHARACTERISTICS

Monetary losses are a function of the ground motion characteristics at a given point and the building's damage control characteristics (if any). The Modified Mercalli Intensity scale is quite useful in this regard when properly interpreted for long period effects.

For our analysis purposes, the lower intensity limit is the threshold of damage, with this threshold varying with the kind of building as well as the kind of ground motion. The upper intensity limit is determined by that intensity where ground vibration effects to buildings are overshadowed by geologic effects such as landsliding, faulting, and failures of structurally poor ground. This upper limit is normally given as Modified Mercalli Intensity IX for insurance practice. The cut-off at IX is somewhat arbitrary since vibrational effects on buildings will increase with increasing intensity, but become overshadowed by building damage due to faulting, etc.

The shapes of the characteristics curves for intensity-loss relationships are quite variable, depending upon numerous factors. The lower limit of the loss for each curve is zero at intensities within a range from MM IV to MM VI. The upper limit is at MM IX. The shape in-between is variable.

Let us next consider curves #1 and #2 in Figure 1 which show the characteristic damage patterns for certain kinds of flexible frame multi-story buildings. Both buildings are considered to be equally earthquake resistive from a design standpoint, with certain non-structural elements being the only construction variable. The lower loss vs. intensity values are represented by a flattened curved line to represent, in part, "imaginary" losses assumed by the owner/occupant. If the loss is less than 100% (i. e., no collapse), then the curve flattens out at the top. In this case, the curve flattens since increasing non-structural damage no longer requires proportionate repair costs (for example, patching and painting may cost little more between a badly cracked wall and excessively cracked wall).

One possible effect of occupancy can be seen by comparing curves #1 and #2 in Figure 1. A warehouse or manufacturing structure might have a minimal number of partitions (curve #2) while a hotel would have numerous partitions (curve #1). The vertical spread between the curves represents the difference in loss due to occupancy related construction. Significant exceptions may exist to this vertical spread between curves. For example, if the partitions are of a high value type which are subject to little damage prior to building collapse, then the two curves may essentially coincide. It should be added that these two curves are principally applicable to Class III and Class IV structures which do not have shear walls.

Curves #3 and #4 in Figure 1 have the characteristic shapes for loss to rigid unit masonry buildings, and these curves are generally applicable to Class V structures as well as some Class III and IV buildings. The beginning of the curves at low loss levels represents hairline cracks at partition-masonry wall intersections and similar kinds of minor damage. The steepness of the straight line represents brittle failure of the walls and/or roof-to-wall connections. Actually for a specific building, the straight line could be replaced by a jagged line since loss would really be a series of step functions, with each step representing another brittle failure. Numerous acceptable variants exist.

COMPUTATIONAL RESULTS

Computation of the average annual loss by class of construction for the San Francisco, California metropolitan area required us to estimate the distribution of ground shaking likely to occur in all of the census tracts in the area considered. To compute the distribution of shaking, we made use of the historical record of earthquakes from 1800-1974 with maximum Modified Mercalli Intensities greater than or equal to VI. Existing isoseismal maps were used when available. For earthquakes for which only maximum intensities are known, theoretical isoseismal maps were developed using intensity data from well studied earthquakes with similar maximum intensities. Using the distribution of intensity in each census tract and the percent loss by class of construction, the average yearly loss was computed using the historical seismicity over four different time intervals. While the historical record is certainly incomplete for at least the smaller shocks in the 19th century, the average losses based on the period 1800-1974 and 1800-1899

are still larger than for losses computed using the seismicity in the 20th century (Table 1). This is a result of the higher seismicity in the San Francisco area in the 19th century. The implication is that earthquake losses in the San Francisco area have been low in the 20th century, particularly since 1906. Should seismicity in the San Francisco area return to pre-1907 historical levels, substantially higher losses than those experienced over the past 70 years are likely to occur. It should be clearly understood that the values given in Table 1 are not insurance rates, since these values do not include taxes and other business costs.

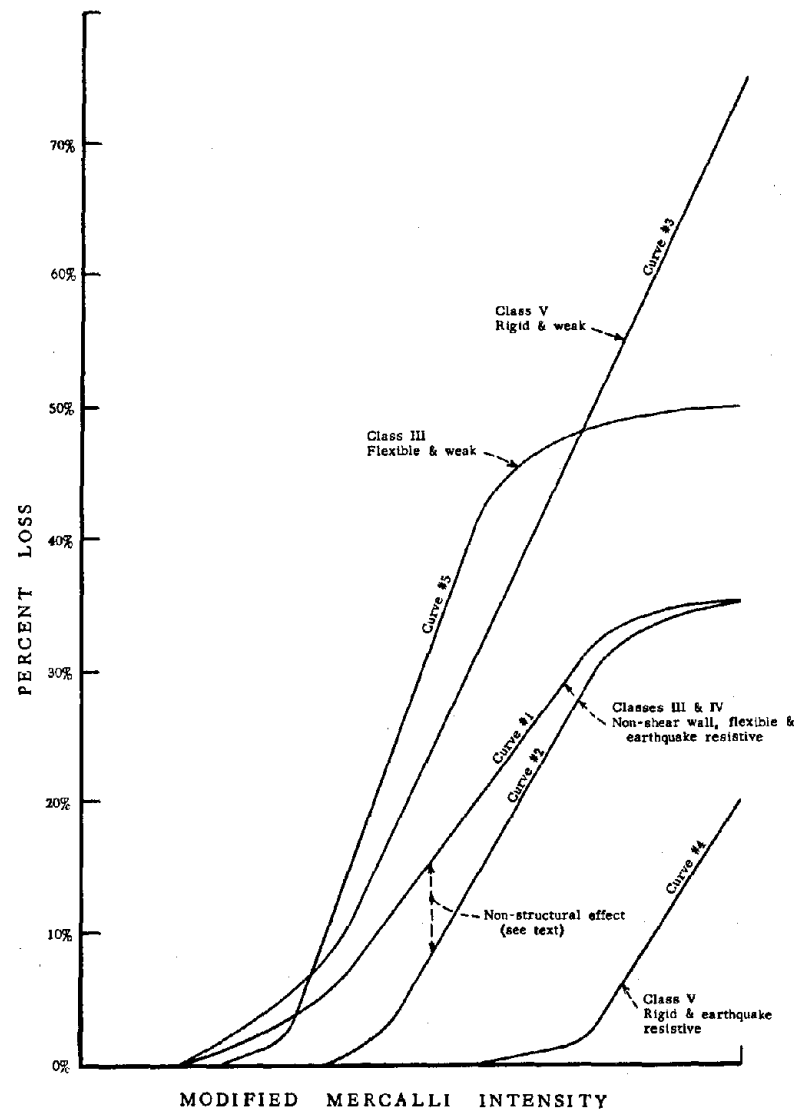

FIGURE 1. Characteristic loss patterns for selected building classes.

TABLE 1

EXAMPLES OF AVERAGE ANNUAL LOSS BY CLASS OF CONSTRUCTION

San Francisco, California, Metropolitan Area

Selected Building Classes (Simplified Construction Description)	**Average Annual Loss in Percent of Replacement Value			
	*1800-1974	*1800-1899	*1900-1974	*1907-1974
All metal buildings:				
II A - One story, all metal.	.118	.130	.102	.043
II B - Larger than II A.	.141	.168	.106	.028
Steel frame buildings:				
III A - Steel frame carries vertical loads, reinforced concrete and/or metal deck roof and floors, reinforced concrete or reinforced masonry walls, special damage control features.	.214	.275	.132	.008
III B - Similar to III A, but non-reinforced masonry walls. No special damage control features.	.452	.553	.317	.098
III C - Includes III A and III B having intermediate damage control features.	.269	.345	.168	.011
III D - Steel frame with wood floors/roof. Walls are non-bearing concrete or masonry.	.452	.553	.317	.098
Reinforced concrete buildings:				
IV A - Poured-in-place reinforced concrete (a) frame or (b) bearing walls or (c) mixed with steel frame having poured-in-place reinforced concrete floors, roofs, and walls. Special damage control features.	.269	.345	.168	.011
IV B - Similar to IV A, but non-reinforced masonry walls. No special damage control features.	.646	.790	.453	.139
IV C - Includes IV A and IV B having intermediate damage control features.	.374	.482	.231	.014
IV D - Precast concrete construction with average damage control features.	.775	.948	.543	.167

*Time periods are inclusive.

**Values are representative and taken from families of loss-intensity curves.

SEISMIC RISK ANALYSIS FOR A METROPOLITAN AREA

by
Carlos S. Oliveira[I]

SYNOPSIS

A method to analyse the seismic effects over a system extended in space is developed. The system is characterized by the description in space of its dynamic and resisting properties. The seismic activity is controlled by three parameters β, λ, M_1, and by the spacial distribution of earthquakes. A penalizing function is used to convert the vector of performances into a scalar loss. The probability distribution of losses is generate using simulation. Comparisons between single site and system spread in space are analysed.

INTRODUCTION

The study of seimic risk at a site has been pursued since the late sixties, but only recently consideration of the seismic risk of systems spread in space became apparent[1,2]. The consequences of an earthquake in large systems (simultaneous failure or the non operation of two systems causes more loss than the sum of two separate failures), requires this kind of analysis: the total effect of an earthquake on a region or country cannot be expressed as a sum of individual losses. Rather, it is a nonlinear multiple of this sum, due to the combination of factors. The space problem becomes more complex when dealing with lifeline systems.

Due to uncertainty in determining the parameter values, the probability method is the sole capable of analysing comprehensibly the problem. Two main philosophies have been considered in this respect: on studying economical problems, determination of insurance rates or in optimization one should care for the mean value estimators of the parameters while on studying codes safety of populations, catastrophic insurance reserves or decision-making, an extreme value estimation is more convenient. Fig 1 presents the overall problem of seismic risk analysis in its generalized version[II]. Each box represents a single event and the string of events shows the interrelationships involved. The main parameters of this description are as follows (the quantification of those parameters referred in items (i) through (iv) has been done in great detail and is available in the literature; information is lacking on the parameters covering items (v) through (viii) but further details will be given in this paper): (i) generation of the earthquake process considered as as a stochastic point process random in time, space and magnitude; (ii) propagation of the seismic action from focus and fault to the site or sites according to the formula $y = b_1 e^{b_2 m} [f(R)]^{-b_3}$ in which y is the maximum acceleration, velocity or displacement, m is the magnitude, f(R) is a function of the focal distance R and b_1, b_2, b_3 are empirical constants, and taking into account the changes in the predominant period of ground motion with distance and magnitude; (iii) soil influence considered through a simple parameter ω_{soil}, Fig 2; (iv) structural response of a one degree of freedom system, ω_{st}, ξ_{st}, under the action of a stationary Gaussian stochastic process having a white noise power spectral density $S(\omega)$ filtered by the propagation and soil; (v) performance in terms of response through the damage

I Visiting Assistant Research Engineer, University of California, Berkeley USA. and Assistant Research Engineer, Applied Dynamics Division, L.N.E.C., Portugal.

II The word risk, as used in this paper, is related to those random variables which take into account all probable earthquakes to occur during a period of time; not just a single earthquake.

ratio function, DRF; (vi) individual loss, ILF; (vii) direct loss to the metropolitan area,GLF; (viii) global consequences to the metropolitan area,GCF. The quantification of all these parameters is enhanced with uncertainty some of which has a wide range of variation.

ENVIRONMENTAL RISK (ER)

Based on items (ii) through (iv) response spectra was developed for given m and R, Fig 3. Considering the randomness in time, space and magnitude, a distribution of extreme value for acceleration or response spectra could be obtained. For low risks ($\leq 10^{-3}$) the final distribution that takes into account both the randomness of intensity and the randomness of response, has to be computed using the distribution of intensity and response. It is no longer valid to consider only the distribution of intensity and the mean value of maximum response[3].

Let's look at the extreme value distribution of maximum acceleration felt at a point or over a space element. The second case differs from the first one in the way we define R: an equivalent R_{eq} is the minimum distance between the earthquake epicenter $F(u^1,u^2)$ and the area element $M(u^1,u^2)$

$$R_{eq} = \text{Min}\ [\ \text{Dist}\ (F(u^1,u^2) - M(u^1,u^2))\ ]$$

where u^1,u^2 are the space coordinates. Fig 4 shows the extreme value distribution of acceleration obtained for the case of earthquake generation line paralel to a metropolitan line of variable length. The following values characterize the system: $\lambda=4$/year, $\beta=2$, t=1 year, $m_o=3.5$, $m_1=8.1$, $b_1=1230$, $b_2=0.8$, $b_3=2$, $f(R)=R+25$, $\ell=100$ km, d=20 km. As shown in Fig 4, there is a substantial difference between seismic risk at a point and over a line.

DAMAGE RATIO FUNCTION (DRF)

Data has shown that there is a correlation between the degree of damage or damage ratio (cost of repair to replacement cost at the time of the earthquake) and the intensity of shaking. This observation led to the development of the concept of damage probability matrix[4], which is a global measure of damage and includes the environmental impact and the socio-economic standards of the region. It would seem more convenient to separate, at the beginning of the study of losses, the degree of damage from the costs resulting from such damages. Based on reliability theory and extending the concept of step function describing costs associated to limit states, to a continuous description, we have defined a damage ratio function, DRF,as, Fig 5

$$DRF = \begin{cases} 0 & \text{if} \quad Z<Yd \\ \left(\frac{Z-Yd}{C-Yd}\right)^{\alpha} & \text{if} \quad Yd\leq Z\leq C \\ 1 & \text{if} \quad Z>C \end{cases}$$

where Z is the response of the building, Yd is the yield displacement, C is the collapse point and α is a parameter characterizing the type of building system. In order to take into account the dispersion of the building resistance, Yd and C are considered as random variables,RV. Using the standard techniques of transformation of RV, the probability density function, pdf, of DRF is obtained as, Fig 5,

$$f_{DRF}(dr) = \int_E \int_F f_{Z,Yd,C}\left(E, \frac{E-dr^{1/\alpha}F}{1-dr^{1/\alpha}}, F\right) \left|\frac{1}{\alpha} dr^{1/\alpha-1} \left(\frac{E-F}{(1-dr^{1/\alpha})^2}\right)\right| dE\,dF \qquad 1)$$

where the pdf of Z,Yd,C in most cases, is expressed as the product of the density of Z and the joint density of Yd and C, with correlation coeffidient ρ. Fig 6 shows the influence of ρ on the pdf of DRF given Z for Z=1.25,..., 5.75, when Yd and C have bivariate normal densities with mean values 2 and 5 respectively and coefficient of variation $V_{Yd}=V_C=0.2$ and Z has an extreme

type I distribution with mean value 1 and V_Z=0.2. Fig 7 shows the pdf of DRF for some combinations of values mentioned before. The influence of V_Z is also analysed.

While the DRF is a measure of structural response or an index of the level of damage suffered by the building during an earthquake, the individual loss function, ILF, is the translation of those damages into losses. It may include (i) direct losses such as cost of repair and replacement, fire, (ii) indirect losses such as losses caused to other buildings, decrease in productivity, operational losses and (iii) losses to people, Fig 8, and it may be obtained directly from the definition of DRF.

ANALYSIS OF LOSSES IN A METROPOLITAN AREA FOR A GIVEN EARTHQUAKE

In the previous discussion, the existence of buildings spread over a metropolitan area was not considered. The interaction between environmental risk and the space distribution of population and property is most important in the characterization of global losses, due to earthquake action. In the location of disaster relief facilities, predictions of the total amount of damage to be expected in large metropolitan areas, planning, etc. require the development of a method to analyse the seismic risk in an element of area. The knowledge of seismic intensity at a point is not sufficient. The analysis of risk in a given time interval T, for a metropolitan area cannot make use of the environmental curves for a site and sum the individual losses over the entire area because the RV that measure the individual risk are not independent. To find the solution of this problem we should look at the dependence among the different ILF for a given earthquake (m and R) and compute the global loss function, GLF, as

$$GLF_{m,R} = \int_{area} d(ILF(u^1,u^2)\ Morph(u^1,u^2)) \qquad 2)$$

where Morph (u^1,u^2) is a scalar quantity that represents the building characteristics for the area coordinate $r(u^1,u^2)$. If the ILF are essentially governed by shaking intensity, then the correlation coefficient ρ_{ILF} for two different buildings is approximately equal to one. In other cases is smaller then one. At the lower bound , ρ_{ILF}=0, the problem of spacial dependence no longer has any meaning. Making use of the probability laws that regulate the mean and variance of the sum of dependent RV, in the case of a line of length ℓ, one gets

$$E[GLF_{m,R}] = \int_0^{\ell} Morph(u)\ E[ILF(u)]\ du \qquad 3)$$

$$\sigma^2[GLF_{m,R}] = \int_0 (Morph(u))^2\ \sigma^2[ILF(u)]\ du + 2\rho \int_{u=0}^{\ell} \int_{v=u}^{\ell} Morph(u)Morph(v)\ [ILF(u)]\ [ILF(v)]\ du\ dv \qquad 4)$$

To obtain the global consequence function, GCF, we should penalize the GLF according to the total number of loss of life and/or according to the degree of extension of damage. The aversion function which relates the number of fatalities with the effects on the society might be used.

ANALYSIS OF RISK

To compute the total amount of losses in an interval T, one should sum the individual contribution occurring during the interval

$$GRF = \sum_{t_i=0}^{T} GLF\ (m_i,R_i,t_i)\ C\ \ e^{-\gamma t_i} \qquad \text{or} \qquad GRF(t) = \sum_{i=1}^{N(t)} GLF_i\ C\ \ e^{-\gamma T_i} \qquad 5)$$

where $GLF(m_i, R_i, t_i)$ is the GLF for a given area and for an earthquake m_i and R_i occuring at time t_i, C is the cost per unit of time and γ is the discount factor. It is assumed that after each event the metropolitan area is rebuilt to its original condition. Making use of the moment generating func-

tions,one can compute the expected values of GRF

$$E[GRF^{(j)}] = \sum_{t_i=0}^{I} E[GLF(m_i,R_i,t_i)\,C\,)^j e^{-j\gamma t_i}] \quad j=1,2 \qquad 6)$$

The pdf of GRF approach the Gaussian distribution when the number of terms in 5) increases. Assuming that the GLF can be reduced to a simple RV with known pdf, occuring at arrival times $T_1,\ldots T_n$ of a Poisson process N(t) with mean value λ_N, the process 5) has

$$E[GRF(t)] = \lambda_N E[GLF]\,C\,\frac{1-e^{-\gamma t}}{\gamma} \qquad 7) \qquad \sigma^2[GRF(t)] = \lambda_N E[GLF^2]\,C^2\,\frac{1-e^{-2\gamma t}}{2\gamma} \qquad 8)$$

To illustrate this method, the following example of a metropolitan line paralel to the fault line is given. The values used in this simulation are hypothetical and do not represent a real case. Earthquakes with the characteristics presented before were generated uniformly for a 100 km line. The metropolitan line with 20 km has uniform distribution of construction: T_{st}=1 s; ξ_{st}=0.05; E[Yd]=2; E[C]=8; $V_{Yd}=V_C$=0.2; α=1; ρ=0; ILF=DRF; γ=0.08; C=0.5/km; population=50inhab/km; T_{soil}=0.4sec. For these values computations show that V_Z varies from 0.27 to 0.32. Using the value 0.3 and a type I distribution to represent Z, it was assumed that

$$E[DRF] = \frac{1}{2\pi}\left(\arctan(m_Z - 5.0) + \frac{\pi}{2}\right) \qquad 9) \qquad \sigma^2[DRF] = 0.05\left(\cos\left(\frac{2\pi}{5}\,m_Z - 2\pi\right) + 1\right) \qquad 10)$$

Fig 9 compares the values obtained using the integration procedure,1) with 9) and 10). It also shows the mean value of casualties if loss of life is considered (when DRF=1). Fig 10 shows the variation of E[ILF] ,σ^2[ILF] and mean loss of life along the metropolitan line. Fig 11 shows the distribution of E[GRF] obtained from the simulation of 16 members of the family of earthquakes, based on 6). From the mean value and variance of GLF per year,using 7) and 8), the mean value and the variance of GRF for the period of 50 years, are respectively 53.12 and 30.70, V_{GRF}=0.10 while in the simulation E[GRF]= 52.172, σ^2[GRF]=87.486 and V_{GRF}=0.179.

CONCLUDING REMARKS

The results in the present simulation suggest: (1)risk for a metropolitan area must be defined in terms of global quantity,ie, total losses; not a single parameter has been identified to represent this risk and the entire pdf should be generated, (2) moderated earthquakes contribute in large part to the total losses, (3) the pdf of GLF shows a concentration corresponding to the moderate events and a spike due to the large ones, (4) for small λ and short interval of time, the normal approach cannot be used to generate the pdf of GRF, (5) the GRF has a wide dispersion that tends to decrease when the metropolitan area spreads, (6) based on the pdf of material and human losses, application of the present methodology can be carried on to the study of optimization,insurance, etc., Fig 12.

REFERENCES

1. Keilis-Borok, V.I., T.L. Kronrod and G.M. Molchan, 1974: "Algorithm for the Estimation of Seismic Risk", Computation Seismology, Institute of Geophysics, Moscow, Vol 6 (in russian)
2. Whitman, R.V., C.A. Cornell and G. Taleb-Agha, 1975: "Analysis of Earthquake Risk for Lifeline Systems", Proc. U.S. National Conference on Earthquake Engineering
3. Oliveira, C.S., 1975: "Seismic Risk Analysis for a Site a Metropolitan Area", Report EERC 75-3, University of California, Berkeley
4. Whitman, R.V., J.M. Biggs, J. Brennan III, C.A. Cornell, R. de Neufville and E.H. Vanmarcke, 1975: "Seismic Design Analysis", Journal of Structural Division, Proc. ASCE, Vol 101, ST.5

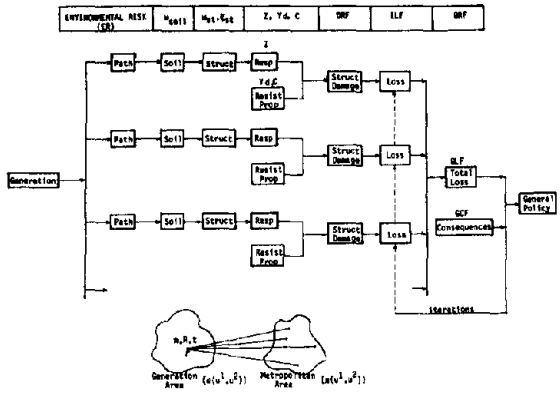

Figure 1. General sketch of the seismic risk event

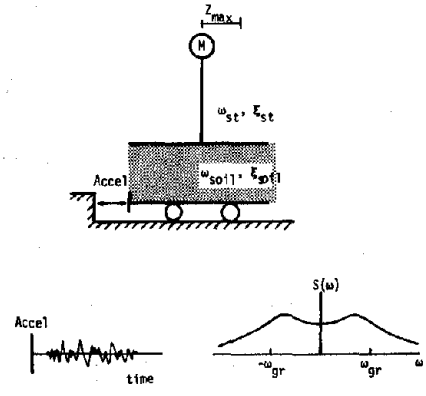

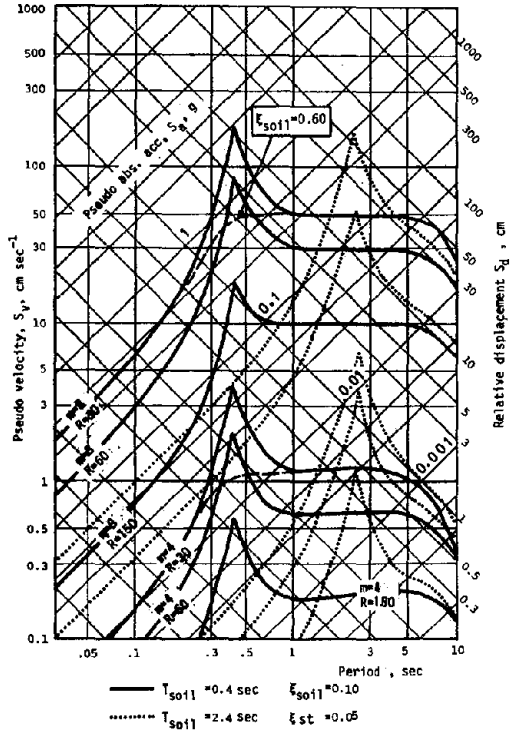

Figure 3. Response spectra for different combinations of T_{soil}, m and R

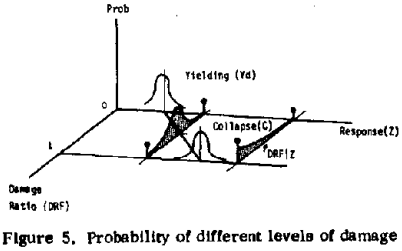

Figure 5. Probability of different levels of damage

Figure 2. Model for soil and structure

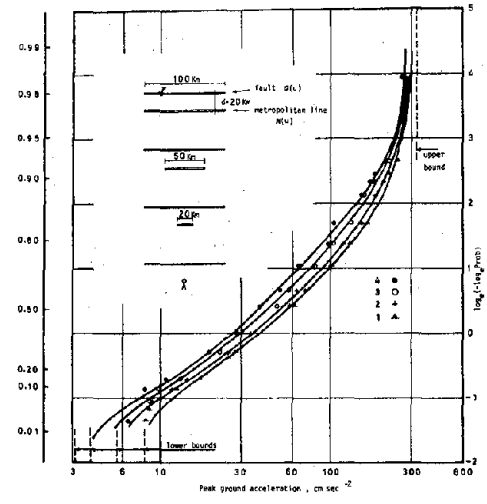

Figure 4. Environmental risk over a line segment

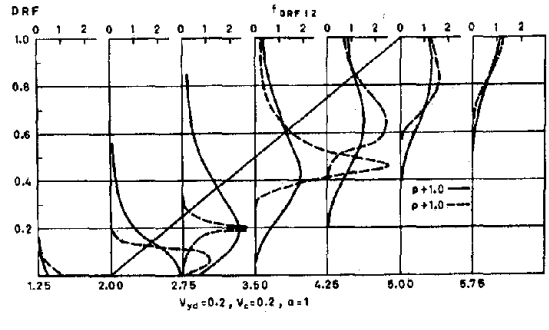

Figure 6. Influence of ρ

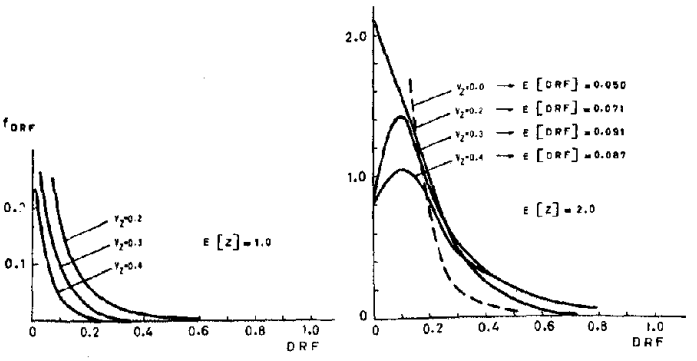

Figure 7. Probability density function of DRF; $V_{Y_d} = 0.2$; $V_C = 0.2$; $\beta = 0$; $\alpha = 1$

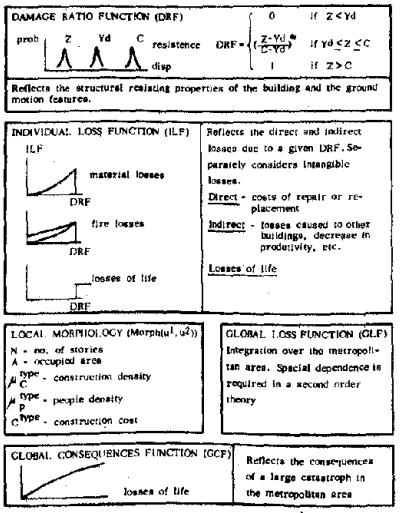

Figure 8. Sketch of the entire process to compute losses for a given earthquake

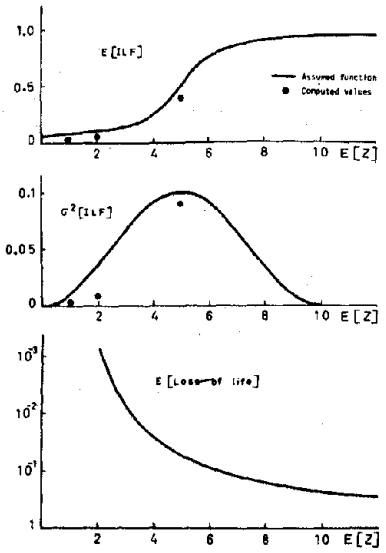

Figure 9. Functions used in simulation to compute ILF and mean loss of life

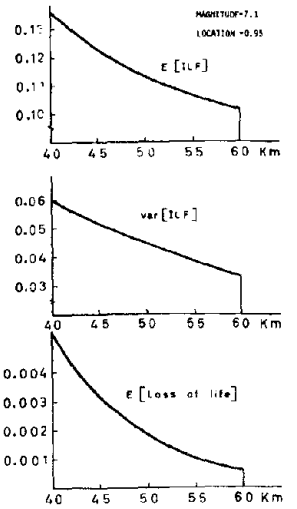

Figure 10. Variations of ILF and mean loss of life along the metropolitan line

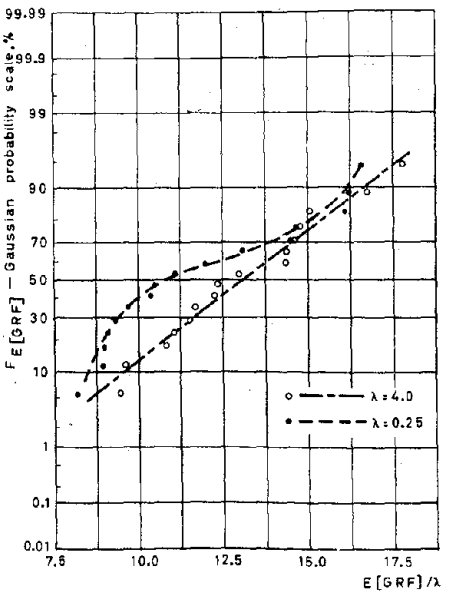

Figure 11. Probability distribution function of E [GRF]/λ

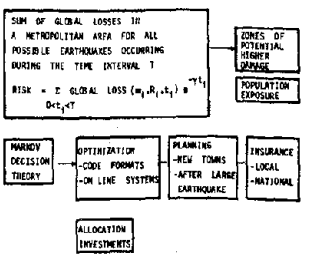

Figure 12. Some possible applications of the present theory

SEISMIC DESIGN REGIONALIZATION MAPS FOR THE UNITED STATES

by

Robert V. Whitman[I], Neville C. Donovan[II], Bruce Bolt[III]
S.T. Algermissen[IV], and Roland L. Sharpe[V]

SYNOPSIS

Two maps give the geographical variation of effective peak acceleration EPA and effective peak velocity EPV. The map for EPA is based primarily upon a seismic risk study involving selection of source zones, seismicity parameters and attenuation laws. The map for EPV is a modification to the map for EPA. The probability that EPA and EPV will not be exceeded at any location is estimated as 80% to 95%. EPA and EPV are used as input to an equation for design base shear.

INTRODUCTION

This paper describes a portion of recommended nationally applicable seismic design provisions. These provisions have been produced by the Applied Technology Council, associated with the Structural Engineers Association of California, under contract with the National Bureau of Standards (NBS) with funding by NBS and the National Science Foundation Research Applied to National Needs Program, as part of the Cooperative Federal Program in Building Practices for Disaster Mitigation initiated in 1972 under the leadership of NBS.

The preparation of design regionalization maps is being carried out by a committee composed of the authors plus Drs. Jack Benjamin, John Foss, John Reed and John Wiggins. Such maps cannot be drawn without consideration of the totality of the recommended design provisions. Hence, some of the material presented in this paper represents input from other committees involved in the overall ATC effort, especially a Committee on Ground Motion Spectra chaired by Dr. H.B. Seed. The maps are not yet in final form, and this paper emphasizes basic principles and procedures and displays the maps as drawn at the time of this writing (June 1976).

POLICY DECISIONS

The proposed ground shaking hazard maps are based upon two policy decisions which are departures from past practice in the United States. First, the relation between design lateral forces and building period should take into account the distance from anticipated earthquake sources. To accomplish this objective it was necessary to use two ground motion parameters and

---

I Professor of Civil Engineering, Massachusetts Institute of Technology, Cambridge, Mass.
II Dames and Moore, San Francisco, California.
III Director, Seismographic Station, University of California, Berkeley, California.
IV U.S. Geological Survey, Golden, Colorado.
V Project Director, Applied Technology Council, Palo Alto, California.

hence to prepare two maps. Second, the probability of exceeding the design ground shaking should be roughly the same in all parts of the country. Zoning maps previously in use had been based upon the maximum ground shaking experienced during the historical period without consideration of the frequency with which such motions might occur.

GROUND MOTION PARAMETERS - EPA AND EPV

In the recommended provisions, the strength of gound shaking is represented by two parameters: effective peak acceleration (EPA) and effective peak velocity (EPV). EPA and EPV are normalizing factors for construction of smoothed elastic response spectra (6). EPA is proportional to spectral ordinates for natural periods in the range of 0.1 to 0.5 second, while EPV is proportional to spectral ordinates for a period of about 1 second (5). The constant of proportionality in both cases is 2.1 for 5% damping.

For any one ground motion, EPA and EPV would be chosen such that the resultant smooth response spectra are a reasonable fit to the actual spectra for periods larger than about 0.2 second. For motions of very short duration, EPA and EPV would be reduced to reflect the observed fact that only one or two cycles of motion cause little inelastic motion even if a structure yields. Thus, the EPA and EPV for a motion may be either greater or smaller than the peak ground acceleration and velocity. However, when the duration is very short and/or when very high frequencies appear in the ground motion, EPA may be significantly less than peak acceleration. On the other hand, EPV is generally greater than peak velocity at large distances from a major earthquake (5).

MAP FOR EPA

Fig. 2 is the recommended map for the contiguous 48 states. EPA is contoured, and interpolation between contours is appropriate. There may be locations inside of the 0.4g contour where higher values of EPA would be appropriate; however, contouring such small areas would amount to microzoning, and was beyond the scope of this effort.

A prime reference for the preparation of Fig. 2 was a map prepared by Algermissen and Perkins (2) using the principles of seismic risk zoning (2,4). In the preparation of that map, seismic source areas were identified from historical seismicity and geology, and rates of occurrence and maximum credible magnitudes were established for each source area. Different attenuation laws were used west (8) and east (7) of the Rocky Mountains.

The Algermissen and Perkins map was modified through the judgement of the committee to reflect the most up-to-date thinking concerning active faults and seismic source areas. Suggestions were received from a panel of seismologists from different parts of the country.

MAP FOR EPV

Fig. 3 was constructed by modifying the map for EPA. First an EPV = 12 inches/sec was assigned to contour 4 on Fig. 2. This value of EPV together with an EPA = 0.4g defines the standard shape of response spectra recommended by Prof. Seed's committee as applying for nearby earthquakes. A similar approach was used for all contours which are regional "highs" of EPA; for example, EPV was set at 3 inches/sec along contour 2 (EPA = 0.1g) around the

Appalachian Mountains and South Carolina in the southeastern part of the country.

Strong motion recordings from California were used to determine the distance required for EPV to halve with distance from a large earthquake (5). This distance is about 80 miles. Data on attenuation of Modified Mercalli Intensity indicated that velocity should continue to halve in about 80 mile intervals. Thus a contour spacing of about 80 miles was used around all regional "highs" in the west, with the proviso that a contour 2 for EPV should never fall inside a contour 2 for EPA, etc.

For the east, data on attenuation of Modified Mercalli Intensity (3) indicated that within 100 miles of a large earthquake attenuation was the same as in the west. Thereafter, however, the distance required for the velocity to halve nearly doubled. Hence, around the New Madrid "high" in the central United States, the first contour interval is about 80 miles while the next contour interval is 160 miles.

RISK ASSOCIATED WITH EPA AND EPV

The probability that the recommended EPA and EPV at a location will not be exceeded during a 50 year period is estimated to be roughly 90% - at least it is in the general range of 80 to 95%. Thus the ground motion envisioned for design, at any location, is not necessarily the most intense motion that can occur at the location. In this connection, several points must be emphasized. First, considering the significant cost of designing a structure for extreme ground motions, it is undesirable to require such a design unless there is a high probability that the extreme motion will occur or if there is a particularly severe penalty associated with failure or non-functioning of the structure. Second, a building properly designed for a particular ground motion will provide considerable protection to life safety during a more severe ground motion. Third, even if it were desirable to design for the extreme gound motion, it is impossible, at this time, to get agreement among experts as to the largest credible EPA and EPV. This is especially true for the less seismic portions of the country.

SEISMIC DESIGN COEFFICIENTS

The base shear to be used for design is given by $V = C_s UW$ where W is the weight and U is an importance factor. The seismic design coefficient is

$$C_s = \frac{1.2\, A_2\, G}{R\, T^{2/3}} \qquad (1)$$

but need not exceed $2.5A_1/R$ for stiff or deep soils nor $2.0IA_1/R$ for soft soils. G is a soil profile factor, ranging from 1.0 to rock and shallow stiff soils to 1.5 for profiles with soft to medium stiff clays and soils. R is a response modification coefficient discussed in a companion paper by Newmark et al. T is the fundamental period of the building; the exponent on T reflects a need for greater conservatism in the design of flexible buildings. A_1 and A_2 are coefficients related to EPA and EPV as indicated in Figs. 2 and 3. To illustrate the use of Eq. (1) and Figs. 2 and 3, Fig. 1 gives values of A_1 and A_2 for several cities together with curves of C_sR for shallow stiff soil.

For possible use by code authorities, alternate versions of Figs. 2 and

3 are being prepared. On each map, the contours will be replaced by 8 zones, with increments of 0.05 between zones. The boundaries between zones will generally be drawn along county lines.

REFERENCES

1. Algermissen, S.T. and D.M. Perkins, 1972: "A Technique for Seismic Risk Zoning: General Considerations and Parameters," Proc. Microzonation Conf., Univ. Washington, Seattle, pp. 865-877.
2. Algermissen, S.T. and D.M Perkins, 1976: Open File Map, U.S. Geological Survey, Golden, Colorado.
3. Bollinger, G., 1976: "Reinterpretation of the Intensity Data for the 1886 Charlestown South Carolina Earthquake," Bull. Seismological Soc. Am. in pub.
4. Cornell, C.A., 1968: Engineering Seismic Risk Analysis, Bull. Seismological Soc. Am., Vol. 58, pp. 1583-1606.
5. McGuire, R.K., 1975: "Seismic Structural Response Risk Analysis, Incorporating Peak Response Progressions on Earthquake Magnitude and Distance," Report R74-51, Dept. Civil Eng., M.I.T., Cambridge, Mass.
6. Newmark, N.M. and W.J. Hall, 1969: "Seismic Design Criteria for Nuclear Reactor Facilities," Proc. 4th WCEE, Santiago, Chile.
7. Nuttli, O.W., 1973: "Seismic Wave Attenuation and Magnitude Relations for Eastern North America," J. Geophysical Research, Vol. 78, pp. 876-895.
8. Schnabel, P.B. and H.B. Seed, 1973: "Accelerations in Rock for Earthquakes in the Western United States," Bull. Seismological Soc. Am., Vol. 63, No. 2, pp. 501-528.

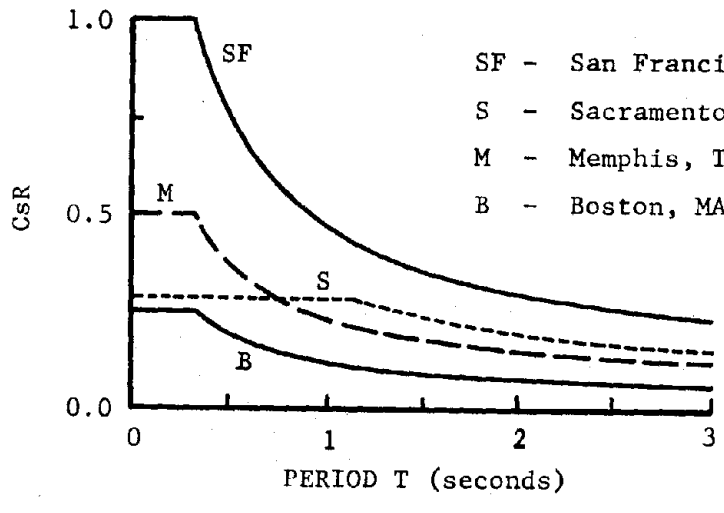

		A_1	A_2
SF	San Francisco, CA	0.4	0.4
S	Sacramento, CA	0.12	0.25
M	Memphis, TN	0.2	0.2
B	Boston, MA	0.1	0.1

NONLINEAR RESPONSE SPECTRA FOR PROBABILISTIC SEISMIC DESIGN OF REINFORCED CONCRETE STRUCTURES

Masaya Murakami[I] and Joseph Penzien[II]

SYNOPSIS

Twenty each of five different types of artificial earthquake accelerograms were generated for computing nonlinear response spectra of five structural models representing reinforced concrete buildings. To serve as a basis for probabilistic design, mean values and standard deviations of ductility factors were determined for each model having a range of prescribed strength values and having a range of natural periods. Adopting a standard design philosophy, required strength levels were investigated for each model. Selected results obtained in the overall investigation are presented and interpreted in terms of prototype behavior.

INTRODUCTION

The general philosophy of seismic resistant design in most countries of the world is that only minor damage is acceptable in buildings subjected to moderate earthquake conditions and that total damage or complete failure should be prevented under severe earthquake conditions. Usually, this design philosophy is applied to performance assessments and to design in a deterministic manner. It should be recognized however that due to the highly variable characteristics of ground motions, even for a given site, as well as the variable properties of structures, large uncertainties exist in predicting structural response. Therefore, nondeterministic methods which formally recognize these uncertainties should be used leading to response predictions in probabilistic terms.

Since it was the intent of this investigation to concentrate on the influence of variability of ground motions on the behavior of reinforced concrete buildings, nondeterministic response analyses were carried out using a stochastic model to represent the expected ground motions. The particular model used is essentially nonstationary filtered white noise as commonly used by many investigators [1,2,3,4]. While this model is admittedly not perfect, it does reflect the main statistical features of real ground motions; therefore, its use in seismic response analyses leads to more realistic predictions than does a single fully prescribed accelerogram.

ARTIFICIAL EARTHQUAKE ACCELEROGRAMS

Five specific types (Types A, B, B_{02}, C, and D) of artificial accelerograms were generated using a modified version of the program (PSEGCN) [1,5], where stationary wave forms having a constant power spectral density function (white noise) of intensity S_0 were modified by multiplying by a prescribed time intensity function, passing the resulting wave forms through both high and low frequency filters, and finally by applying a baseline correction in accordance with the procedure of Berg and Housner [6].

[I] Associate Professor of Architectural Engineering, Chiba University, Japan

[II] Professor of Structural Engineering, University of California, Berkeley, U.S.A.

Five time intensity functions were used as shown in Fig. 1. These functions are identical to those used previously by Jennings, et al. [2]. The selected high frequency filter function is plotted in Fig. 2a for ω_o = 15.6 rad/sec and ξ_o = 0.6. These same values of ω_o and ξ_o were used for four of the five classes of accelerograms, namely, Types A, B, C and D. Accelerograms Type B_{02} used the same value for ω_o, i.e. 15.6, but a different value for ξ_o, namely 0.2. The low frequency filter function used is shown in Fig. 2b. The values of T_f used in this function were 7 seconds for Types A, B, B_{02} and 2 seconds for Types C and D following the suggestion of Jennings, et al.[2].

The constant power spectral intensity S_o, used in generating the stationary wave forms, was assigned the value 0.8952 ft^2/sec^3. Table 1 lists the mean values and standard deviations for the peak accelerations in all five classes of accelerograms. The mean values and standard deviations for the infinite number of accelerograms of each class were estimated in accordance with the method of Gumbel [7]. In view of this mean peak acceleration and the time intensity function used, the Type B accelerograms closely represent that class of motions containing the N-S component of acceleration recorded during the 1940 El Centro, California, earthquake [2,3].

STRUCTURAL MODELS

A. ORIGIN-ORIENTED HYSTERETIC MODEL

One of the five structural models used in this investigation was the so-called "Origin-Oriented" hysteretic model proposed by Umemura, et al. [8]. This model is shown in Fig. 3 where it is characterized by p_{sc}, p_{sy}, v_{sc}, and v_{sy} which represent the concrete shear cracking strength, the ultimate shear strength, the relative displacement produced by p_{sc}, and the relative displacement produced by p_{sy}, respectively. Two other parameters are used in generating response spectra, namely, period $T_1 = \sqrt{m/k_1}$ and ratio $(p_{sc}/m\ddot{v}_{go})$ where m is the mass of the single degree of freedom system and $\ddot{v}_{go}$ is the mean peak ground acceleration. Through the use of this ratio, the absolute values of mean peak acceleration shown in Table 1 need not be specified separately.

B. TRILINEAR STIFFNESS DEGRADING HYSTERETIC MODEL

Four of the five structural models used in this investigation were the so-called "Trilinear Stiffness Degrading" hysteretic model [8]. This model is shown in Fig. 4 where it is characterized by p_{Bc}, p_{By}, v_{Bc}, and v_{By} which represent the load at which the concrete cracks due to flexure, the load at which the main reinforcing steel starts yielding due to flexure, the relative displacement produced by p_{Bc}, and the relative displacement produced by p_{By}, respectively. As in the case of the origin-oriented model, two other parameters are used in generating response spectra, namely, period $T_1 = \sqrt{m/k_1}$ and ratio $(p_{By}/m\ddot{v}_{go})$.

One characteristic feature of the trilinear stiffness degrading model worth noting is that when subjected to full-reversal cyclic displacements at a constant amplitude the bilinear hysteretic loops are perfectly stable. Using period $T_2 \equiv 2\pi\sqrt{m/k_y}$ one can calculate the equivalent damping ratio ξ_e for a linear viscously-damped single degree system which represents the same energy absorption per cycle of oscillation. This damping ratio is shown in

Fig. 5 for each of four different bylinear models together with the parameters of each model.

DUCTILITY RESPONSE SPECTRA

Mean maximum ductility factors $\bar{\mu}$ and their corresponding coefficients of variation were generated for the origin-oriented shear model and the four trilinear stiffness degrading flexure models using the 20 response time histories for each class of earthquake ground motions. Two examples of the results obtained are shown in Figs. 6 and 7 for the origin-oriented models and for one of the four trilinear models, respectively, when subjected to Type A excitations.

For each type of earthquake excitation, the maximum ductility factors generally increase with decreasing period and the spread of these ductility factors over the full strength range increases with decreasing period. Also these ductility factors for a fixed period increase with decreasing structural strength. The trends of the coefficients of variation for the maximum ductility factors with period are similar to the trends just described for mean maximum ductility factor, particularly regarding strength level and strength variation. It is most significant to note that the coefficients of variation are low when the response is essentially elastic ($\mu < 1$) but they can become very large with increasing inelastic deformations.

USE OF DUCTILITY RESPONSE SPECTRA FOR PROBABILISTIC SEISMIC DESIGN

A. SELECTION OF REQUIRED DUCTILITY LEVELS

Previous investigations have shown that the probability distribution function for extreme value of structural response for a single class of earthquakes follows closely the Gumbel Type 1 distribution [1,3]

$$P(\mu) = \exp \{- \exp [- \alpha (\mu - u)]\} \qquad (1)$$

where μ is the maximum response measured in terms of ductility factor, and α and u are parameters which depend on the average and standard deviation of μ. If only 20 sample values of μ are available as in this investigation, α and u can be obtained using the relations [7]

$$\alpha = 1.063/\sigma_{\mu} \quad \text{and} \quad u = \bar{\mu} - 0.493\, \sigma_{\mu} \qquad (2)$$

Suppose for example, it was decided that a 15 percent probability of exceedance was acceptable, i.e. $P(\mu) = 0.85$. Using Eq. (1) and the data provided in Figs. 6-7, one can easily establish that ductility factor μ_{85} associated with $P(\mu) = 0.85$. This has been done for two trilinear stiffness degrading models subjected to Type A ground motions giving the results shown in Fig. 8.

B. SELECTION OF REQUIRED STRENGTH LEVELS

To establish the required strength levels of the various structural models for each class of earthquake motions, one must first prescribe basic criteria consistent with the basic design philosophy. It will be assumed

that moderate and severe earthquake conditions are represented by 0.30g and 0.45g, respectively, for the corresponding peak ground accelerations. Further, the two ductility factors, consistent with light and heavy (but controlled) damage, are chosen as 2 and 10 for the origin-oriented shear model and 2 and 4 for the trilinear stiffness degrading model. The values of mean peak accelerations and ductility factors selected above follow the suggestions of Umemura, et al. [8].

Using data such as shown in Fig. 8 for each structural model and for each type of earthquake motion, i.e. using curves of μ_{85} vs. T_1, one can easily obtain the required strength ratios ($\beta \equiv p_y/m\ \ddot{v}_{go}$) for discrete values of T_1. Linear interpolation between the curves (μ_{85} vs. T_1) for a fixed value of T_1 can be used for this evaluation. The resulting required strength ratios can then be plotted as functions of period T_1 as shown in Fig. 9. When judging which of the two prescribed ductility factors control a particular design, one should be careful not to base the decision on a direct comparison of the required strength ratios as shown in Fig. 9, but to select the larger of the two strength ratios required to satisfy the prescribed maximum ductility factors under moderate and severe earthquake conditions. The required strength ratios for the trilinear models are shown only for $\mu_{85} = 4$ since the heavy damage criterion always controls the design.

Two characteristic features shown in Fig. 9 are that the four curves representing earthquake Types A, B, C, and D are quite close together in each case showing that the influence of duration of ground motions is not large, and that the required strength ratios for relatively larger periods vary in a linear manner with negative slopes along the log scale for T_1, i.e. converting to a linear scale, the strength ratios would vary in inverse proportion to the square root of T_1.

One significant feature shown in Fig. 1 where the required strength ratios are plotted as functions of periods T_2, is that the ratios vary considerably with period T_2 and the equivalent damping ratio ξ_e (see Fig. 5); therefore, these two parameters are important to the seismic response of reinforced concrete structures of the flexural failure type.

When using the results in Figs. 9 and 10, one should remember that they are based on the ground motion parameters $\omega_o = 15.6$ rad/sec ($T_o = 0.4$ sec) and $\xi_o = 0.6$ which represent firm ground conditions. If one should have quite different ground conditions, these parameters should be adjusted appropriately. These adjustments shift the level of the predominant frequencies in the ground motions and also change the mean intensity level $\ddot{v}_{go}$. With considerable experience and using engineering judgment, certain modifications to the data in Figs. 9 and 10 can be made to reflect these new conditions.

CONCLUDING STATEMENT

The mean maximum ductility factors and their corresponding coefficients of variation presented herein provide the necessary data for carrying out probabilistic seismic resistant designs consistent with basic design criteria and the statistical nature of earthquake ground motions.

ACKNOWLEDGMENT

The authors express their sincere thanks and appreciation to the National Science Foundation for its financial support of this investigation.

BIBLIOGRAPHY

[1] Ruiz, P., and Penzien, J., "Probabilistic Study of the Behavior of Structures during Earthquakes," Earthquake Engineering Research Center, No. EERC 69-3, University of California, Berkeley, California, March, 1969.
[2] Jennings, P. C., Housner, G. W., and Tsai, N. C., "Simulated Earthquake Motions," Earthquake Engineering Research Laboratory, California Institute of Technology, Pasadena, California, April, 1968.
[3] Penzien, J., and Liu, S-C., "Nondeterministic Analysis of Nonlinear Structures Subjected to Earthquake Exitations," Proceedings of the 4th World Conference on Earthquake Engineering, Santiago, Chile, January, 1969.
[4] Amin, M., and Ang, A. H. S., "A Nonstationary Stochastic Model for Strong-Motion Earthquake," Structure Research Series 306, University of Illinois, Urbana, Illinois, April, 1966.
[5] Murakami, M., and Penzien, J., "Nonlinear Response Spectra for Probabilistic Seismic Design and Damage Assessment of Reinforced Concrete Structures," Earthquake Engineering Research Center, No. EERC 75-38, University of California, Berkeley, 1976.
[6] Berg, G. V., and Housner, G. W., "Integrated Velocity and Displacement of Strong Earthquake Ground Motion," Bulletin of the Seismological Society of America, Vol. 51, No. 2, April, 1961.
[7] Gumbel, E. J., and Carlson, P. G., "Extreme Values in Aeronautics," Journal of the Aeronautical Sciences, 21, No. 6, June, 1954.
[8] Umemura, H., et. al., "Earthquake Resistant Design of Reinforced Concrete Buildings, Accounting for the Dynamic Effects of Earthquake," Giho-Do, Tokyo, Japan, 1973 (in Japanese).

TABLE 1

MEAN VALUES AND STANDARD DEVIATIONS OF PEAK GROUND ACCELERATIONS

Type of Earthquake	Statistical Quantity	Number of Earthquakes		
		20	40	Infinity
A	Mean	0.327	0.331	0.332
	Std. Deviation	0.023	0.036	0.040
B	Mean	0.300	0.308	0.309
	Std. Deviation	0.032	0.037	0.041
C	Mean	0.240	0.243	0.244
	Std. Deviation	0.022	0.035	0.039
D	Mean	0.191	0.188	0.189
	Std. Deviation	0.041	0.039	0.044
B_{02}	Mean	0.346	0.336	0.337
	Std. Deviation	0.048	0.049	0.055

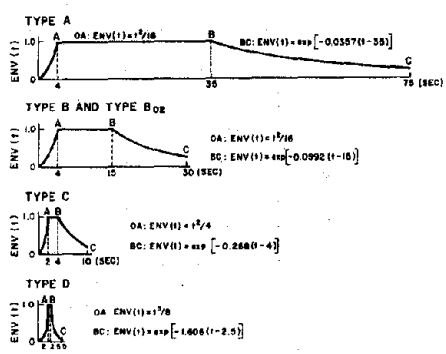

Fig. 1 Time Intensity Functions

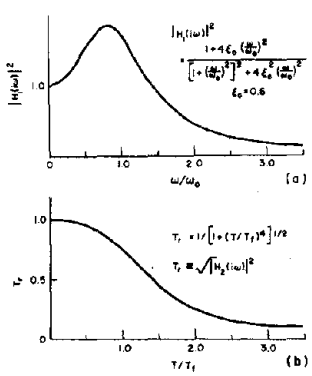

Fig. 2 Filter Transfer Functions

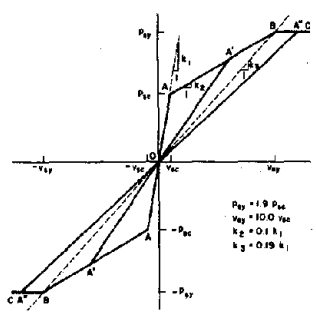

Fig. 3 Origin-Oriented Hysteretic Model

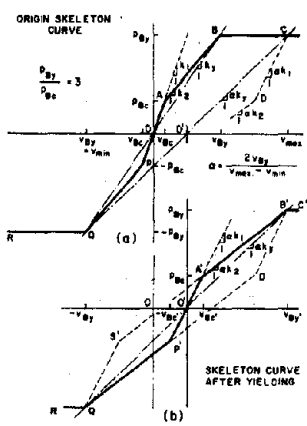

Fig. 4 Trilinear Hysteretic Model

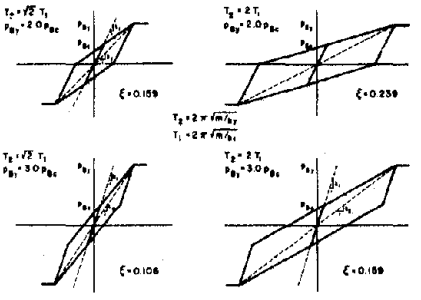

Fig. 5 Stable Bilinear Hysteretic Loop for Trilinear Stiffness Degrading Model

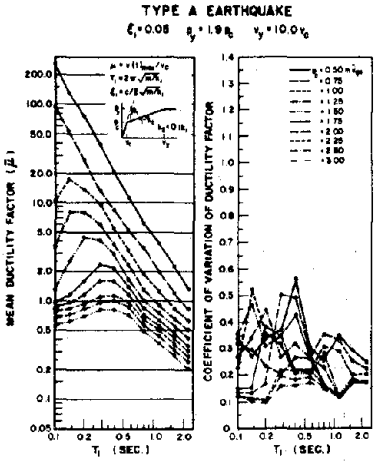

Fig. 6 Mean Ductility Factors and Corresponding Coefficients of Variation for Origin-Oriented Model

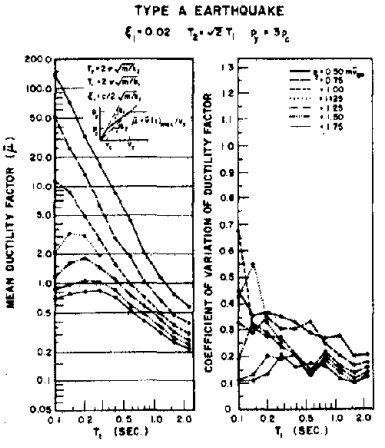

Fig. 7 Mean Ductility Factors and Corresponding Coefficients of Variation for Trilinear Stiffness Degrading Model

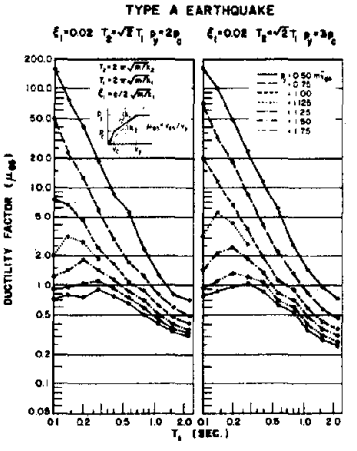

Fig. 8 Response Ductility Factors for 85% Level on Probability Distribution Functions

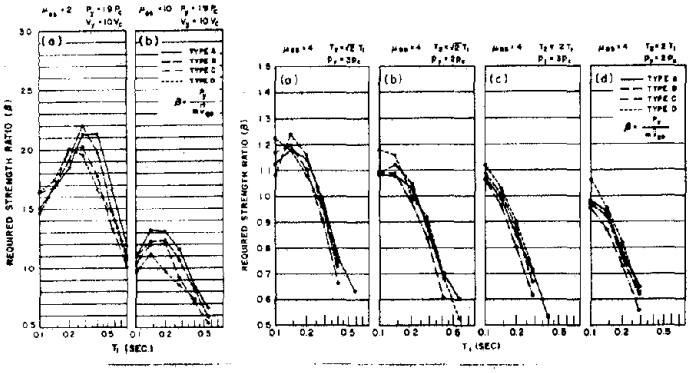

Fig. 9 Required Strength Ratios for Origin-Oriented Model and Trilinear Stiffness Degrading Models at the 85 % Probability Distribution Level

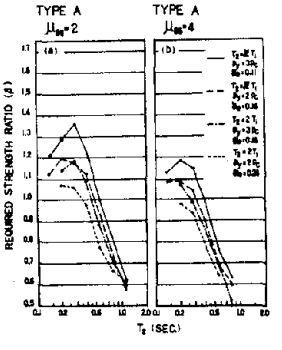

Fig. 10 Required Strength Ratios vs. T_2 for Trilinear Stiffness Degrading Models at the 85 % Probability Distribution Level

GENERAL PURPOSE COMPUTER PROGRAM FOR DYNAMIC NONLINEAR ANALYSIS

by

D.P. Mondkar[I] and G.H. Powell[II]

SYNOPSIS

This paper presents a brief description of the concepts, features, organization and usage of a general purpose finite element computer program ANSR (Analysis of Nonlinear Structural Response) for the static, dynamic and earthquake response analysis of nonlinear structures. The program is intended ultimately to form a practical analysis tool for use in design studies as well as to satisfy research needs in various aspects of nonlinear analysis.

INTRODUCTION

Because of the need for rational investigations of nonlinear structures subjected to severe loading conditions such as would occur in strong motion earthquakes, a study was initiated with the objective of developing a general purpose computer program for nonlinear structural analysis. This study progressed through two phases. Phase one consisted of review and development of theories, computational techniques and algorithms that can be applied in nonlinear structural analysis, and phase two resulted in development of a general purpose computer code based on the studies in phase one. The results and findings of these two study phases have been documented in [1,2]. The purpose of this paper is to summarize the features of the computer program ANSR [2].

THEORETICAL BASIS

The program is based on the finite element discrete equations obtained from the variational form of the incremental equations of motion described in a Lagrangian coordinate system. In the Lagrangian description, the kinematics of deformation of a body is described by three configurations, namely, the initial configuration, current deformed configuration and a neighboring configuration; the initial undeformed configuration C_o (time $t = 0$) is taken as the reference configuration and the kinetic variables are the conjugate pair consisting of the second (symmetric) Piola-Kirchhoff stress and Lagrangian strain.

The incremental equations can be used to study nonlinearities due to large displacements, large strain effects and/or nonlinear material behavior. The material nonlinearity is specified by an appropriate relationship between stress and strain.

[I]Assistant Research Engineer, Division of Structural Engineering and Structural Mechanics, Department of Civil Engineering, University of California, Berkeley, California, U.S.A.

[II]Professor of Civil Engineering, University of California, Berkeley, California, U.S.A.

The dynamic response is obtained by a step-by-step numerical integration of the equations of motion using Newmark's generalized implicit operator. Equilibrium iterations can be performed, if desired, in each time step to satisfy equilibrium subject to a specified tolerance. A variety of iterative schemes are included so as to give considerable flexibility to the analyst to design a solution scheme giving results as accurately as possible with minimum computation times.

PROGRAM FEATURES AND LIMITATIONS

A. Structural Idealization

(1) The structure to be analyzed is idealized as an assemblage of discrete finite elements connected at nodes. The theory and solution procedure are based on the finite element formulation of the displacement method, with the nodal displacements as the unknown field variables.

(2) Each node may possess up to six displacement degrees of freedom, as in a typical three dimensional frame analysis.

(3) Certain degrees of freedom can be deleted or combined. This feature provides the program user ample flexibility in the idealization of the structure, and may permit the size of the problem to be substantially reduced.

(4) The structure mass is assumed to be lumped at the nodes only, so that the mass matrix is diagonal. The program could be modified to consider a coupled (consistent) mass matrix.

(5) Viscous damping effects proportional to mass, initial elastic stiffness and/or tangent stiffness can be included. These effects may be specified to vary in magnitude from one group of elements to the next.

B. Static and Dynamic Loadings

(1) Loads are assumed to be applied only at the nodes. Static and/or dynamic loads may be specified; however, static loads, if any, must be applied prior to the dynamic loads.

(2) For static analysis, a number of static force patterns must be specified. Static loads are then applied in a series of load increments, each load increment being specified as a linear combination of the static force patterns. This feature permits nonproportional loads to be applied. Each load increment can be specified to be applied in a number of equal steps.

(3) The dynamic loading may consist of earthquake ground accelerations time dependent nodal loads, and prescribed initial values of the nodal velocities and accelerations. These dynamic loadings can be specified to act singly or in combination.

(4) Earthquake excitations are defined by time histories of ground acceleration. Three different time histories may be specified, one for each of the X, Y and Z axes with which the structure geometry is defined. For any given axis, all support points are assumed to move identically

and in phase. The accelerations for any time history may be specified at equal time intervals (as in an artificially generated earthquake record) or at unequal time intervals (as in a measured earthquake record).

(5) Any number of time histories of dynamic force may be specified. As with the earthquake records, these time histories may be input at equal or unequal time intervals. Any dynamic force record may be prescribed to act at a node or a group of nodes, either as forces in the X, Y or Z directions, or as moments about the X, Y or Z axes.

(6) Values of initial translational and/or rotational velocity and acceleration may be specified at each node. Structures subjected to impulsive loads can be analyzed by prescribing appropriate initial velocities. For the case of static analysis followed by dynamic analysis, the displacements at the start of the dynamic analysis are assumed to be those at the end of the static analysis.

C. Finite Element Library

(1) The finite element library is limited at the time of writing, consisting of the following.

(a) Three dimensional truss element, which may yield in tension and yield or buckle elastically in compression. Large displacement effects may be included.

(b) Three dimensional beam-column element, which may be of variable cross section and strength, and which yields through the formation of concentrated plastic hinges at its ends. The inelastic behavior is considered using interaction between axial force and major axis bending moment only, and this interaction may be specified to be either for cross sections of steel or concrete. Eccentricities at the element ends may be specified for analysis of coupled frame-shear wall structures.

(c) Two dimensional variable number (4-to-8) node finite element for plane stress and plane strain analysis. Large displacement effects may be included. The material description may be specified to be isotropic linearly elastic, orthotropic linearly elastic, or isotropic elasto-plastic with either von Mises or Drucker-Prager yield function.

(d) Two dimensional variable number (4-to-8) node finite element for axisymmetric solid or shell analysis. Large displacement effects may be included. The material descriptions available are the same as those for two dimensional plane stress/strain analysis.

(e) Three dimensional variable number (8-to-20) node solid element for analysis of solids and thick shells/plates. Large displacement effects may be included. The material law may be specified to be isotropic linearly elastic, orthotropic linearly elastic or isotropic elastic-plastic with von Mises yield function.

(f) Boundary (spring) element for use in specifying flexible supports, prescribed displacements, and for idealizing gaps between the structure and supporting system.

(2) The program is organized to permit the addition of new finite elements to the library with relative ease, without modifying the original program. Also, for the currently developed elements in the library, new material constitutive laws can be added by developing a few new "material" subroutines.

(3) Nonlinearities are introduced at the element level only, and may be due to large displacements, large strains and/or nonlinear materials. The programmer adding a new element may include any type or degree of nonlinearity in the behavior of the element.

D. Solution Procedure

(1) The program incorporates a solution strategy defined in terms of a number of control parameters. By assigning appropriate values to these parameters, a wide variety of solution schemes, including step-by-step iterative and mixed schemes, may be constructed. This permits the program user considerable flexibility in selecting optimal solution schemes for particular types of nonlinear behavior.

(2) For static analysis, a different solution scheme may be employed for each load increment. The use of this feature can reduce the solution time for structures in which the response must be computed more precisely for certain ranges of loading than for others. In such cases a sophisticated solution scheme with equilibrium iteration might be used for the critical ranges of loading, whereas a simpler step-by-step scheme without iteration might suffice for other loading ranges.

(3) The dynamic response is computed by step-wise time integration of the incremental equations of motion using Newmark's β-γ-δ operator. A variety of integration operators may be obtained by assigning appropriate values to the parameters β and γ. However, the most commonly used scheme will be the "constant average acceleration" scheme ($\beta=1/4$, $\gamma=1/2$, $\delta=0$). Viscous damping effects may be introduced by specifying a positive value to the parameter δ. In most cases, however, damping effects will be introduced more explicitly, in mass proportional and/or stiffness proportional form.

E. Other Features

(1) Data checking runs may be made prior to execution runs. During data checking, the program reads and prints all input data, and also prints any generated data, but performs no substantial analysis.

(2) In its current version the program requires that the stiffness matrix be stored in core. This matrix is stored column-wise in a compacted form omitting most zero elements. Because the stiffness matrix is updated, rather than completely reformed, as the tangent stiffness changes, it is also necessary to save a duplicate stiffness matrix. Updating of the matrix requires least numerical operations if the duplicate stiffness matrix can be held in core. However, this may not always be possible, and hence provision is made for the user to specify whether the duplicate matrix should be stored in core or on disc. Modifications for very large systems, using

blocking and out-of-core storage of the stiffness matrix, are planned for a future version of the program.

(3) During solution, the decomposition (triangularization) of the structure stiffness matrix is carried out on only that part of the updated stiffness matrix which follows the first modified coefficient. Significant savings in solution time can sometimes be obtained by numbering those nodes connecting nonlinear elements to be last, so that the operations on the structure stiffness matrix are limited to the end of the matrix.

(4) The element information is stored either in core or on disc. When stored on disc, the information is blocked to minimize input/output cost for data transfer between core and disc storages. Thus, the number of finite elements is not limited by the available core storage, except that this storage must be sufficient to hold the information for at least one element.

(5) Because the structure stiffness matrix is stored in compacted form, rather than in banded form, there will be relatively small penalties in storage requirements and equation solving time if there are local increases in the matrix band width. Hence, if a few nodes are to be added to a structure for which an input data deck has already been prepared, the additional computational cost incurred by numbering these nodes last may be less than the man-hour cost involved in renumbering all of the nodes and preparing a new input data deck.

(6) Because all nonlinearities are introduced at the element level, and because the structure stiffness matrix is updated, not reformed, due to nonlinearities, there is no loss of efficiency in computing dynamic response of purely linear structures.

(7) At present no restart capability is included in the program. Such a capability will be added in a future version.

PROGRAM STRUCTURE

The program is divided into two parts, namely, (1) the base program consisting of a series of subroutines performing specific tasks required for static and dynamic analysis, and (2) a number of auxiliary programs, each program consisting of a package of subroutines required for a specific type of finite element in the element library. The base program reads and prints the structure geometry and loading data, carries out a variety of bookkeeping operations, assembles the structure stiffness matrix and loading, and using the user-specified solution scheme computes the displacement response of the structure. The base program is then combined with element subroutines of the auxiliary programs to produce a complete package. The auxiliary program for any one specific type of element performs four main functions, namely, (1) reading and printing of element data, (2) computing tangent stiffness, (3) calculating new state, and (4) outputing response results. Each of these functions is performed by a separate subroutine, and information returned to the base program. The rules for the linkage and information transmittal between the base program and the auxiliary program have been simplified, so that auxiliary programs for new structural elements can be developed and added to the base program relatively easily. The currently developed auxiliary programs also have the capability of accepting new material constitutive laws. This is achieved by performing all computations associated with a particular material in a package of

"material" subroutines, and returning the information to the auxiliary program. Again, rules for the linkage and transmittal of information between the "material" subroutines and the auxiliary program have been designed to give the programmer the ability to code new material models with relative ease. The capability to add new structural elements and new material models is an important feature of the program for use as a research tool as well as a practical analysis tool.

The available core storage is allocated dynamically at execution time. As mentioned previously, the element data is blocked to reduce input/output cost for data transfer between disc and core storage. If all element data can be held in core then no data transfer operations are required. The program incorporates efficiently designed computational algorithms for equation solving and stress computations.

SAMPLE APPLICATIONS

The program has been used to analyze a number of structures with widely different nonlinear characteristics. The main objective of these analyses has been verification of the program features and the various solution schemes implemented in the program. Wherever possible the results of these analyses have been compared with the analytical, numerical and/or experimental studies of other investigators, and close agreement has been obtained; see reference [2] for descriptions of these analyses.

FUTURE DEVELOPMENTS

A number of new capabilities will be added to the program. These include restart options, new constitutive material laws such as elasto-plastic isotropic and kinematic hardening models, a parallel component model, and soil material models. The program will also be modified to handle out-of-core blocking of the structure stiffness matrix for use in large scale structures. A special purpose version of the program is also being developed for exclusive use in three dimensional nonlinear analysis of building systems. Thermal stress analysis capability including some simple thermo-plastic material models have been developed. This paper should be regarded as a preliminary documentation paper. It is anticipated that the program ANSR will be continually updated to satisfy both research and industrial needs in nonlinear analysis.

ACKNOWLEDGEMENTS

The work presented in this paper was supported partly by the National Science Foundation, under Grant NSF-GI-36387. Computer Facilities were provided by the Computer Centers of the University of California, Berkeley and the Lawrence Berkeley Laboratory.

REFERENCES

1. Mondkar, D.P., and Powell, G.H., "Static and Dynamic Analysis of Nonlinear Structures", Report No. EERC 75-10, Earthquake Engineering Research Center, University of California, Berkeley, March 1975.
2. Mondkar, D.P., and Powell, G.H., "ANSR-I, General Purpose Program for Analysis of Nonlinear Structural Response", Report No. EERC 75-37, Earthquake Engineering Research Center, University of California, Berkeley, December 1975.

EARTHQUAKE RESPONSE OF A CLASS OF TORSIONALLY COUPLED BUILDINGS

by

C. L. Kan[I] and Anil K. Chopra[II]

SYNOPSIS

Results of an investigation of earthquake response of an important class of buildings for which the lateral motion is coupled with the torsional motion are summarized. The relationships between the story forces in a torsionally coupled system and those in a corresponding torsionally uncoupled system are presented, and the effects of torsional coupling on earthquake forces are identified.

INTRODUCTION

Buildings with eccentric centers of mass and resistance respond in coupled lateral torsional motions to earthquake ground motion, even when the motion is uniform over the base and contains no rotational components. Analysis of torsionally coupled buildings requires that, in addition to the usually considered translational degrees of freedom, the torsional degree of freedom be included for each floor. It is possible, however, to establish relationships between the response of a torsionally coupled building to that of one which is torsionally uncoupled but otherwise possesses identical properties. These relationships are presented here and some of the effects of torsional coupling on response are identified.

THE IDEALIZED SYSTEM

Characteristic of many multistory buildings are the following features: (i) All floors of the building have the same geometry in plan and the same locations for columns and shear walls. (ii) The ratio of the story stiffness in the two principal directions of resistance is about the same for all stories. With reference to the building idealization consisting of rigid floors supported on massless, axially inextensible columns and walls (Fig. 1), the class of buildings mentioned is assumed to satisfy the following restrictions:

1. The principal axes of resistance for all the stories are identically oriented, along the x- and y-axes shown.
2. The centers of mass of the floors all lie on one vertical axis.
3. The centers of resistance of the stories all lie on another vertical axis, i.e., the static eccentricities e_x and e_y are the same for all the stories.
4. All the floors have the same radius of gyration r about the vertical axis through the center of mass.
5. The ratios of the three stiffness quantities -- translational stiffnesses in x- and y-directions, K_{xi} and K_{yi}, and torsional stiffness $K_{\theta i}$ -- for any story:

$$K_{yi}/K_{xi} = \beta_y , \qquad K_{\theta i}/(r^2 K_{xi}) = \beta_t$$

[I]Graduate Student, [II]Professor of Civil Engineering, University of California, Berkeley, California, U.S.A.

are independent of the story number i, i.e., the ratios are the same for all stories.

For this system, each floor has three degrees of freedom: x- and y-displacements, relative to the ground, of the center of mass and rotation about a vertical axis -- resulting in a total of 3N (N=number of stories) degrees of freedom.

STORY FORCES

Considering ground motion only in the x-direction, characterized by hyperbolic or flat acceleration response spectrum (Fig. 2), the forces in a story of the torsionally coupled system -- the shear in x-direction, V_x, shear in y-direction, V_y, and torque T defined at the mass center or T_R defined at the center of resistance -- can be expressed in terms of the shear, V_{xo}, in the same story of the corresponding torsionally uncoupled system -- a system with coincident centers of mass and resistance but all other properties identical to the actual system (1):

$$V_x = \bar{V}_x V_{xo}, \quad V_y = \bar{V}_y V_{xo}, \quad T = r \bar{T} V_{xo}, \quad T_R = r \bar{T}_R V_{xo} \tag{1}$$

The dimensionless coefficients $\bar{V}_x$, $\bar{V}_y$, $\bar{T}$ and $\bar{T}_R$ are the same for every story of the building. They are also the normalized forces -- normalized in accordance with Eq. 1 -- in an associated one-story system having the following properties: $K_\theta/(r^2 K_x) = \beta_t$, $K_y/K_x = \beta_y$, e_x/r and e_y/r same as for all the stories of the multistory building.

It can also be shown that the overturning moments $\mathcal{M}_x$ and $\mathcal{M}_y$ at any level in the torsionally coupled system are

$$\mathcal{M}_x = \bar{V}_x \mathcal{M}_{xo}, \qquad \mathcal{M}_y = \bar{V}_y \mathcal{M}_{xo} \tag{2}$$

where $\mathcal{M}_{xo}$ is the overturning moment at that particular level of the corresponding torsionally uncoupled system.

NORMALIZED FORCES

Interaction Equations

It can be shown analytically (1) that the normalized forces for earthquake motion in the x-direction, characterized by either a flat or hyperbolic acceleration spectrum, satisfy the interaction equation

$$\bar{V}_x^2 + \bar{V}_y^2 + \bar{T}^2 = 1 \tag{3}$$

It is apparent from Eqs. 1 and 3 that, for flat or hyperbolic acceleration response spectra, story shears and overturning moments in a torsionally coupled system are less than in the corresponding uncoupled system. Earlier studies (2,3) arrived at the same conclusion but in a restricted sense: The conclusion was based on numerical results for specific systems, and hence applicable only to those systems.

Interaction equations can also be derived (1) in terms of the torque at the center of resistance. For ground motion in the x-direction, these are:

$$\bar{V}_x^2 + \frac{\bar{V}_y^2}{\beta_y} + \frac{\bar{T}_R^2}{\beta_t - (e_y/r)^2 - (e_x/r)^2 \beta_y} = 1 \qquad (4)$$

for hyperbolic acceleration spectrum, and

$$\bar{V}_x^2 + \frac{\bar{V}_y^2}{\beta_y} + \frac{\bar{T}_R^2 - (e_y/r)^2}{\beta_t - (e_y/r)^2 - (e_x/r)^2 \beta_y} = 1 \qquad (5)$$

for flat acceleration spectrum. For structures symmetric about the y-axis, $\bar{V}_y = 0$ in Eqs. 3-5. Replacing V_{xo} by V_{yo} in Eq. 1 and interchanging the subscripts x and y in Eqs. 4 and 5 results in the interaction equations for forces due to ground motion in the y-direction.

Numerical Results

Numerical results for the normalized shear forces $\bar{V}_x$ and $\bar{V}_y$ and a normalized measure of the torque:

$$\tilde{T}_R = \frac{T_R}{V_{xo}\, e_y} = \frac{\bar{T}_R}{(e_y/r)} \qquad (6)$$

are presented next. This particular definition of normalized torque is chosen as it may be interpreted as the ratio of dynamic eccentricity to static eccentricity: e_d/e_y, where $e_d = T_R/V_{xo}$ is the dynamic eccentricity, the distance from the center of resistance at which the shear V_{xo} must be applied to result in the torque T_R.

The three normalized forces depend only on the shape of the acceleration response spectrum -- flat or hyperbolic, frequency ratios ω_θ/ω_x and ω_y/ω_x, static eccentricities e_x/r and e_y/r and damping factor ξ. The three frequency parameters ω_x, ω_y and ω_θ may be interpreted as the uncoupled frequencies of the associated one-story system, the natural frequencies of the system if it were torsionally uncoupled ($e_x = e_y = 0$); $\omega_y/\omega_x = \sqrt{\beta_y}$ and $\omega_\theta/\omega_x = \sqrt{\beta_t}$. The results of Fig. 3-5 and other numerical results (1) not presented here lead to the following conclusions:

1. The shear in the direction of ground motion, V_x, and the torque are essentially independent of ω_y/ω_x, except for a relatively narrow band of ω_y/ω_x around $\omega_y/\omega_x = 1$ (Fig. 3).
2. The torque generally increases with increase in e_y/r, the component of eccentricity perpendicular to the direction of ground motion. But it may decrease (Fig. 4), and often does, when e_x/r, the component of eccentricity along the direction of ground motion increases.
3. The effect of torsional coupling depends strongly on ω_θ/ω_x, the ratio of natural frequencies for uncoupled torsional and lateral motions of the corresponding uncoupled system (Figs. 3-5).
4. The effect of torsional coupling decreases as damping increases.

CONCLUDING REMARKS

In the preceding sections, Eq. 1 formed the basis for studying the

effects of torsional coupling on earthquake response of buildings. The equation also suggests that for a torsionally coupled building belonging to the particular class considered, the maximum response forces can be determined by analyzing (i) the corresponding torsionally uncoupled building, a system with N degrees of freedom, and (ii) the associated one-story system -- with 3 degrees of freedom. This procedure and its extension to buildings that do not belong to the particular class is presented elsewhere (1).

ACKNOWLEDGEMENT

This study was sponsored by the National Science Foundation.

REFERENCES

1. Kan, C. L., and Chopra, A. K., "Coupled Lateral Torsional Response of Buildings to Ground Shaking," Report No. EERC 76-13, Earthquake Engineering Research Center, University of California, Berkeley, California, May 1976.

2. Bustamante, J. I., and Rosenblueth, E., "Building Code Provisions on Torsional Oscillations," Proceedings of the Second World Conference on Earthquake Engineering, Vol. 2, Tokyo, Japan, 1960, pp. 879-894.

3. Elorduy, J., and Rosenblueth, E., "Torsiones Sismicas en Edificios de Un Piso," Segundo Congreso Nacional de Ingenieria Sismics, Veracruz, Mexico, 1968.

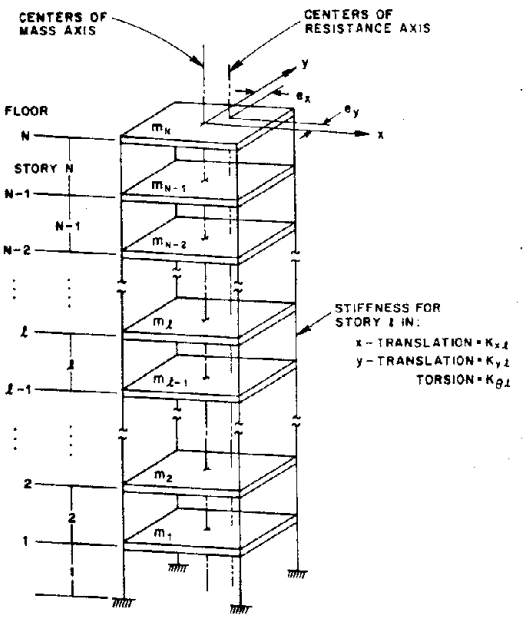

FIG. 1 IDEALIZED MULTISTORY BUILDING

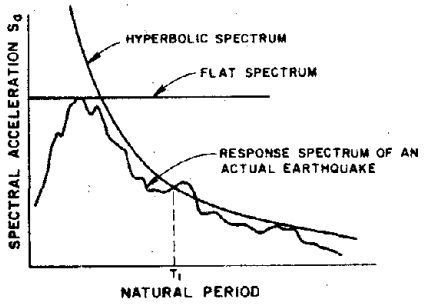

FIG. 2 IDEALIZED RESPONSE SPECTRA

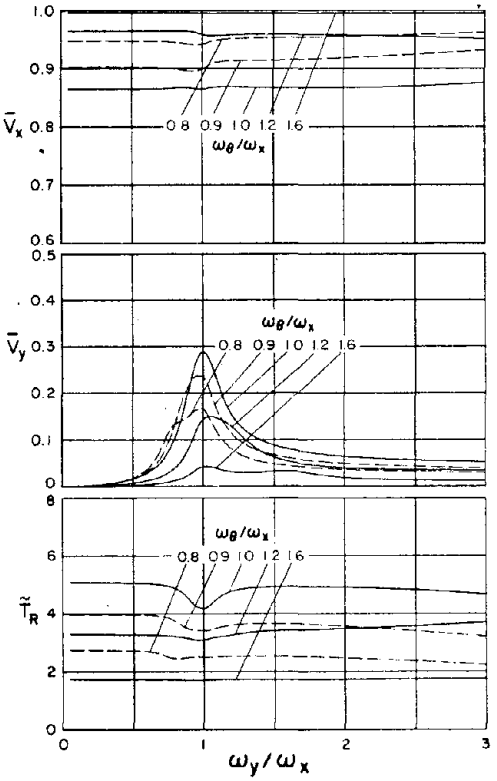

FIG. 3 NORMALIZED FORCES FOR TORSIONALLY COUPLED SYSTEMS WITH $e_x/r = e_y/r = 0.1$ AND FLAT ACCELERATION SPECTRUM

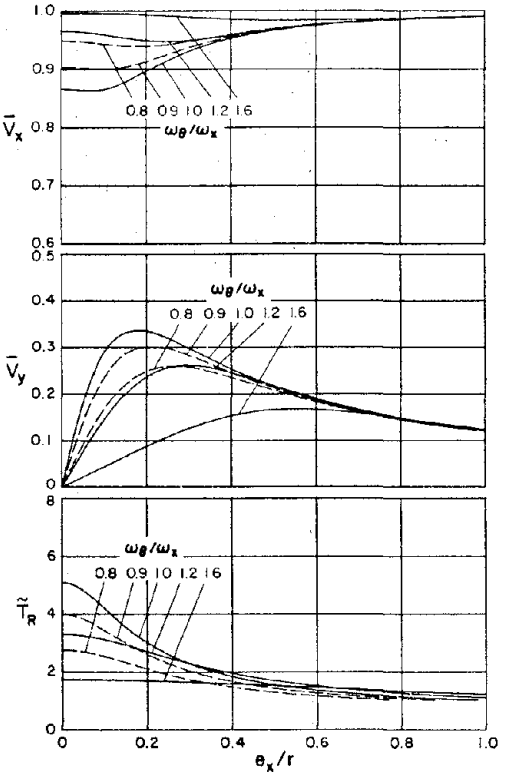

FIG. 4 NORMALIZED FORCES FOR TORSIONALLY COUPLED SYSTEMS WITH $\omega_y/\omega_x = 1$, $e_y/r = 0.1$ AND FLAT ACCELERATION SPECTRUM

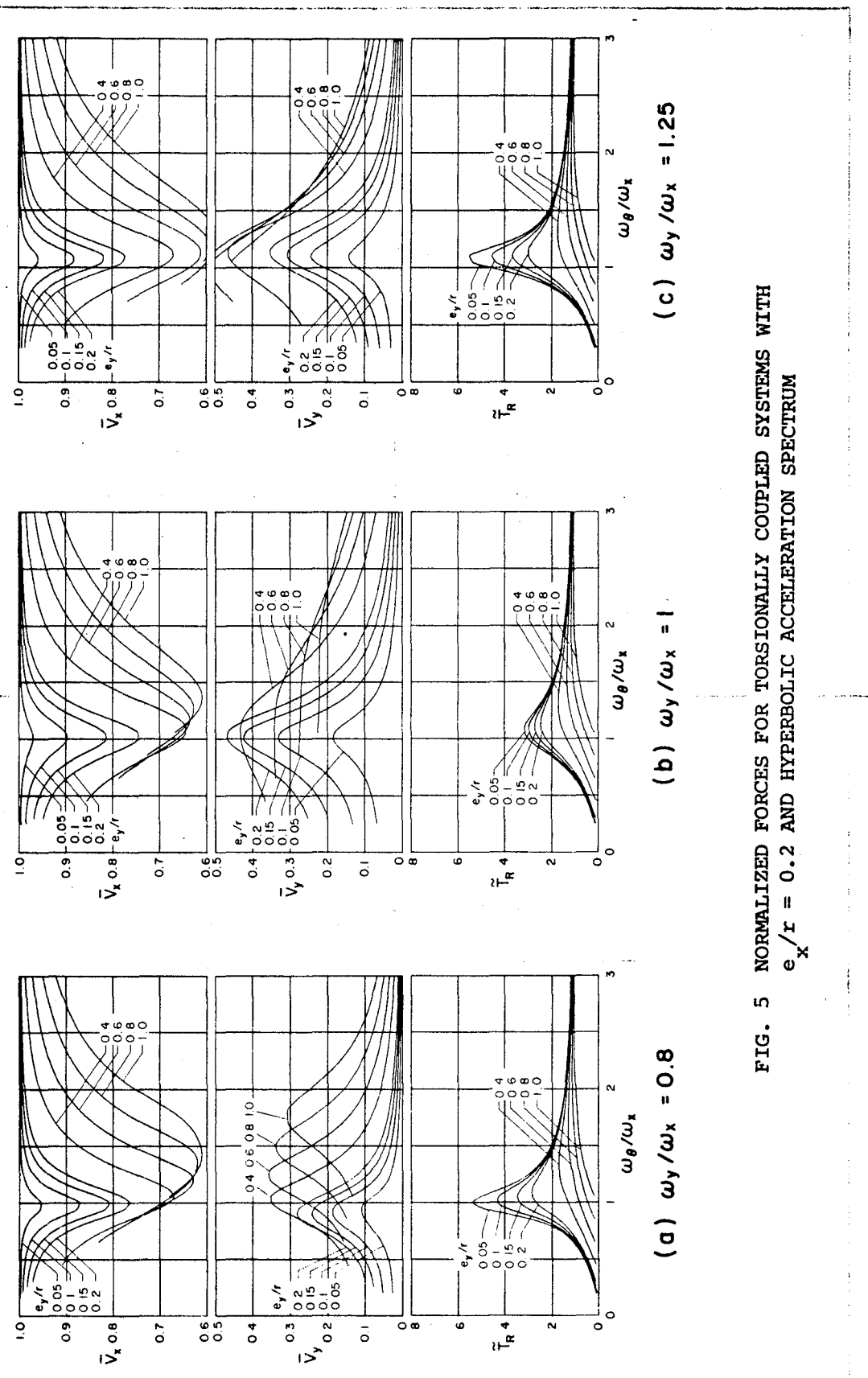

FIG. 5 NORMALIZED FORCES FOR TORSIONALLY COUPLED SYSTEMS WITH $e_x/r = 0.2$ AND HYPERBOLIC ACCELERATION SPECTRUM

ENERGY ABSORBING DEVICES IN STRUCTURES UNDER EARTHQUAKE LOADING

by

J. M. Kelly[I] and D. F. Tsztoo[II]

SYNOPSIS

Several different types of energy absorbing devices have been proposed for incorporation into structures designed to resist earthquake attack. The basic concept is that the energy dissipating, needed to absorb the kinetic energy imparted to the structure by earthquake loading, can be concentrated in devices specifically designed for that purpose. In previous work we have described a particular type of device which operates on the principle of large plastic deformation of mild steel in torsion. It has been shown that the device can provide substantial energy absorption over many cycles of plastic deformation, that the lifetime of the device and its absorption capacity are not decreased by increasing strain rates or by random loading.

In this paper we describe a series of tests in which a half scale three story single bay steel frame fitted with these torsion type energy absorbing devices was subjected to simulated earthquake loading on the 20 ft. square Earthquake Simulator Facility. The results of the tests are compared in this paper to those for two other series on the same frame when the devices were not used. The test series are taken as establishing the feasibility of the energy absorbing device concept.

INTRODUCTION

Many structures are currently designed for multiple load carrying and resisting capacities. Where earthquakes constitute a hazard, a serious problem may exist in that multi-functional structures may not only suffer damage to their seismic resistance capabilities but also to their normal load carrying capacities as well. All structural mechanisms for the absorption of seismic energy simultaneously diminish the capabilities of structures to carry loads under normal gravity and wind conditions. Even if repairs are effected after each earthquake attack there is always the possibility that some structural damage has accumulated in the structure.

The underlying theme of the work reported here concerns the separation of structural earthquake resistance from structural load carrying capacity; the structure is designed to resist gravity and wind loads and special energy absorbing mechanical devices are integrated into the structure to provide seismic resistance and thus to protect the major structure at the expanse of the replaceable energy absorbing devices. The effectiveness of such devices may be enhanced by incorporating them into a base isolation system which not only isolates the structure from seismic energy but channels such energy into the devices. Possible isolation systems include designs incorporating flexible first stories or stepping support foundations.

[I] Professor of Civil Engineering, Earthquake Engineering Research Center, University of California, Berkeley, California, U.S.A.

[II] Graduate Student, Department of Civil Engineering, University of California, Berkeley, California, U.S.A.

The benefit/cost ratios of such designs are favorable. The major structure can be designed to be lighter and more economical since much of the damaging seismic energy can be absorbed by the devices. Low maintenance and replacement costs are possible. The devices can be designed to resist corrosion and require little monitoring and to be replaceable without disruption to the main structure. The cost of the devices would be a small percentage of the major structure cost.

A study of the feasibility of such devices has been reported by Kelly, Skinner, and Heine [1,2] in which various mechanisms of energy absorption were studied. The characteristics of these mechanisms which were of primary importance were the load displacement relationships, the energy absorption capacity and the low cycle fatigue resistance. It was shown that the plastic torsion of mild steel is an extremely efficient mechanism for the absorption of energy and that the mode of failure in torsion is a favorable one for use in an energy absorbing device in that it takes the form a a gradual decay.

The research to be reported in this paper is concerned with the experimental verification of the use of energy absorbing devices in earthquake resistant design. We have recently been able to carry out in a series of tests in which a three story model steel frame was fitted with energy absorbing devices and subjected to several earthquake loadings on the 20 ft. square shaking table at the Earthquake Simulator Laboratory of the Earthquake Engineering Research Center. The column bases of the frame were fitted with a special type of footing which provided full horizontal constraint but allowed the bases to move freely vertically. Roller bearings are incorporated to facilitate free vertical movement. The frame so fitted was subjected to a series of simulated earthquake loadings using the El Centro N-S 1940 record scaled up to a maximum intensity of .786g. The results of this series of tests on the free uplift frame has been reported by Huckelbridge and Clough [3].

Following these tests the column bases of the frame were modified to include torsion type energy absorbing devices with one device at each column base. The devices were located in such a way that they operated only when the column foot lifts off the foundation, in this case the shaking table. When the column foot lifts up the device produces a downward restraining force which is almost constant and when the foot moves back downwards the device produces an upward force, thus absorbing energy from the frame.

The results of the present series are compared in this report with previous El Centro tests on the frame with the feet tied down and the feet free as reported in [3].

TEST PROGRAM

The test structure is pictured in Fig. 1. A complete description of member sizes and connection details is given by Clough and Tang [4]. Details of the modifications needed to allow the column feet to uplift are given by Huckelbridge and Clough [3]. It should be noted that the feet although free to move vertically are constrained by the uplift mechanism to follow the horizontal displacement of the table. The modifications of the uplift mechanism to incorporate the energy absorbing device are shown in Fig. 2, and details of the design of the device are given in Fig. 3.

The data acquisition system of the University of California shaking table has been described by Rea and Penzien [5]. Up to 128 channels can

be monitored in discrete sampling intervals, and the digital data stored on the disk of a mini-computer system. Subsequently the data is transferred to magnetic tape for detailed reduction. For the tests described here, 36 table functions and 90 transducer channels on the model were monitored, with a sampling frequency of approximately 50 points per second for each channel.

During the tests 5 types of electrical transducers were utilized to provide data: accelerometers, potentiometers, DC LVDT's, strain gages and half-bridge on-off contact switches. Accelerometers monitored the three horizontal floor accelerations and the table acceleration. Potentiometers and DC LVDT's monitored the three horizontal floor displacements relative to a fixed reference station off the table, the vertical displacements of the four column bases relative to the table surface, and selected frame member displacements. Strain gages were positioned on the various members to give the complete force distribution throughout the structure. The contact switches were placed between each column base and its impact pad to indicate the times of separation of the two elements during uplift.

The tests were carried out with six different intensities of the El Centro N-S 1940 record without vertical component with maximum intensity up to .786g. The intensities used here were the same as those of the tests reported in [3].

EXPERIMENTAL RESULTS

The results of the test series were very positive. At each intensity (from about 10% g max. to about 75% g max.) the uplift of the frame footings and the relative story displacements with devices was much less than when the frame was free to uplift as shown in Figs. 4 and 5. The column tension and base shear with devices were also much less than those experienced when the frame feet were rigidly fixed to the foundation as indicated by Figs. 6 and 7. Although not illustrated comparisons of base overturning moment produced the same results as the base shear. A summary of these results is given in Table 1.

CONCLUSIONS

Comparisons of the results for the case with energy absorbing devices with those for the base fixed and with those for the frame without any anchorages show that the use of the devices is generally beneficial. The devices offer enough base restraint to keep relative story displacements almost the same as in the fixed base case but substantially less than when the frame was uncoupled vertically from its foundation. Yet the devices absorb enough energy and allow partial base uncoupling to reduce column forces to levels much less than those for the fixed base case and to levels comparable for the unanchored case. Another notable fact is that the base shear and overturning moments were reduced by the devices to less than those experienced in both the fixed base and free base cases.

Thus it is believed that the tests have established the feasibility of the use of energy absorbing devices in seismic resistant design, at least in so far as El Centro type earthquakes are concerned. Work on the response to other types of earthquakes is continuing.

BIBLIOGRAPHY

1. J.M. Kelly, R.I. Skinner and A.J. Heine, "Mechanics of Energy Absorption in Special Devices for Use in Earthquake Resistant Structures", Bull. N.Z. Society of Earthquake Engineering, Vol. 5, pp. 63-88, 1972.

2. R.I. Skinner, J.M. Kelly and A.J. Heine, "Hysteretic Dampers for Earthquake Resistant Structures", Earthquake Engineering and Structural Dynamics, Vol. 3, pp. 287-296, 1975.

3. A.A. Huckelbridge and R.W. Clough, "Earthquake Simulation Tests of a Steel Frame Allowed to Uplift", Dynamic Response of Structure: Instrumentation, Testing Methods and System Identification, ASCE/EMD Specialty Conference, March 30 and 31, 1976, University of California, Los Angeles, pp. 318-329.

4. R.W. Clough and David T. Tang, "Earthquake Simulatory Study of a Steel Frame Structure", Report No. EERC 75-6, E.E.R.C., University of California, Berkeley, 1975.

5. D. Rea and J. Penzien, "Dynamic Response of a 20 ft. x 20 ft. Shaking Table", Proceedings of 5th World Conference on Earthquake Engineering, Rome, 1973.

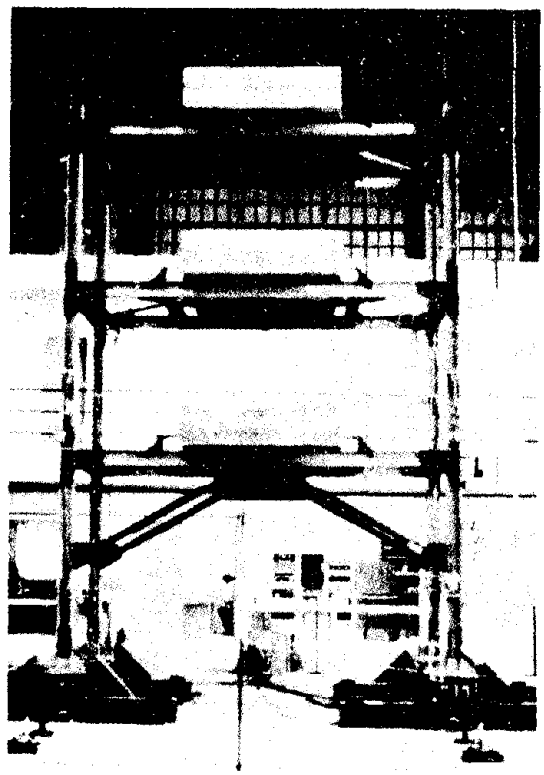

FIG. 1. TEST FRAME.

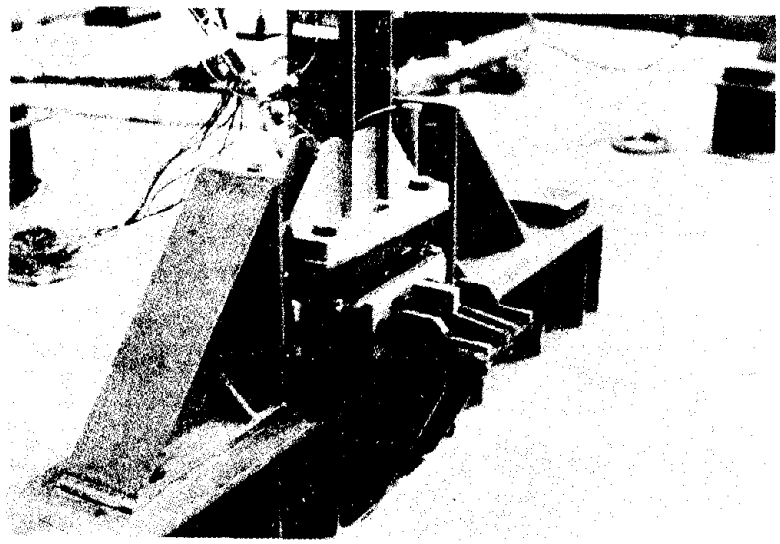

FIG. 2. COLUMN FOOT DETAIL.

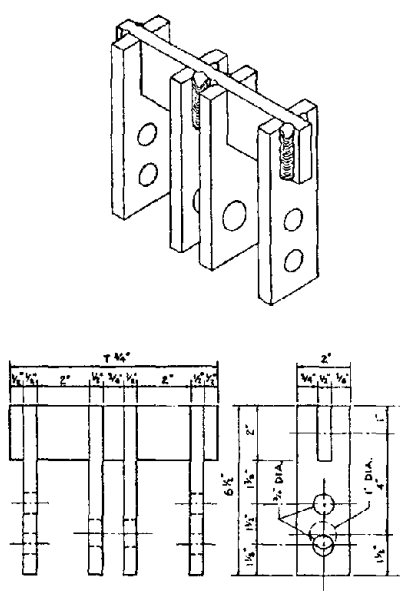

FIG. 3. TORSION DEVICE.

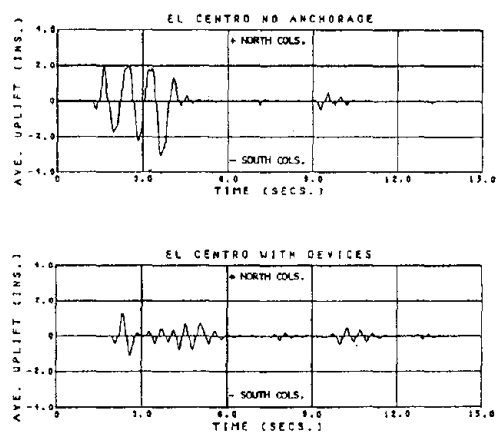

FIG. 4. VERT. UPLIFT DISPL. COMPARISON.

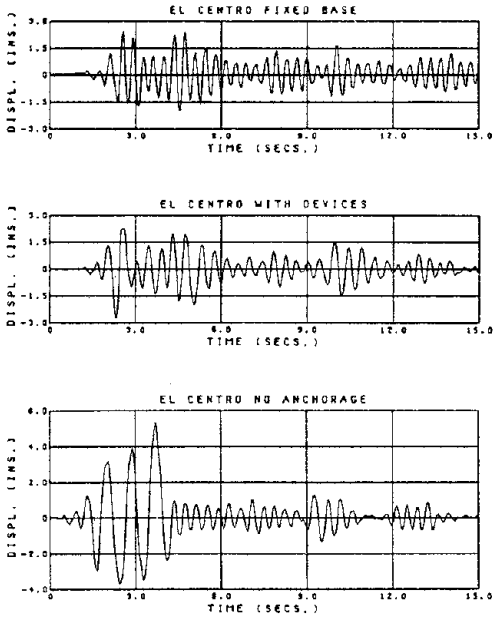

FIG. 5. REL. 3RD. FLR. HORT. DISPL. COMPARISONS.

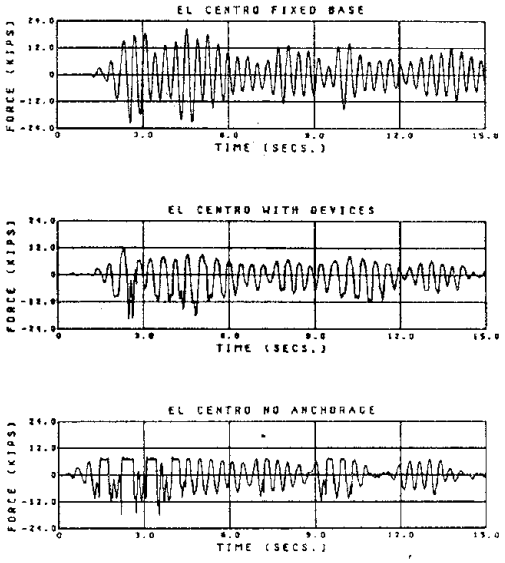

FIG. 6. 1ST. FLR. NORTH COL. AXIAL FORCE COMPARISONS.

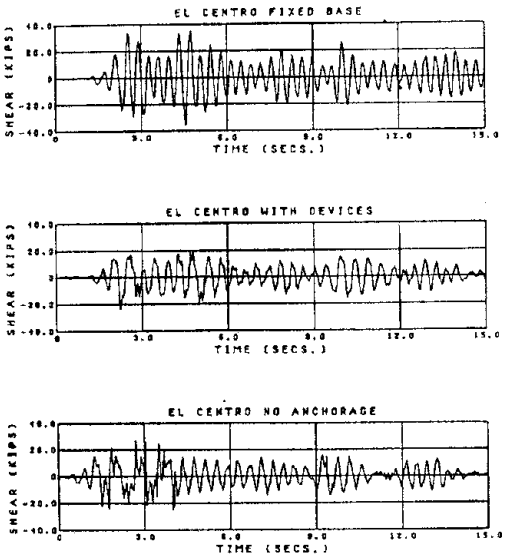

FIG. 7. BASE SHEAR COMPARISONS.

SUMMARY OF EL CENTRO PEAK RESPONSES

	FIXED BASE	WITH DEVICES	WITHOUT ANCHORAGES
AVE. UPLIFT			
NORTH COLS.	0"	1.26"	1.99"
SOUTH COLS.	0"	1.10"	3.03"
REL. 3RD. FLR. DISPL.	+2.43" -2.82"	+2.29" -2.74"	+5.34" -3.72"
1ST. FLR. COL. AXIAL FORCE			
NORTH COL.	+20.75 K -22.14 K	+11.64 K -19.93 K	+7.85 K -18.44 K
SOUTH COL.	+22.10 K -18.93 K	+14.42 K -13.33 K	+8.99 K -20.50 K
BASE SHEAR	+35.21 K -35.53 K	+19.57 K -24.11 K	+26.90 K -25.25 K
BASE OVERTURNING MOMENT	+471.3 K-FT -434.3 K-FT	+278.7 K-FT -297.7 K-FT	+323.2 K-FT -296.1 K-FT

TABLE 1

EVALUATION OF METHODS FOR EARTHQUAKE ANALYSIS OF STRUCTURE-SOIL INTERACTION

by

Jorge A. Gutierrez[I] and Anil K. Chopra[II]

SYNOPSIS

Three methods for analysis of earthquake response of structures including structure-soil interaction are evaluated for their effectiveness and applicability in handling various types of structures and soil conditions encountered in practice. Two of these--a simple substructure method and a direct finite element method--have been employed in analysis of practical problems for sometime, whereas the third, a general substructure method, has been developed only recently.

SIMPLE SUBSTRUCTURE METHOD

In the early research[1], the structure was idealized as a one-dimensional system, the base of the structure as a rigid plate supported on the surface of the soil region idealized as a halfspace. The available results for harmonic vibration of a rigid plate on an elastic halfspace were used. The complex valued stiffness (or impedance) coefficients, which depend on the excitation frequency, relate the harmonic forces applied to the rigid plate and the resulting displacements. By imposing requirements of equilibrium between the interaction forces and of compatibility between displacements at the base plate in the two substructures--the structure and the soil system--these impedance coefficients were incorporated in the governing equations for the structure written in the Fourier-transformed frequency domain. These equations are solved for a range of excitation frequencies and then using Fourier transform methods the response to arbitrary ground motion may be determined.

This analysis procedure is referred to as a substructure method because the system is analyzed in two steps: First the dynamic of a rigid plate on the soil region is analyzed separately from the structure; the resulting foundation impedance coefficients appear in the structural equations, which are then solved to determine the structural response.

The first stage of such analyses, the general problem of dynamic response of rigid footings, has been the subject of considerable research: various footing geometries--circular, rectangular and strip--were considered; the soil was treated as a viscoelastic material thus removing the restriction of linear elasticity; various soil regions--e.g., halfspace, layer, layered halfspace, were considered; embedded footings were analyzed.

This method is especially convenient if the base of the structure, the constitutive properties of the soil, and the geometry of the soil region can be idealized to conform to one of the above-mentioned cases for which foundation impedance coefficients are available. Then, only the second stage of the analysis need be performed.

The computation in the second stage of the analysis can be drastically reduced as follows. The displacements are decomposed into two parts as shown in Fig. 1. The part r_j^s may be interpreted as the quasistatic displacement in the jth degree of freedom due to base translation r_{1b} and

---

I Associate Professor, Universidad de Costa Rica, San Jose, Costa Rica, formerly Graduate Student, University of California, Berkeley.

II Professor of Civil Engineering, University of California, Berkeley.

rotation r_{2b}. The part r_j^d which then represents the dynamic displacements relative to the quasistatic displacements is expressed as the superposition of the natural modes of vibration of the structure on fixed base. Because excellent results can be obtained by including only the first few modes, the number of algebraic equations that need to be solved for each excitation frequency are considerably reduced, thus drastically reducing the computational effort, because the solution of equations has to be repeated for several hundred values of the excitation frequency[2].

The simple substructure method of analysis outlined above has a number of important limitations: The assumption of a rigid base plate is not appropriate in many situations; e.g., buildings with stiff central core combined with flexible frames[3], buildings supported on a number of individual footings, concrete gravity dams, and earth dams. Only approximate solutions are available for foundation impedance coefficients for embedded foundations. Solutions have not been completely developed for foundation impedances required in analysis of two or more adjacent structures involving structure-soil-structure interaction. Arbitrary non-homogeneities in the halfspace cannot be tackled.

In the simple substructure method, the specified free-field earthquake motion at the base of the structure is directly treated as the excitation.

DIRECT FINITE ELEMENT METHOD

The direct method for analysis of structure-soil systems is the result of an obvious application of the finite element method[4,5]. The system to be analyzed is defined simply as the structure combined with a portion of the soil. While this method has the obvious advantage in that it can routinely handle non-homogeneous soil properties and embedded structures, it has a number of serious limitations, the more important of which are discussed in what follows.

A boundary is introduced to define the portion of the soil to be included in the system to be analyzed, whether a natural dividing line such as a soil-rock interface exists at the site or not. To overcome this definiency, transmitting boundaries to limit the lateral extent of the soil portion have been developed[6], but the horizontal boundary to define the vertical extent must be assumed as rigid. To evaluate the errors that may be caused by the introduction of such a rigid boundary, the recently developed general substructure method[7] was employed to determine the dynamic response of an example structure supported on a viscoelastic soil with specified properties; two idealizations for the geometry of the soil region: a layer of depth equal to the base width of the structure, as recommended for analysis by the direct method[5], and a halfplane. Numerical results (not presented here but will be reported elsewhere) demonstrated that if essentially similar soils extend to large depths at the site under consideration, the direct finite element analysis would be in error to an unacceptably large degree.

Because essentially all of the information on ground motion during earthquakes is based on records from accelerographs located on the ground surface or at shallow depths--in basements of buildings, the design earthquake is specified at the ground surface. However, in the direct finite element method the earthquake input is defined at the base of the finite element mesh at considerable depth. This input is determined by deconvolution of the surface level motions, assuming that they were produced exclusively by vertically propagating shear waves. This assumption

excludes surface waves as well as non-vertically incident body waves. The latter can cause significant torsional response even when the structure is symmetric, whereas a vertically incident body wave would not cause any torsional response in such a structure[8].

Enormous computational effort is required in direct analysis of structure soil systems because finite element idealizations that are typically used for such analyses have several hundred to a few thousand degrees of freedom. Furthermore, modal analysis cannot be used with advantage to reduce the number of unknowns because the natural modes of vibration of the complete structure-soil system are generally inefficient in representing the deformations of the structure.

In its commonly used form[5], the direct method is limited to two-dimensional finite element systems, leading to significant errors in analysis of even an isolated structure and requiring unrealistic simplifications in modelling of a complex of structures encountered in analysis of nuclear power plants[10].

GENERAL SUBSTRUCTURE METHOD

To overcome the limitations of the direct finite element method, a substructure method which is a generalization of the simpler version discussed first has been developed[7]. This method can analyze structure-soil systems with the structure idealized as a finite element system and the soil region as either a continuum, for example as a viscoelastic halfspace, or as a finite element system. The free-field earthquake motion, including spatial variations if any, at the structure-soil surface is treated directly as the excitation, thus eliminating the deconvolution calculations and the related assumptions required in the direct method.

The concept of the foundation impedance coefficients is generalized as shown in Fig. 2 to avoid the restrictions of a rigid base plate in the simple substructure method. Methods have been developed to determine the foundation impedance matrix considering a deformable structure-soil interface for soil regions idealized as a finite element system[7] or as a viscoelastic half plane[11].

Theoretically, for structure-soil systems idealized as an assemblage of finite elements, the general substructure method will lead to results identical to those from the direct method, provided the free-field motion prescribed at the structure-soil interface in the substructure method is consistent with--i.e., represents the free field response of the soil region to--the motion prescribed at the base of the finite element mesh in the direct method[7]. Computationally, however, the substructure method is more efficient[7].

The substructure method is computationally efficient because it works with two smaller systems--the structure and the soil region--and more important, it takes advantage of an extension of the modal analysis concepts discussed earlier in context of the simple substructure method. By separating the structural displacements into two parts, the quasistatic displacements associated with the interaction displacements at the structure-soil interface and the remaining dynamic displacements, and expressing the latter as superposition of the first few modes of vibration of the structure on fixed base, a drastic reduction in the computational effort is achieved. Accurate solutions are obtained by including only those modes with natural frequencies within--or slightly beyond--the frequency range of interest.

For example, accurate solutions over the frequency range 0-10 cps were obtained for a structure with 96 degrees of freedom by considering only the first four vibration modes on fixed base[7].

The substructure method is applicable to complex structural idealizations, with the soil region idealized as a viscoelastic halfspace or as a finite element system, whichever is appropriate for the particular site. For finite element idealization of the soil region, the substructure method provides, for the reasons discussed above, a better alternative to the direct method. For sites where essentially similar soils extend to large depths and there is no obvious rigid boundary such as a soil-rock interface, numerical results (not presented here to keep this presentation within limits) have demonstrated that the direct method would generally result in unacceptable errors and the general substructure approach provides the only reliable analysis technique.

Combining the attractive features of the two commonly used methods--simple substructure method and direct finite element method--the general substructure method provides an effective approach to earthquake analysis of structure-soil systems, capable of analyzing any system that the commonly used methods can, and more.

ACKNOWLDEGMENT

The financial support provided for this study by the National Science Foundation is gratefully acknowledged.

BIBLIOGRAPHY

1. Parmelee, R. A., "Building-Foundation Interaction Effects," Journal of the Engineering Mechanics Division, ASCE, Vol. 93, No. EM2, April 1967, pp. 131-152.

2. Chopra, A. K., and Gutierrez, J. A., "Earthquake Response Analysis of Multistory Buildings Including Foundation Interaction," International Journal of Earthquake Engineering and Structural Dynamics, Vol. 3, No. 1, 1974, pp. 65-77.

3. Foutch, D. A., et.al., "Full Scale 3-Dimensional Tests of Structural Deformations during Forced Vibration of a 9-story Reinforced Concrete Building," Proceedings of U.S. National Conference on Earthquake Engineering, Ann Arbor, Michigan, June 1975, pp. 206-215.

4. Wilson, E. L., "A Method of Analysis for the Evaluation of Foundation-Structure Interaction," Proceedings 4th World Conference on Earthquake Engineering, Santiago, Chile, 1969.

5. Lysmer, J., Udaka, T., Seed, H. B., and Hwang, R., "LUSH - A Computer Program for Complex Response Analysis of Soil-Structure Systems," Report No. EERC 74-4, Earthquake Engineering Research Center, University of California, Berkeley, California, April 1972.

6. Waas, G., "Linear Two-Dimensional Analysis of Soil Dynamics Problems in Semi-infinite Layered Media," Dissertation, Submitted in partial satisfaction of the requirements for the degree of Doctor of Philosophy in Engineering, University of California, Berkeley, California, September 1972.

7. Gutierrez, J. A., "A Substructure Method for Earthquake Analysis of Structure-Soil Interaction," Report No. EERC 76-9, Earthquake Engineering Research Center, University of California, Berkeley, April 1976.

8. Luco, J. E., "Torsional Response of Structures to Obliquely Incident Seismic SH Waves," International Journal of Earthquake Engineering and Structural Dynamics, Vol. 4, No. 3, January-March 1976, pp. 207-219.

9. Luco, J. E., and Hadjian, A. H., "Two-Dimensional Approximations to the Three-Dimensional Soil-Structure Interaction Problem," Nuclear Engineering and Design, 31, 1974, pp. 195-203.

10. Hadjian, A. H., "Soil-Structure Interaction - An Engineering Evaluation," to appear in Nuclear Engineering and Design.

11. Chopra, A. K., et.al., "Dynamic Stiffness Matrices for Viscoelastic Halfplane Foundations," Journal Engineering Mechanics Division, ASCE, Vol. 102, No. EM3, June 1976.

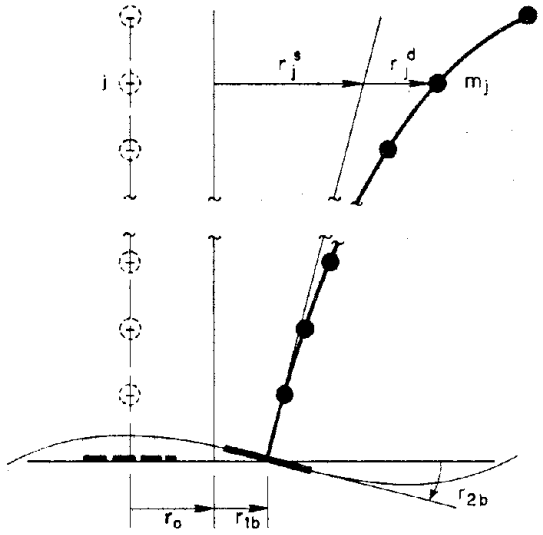

FIG. 1 SEPARATION OF DISPLACEMENTS INTO QUASI-STATIC AND DYNAMIC DISPLACEMENTS

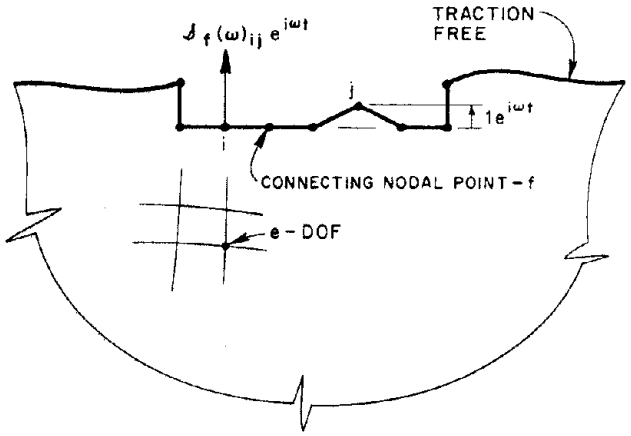

FIG. 2 PHYSICAL INTERPRETATION OF THE FREQUENCY DEPENDENT FOUNDATION STIFFNESS MATRIX $\underline{\mathcal{S}}_f(\omega)$

PROBLEMS IN PRESCRIBING RELIABLE DESIGN EARTHQUAKES

by

Vitelmo V. Bertero,[I] Stephen A. Mahin,[II] and Ricardo A. Herrera[III]

SYNOPSIS

Earthquake ground motion characteristics controlling the elastic and inelastic response of structures are shown to be fundamentally different. Limitations of present methods for specifying design earthquakes for buildings located near potential sources of a major earthquake are examined. In particular, the reliability of inelastic design response spectra derived directly from linear-elastic design response spectra is evaluated on the basis of the nonlinear dynamic response of single and multiple degree-of-freedom systems to near-fault accelerograms obtained during the San Fernando earthquake. Guidelines for prescribing inelastic design response spectra for near-fault sites and recommendations for further research are offered.

INTRODUCTION

To achieve an efficient aseismic design it is necessary to predict structural behavior for various critical combinations of loads and seismic excitations for each of a structure's limits of usefulness (limit states). While evaluation of all possible limit states in accordance with the philosophy of comprehensive design[1] is impracticable at present, satisfaction of the requirements for service and ultimate limit states is generally desirable and appears feasible. To prevent functional failure during relatively frequent seismic events (service limit states), structures should generally be designed to behave elastically. For unusually severe ground shakings, inelastic behavior up to the point of incipient dynamic collapse (ultimate limit states) may be tolerated. While analytical methods for predicting the mechanical behavior of structures are rapidly improving, considerable uncertainty remains regarding the characterization of design earthquakes. Resolution of this problem is complex because the critical ground motion varies according to the limit state considered.

The results of several studies[1,2] conducted to identify special problems encountered in prescribing design earthquakes for buildings located close to potential sources of major earthquakes are summarized in this paper. Methods currently used to specify design earthquakes, as well as some recent information regarding the characteristics of ground motions at near-fault sites, are reviewed and evaluated. The aseismic design implications of this evaluation are examined.

PRESENT METHODS OF PRESCRIBING DESIGN EARTHQUAKES

The ground motion experienced at a site is a complex function of the type and characteristics of the source mechanism, the nature of the intervening geological structure, and the topographical and soil conditions near the site. A usual design simplification is to consider only nonconcurrent action of horizontal ground translational components. It should be recognized that, for sites near the earthquake source, it may be necessary to base structural response evaluations on the simultaneous action of all six ground components[3] and to consider realistically the nonlinear soil-structure interaction.

I Professor of Civil Engineering, University of California, Berkeley.
II Assistant Research Engineer, University of California, Berkeley.
III Engineer, Capacete-Martin and Associates, San Juan, Puerto Rico; formerly Junior Specialist, University of California, Berkeley.

SERVICE LIMIT STATE DESIGN EARTHQUAKES. - Design earthquakes have been specified in terms of a building code zone, a site intensity factor, or more increasingly, an effective site acceleration.[4] However, for structures located at moderate distances from the source, it is generally agreed that one of the best ways to specify the service limit state design earthquake is by an average or smooth linear-elastic design response spectrum (LEDRS). Such a spectrum can be constructed by statistical analysis of elastic spectra obtained for appropriate real or simulated accelerograms, or by scaling the peak ground acceleration, velocity and displacement by spectral amplification factors statistically derived for various amounts of damping.[5] When only estimates of peak ground acceleration are available, it has been suggested that reasonable values for the peak ground velocity and displacement can be obtained by multiplying the ground acceleration (expressed as a fraction of gravity) by 122 cm/sec and 91 cm, respectively.[5]

ULTIMATE LIMIT STATE DESIGN EARTHQUAKES. - Design forces significantly lower than those derived from LEDRS for major earthquakes may be used in some cases by taking advantage of a structure's inelastic energy dissipation capacity. Preliminary ultimate limit state loads can be obtained using inelastic design response spectra (IDRS) derived by statistically evaluating the dynamic response of realistic nonlinear structural models to various appropriate ground motions.[6] Because of the complexities involved in such nonlinear dynamic analyses, a simpler method which derives IDRS by directly modifying LEDRS is more commonly used.[5] In this method, the LEDRS is modified using factors for a specified displacement ductility ratio. These factors were derived on the basis of analyses of elasto-perfectly plastic responses of single degree-of-freedom (SDOF) systems to several strong motion records obtained at moderate epicentral distances.[5] Caution should be exercised when applying this simplified method to sites subjected to significantly different types of ground motions, to multiple degree-of-freedom systems, or to systems with hysteretic behavior different from the assumed elasto-plastic idealization.[1,4,5]

CHARACTERISTICS OF NEAR-FAULT GROUND MOTIONS

Very little empirical data are available on ground motion characteristics, especially peak ground acceleration and velocity, for epicentral distances less than 15 km. Theoretical estimates of the upper limit for peak particle velocities range from 100-150 cm/sec.[5,7,8] Analytical studies based on simple two- and three-dimensional fault dislocation models (9,10) have indicated that the near-fault ground motions of the San Fernando earthquake were characterized by large ground velocity pulses. The Pacoima Dam (PD) record (which was the only accelerogram recorded in the area of heaviest shaking), and derived records for the base of the PD (i.e. the DPD record) and for the motion needed to produce the lower Van Norman Dan (VND) seismoscope trace, are shown in Fig. 1. These records contain severe, long duration acceleration pulses which resulted in unusually large incremental ground velocities (Fig. 1) and spectral velocities for periods greater than 0.8 sec. (Fig. 2). Such severe, long duration acceleration pulses can be directly related to the faulting process[9] and they have been detected in other near-fault accelerograms.[4]

RELIABILITY OF IDRS BASED ON LEDRS

The basic approach of deriving IDRS directly from LEDRS can seriously be questioned since the types of excitations that induce the maximum response in linear and inelastic systems are fundamentally different. In the case of a linear-elastic system, the critical dynamic excitation is of a periodic type having a frequency equal to that of the system; this induces an

engineering resonance phenomenon. Since the largest dynamic amplification factor for an impulsive excitation is only 2, severe, relatively long duration acceleration pulses are not usually critical for elastic systems. On the other hand, the larger the intensity of the effective acceleration of a pulse with respect to the structure's yield strength, and the shorter the time to reach the peak acceleration and the longer the duration of the pulse relative to the fundamental period of the structure, the larger the inelastic deformations that will develop. Relatively short, periodic acceleration pulses are usually not critical for inelastic systems because, one yielding occurs, engineering resonance is depressed by the large energy dissipated by even small inelastic deformations.

Several nonlinear dynamic analyses of single and multiple degree-of-freedom systems were performed to assess the reliability of present methods of constructing IDRS from LEDRS for near-fault sites in view of possible severe, long duration acceleration pulses. For example, the actual ductility requirements for elasto-perfectly plastic SDOF systems with 5% viscous damping designed according to the IDRS in Ref. 5 for a desired ductility of four are shown in Fig. 3a for the El Centro and DPD records. While the maximum displacement ductilities required for the El Centro record are generally smaller than those predicted by the IDRS, ductilities required by the DPD record exceeded the specified value by factors as great as 2.2 for periods longer than 0.4 sec. IDRS based on ductility factors larger than 4 are even less reliable for near-fault motions.

Nonlinear analyses[1] of a ten-story, three-bay frame[2] designed using an IDRS for a ductility, μ, of four and with spectral velocities in the constant velocity range 31% higher than conventional values[5] also indicate that IDRS derived directly from LEDRS may not adequately define ultimate limit state design earthquakes. The frame's nonlinear response to records obtained at moderate epicentral distances was adequate[2], while not so for the DPD and VND records.[1] The response of the frame to near-fault records was characterized by a few large inelastic displacement excursions rather than by numerous intense oscillations, Fig. 4. The results in Fig. 4 also indicate that inelastic response cannot be reliably predicted by elastic analyses.

Derivation of IDRS directly from LEDRS implicitly assumes that increasing damping is as benefitial to the response of inelastic systems as it is to that of elastic systems. This is not the case, however. It has been found that the spectral amplification factors used to construct LEDRS[5] may significantly overestimate the effect of damping on inelastic response,[1] resulting in lower design forces than actually required to achieve a given μ. The typical effect of this is illustrated by Fig. 3b which shows that ductility requirements for elasto-perfectly plastic SDOF systems designed using suggested IDRS[5] for a μ of four increase with increasing values of the viscous damping ratio, ξ.

IMPLICATIONS FOR ASEISMIC DESIGN

LEDRS offer relatively simple and reliable methods for specifying design earthquakes for service limit states. At near-fault sites, however, ground spectrum shapes based on strong motion records obtained at moderate source distances may significantly underestimate the peak ground velocity and displacements. Realistic spectral shapes based on analyses of available near-fault records, or from theoretical predictions accounting for the faulting process and the nonlinear mechanical characteristics of a building's foundation media, should be used. To better define design earthquakes,

strong motion instrumentation capable of recording all six ground motion components is needed at sites close to potential sources of major earthquakes.

DESIGN EARTHQUAKES FOR ULTIMATE LIMIT STATES. - Near-fault records can contain severe, relatively long duration acceleration pulses. Such pulses substantially increase the spectral velocity and, more importantly, the required seismic resistance coefficient, C_y, of buildings, particularly those with relatively long periods. To illustrate this, the values of C_y needed to limit ductility to four for the El Centro, DPD and VND records (normalized to 0.5g peak acceleration) are compared in Fig. 5 to current IDRS[5] and code values.[1] Unless the values of damping and ductility usually assumed in design can be substantially increased, structures located at near-fault sites must be designed for much higher forces than currently specified in codes. The IDRS requires sufficiently high C_y values in the short period range, while underestimating them for the near-fault records at periods greater than 0.5 sec.

Although structures can be detailed to accommodate the large ductilities that might result at near-fault sites if they were designed using current code or IDRS forces, this may not be desirable except for short period structures. The danger of underestimating design forces at near-fault sites is illustrated by the performance of the Olive View Hospital Main Building during the 1971 San Fernando earthquake.[1] Although this six-story reinforced concrete building, located near the fault rupture, had C_y values in excess of 0.3 (which would correspond to a ductility requirement of about 4 for 5% damping and peak ground acceleration of 0.5g), it suffered permanent drifts exceeding 75 cm and had to be demolished.

Since ultimate limit state design criteria are not only controlled by the energy dissipation capacity of the structural system but also by the deformations that can be tolerated due to economic, safety or stability considerations, selection of displacement ductility based on energy dissipation alone may not be a sufficient basis for establishing design earthquakes. In particular, the selection of a design ductility factor without regard to structural period or earthquake type (magnitude, source distance, duration, etc.) is inadequate. Furthermore, current IDRS do not give any indication of the total amount of inelastic action, or numbers and magnitudes of inelastic reversals which are essential for detailing critical regions. Comprehensive studies to determine more rational methods for establishing acceptable ductilities, particularly for flexible structures, are needed. Investigations are also needed regarding the economic impact of designing structures for either seismic resistance coefficients or design ductility ratios higher than those presently assumed.

Extensive research is also needed to fully characterize near-fault ground motions (particularly, duration of shaking and the number, sequence and features of intense, relatively long duration acceleration pulses). Misleading results can be obtained for near-fault sites if accelerograms characteristic of earthquakes with different magnitudes, source distances and soil conditions are used. For example, accelerograms obtained on soft soil at sites distant from the source often contain very long, but rather moderate acceleration pulses. Normalization of these records to larger peak accelerations, may be unrealistically severe for inelastic systems.

CONCLUDING REMARKS

Prediction of inelastic response on the basis of linear-elastic analysis, and correspondingly, direct derivation of IDRS from LEDRS, have

been shown to be unreliable since the ground motion characteristics that control elastic and inelastic dynamic response are fundamentally different, and the effect of viscous damping is different. The reliability of simple relationships for constructing IDRS from LEDRS is expected to remain small even if more refined ground spectrum shapes for near-fault events and spectral amplification factors for yielding systems are developed. Thus, it may be preferable to obtain IDRS from a statistical analysis of the nonlinear dynamic response of SDOF systems with realistic hysteretic models to numerous types of ground motions. Nondimensional nonlinear response spectra, Fig. 6, can be developed for a particular record in terms of period, damping ratio, ductility and the parameter, η, defined as the ratio of the seismic resistance coefficient to the peak ground acceleration expressed as a fraction of gravity.(1) For given values of period, damping and peak ground acceleration, the seismic resistance coefficient required to limit the ductility to a desired value can be determined. Statistical analysis of such nonlinear spectra could lead to a better definition of the design earthquake which could explicity account for the variability of response.

It should be reiterated that design methods based on SDOF systems are only approximate guidelines for multiple degree-of-freedom (MDOF) systems. The seismic response of such systems designed using these methods should be thoroughly investigated to determine ways that IDRS obtained for SDOF systems should be modified for MDOF systems or to formulate new procedures for establishing design earthquakes for the inelastic design of MDOF systems.

ACKNOWLEDGMENTS

The financial support of the National Science Foundation is gratefully acknowledged.

REFERENCES

1. Bertero, V. V., Herrera, R. A. and Mahin, S. A., "Establishment of Design Earthquakes--Evaluation of Present Methods," Proc. of Int'l. Symp. on Eq. Str. Engng., St. Louis, August 19-21, 1976.
2. Bertero, V. V. and Kamil, H., "Nonlinear Seismic Design of Multistory Frames," Canadian Jnl. of Civ. Engng., Vol. 2, Ottawa, December 1975.
3. Rosenblueth, E., "The Six Components of Earthquakes," Jnl. of Struc. Div., ASCE, Vol. 102, No. ST2, 1976.
4. Newmark, N. M. and Rosenblueth, E., Fundamentals of Earthquake Engineering, Prentice-Hall, Inc., Englewood Cliffs, N.J., 1971.
5. Newmark, N. M. and Hall, W. J., "Procedures and Criteria for Earthquake Resistant Design," Bldg. Sci. Series 46, NBS, February 1973.
6. Murakami, M. and Penzien, J., "Nonlinear Response Spectra for Probabilistic Seismic Design of Reinforced Concrete Structures," Proc. of the U.S.-Japan Coop. Res. Prog. in Earthq. Engng., Tokyo, 1976.
7. Ambraseys, N. N., "Maximum Intensity of Ground Movements Caused by Faulting," Proc. of the 4th Wld. Conf. on Earthq. Engng., Vol. 1, Santiago, Chile, 1969.
8. Brune, J. N., "Tectonic Stress and the Spectra of Seismic Shear Waves from Earthquakes," Jnl. of Geophys. Res., Vol. 75, 1970.
9. Boore, D. M. and Zoback, M. D., "Two-dimensional Kinematic Fault Modeling of the Pacoima Dam Strong-motion Recording of the February 9, 1971, San Fernando Earthquake," BSSA, Vol. 64, No. 3, June 1974.
10. Trifunac, M. D., "A Three-dimensional Dislocation Model for the San Fernando, California, Earthquake of February 9, 1971," BSSA, Vol. 64, No. 1, February 1974.

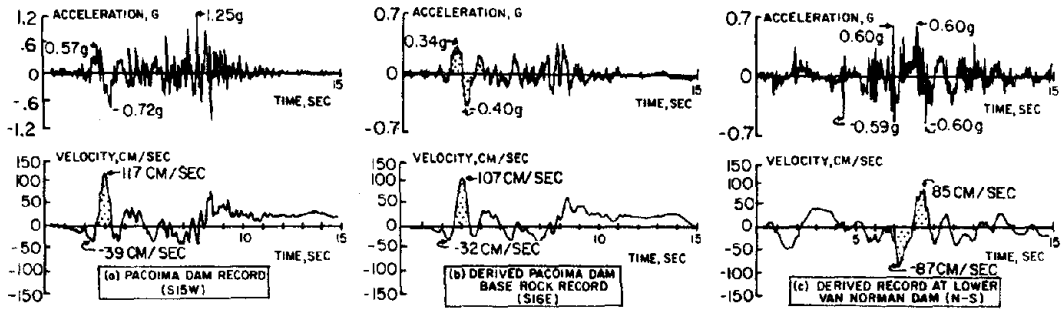

FIG. 1 NEAR-FAULT GROUND MOTION RECORDS OF THE SAN FERNANDO EARTHQUAKE

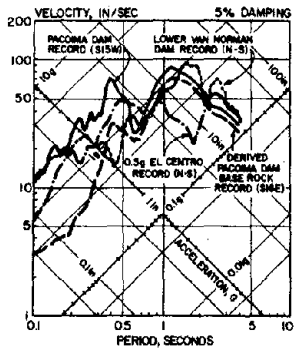

FIG. 2 RESPONSE SPECTRA

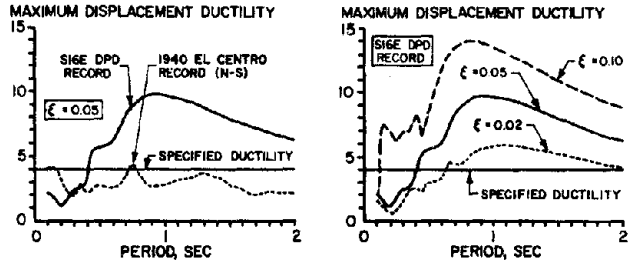

a. FOR DIFFERENT RECORDS

b. FOR DIFFERENT DAMPING RATIOS

FIG. 3 COMPARISON OF SPECIFIED AND REQUIRED DUCTILITIES

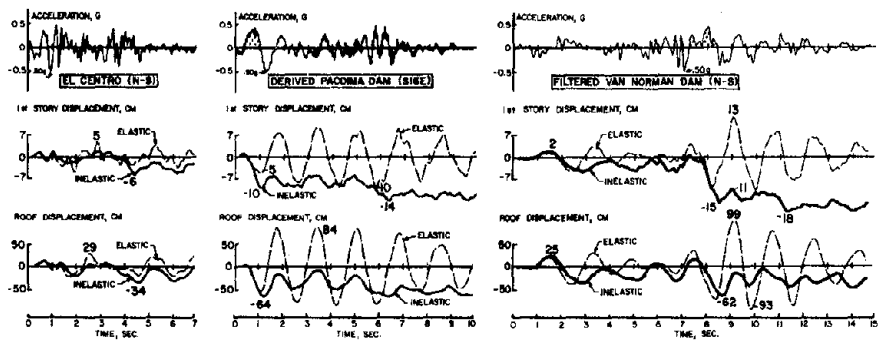

FIG. 4 RESPONSE OF 10-STORY FRAME TO DIFFERENT ACCELEROGRAMS

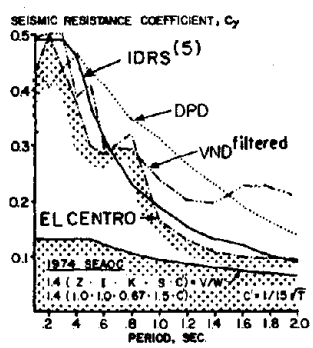

FIG. 5 C_y FOR μ=4 AND ξ=5%

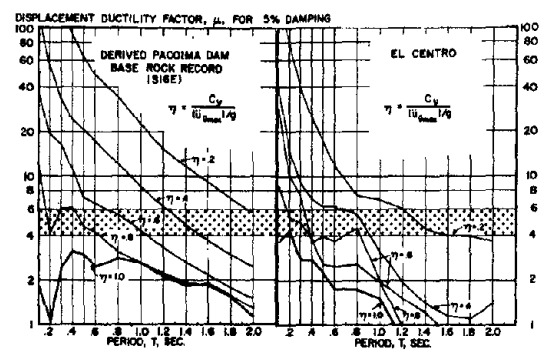

FIG. 6 SAMPLE NONLINEAR RESPONSE SPECTRA

SEISMIC DESIGN IMPLICATIONS OF HYSTERETIC BEHAVIOR OF REINFORCED CONCRETE STRUCTURAL WALLS

by

V. V. Bertero,[I] E. P. Popov,[I] T. Y. Wang,[II] and J. Vallenas[II]

SYNOPSIS

After reviewing current code aseismic design provisions for R/C structural wall systems and present knowledge of their hysteretic behavior, research being conducted on this subject at Berkeley is summarized. The facility selected for testing frame-wall subassemblages, details of the 1/3-scale wall subassemblage models tested, the fabrication procedure, mechanical characteristics of the materials, and the selection of the test loadings for these models are discussed. The main results obtained are evaluated and their implications for aseismic design of frame-wall structural systems are discussed.

INTRODUCTION

In buildings with frame-wall structural systems, the interaction between wall and frame, particularly during their hysteretic behavior under severe earthquake-like conditions, is not very well understood at present. While the UBC and SEAOC recommend increasing the value of earthquake forces in calculating shear stresses in shear walls of buildings without a 100% moment-resisting frame, the ACI does not. Although it is convenient to have a greater safety factor against nonductile shear failures, it is not believed that merely increasing the value of the design seismic loads is the best way of achieving this. To achieve ductile hysteretic behavior, a wall should be designed against the maximum shear that can be developed according to the actual flexural capacity (as affected by the axial force) of its critical region and considering the critical moment-shear ratio that can exist at such a region. Even if the maximum shear can be estimated with sufficient engineering accuracy, there still remains the problem of designing against it. Up until 1970, most of the available experimental results on the behavior of wall elements were obtained from tests of one- or two-story R/C walls, or infilled R/C frames which were subjected to simplified loading conditions which did not simulate the actual effects of earthquake excitations. Only in some recent investigations[1,2,3] have attempts been made to simulate the loading conditions expected in slender flexural walls subjected to earthquake excitations. Need for improvements in predicting the mechanical behavior of wall systems has led to the initiation of the investigation partially described herein.

Objectives and Scope. - The ultimate objective of this investigation is to develop practical methods for the aseismic design of combined frame-wall structural systems. To achieve this objective, integrated analytical and experimental studies are being conducted.[4] In this paper emphasis is placed on the discussion of experimental studies. The main objective of these studies is to obtain reliable data regarding the linear and nonlinear (particularly hysteretic) behavior of such wall systems. Only those analytical results needed for planning the design of the testing facility and specimen loading programs, and for judging the possible aseismic design implications of the behavior observed in the experiments will be briefly discussed.

[I]Professor of Civil Engineering, University of California, Berkeley, Calif.
[II]Research Assistant, University of California, Berkeley, Calif.

SELECTION OF TYPE, DESIGN AND CONSTRUCTION OF TESTING FACILITY

To investigate in detail the mechanical behavior of frame-wall systems, it was decided to develop a loading facility capable of simulating earthquake effects rather than to use the existing shaking table. For economic reasons, it was decided to test significant subassemblages of the structural system rather than large-scale models of entire buildings. Predicting the in-plane seismic behavior of frame-wall systems requires information on the variation of the lateral shear-displacement relationship for each story (Fig. 1). To simulate the actual boundary conditions of a particular story, subassemblages of at least two or three stories have to be tested (Fig. 1).[4]

Two buildings, ten (Fig. 1)- and 20-stories, 61 ft x 180 ft each, were designed according to present UBC provisions. From analyses of the response of these buildings to different ground motions, it was possible to estimate the relative intensity of the forces acting on the bottom three-story subassemblages. The results led to the design of a facility capable of testing 1/3-scale models of this type of subassemblage. The principal feature of this facility is its ability to simulate pseudo-statically the dynamic loading conditions which could be induced in subassemblages of buildings during earthquake ground shaking (Fig. 2). Assuming that the wall alone resists most of the lateral inertial forces, it would not only be necessary to apply lateral forces, but also, forces which would simulate the effect of overturning moments and gravity loads existing above the top floor of the subassemblages [Fig. 2(c)]. Therefore, to simulate the actual inelastic behavior of this subassemblage when it forms part of the whole wall, the synchronized shear, overturning, and axial forces must be applied simultaneously.

The walls are tested in a horizontal position (Fig. 3). The testing facility consists of a set of reaction blocks, loading devices, ancillary devices, instrumentation and data acquisition systems.[4] Specimens from 1/2- to 1/4-scale of two- to four-story prototype subassemblages can be tested in this facility.

FABRICATION AND MATERIAL MECHANICAL CHARACTERISTICS OF TEST SPECIMENS

A series of tests have been conducted on four 1/3-scale wall component models of the bottom three stories of the ten-story frame-wall system shown in Fig. 1. The four specimens consisted of a 4-in. thick wall framed by two 10-in. sq. columns and a portion of 3-in. thick floor slabs (Fig. 4). The only difference between the four specimens was in the way that the concrete of the edge members was confined. While spirals were used in specimens 1 and 2 (series 1), Fig. 4(a), square ties were used in specimens 3 and 4 (series 2), Fig. 4(c). To simulate the construction work in the field, the specimens were cast story by story in their vertical position. The two specimens of each series were cast simultaneously to minimize variation in the mechanical characteristics of the concrete. The material mechanical characteristics are summarized in Table 1 which shows that the actual concrete compressive strength and yielding strengths of the reinforcing bars were considerably higher than those specified.

LOADING CONDITIONS AND TESTING PROCEDURE

Loading Conditions. - Rather than simulate the critical load combinations of gravity (dead and live) and seismic loads as specified by the 1973 UBC, it was decided to investigate the behavior of these code designed walls under

the most critical load combination which could be developed in the case of an extreme earthquake ground shaking. Table 2 illustrates the differences in some of the loading conditions that were derived for the wall model of the prototype of Fig. 1 using different methods for evaluating the seismic forces. The considerable discrepancies between the resulting shear span values point out not only the difficulties in selecting the critical combination of inertial forces, but also, the need for carefully interpreting results obtained in experimental investigations in terms of the actual seismic behavior of structures. Specimens were tested under the load combination corresponding to the last case presented in Table 2.

Testing Procedure. - The two axial forces necessary for simulating the effects of gravity forces were applied first and were the same for the four specimens. The effects of seismic forces were introduced following a different loading pattern in each of the specimens tested. The four specimens were first subjected to cycles of full seismic force reversals in the working load range. In walls 1 and 3, the lateral force and change in column axial forces needed to reproduce the corresponding change in overturning moment were supposed to increase monotonically until a reduction in the lateral resistance could be observed. In the test of wall 1, however, a cycle with significant inelastic displacement reversal was introduced long before the drop in lateral resistance (Fig. 5). Walls 2 and 4 were subjected to a history of lateral shear and corresponding overturning moment that induced gradually increasing cycles of full reversal lateral displacement with at least three cycles at each displacement amplitude (Fig. 6).

TEST RESULTS AND THEIR EVALUATION

Overall Response. - Figures 5 and 6 are composite graphs illustrating the overall responses for the four specimens tested. These graphs facilitate evalution of the two main variables of the tests reported herein, i.e. the effect of (1) cycling with reversal deformations versus monotonically increasing loads; and (2) different ways of confining concrete of edge members.

Cycling with Displacement Reversals vs. Monotonic Loading. - The curves obtained under monotonically increased loading for walls 1 and 3 provide approximate envelopes for the hysteretic behavior obtained for walls 2 and 4, respectively (Figs. 5 and 6). Before any significant reduction in strength was observed, wall 3 deformed up to nearly 7 in., giving a displacement ductility, $\mu_\delta = \delta/\delta_y$, of about 10. However, when the load was reversed, the wall buckled under a lateral load of only 80 kips. With wall 1 (which was subjected to only one significant cycle of reversal of inelastic deformation), the maximum μ_δ was 6.1, i.e. a reduction of about 40%; and with walls 2 and 4, the maximum μ_δ was 4.2, i.e. a reduction of nearly 60%. It can therefore be concluded that while repeated reversals of lateral loads did not affect the strength of the wall, they did reduce the ductility by as much as 60%. It should be noted, however, that the maximum cyclic ductility, $\mu_{\delta_{cyc}}$, for walls 2 and 4 ($\doteq$ 7.5) was only 25% less than the μ_δ of wall 3. Analysis of the hysteretic loops for walls 2 and 4 (Fig. 6) indicates that each time the absolute value of peak deformation was increased, there was a degradation in the initial stiffness and energy dissipated during the following cycle. Although there was a loss in strength with repetition of cycles at same tip deflection, this was noticeable only after the first cycle and it stabilized at the third cycle except when the tip deflection reached a value of 2.8 in. (where crushing of the wall panel was observed). At this displacement, no stabilization of the hysteretic loop was obtained.

Different Ways of Confining Column Concrete. - From comparisor of the curves for walls 2 and 4 (Fig. 6) it can be concluded that the hysteretic behavior of these two walls were very similar except for the following differences: (1) for the same tip deflection the resistance of wall 2 was greater than that of wall 4; and (2) there was slightly less stiffness degradation and pinching in the curves of wall 4. These two observed differences are interrelated and consistent because the larger the shear developed in a cycle, the larger the stiffness degradation and pinching during the next cycle. However, these differences are not a consequence of the differences in the concrete confinement of columns. The reason for the smaller resistance of wall 4 is the lower strength at yielding and in the strain-hardening range of the #6 bars used in the columns when compared with those of wall 2 (see Table 1). Thus, it can be concluded that the closely spaced square ties were as effective as the spirals. The only noticeable difference was observed in the pattern of failure of the columns after the wall panel failed: the columns of wall 4 were bent (kinked) into a double curvature along a length smaller than that of wall 2, with more pronounced buckling of its main reinforcement and crushing and spalling of its confined concrete in this region.

Contribution of Different Sources of Deformation: The analysis of data recorded permitted study of the contributions of: (1) flexural deformation; (2) shear deformations at each story; (3) slippage along the construction joints; and (4) fixed-end rotation due to slippage of the reinforcement along its embedment length at the foundation. As illustrated in Fig. 7, for the walls subjected to cyclic loading, the first two sources of deformation were the most significant. Up to first yielding, the shear deformation at each story was similar, the first story deformation being somewhat higher because of the greater amount of cracking. After yielding, most of the shear deformation was concentrated in the first story. Furthermore, at a total tip displacement of 1.4 in., there was already a considerable increase in shear deformation of the first story upon repetition of cycles having the same peak displacement (compare Figs. 6 and 8). At a tip displacement of 2.8 in., the shear deformation was concentrated in the lower part of the first story where the concrete crushed and spalled along a horizontal band (Fig. 9). As a consequence of this type of wall panel failure, the columns began deflecting in a double curvature chape, leading to the failure mechanism shown in Fig. 9.

ASEISMIC DESIGN IMPLICATIONS OF EXPERIMENTAL RESULTS

Despite the limited amount of specimens tested, analysis of the data obtained enables the following observations to be formulated. These observations, however, should be evaluated as tentative and subject to modification as more data become available: (1) It is possible to design structural wall components capable of developing large ductilities even when subjected to full deformational reversals inducing nominal unit shear stresses up to $10\sqrt{f'_c}$. Although the μ_δ under monotonic loading reached a value of 10, this large μ_δ should not be used for design since its development can lead to instability of the wall under loading reversal. (2) Although the μ_δ was reduced significantly due to full reversals, from 10 to about 4, it should be noted that this reduced μ_δ corresponded to a $\mu_{\delta_{cyc}}$ of 7 and that it can be considered large enough to permit the development of energy absorption and energy dissipation capacities exceeding even those that would be demanded in the case of very severe earthquake shaking. Furthermore, at this reduced μ_δ the confined core of the columns remained sound and capable of resisting both the effects of axial forces imposed by gravity loads and by lateral

loads in the working load range. (3) Present code specifications for design forces, load factors, and design and detailing of critical regions can lead to a wall design which considerably underestimates the amount of shear that can actually develop. The design of flexural walls against shear should be based on the maximum shear that can be developed according to the flexural capacity of the critical region, and on the largest possible shear/bending moment ratio (V_B/M_B) according to the expected dynamic response of the entire building to severe ground motions of different dynamic characteristics. After the tests, several nonlinear dynamic analyses assuming an infinitely ductile model of the prototype were carried out according to the experimentally obtained stiffnesses and strengths of the walls. The results obtained reveal that the shear force in the first two stories of the wall exceeded its shear capacity before the base moment reached the moment capacity of the wall, and that the critical ratio, V_B/M_B, was about 1.46 times the larger value obtained in the elastic analyses. Thus, the shear and overturning moment ratio used in the experiments was unconservative.

ACKNOWLEDGEMENTS

These studies have been supported by the National Science Foundation.

REFERENCES

1. Portland Cement Association, Recent Research on Earthquake Resistant Shear Walls and Frames, Aug. 1973.
2. Paulay, T., "Design Aspects of Shear Walls for Seismic Areas," Res. Rept. 74-11, Univ. of Canterbury, Christchurch, N. Z., Oct. 1972.
3. Hirosawa, M. and Goto, T., "Strength and Ductility of R/C Shear Wall Subjected to Shear Moment and Axial Load," Bldg. Res. Inst., Tokyo, Sept. 1973.
4. Wang, T. Y., Bertero, V., and Popov, E., "Hysteretic Behavior of R/C Framed Walls," Rept. No. EERC 75-23, Univ. of Calif., Berk. (in press).

TABLE 1 MECHANICAL CHARACTERISTICS OF MATERIALS

CHARACTERISTICS		AVERAGE STRENGTH AT TIME OF TESTING	
		Walls 1&2	Walls 3&4
Concrete Compressive Strength * (psi)	1st Fl. 2nd Fl. 3rd Fl.	5,340 5,120 4,770	5,100 5,130 4,900
Concrete Splitting Tensile Strength (1st Fl.) (psi)		495	480
Concrete Flexural Tensile Strength (1st Fl.) (psi)		645	632
Wall Steel ** (#2 Bars) (psi)	f_y f_{max}	73,400 105,800	73,400 105,800
Col. Long. Steel ** (#6 Bars) (psi)	f_y f_{max}	72,700 106,900	64,400 92,740
Col. Transverse Steel ** (0.21" ϕ) (psi)	f_y f_{max}	82,000 101,000	63,750 69,500

*The specified design strength of concrete was 4000 psi at 28 days.

**The specified yield strength of steel was 60,000 psi.

TABLE 2 COMPARISON OF LOADING CONDITIONS FOR MODEL DERIVED FROM ANALYZING PROTOTYPE STRUCTURES USING DIFFERENT SEISMIC ANALYSIS METHODS

DESIGN CRITERIA	METHODS OF DETERMINING SEISMIC FORCES		SIMPLIFIED LOADING CONDITIONS FOR WALL SUBASSEMBLAGE MODEL: COMPUTED FORCES	SIMPLIFIED LOADING CONDITIONS FOR WALL SUBASSEMBLAGE MODEL: ULTIMATE FORCES BASED ON ESTIMATED FLEXURE STRENGTH OF 42,000 K-IN.	SHEAR SPAN $\frac{M(IN)}{V(K)}$ ($\frac{h}{d}$)
WALLS ALONE RESIST TOTAL SEISMIC LATERAL FORCES	UBC		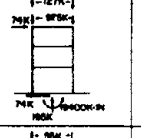	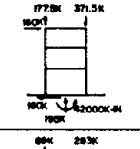	263 (2.8)
FRAMES AND WALLS RESIST TOTAL SEISMIC LATERAL FORCES	UBC		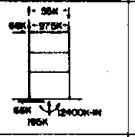	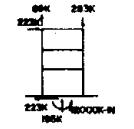	189 (2.0)
	LINEAR ELASTIC RESPONSE SPECTRUM $\ddot{U}_g = 0.33g$ and $\zeta = 5\%$	FIRST THREE MODES	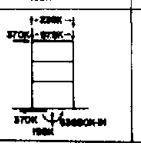	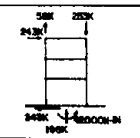	173 (1.9)

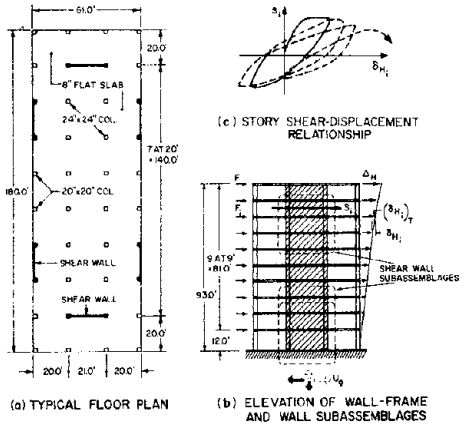

FIG. 1 PROTOTYPE BUILDING, WALL SUBASSEMBLAGES AND STORY SHEAR - DISPLACEMENT RELATIONSHIP

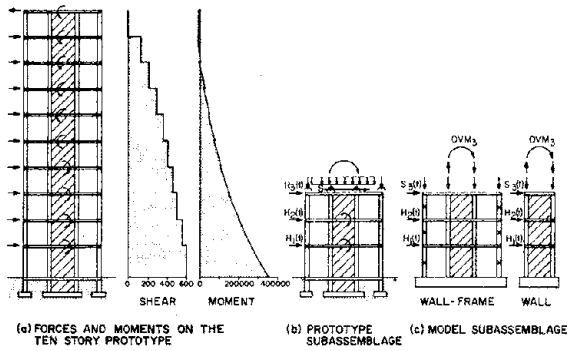

FIG. 2 COMPARISON OF ACTUAL AND SIMULATED LOADING AND SUPPORT CONDITIONS

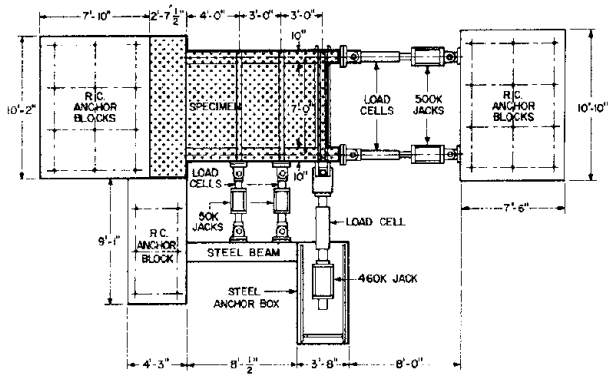

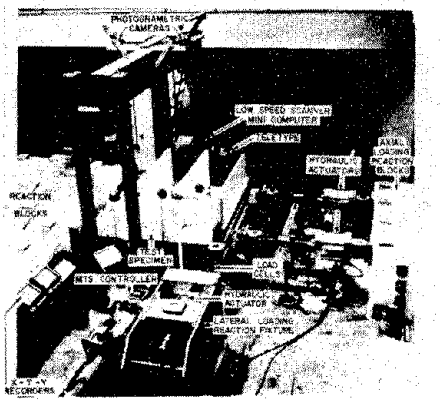

FIG. 3 PLAN AND GENERAL VIEW OF TESTING FACILITY

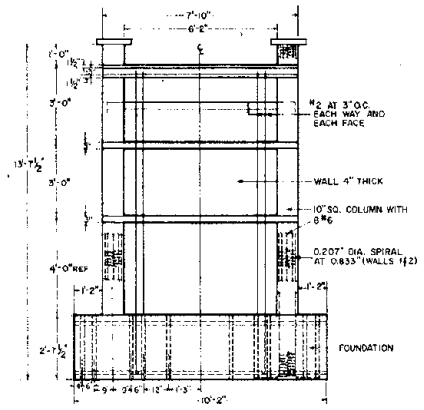

(a) Elevation of Walls 1 & 2

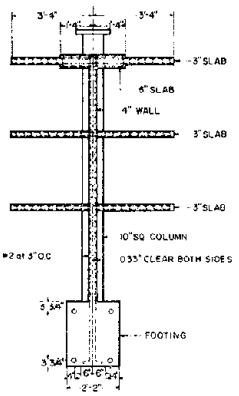

(b) Vertical Cross-section

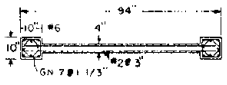

(c) Horizontal Cross-section of Walls 3 & 4

FIG. 4 DIMENSIONS AND DETAILS OF WALL SPECIMENS

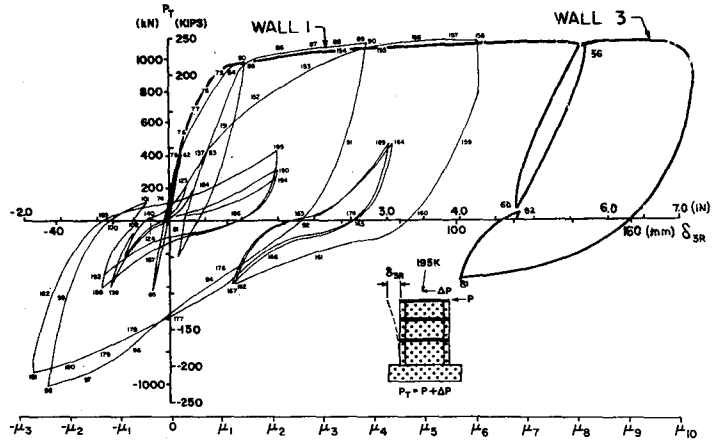

FIG. 5 P_T-δ_{3R} DIAGRAMS - WALLS 1 & 3

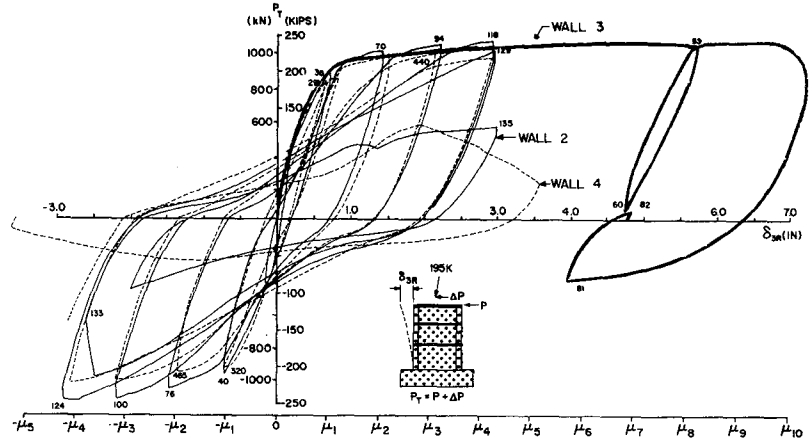

FIG. 6 P_T-δ_{3R} DIAGRAMS - WALLS 2, 3 & 4

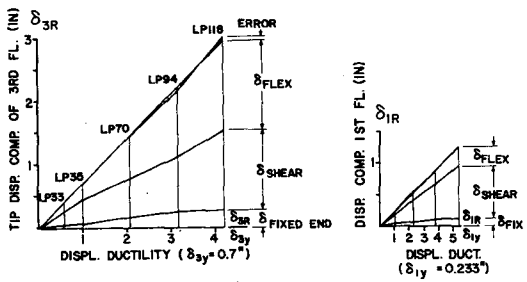

FIG. 7 CONTRIBUTION OF DIFFERENT SOURCES OF DEFORMATION

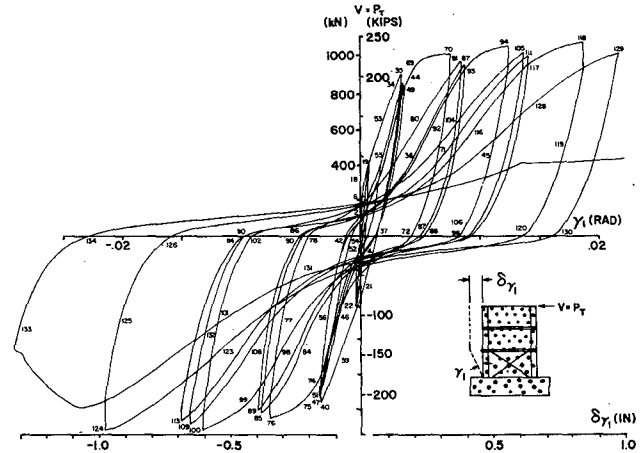

FIG. 8 P_T-γ_1 DIAGRAM - WALL 2

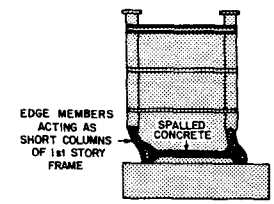

FIG. 9 MECHANISM OF FAILURE OF WALL SPECIMENS

INFILLED FRAMES IN ASEISMIC CONSTRUCTION

by

Richard E. Klingner[I] and Vitelmo V. Bertero[II]

SYNOPSIS

Results obtained in the experimental phase of an investigation of the effects of engineered masonry infill panels on the seismic hysteretic behavior of R/C frames are presented and evaluated. This experimental phase consists of quasi-static cyclic load tests on a series of 1/3-scale model subassemblages of the lower three stories of an 11-story, 3-bay frame with infills in the two outer bays. Emphasis is placed on simulation of the proper force and displacement boundary conditions, and on the reinforcing details required to attain ductile frame action. The engineered infilled frames offered several advantages over comparable bare frames, particularly with respect to their performance under strong ground motions.

INTRODUCTION

Analyses of building damage from strong earthquakes reveal many instances in which the presence of masonry infills has adversely affected the seismic resistance of R/C multistory structures. Some of these effects may be explained in the light of previous research. Experimental investigators[1,2] have concluded that in the elastic range, infill panels act essentially as equivalent diagonal compression struts, stiffening the bounding frame. In the inelastic range, distributed infill cracking produces considerable energy dissipation through friction.[3] Several investigations have shown that the usual failure mode of a bare frame may be significantly affected by the presence of infilling. Early studies by Benjamin and Williams[4] have indicated that after the onset of panel cracking, the ultimate lateral resistance of the infilled frame depends on the resistance of the columns to flexure, compression, and the shear induced by the action of the equivalent compression strut. Fiorato et al.[5] found that after panel cracking, a five-story, single-bay infilled frame model behaved as a knee-braced frame. Kahn[6] has recently observed that the action of the infill on the bounding frame increased the tendency for the frame members to fail in shear.

OBJECTIVES AND SCOPE. - After a comprehensive review of the literature,[7] integrated experimental and analytical studies were planned to investigate the hysteretic behavior of specially designed infilled frames under actions similar to those expected under severe earthquake ground motions. The study reported herein is concerned only with the results obtained in a first series of tests of frame models under quasi-static loads simulating the principal effects of severe seismic excitations. A bare frame was first tested to obtain its mechanical behavior; all other tests were carried out on infilled frames. The frames and infill panels were designed according to the following guidelines: (1) to maximize energy dissipation through distributed infill cracking, closely-spaced horizontal and vertical reinforcement was adopted; and (2) to minimize the possibility of brittle frame failure which could result from panel failure, the frames were specially reinforced against

---

[I]Graduate Student, University of California, Berkeley.
[II]Professor of Civil Engineering, University of California, Berkeley.

shear, and the thickness of the infill was based on the column shear resistance.

DESCRIPTION OF TEST SPECIMENS

PROTOTYPE SUBASSEMBLAGE. - An eleven-story apartment building having plan dimensions of 18.3 m by 61.0 m was selected as the prototype. Each story had a height of 2.74 m. The structural system consisted of R/C moment-resisting space frames supporting a two-way slab floor system. Other details may be found in Ref. 8. Although the preliminary design of a transverse frame (Fig. 1) was carried out using the seismic design provisions of the 1970 UBC and the 1971 ACI Code, the final proportioning and detailing of the frame members to resist strong earthquakes were done using Newmark's standard inelastic response spectra[9] and accepted principles of inelastic analysis and limit state design for high rotational ductility. To increase the lateral stiffness of the frame, it was decided to infill the two outer bays with 15-cm thick panels. In accordance with the capacity of the available testing facility, it was decided to test models of the lower three stories of this transverse end frame. Geometric and structural symmetry about the frame centerline suggested a realistic simulation of actual boundary conditions using a model of a prototype subassemblage 1-1/2 bays wide and 3-1/2 stories high (Figs. 1 and 2). It is believed that the lack of symmetry in the inelastic range due to the effect of axial forces in the infilled frames, and the effect of gravity forces in the coupling girders, are of secondary importance.

MODEL SUBASSEMBLAGES. - The prototype subassemblage was modeled to 1/3-scale. To facilitate loading and instrumentation, the models were tested in a horizontal position. As shown in Fig. 2, the loads and/or deformations to the specimens were applied by hydraulic actuators which form part of a servo-hydraulic system specially designed for this type of test.[10] This system permits any selected ratio to be maintained between the axial forces (simulating the effect of gravity loads and overturning moment), and the lateral force. The model was extensively instrumented; while all the transducer output was read at discrete intervals using a low-speed scanner, some data were monitored continuously.

The results presented herein correspond to tests carried out on the following models: (1) a bare frame (test #1); (2) this same frame, infilled with clay blocks after test #1; (3) a virgin frame, infilled with clay blocks; and (4) a virgin frame, infilled with concrete blocks. Each frame model was cast in the horizontal position using a single pour. All frames were identical. The sizes and detailing of the main members of the frame (Fig. 2) are given in Fig. 3. The main reinforcement for these members consisted of steel bars conforming to ASTM Designation A-615-68 Grade 60 (422,000 KPa). The strength of the concrete was about 27,000 KPa. After casting, the frames were rotated to a vertical position and infilled with hollow-core blocks, and were grouted one story at a time by the "high-lift" technique. Infills were approximately 5 cm thick, reinforced horizontally and vertically every 10 cm by deformed #2 bars (f_y = 422,000 KPa) spliced to dowels anchored in the frame members. Prism tests showed the compressive strength of both types of infill to be about 24,700 KPa.

TEST RESULTS

BARE FRAME TEST. - After the application of simulated gravity loads using the axial jacks (Fig. 2), this frame was subjected to the first few cycles

of the history of lateral load (and the associated overturning moment) shown in Fig. 4. Figure 6 shows the resulting tip displacement as a function of the lateral load. Failure occurred through the formation of a sidesway mechanism, at a maximum lateral load which agreed very well with that predicted by a collapse analysis using individual member resistances and a failure mechanism consistent with the observed damage. The seismic resistance of the bare frame was significantly affected by its lateral flexibility and consequent susceptibility to P-Δ effects.

INFILLED FRAME TESTS. - The loading program and lateral load-deflection curves for the three infilled models are shown in Figs. 4, 5, 7, 8 and 9. The general failure sequence was similar for all three frames: initial cracking patterns in each panel were consistent with the principal tensile stress orientations predicted by deep beam theory. After the formation of cracks along the boundary between the frame and infills, the assemblage behaved essentially as a frame braced by equivalent diagonal compression struts. Spalling occurred at those frame regions subjected to critical combinations of axial load, moment, and infill-induced shear. Reduced frame member stiffness at these regions resulted in increasing local inelastic deformations. Eventually, the number of such regions increased sufficiently to produce a sidesway mechanism (shown schematically in Figs. 7-9), whose lateral resistance was controlled by the strength of these inelastic regions as well as the residual infill resistance. Repeated cycles of reversals produced an increased amount of pinching in the load deflection curve, characteristics of shear-degrading structures, and the strength of the subassemblages asymptotically approached that of the corresponding bare frame mechanism. As may be seen from Figs. 7-9, although all three infilled frame models exhibited a decrease in strength following the initial drop in panel resistance, this decrease was gradual. All models exhibited excellent energy dissipation characteristics, even at tip deflections greater than ±10 cm., corresponding to average story drifts in excess of 0.03. As an index of the efficiency of these different systems against a major earthquake, Fig. 10 shows, for each specimen tested, the energy dissipated per complete cycle. When the results presented in Fig. 10 as well as those of Figs. 6-9 are compared, it is clear that with respect both to the stiffness at service levels and to the maximum energy absorption and dissipation capacity, tremendous gains were effected by infilling the frames. In all cases, it was possible to achieve distributed infill cracking and high energy dissipation and to minimize brittle shear failure.

CONCLUSIONS

Infilled frames designed and constructed in accordance with the guidelines mentioned in the introduction have several advantages over comparable bare frames, particularly if they may be subjected to severe ground motions:

(1) Owing to the increased stiffness (500%) and strength (from 60 kN to 280 kN) provided by infills, behavior is greatly improved under service loads, moderate ground shaking, and even under the largest expected overload of standard live loads. The increase in strength and energy absorption and dissipation capacities achieved by the addition of engineered infills is so large that it far exceeds the detrimental effects of possible increases in inertial forces due to increased stiffness. Architectural damage due to interstory drifts is reduced.

(2) For severe ground motions demanding elastic base shears in excess

of that corresponding to the bare frame collapse load, the stiffness provided by infills significantly reduces the influence of P-Δ effects on seismic response. Local panel failures occurred at tip deflections of at least 1.3 cm (average story drifts of 0.004). Prior to this, infilled frame damage was restricted to cracks less than 1.6 mm in width.

(3) For extreme ground motions demanding average story drifts in excess of 0.02, the engineered infilled frame is superior to the bare frame with respect to energy dissipation and resistance to incremental collapse. A bare frame dissipates energy primarily through large inelastic rotations at hinge regions near beam-column connections. Strain-hardening at these regions often results in anchorage deterioration at beam-column connections. The consequent loss of connection stiffness increases the danger of incremental collapse of the bare frame. However, in the engineered infilled frame, the panels dissipate very large amounts of energy through hysteretic behavior (gradual degradation of their high initial stiffness and strength). Because of this, the danger of incremental collapse is reduced. Gradual panel degradation is achieved by closely-spaced infill reinforcement, and by frame details providing high rotational ductility and cyclic shear resistance.

ACKNOWLEDGEMENTS

This study was supported financially by the National Science Foundation under Grant No. AEN 73-07732 A02, subproject 0-21997. Thanks are due to Mr. W. L. Dickey, Consulting Structural Engineer of the Masonry Institute of America, for his assistance throughout the testing program.

REFERENCES

1. Polyakov, S. V., "Masonry in Framed Buildings," Moscow, 1957 (English translation).
2. Stafford Smith, Bryan, "Lateral Stiffness of Infilled Frames," Journal of the Structural Division, ASCE, Dec. 1972.
3. Esteva, Luis, "Behavior under Alternating Loads of Masonry Diaphragms Framed by Reinforced Concrete Members," Proc. Int. Symp. on the Effects of Repeated Loading... (RILEM), Vol. V, Mexico City, 1966.
4. Benjamin, Jack R. and Williams, Harry A., "The Behavior of One-story Brick Shear Walls," Journal of the Structural Division, ASCE, July 1958.
5. Fiorato, A. E., et al., "An Investigation of the Interaction of Reinforced Concrete Frames with Masonry Filler Walls," Univ. of Illinois, Nov. 1970.
6. Kahn, Lawrence F., "Reinforced Concrete Infilled Shear Walls for Aseismic Strengthening," Univ. of Michigan, 1976.
7. Klingner, Richard, "Infilled Frames in Aseismic Construction, Ph.D. thesis in preparation, Univ. of California, Berkeley, 1976.
8. Biggs, John M. and Grace, Peter H., "Seismic Response of Buildings Designed by Code for Different Earthquake Intensities," MIT Structures Publication No. 358, Jan. 1973.
9. Newmark, N. M. and Hall, W. J., "Procedures and Criteria for Earthquake Resistant Design," Bldg. Sci. Ser. 46, NBS, Feb. 1973.
10. Bertero, V. V., et al., "Pseudo-dynamic Testing of Wall Structural Systems," Proc. ASCE-EMD Specialty Conf., Univ. of California, Los Angeles, March 1976.

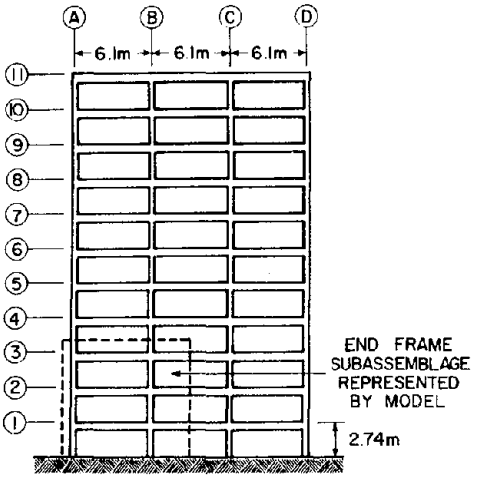

FIG. 1 END FRAME ELEVATION - PROTOTYPE

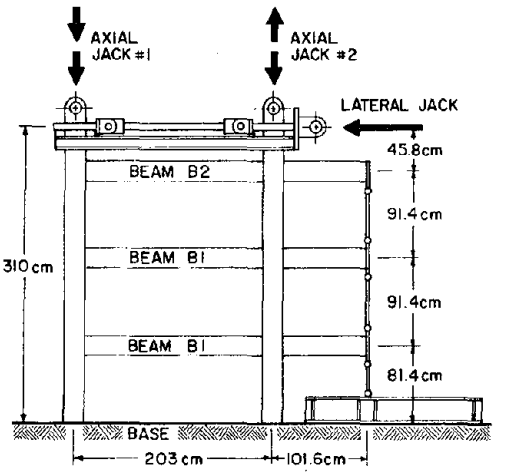

FIG. 2 TEST SPECIMEN AND TESTING ARRANGEMENT

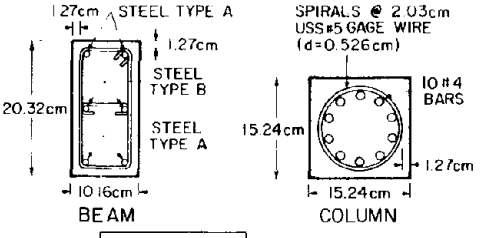

BEAM TYPE*	STEEL TYPE A	STEEL TYPE B	TRANSVERSE REINFORCEMENT
B1	#3	#2 DEFORMED	HOOPS AND CROSSTIES @ 2.54 cm
B2	#3	USS #11 GAGE WIRE	USS #11 GAGE WIRE (d=0.306 cm)

*REFER TO FIG. 2

GRADE 60 STEEL
NOMINAL f_y=4220 $\frac{kg}{cm^2}$

FIG. 3 DESIGN DETAILS OF FRAME MEMBERS

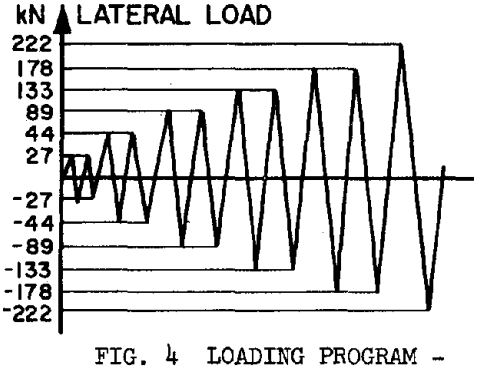

FIG. 4 LOADING PROGRAM - TESTS #1, 2 & 4

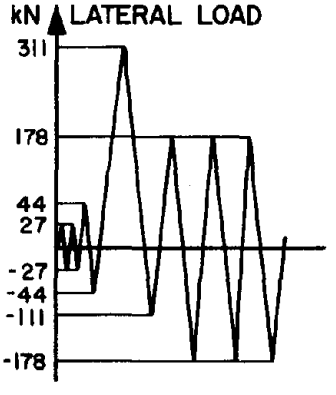

FIG. 5 LOADING PROGRAM - TEST #3

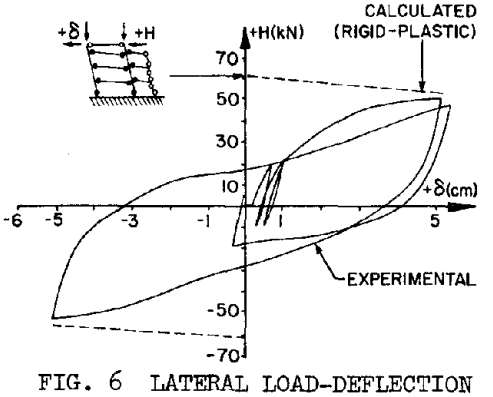

FIG. 6 LATERAL LOAD-DEFLECTION RELATIONSHIP - BARE FRAME

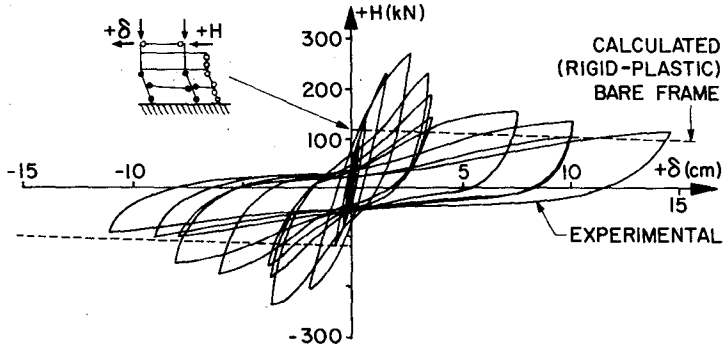

FIG. 7 LATERAL LOAD-DEFLECTION RELATIONSHIP - INFILLED BARE FRAME

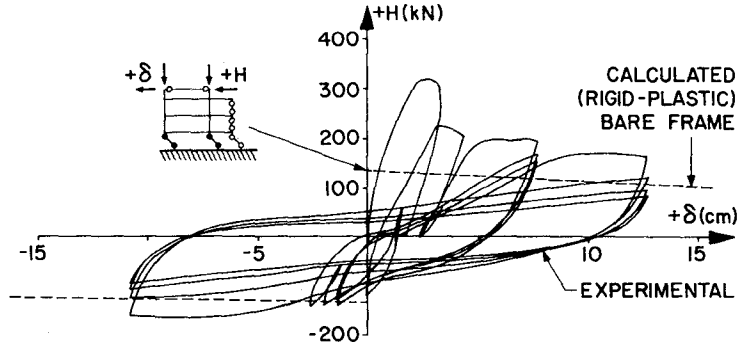

FIG. 8 LATERAL LOAD-DEFLECTION RELATIONSHIP - VIRGIN FRAME, CLAY INFILL

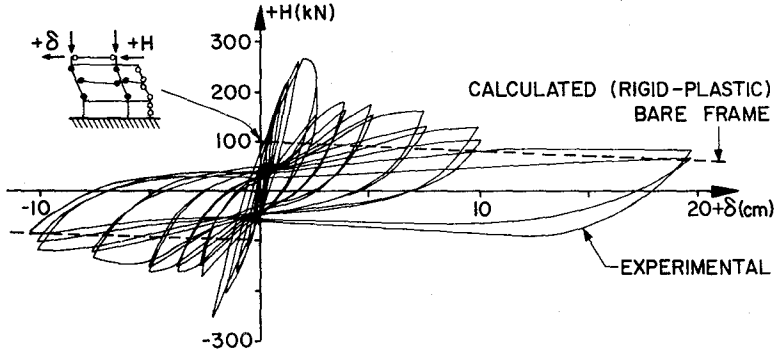

FIG. 9 LATERAL LOAD-DEFLECTION RELATIONSHIP - VIRGIN FRAME, CONCRETE INFILL

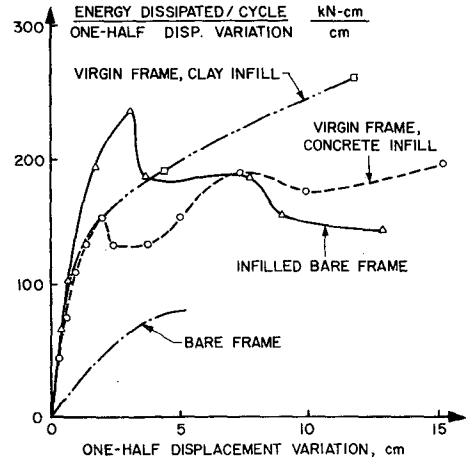

FIG. 10 ENERGY DISSIPATION

ON SEISMIC DESIGN OF R/C INTERIOR JOINTS OF FRAMES

by E.P. Popov[I], V. V. Bertero[I], B. Galunic[II] and G. Lantaff[II]

SYNOPSIS

Two alternative designs for beam reinforcement at the interior joints of moment-resisting reinforced concrete frames are discussed. The proposed details, verified by experiments, avoid the danger of bond degradation of the main beam bars within the column.

INTRODUCTION

A rational design of R/C frames for successfully resisting seismic loadings is one of the more important problems in earthquake engineering. Such frames are widely used either as the principal structural system or in conjunction with infill or structural walls. To assess the behavior of such R/C frames, a good deal of experimental work was done on individual beams and columns. The behavior of these elements was studied under cyclic loadings simulating seismic disturbances. The separate study of these members, however, is not sufficient to determine the behavior of whole frames, as a very complex action develops in the joints. Improperly designed joints may change dramatically the behavior of the whole frame. Therefore, in addition to studying the beams and columns as separate entities, these elements must also be studied interconnected, forming typical frame subassemblages.

At Berkeley, a series of half-scale subassemblages of a tall R/C building was tested according to a procedure described later in this paper, and after some damage and repair, was re-tested [1]. The model simulated the basic subassemblage of a third floor level of a 20-story office building. The overall dimensions of the specimens were kept constant while changing the amount and type of reinforcement details in the joints and beams. The test arrangement was such that a Pδ effect could be induced. The specimen design was based on the concept of strong columns-weak beams, i.e., the inelastic action was to take place primarily in the beams.

In a previous test on specimen BC3, the beams were designed with four #6 bars on the top and three #5 bars or 50 percent of negative steel on the bottom. Since the bars were continuous, the beam plastic hinges formed at both faces of the column. The maximum shearing stresses in the beams were on the order of $3\sqrt{f'_c}$ (psi). This resulted in failures of the beams in the flexural mode[2,3]. The expected degradation of beam stiffness and strength during reversals of large shear did not occur, although the subassemblage showed severe degradation due to the bond failure of the main beam bars within the column. To remedy this objectionable condition in the joint, two alternative designs were made and tested, and the results are presented in this paper.

DESIGN OF NEW SPECIMENS

Both of the new specimens are so designed as to force the formation of plastic hinges away from the column faces. It is believed that by this scheme, the bond failure of the main beam bars within the column will be delayed or prevented. This should result in a superior ductile behavior of the whole subassemblage. The details of the specimens are shown in Fig. 1. For both specimens, the reinforcement of the beams at the face of the column consists of four #6 bars on the top and bottom. Thus, unlike the previous

I Professor of Civil Engineering, Univ. of Calif., Berkeley, California.

II Research Assistant, Univ. of Calif., Berkeley, California.

specimens, 100 percent of the negative steel is placed on the bottom of the beams. The plastic hinge was designed using two different schemes. In one specimen, BC5, the two top interior main bars were bent downward, and the two corresponding bottom bars were bent upward intersecting 16 in. away from the face of the column as shown in Fig. 1. The bars were inclined 60° from the horizontal. After additional bending, the bars extended to the end of the beam. All corner bars are both straight and continuous. In the second specimen, BC6, half of the main bars on the top and bottom of the beams were cut off at 24 in. away from the face of the column. The location of the plastic hinge is determined by the requirement that the steel at the column face begins to yield just shortly before the critical section reaches ultimate condition, where the bars are at their ultimate strength. The plastic hinge in BC5 was closer to the column because the large amount of diagonal steel at that section gave a substantial increase to the moment capacity of the section. In BC6 the bars were cut off at a point just slightly beyond where analysis indicated the plastic hinge would occur, because it was anticipated that the plastic hinge would gradually move toward the column. In both specimens, the beams were reinforced against shear with #2 double stirrups placed 3-1/2 in. apart except in the plastic hinge region where a more conservative stirrup spacing of 4.5 times the bar diameter (or 2 in.) was used to avoid any buckling of the main reinforcement. The columns were reinforced with twelve #6 bars and #2 bar triple ties at 1.6 in. on center. In the column joint the ties were spaced at 2 in. on center. Grade 60 steel was used for all reinforcement.

CASTING PROCEDURE

The specimens were cast in a vertical position in the course of the same day, in three separate lifts with a stopover after each to allow for the shrinkage of the concrete. The lower section of the column was cast first, up to the bottom of the beams. Later, the beams were cast and, finally, the top part of the column was cast to complete the process. Because of an error in the mixing process, the concrete for specimen BC5 was not of uniform quality. The design called for a 28-day concrete strength of 4000 psi, but the actual strength obtained in the beams was only 2100 psi. However, since the tests were conducted primarily to study the behavior of the subassemblages after the steel has yielded, the steel had a greater influence on the specimen's performance in the inelastic range than the concrete, and the overall results were not strongly affected. The concrete strength in specimen BC6 was uniform throughout. The material properties are listed in the table below. After the specimens were cured and the forms removed, metal hinge assemblies were attached at all four ends of the specimens. These were made of steel for the column and of aluminum for the beams. The aluminum hinge assemblies were designed to act as transducers for measuring the reaction forces acting on the beams during the experiments.

Subassemblage Material Properties

SPECIMEN	CONCRETE ULTIMATE STRENGTH		REINFORCING STEEL				
			BAR SIZE	YIELD STRENGTH		ULTIMATE STRENGTH	
	ksi	MPa		ksi	MPa	ksi	MPa
BC5	2.1	14.4	#2	65.0	448	106	731
BC6	4.0	27.5	#6	64.0	441	106	731

EXPERIMENTAL SET-UP AND TESTING PROCEDURE

The specimens were tested in a large steel testing frame. The top hinge of the column was connected to a pin fixed to the frame and prevented from

translation. The hinges in the beams were restrained from vertical translation but were free to displace horizontally. The lateral load was applied at the bottom hinge of the column by means of a double acting hydraulic cylinder which moved the hinge back and forth. Also, a large axial load was applied to the bottom hinge by means of a hydraulic jack which was supported by a movable cart. The axial load of 470 kips represents the dead and live loads acting on the specimen and it was kept constant in these experiments. The loads applied and the beam reactions are shown schematically in Fig. 3. As can be seen from the figure, the reactions in the beams are caused not only by the applied horizontal force, but also, by an extra $P\delta$ moment caused by the vertical force, P. The additional beam reaction at each end caused by the vertical loads is equal to $P\delta/(L)$, where P is the total vertical load, δ is the bottom hinge displacement measured from the top of the column, and L is the distance between the two beam hinge supports. In the lower stories of a structure where the axial load is large, the $P\delta$ effects are very significant for large story displacements.

The applied displacement program is shown in Fig. 2. The specimens were first subjected to a few loading reversals in the working stress range. After the first yield, the specimens were subjected to increasing displacements in a stepwise manner. Two cycles were made at each particular displacement. The cyclic loading applied to BC5 and BC6 was very similar to that of the previously tested BC3.

Extensive instrumentation was used to record the specimens' behavior. Strain gages were placed at various locations on the main beam reinforcement to study the variation of strain and to check for yielding. Clip gages were used on the top and bottom of the beams to measure curvature. Shear distortion was measured by a set of clip gages diagonally placed at two adjoining locations near the plastic hinge on each beam. Measurement of beam reactions was made by the aluminum transducers in the hinges. Photogrammetric measurements were made of the beams to study the deformation pattern.

EXPERIMENTAL RESULTS

In representing the overall performance of the members, the H_{eq} vs. δ graphs were used instead of the H vs. δ, because they give a better measure of the main beam's strength. A comparison of the H_{eq} vs. H curves was made for a previously tested specimen and is shown in Fig. 4. The H value is seen to decrease after L.P. 17 with increasing displacement. However, because of the $P\delta$ effect, the equivalent horizontal force, H_{eq}, actually increases, indicating that the beam gains strength after first yield. Similar behavior was evidenced in specimens BC5 and BC6 (Figs. 5 and 8).

Excellent results were obtained from specimen BC5 in terms of overall member performance as well as of solving the problem of anchorage loss. Slippage of the bars through the column was completely eliminated and smooth stable hysteretic curves were recorded throughout the duration of the experiment. The steel at the face of the column yielded at a ductility ratio of approximately 4.5, which represents a ratio of maximum displacement to displacement at yield. Large plastic rotations in the plastic hinge of .058 rad. (.110 rad. for a complete cycle) were observed during the last few cycles of the test. The large increase in strength of the specimen after yielding is caused by the strain-hardening of the continuous bars and by the increasing effectiveness of the inclined bars due to the large strains in that region. From Fig. 5, it can be seen that strength increases to a maximum with increasing displacement and then begins to decrease. The lateral resistance and stiffness decrease with repetition of a reversal cycle with same peak

displacement. Shear distortions were very small due to the excellent reinforcement provided by the inclined bars. The deformation characteristics of the beam in the area of the plastic hinge is shown in Fig. 6.

Slippage of the bars through the column was also eliminated in BC6; however, there was a large amount of shear deformation at the plastic hinge. This plastic hinge formed as expected at the cutoff point of the main interior bars, but progressively moved toward the face of the column as the bond at the end of the cutoff bars deteriorated and the moment capacity of the severely cracked section decreased. The bars at the face of the column did not yield, although during the last several cycles the strains were very large. Under repeated application of displacement reversal in the inelastic range, the flexural-diagonal cracks at the top and bottom of the critical region of the beam increased in width and propagated until they crossed. At this stage, resistance to shear deformation decreased significantly because the only effective mechanisims of shear resistance that remained were the aggregate interlocking and friction along the crack faces and the dowel action of the main steel bars. All of these sources of resistance degrade with increasing severity of reversals. During shear reversal, at small shear force there is a small amount of slippage between the two adjacent sides of the main crack, which causes a drop in the overall stiffness. This shear distortion at the critical region reached 3/4 in. at the last cycle of the test. The deformation pattern at the plastic hinge was obtained by a photogrammetric technique and is shown in Fig. 7.

CONCLUSION

Both specimens were successful in avoiding the problem of bond loss by the main beam bars in the column core. However, to permit the development of large plastic rotations, special shear reinforcement should be provided to prevent an early shear failure. The crossing steel of BC5 offered excellent resistance to shear. In BC6 only vertical stirrups were used for shear reinforcement. Such vertical stirrups are very effective when the cracks in the concrete form at approximately 45°. But, after several cycles into the inelastic range, the plastic hinge of BC6 had many vertical cracks for which vertical stirrups were ineffective. Therefore, with little effective shear reinforcement, large amounts of shear deformation developed in the plastic hinge region. Diagonal shear reinforcement should be used to prevent this type of failure.

When the plastic hinge is forced to form away from the column face, larger amounts of rotation are required in the plastic hinge for the same story drift. Because of these large rotational demands, it is very important that the steel and its detailing be carefully selected so as to develop large strains.

ACKNOWLEDGEMENTS

This work was supported by the National Science Foundation Grants GI-36387 and ENV76-04263 for which the authors are most grateful. Several graduate students among whom D. Soleimani, S. Viwathanatepa, T. Y. Wang and Messrs. B.Lutz, D. Clyde, and R. Osborne were most helpful with the tests.

REFERENCES

[1] E.P. Popov and V.V. Bertero, "Repaired R/C Members Under Cyclic Loading", Earthquake Engineering and Structural Dynamics, Vol. 4, 129-144 (1975).

[2] V.V. Bertero and E.P. Popov, "Hysteretic Behavior of Ductile Moment-Resisting Reinforced Concrete Frame Components", Report EERC 75-16, Earthquake Engineering Research Center, University of California, Berkeley, (April 1975).

[3] E.P. Popov, V.V. Bertero and S. Viwathanatepa, "Analytic and Experimental Hysteretic Loops for R/C Subassemblages", Proceedings, Fifth European Conference on Earthquake Engineering, Istanbul, (September 22-25, 1975).

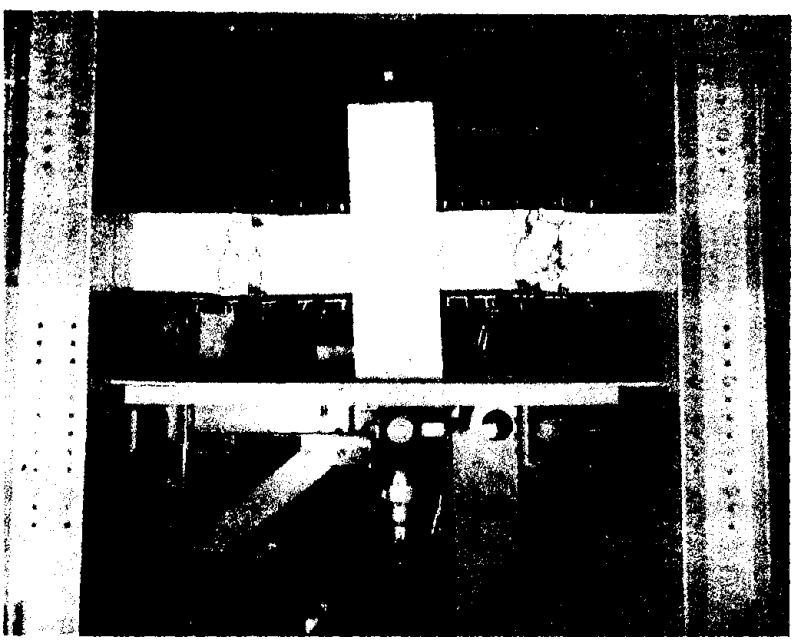

General Experimental Set-up

Specimen BC6 after last load cycle. Note the large shear slippage in the plastic hinge regions.

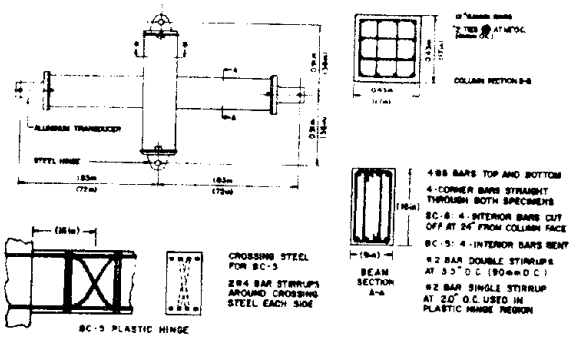

Fig. 1.

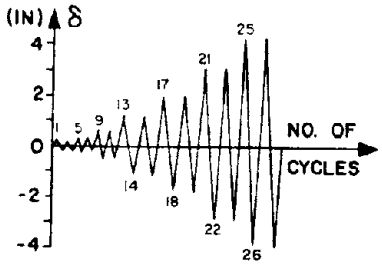

Fig. 2.

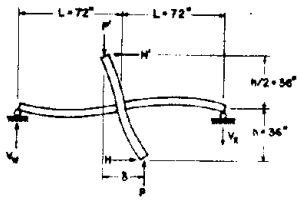

Fig. 3.

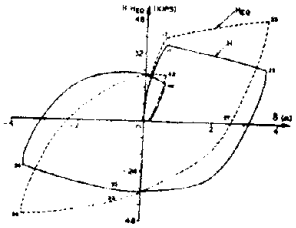

Fig. 4.

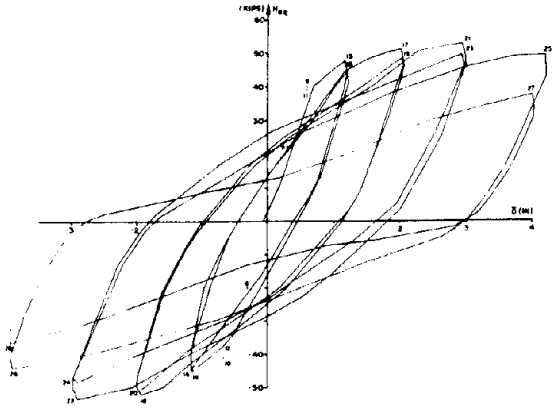

Fig. 5. BC5

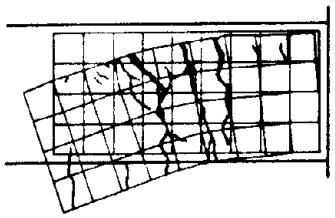

Fig. 6. BC5

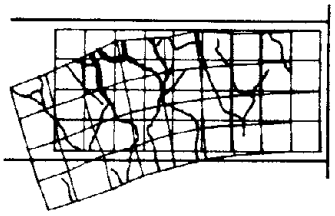

Fig. 7. BC6

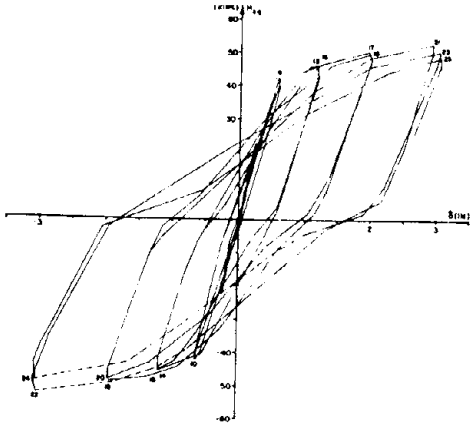

Fig. 8. BC6

SEISMIC DESIGN AND ANALYSIS PROVISIONS FOR THE UNITED STATES

by

Nathan M. Newmark[I], Henry J. Degenkolb[II], Anil K. Chopra[III], Anestis S. Veletsis[IV], Emilio Rosenblueth[V], and Roland L. Sharpe[VI]

SYNOPSIS

The seismic design and analysis requirements presently used in U.S. building codes were largely developed in the Recommended Lateral Force Requirements and Commentary published by the Seismology Committee of the Structural Engineers Association of California in 1959-1960. Since that time, improvements and modifications have been made at frequent intervals. Several years ago it became apparent that a comprehensive review should be made of the provisions, the latest state of knowledge should be evaluated, and a coordinated set of provisions should be developed. This paper describes the basic concepts and summarizes some of the details of the structural design provisions of a new code developed by the Applied Technology Council.

INTRODUCTION

A cooperative program to develop new provisions was initiated in the Fall of 1974 by the Applied Technology Council (ATC) under a contract with the National Bureau of Standards (NBS) funded by the National Science Foundation (NSF) - RANN program and NBS. The performance of buildings during recent earthquakes was evaluated and weaknesses in present code provisions were studied.

The new provisions represent the efforts of 85 participants in 14 Technical Committees organized into 5 Task Groups. This paper is concerned primarily with the effort of Task Group II, on Structural Analysis and Design, although it draws in part on the work done by other Task Groups. Professor Newmark is Chairman of Task Group II and also Chairman of the Task Group Coordinating Committee. Mr. Degenkolb and Professors

I. Professor Nathan M. Newmark, Department of Civil Engineering, University of Illinois, Urbana, IL 61801.

II. Henry J. Degenkolb, President, H. J. Degenkolb & Associates, 350 Sansome Street, San Francisco, CA 94104.

III. Professor Anil K. Chopra, Department of Civil Engineering, University of California, Berkeley, CA 94720.

IV. Professor Anestis S. Veletsos, Department of Civil Engineering, Rice University, Houston, TX 77001.

V. Professor Emilio Rosenblueth, Institute of Engineering, University of Mexico, Mexico 20, D.F., Mexico.

VI. Roland L. Sharpe, Project Director, Applied Technology Council, 480 California Avenue, Suite 301, Palo Alto, CA 94306.

Chopra and Veletsos are Chairmen of the 3 Technical Committees in Task Group II, Professor Rosenblueth is a major contributor to the work of the Group, and Mr. Sharpe is Project Director of the program for the ATC.

A working draft of the new provisions was distributed in February 1975 to some 500 reviewers in practice, industry, professional organizations, government agencies, and universities. Upon completion of a review by the Technical Committees of the comments received, another draft for limited review will be completed this fall, and the final report will be issued in the late spring of 1977.

It is intended that the final recommendations will be of such a form that they can be adopted by jurisdictions through the United States.

BASIC CONCEPTS

The new ATC design recommendations are intended to be logically based, with explicit consideration given to factors that are generally implicit in previous codes and design provisions. The earthquake hazard is defined in the code by a map with contours indicating the "Effective Peak Acceleration" (EPA) in various regions of the United States. Interpolation between contours is permitted. These values range from 0.05 g to 0.4 g, with these extremes being the lowest and the highest values considered in any region of the country. In some regions, consideration is given to the longer durations of somewhat less intense motions by using a map showing Effective Peak Velocity (EPV). Rules are prescribed for determining the design spectrum corresponding to any given levels of EPA and EPV. These are discussed more completely in a companion paper by Whitman et al.

Buildings are classified from the point of view of design by hazard exposure factors and building design categories. When these are selected, the procedure that follows depends on the design spectrum. This design spectrum is used both for simplified analyses through the use of an equivalent lateral force factor or with a modal analysis. The design spectrum is modified by a soil factor which is a function of the type of soil conditions, considered in three categories, as firm soil or rock sites, deep soil sites, and soft soil sites. The response spectrum is also modified by a spectral reduction factor, R, which is used to divide the basic spectrum to obtain the design spectrum appropriate for the particular category of structural framing and materials.

The spectral reduction factor is a function of the ductility factor appropriate to the particular structural type, materials, framing, and category, and any variation in damping consistent with those parameters, if the damping differs from the standard level of 5% of critical damping. The factor also includes an experience or judgment factor to take account of the inherently better capabilities and performance in actual earthquakes of some types of structures and materials compared with others. Tables are given in the recommendations for the selection of the spectral reduction factor.

The base shear is determined in standard ways from the design spectrum and the mass of the building, through the use of an appropriate fundamental

period of vibration for the building. The latter can be determined from relations given in the text for different building framings and types or may be computed by fundamental methods of structural dynamics.

The distribution of seismic forces over the height of the building for the purpose of computing shears and overturning moments, is based on an extrapolation between a linear and a parabolic distribution of accelerations over the height, by means of relations which prescribe a linear distribution for periods less than 0.5 seconds, and a parabolic distribution for periods greater than 3.5 seconds, with a linear interpolation between those limits.

Overturning moments computed from the seismic force distributions may be reduced under certain conditions, but generally not in the upper ten stories of the building, and not by more than 20% in the building itself, with an additional 10% reduction being permitted in determining the foundation forces under the building.

Provisions are given in the code for calculation of drift, and for torsional requirements. Recommendations for construction and design details, in lieu of requiring detailed analyses, are stated for buildings in areas with nominal seismicity.

All of the above factors are stated explicitly in the design provisions. Of particular interest are the requirements for construction and design details, varying in degree of rigor with the seismic zone or acceleration level for the building and its seismic hazard exposure factor. Also, as a function of these quantities, methods of analysis are specified, including a constant coefficient method which may be used in only the least hazardous seismic zones, for buildings of lowest hazard exposure factors, an Equivalent Lateral Force method (ELF) for buildings in general in all zones, and modal analysis which may be used and is recommended under some conditions for the most highly seismic zones for buildings with the highest hazard exposure factors.

The design base shear is computed from the product of the design spectral coefficient C_s multiplied by the effective weight of the building W. The quantity C_s is given by the relationship:

$$C_s = 1.2\ AG/RT^{2/3}$$

In this relationship, the quantities are defined as follows:

A = Effective Peak Acceleration value based on the EPA or EPV maps.

G = soil profile factor ranging from 1.0 for rock and stiff soil sites to 1.5 for soft soil sites.

R = response modification coefficient depending on type of structural system, including vertical and horizontal lateral force distribution systems.

T = measure of fundamental period of vibration based on framing method and geometry of building.

The value of C_s need not exceed 2.5 A/R for rock or stiff soil sites or deep soil sites nor 2.0 A/R for soft soil sites.

Finally, provisions are made for increased seismic forces when the safety of the building is dependent on the survival of a single major force resisting element; and similar provisions are made for increases in seismic factors when large discontinuities in story strengths or stiffness occur.

SOIL-STRUCTURE INTERACTION

Two different approaches can be used to assess the effects of soil-structure interaction on the seismic response of structures. The first consists in modifying the stipulated free-field design ground motion and evaluating the response of the structure to the modified base motion, whereas the second consists in modifying the dynamic properties of the structure and evaluating the response of the modified structure to the prescribed free-field ground motion. The design provisions used are based on the second approach.

The interaction effects in this approach are expressed by (1) an increase in the fundamental natural period of the structure; and (2) a change (usually increase) in its effective damping. The increase in period accounts for the compressibility of the foundational soil, whereas the change in damping accounts primarily for the effects of the energy dissipated in the supporting soil by radiation and hysteretic action.

For the assumptions made in the development of the recommended design provisions for fixed-base structures, soil-structure interaction reduces the design forces below those applicable to a fixed-base condition. Accordingly, the structure may be designed conservatively without consideration for interaction. Hence the use of the relations for soil-structure interaction is optional with the designer. Because of the effect of foundation rocking, however, the displacements of the floors relative to the base may increase, and this would increase the requirements on separation of buildings and the P-Delta effects.

Formulas are given in the recommended provisions for the reduction in total lateral force or base shear for the structure, as a function of the effective weight of the structure, and the seismic coefficients applicable to the fundamental natural periods of vibration and the effective damping factors of the structure (a) with a fixed base and (b) with interaction with the soil. It is assumed that the soil-structure interaction affects only the response component contributed by the fundamental mode of vibration of the fixed base structure.

In defining the effective coefficient of damping, account is taken of the damping in the structure and both material and radiation damping in the foundation. The fundamental period of the structure and foundation takes into account the translational and rotational stiffness of the foundation material when forces are applied to a rigid slab on the foundation. These stiffnesses are given in terms of the shear modulus of the foundation, which is taken as a fraction ranging from about 0.4 to 0.8 times the shear modulus for very low foundation strains.

COMMENTS ON PROCEDURES

Some of the departures from previous procedures and codes are of special interest. The design acceleration spectrum decreases with the 2/3rds power of the fundamental period, in contrast to the theoretical value of decrease with the period on firm ground and with the period squared on very deformable ground. The reasons for using the rate of decrease in the ATC code are to provide uniformity and simplicity, and to take account of the fact that for long periods the cost of the building is less sensitive to seismic reliability in general and one can afford to design more conservatively. Moreover, the longer the period the higher are the losses likely to be caused by failure. It is desirable to be more conservative for long periods because of the higher probable number of significant degrees of freedom, and the likelihood that there may be a concentration of ductility requirement over a small portion of the structure in a tall building compared with a short building. Other reasons for the conservatism in the requirement include the uncertainty in the computed periods and the changes in the periods and mode shapes due to nonlinear behavior.

Accidental torsion is considered by use of an eccentricity of horizontal seismic force corresponding to 5% of the width of the building in the direction of the force considered. This provision is believed to be adequately conservative although under some extreme circumstances, occasional values somewhat higher than 5% may be found.

The maximum overturning moment arises from combinations of modes that are different from those corresponding to those that contribute to the maximum shear in the lower levels of the building, and some reduction is necessary in the seismic coefficients that are used for computing overturning moments from those used in computing maximum shear. The reduction factor is limited, however, for conservatism.

When the shape of the fundamental mode of vibration is unusual, due to large discontinuities in mass and/or stiffness of adjacent stories, criteria have been developed to identify these conditions and are used as a basis for then specifying that modal analysis is mandatory. These criteria involve making a static analysis plus one cycle of a Stodola-Vianello deflection calculation, and a comparison of the story shears in the static analysis compared with those of the single cycle calculation. If the difference is greater than some factor, say approximately 30%, modal analysis is required.

For simplicity the spectral reduction factor R is kept constant over the whole range of the frequencies of the design spectrum, rather than to use two factors with the smaller one applicable only to the acceleration sensitive region of the response spectrum.

Stresses and deformations due to earthquake motions in two directions at right angles horizontally are considered by taking into account the forces due to the motions in each direction plus 30% of the forces due to the motions in the horizontal perpendicular direction. In addition, under some circumstances, the effects of vertical motions are combined with those for horizontal motions. Also, relationships are given for computing the

increases in forces to account for the vertical dead load effects produced by horizontal displacements, the so-called P-Delta effect.

The specific numerical provisions of the new design recommendations are still under study and may be modified slightly in value but not in principle before the final draft of the provisions is issued.

EMERGENCY POST-EARTHQUAKE INSPECTION & EVALUATION OF DAMAGE IN BUILDINGS

Boris Bresler[I], Leslie Graham[II], & Roland Sharpe[III]

ABSTRACT

Recommended procedures are presented for emergency inspection and evaluation of post-earthquake damage to assess the extent of damage and to evaluate the relative safety for occupancy of buildings. Guidelines for recruiting and training competent field personnel and procedures for carrying out field operations safely and effectively are developed.

INTRODUCTION

This paper describes a portion of recommended nationally applicable seismic design provisions. These provisions have been produced by the Applied Technology Council, associated with the Structural Engineers Association of California, under contract with the National Bureau of Standards (NBS) with funding by NBS and the National Science Foundation Research Applied to National Needs Program, as part of the Cooperative Federal Program in Building Practices for Disaster Mitigation initiated in 1972 under the leadership of NBS. The preparation of the procedures is being carried out by a committee composed of the authors plus Messrs. Thomas Atkinson and David Messinger.

The procedures described herein are intended to reduce the incidence of death and injury to occupants of buildings which have been weakened or placed in jeopardy by seismic activity or by aftershocks. A secondary purpose is to assess damage to service systems which would render buildings unusable and/or pose a health hazard to occupants and the community. Finally, statistical assessments of damage are necessary to estimate the magnitude of the disaster in terms of cost of damage, numbers and types of buildings affected, and to provide data for government planning for aid to communities.

Advance planning is essential for effective inspection and evaluation of post-earthquake damage in buildings. The most effective and efficient means of organizing inspections is generally through established agencies within the local jurisdiction. Accordingly, the agency regulating building inspection and safety within the cognizant jurisdiction would be responsible for conducting damage surveys. Recognizing that such an agency would probably not be adequately staffed for the task, mutual aid from neighboring communities would be required.

Even maximal aid from public and governmental agencies may not be adequate. Local jurisdictions should therefore develop plans to enlist the aid of private sector engineers and others to assist in assessing and evaluating damage to buildings. In an emergency these individuals must be contacted and transported to emergency operation centers, and there must be stockpiles of earthquake damage inspection forms and equipment and transport to the damage areas.

I Professor of Civil Engineering, University of California, Berkeley, CA.
II Structural Engineer, Graham & Kellam, San Francisco, CA.
III Project Director, Applied Technology Council, Palo Alto, CA.

The principal elements in planning for and carrying out effective emergency inspection and evaluation of earthquake damage are: (1) organization, training, and mobilization of inspection personnel, (2) inspection procedures, (3) evaluation of structural and nonstructural damage, (4) evaluation of auxiliary systems, and (5) emergency control actions based on the damage evaluation.

The experience of the Building and Safety Department of the City of Los Angeles, whose 250 building inspectors evaluated 27,160 structures in the month following the 1971 San Fernando Earthquake, helps to define emergency damage inspection procedures: (1) An operative communications system is essential; because telephones may not function after a major disaster, it is imperative that an emergency communications system--probably radio--be available. (2) The boundaries of heavily damaged areas must be quickly defined, and overall damage assessed, preferably by air reconnaissance. (3) Efficient forms for compiling and evaluating statistical data must be devised. (4) Plans for obtaining emergency aid from other jurisdictions must be developed, including orientation for inspectors unfamiliar with the area.

INSPECTION PERSONNEL AND ORGANIZATION

The type of personnel needed for inspection teams will vary depending on the classes of structures to be investigated. Structures in average neighborhood shopping centers and surrounding areas could, for instance, be examined by architects, building inspectors, and construction foremen, while larger and more complex structures should be examined by experienced structural engineers. Inspections teams should be aided by specialists such as photographers, amateur radio operators, and other communications specialists. Recruitment of personnel could be through engineering and architectural societies, technical associations, trade unions, and large engineering and construction firms.

Enrollment in manpower pools should be on a regional basis so as to include personnel from areas not affected by a disaster. Personnel lists should be compiled on both a statewide as well as local basis, and be maintained at local mobilization points and at State Department of Emergency Services headquarters. The lists should be updated at least every two years.

Enrollment forms should show special qualifications, age, physical endurance, commitment to participate in training programs, and commitment to serve on-call for not less than two years. The lists should be processed into a data bank, classifying personnel by geographical location and special skills. To avoid problems with legal liability for actions by personnel and with discipline and control, consideration should be given to mobilizing special inspection teams under government power of conscription with conditions of service and compensation rate as part of the enrollment procedure.

Mandatory training programs should be organized for inspection teams, encompassing the following: (1) disaster relief plan organization, (2) mobilization procedures, (3) team organization, (4) communications procedures, (5) identification of types of damage, (6) structural and nonstructural hazard identification, (7) recording procedures, (8) temporary hazard abatement, and (9) estimation of damage losses and possible repair costs. In addition, special training should be provided for: (1) evaluation of damage with respect to safety for continued occupancy, (2) evaluation of damage to utilities and services for health hazards, (3) evaluation and identification of on-site soil and foundation conditions, (4) identification of structural load-resisting systems without benefit of plans, and (5) identification of

mechanical and electrical systems without benefit of plans. Classroom training, correspondence courses with assignments and periodic examinations, and workshops to discuss problems encountered in recent earthquakes should be used. Field exercises, including simulated disasters and involving all disaster relief agencies, should be held with participation in at least one such exercise mandatory for re-enrollment.

PROCEDURES FOR INSPECTION AND EVALUATION

Before effective identification and evaluation of damage can be undertaken, several operations must be completed, including: (1) identification of areas where damage must be assessed, (2) closing-off of damaged areas, and (3) activation of the central control group or groups.

To define the damage area, photo reconnaissance flights should be initiated as soon as possible with planning the joint responsibility of appropriate federal, state, and local governmental agencies. Damage evaluation by driving through the area on a block-by-block basis is less desirable than overflights because of access problems to heavily-damaged areas and less rapid accumulation of data. Closing-off of damaged areas should be the responsibility of the police. The central control group should be informed of the boundaries so as to plan the mobilization of inspection teams and to arrange for personnel access.

The central control group coordinating the inspection efforts and mutual aid between affected areas would: (1) establish communication with the central disaster relief organization, (2) mobilize headquarter office forces and inspection teams, (3) retrieve stored equipment and arrange for issuance of supplies to inspection teams, (4) arrange transportation and communications, (5) arrange for personnel feeding and housing, (6) process inspection reports, (7) respond to inspection requests, (8) issue preliminary damage assessment data to pertinent agencies and news media, and (9) conduct special inspection parties through damaged areas.

Inspection personnel should report automatically to their mobilization point if they have been unaffected by the earthquake and are located in or near the disaster area. Personnel from other areas should be notified by the appropriate agency. In case of loss of telephone service, notification could be by radio. In reporting personnel must use whatever means of transportation is in operation, including personal vehicles if necessary. Prearrangement for use of government vehicles and car pools should be part of the operations plan. A form of pass familiar to state and local police should be issued in advance to all enrolled persons with blank passes available at mobilization points for emergency use. The head of the Building Inspection Agency should have control of pass issue.

Mobilization points should be established considering that some may be rendered inoperable by the disaster. Preferably, the mobilization point would serve as the coordination center for damage evaluation. If the center also housed police, fire, and other vital functions, coordination of effort would be greatly enhanced.

Inspection teams would be formed as personnel report for duty. Engineers familiar with specific structures should be assigned to investigate same. Inspection priority should be established with essential community facilities heading the list. An emergency radio system with mobile two-way units for each team would be most helpful. If such is not available, the

following might be considered: (1) taxicab two-way radios, (2) walkie-talkies, (3) amateur short-wave, (4) private cars with or without two-way receiver-transmission systems, (5) military vehicles, and (6) foot messengers.

After inspection teams are at a building, they must identify the lateral force resisting system, and evaluate damage to this system and to other building elements to ascertain whether the building should be posted as unsafe for occupancy. To expedite inspection and recording of observations, forms have been developed for recording data on damage to structural and nonstructural elements, mechanical, electrical, and plumbing systems, and on soil and site conditions. These forms were designed so the data can be punched directly on IBM cards for processing. Generally, it is desirable to (1) identify the building, (2) identify the inspection team by code number, (3) record the time and date of inspection, (4) detail the building location, (5) describe the occupancy (use, special contents, and number of occupants, (6) describe number of stories above and below grade, shape and dimensions (plan and elevation) and foundation/soil conditions, (7) describe the structural system (roof, floors, walls, frame, connections), (8) identify all materials of construction, and (9) describe special features and construction details (finishes, lighting, mechanical and electrical systems and special equipment, stairs, parapets, etc.). Information should also be provided on (10) damage in structural and nonstructural elements and distortion or malfunctions of nonstructural elements, (11) the degree of hazard from sources within the building and adjacent buildings, and (12) cost estimates of loss and cost of repair or demolition. Finally, inspection team recommendations and any action taken should be noted.

Several classes of structures should receive special attention. Hospitals: Because of the complexity and interdependence of the service systems, qualified engineers with experience in hospital design should assess their condition. Hospital operating personnel should accompany the team, and consideration should be given to the state of the buildings and the potential hazards of dangerous gases, liquids, or solids, and radiation emission. Utilities: Most utilities have emergency plans for investigating and repairing damage to their facilities, and therefore communication between their staff and the central control group should have top priority. Schools: The service systems of many school buildings can be expected to be severely damaged; however, these systems are usually relatively simple and their potential for creating hazardous conditions is negligible. Cognizant technical and custodial school personnel should be listed at emergency operating centers. Office Buildings: The services provided in most office buildings are relatively simple; however, complex electrical equipment is often present, posing a serious fire hazard if wiring is disrupted; structural complexities may create difficulties for inspectors. In most low-rise office buildings, the mechanical equipment and power supply systems are relatively simple to inspect. The stability of heavy equipment and its supports, and the potential for fire hazard, should be evaluated. In high-rise office buildings, mechanical equipment is often concentrated at mid-height and service distribution systems may be extensive, complex, and difficult to observe. The weight of equipment, and the potential instability of mechanical components, is of concern. The cognizant operating technical personnel should have emergency plans coordinated with the local emergency control group, and should if possible accompany the inspection team. The inspection team for any complex office bulding should be composed of specially qualified personnel. Manufacturing Plants: Although the size and complexity of service systems in manufacturing plants vary

widely, the standard investigative team should be capable of inspecting and evaluating hazards associated with common industrial plants. Where dangerous materials are present and/or there is risk of fire or explosion current information on such conditions should be on file in the emergency operating centers, and investigative teams provided with a checklist of special hazards. Local fire departments often maintain current files on such potential hazards and inspection teams should have access to this information. Elevators: Because of the complexity of controls and potential operating hazards, an initial cursory inspection should be made and followed by a more detailed inspection by specialists. Elevators should be posted as nonoperable unless their continued operation is essential under emergency conditions.

HAZARD POSTING AND REINSPECTION

After an inspection team has concluded its evaluation, all buildings will be posted with one of the following: (1) inspection notice posted: minor damage, no hazard to occupants, (2) posted green: badly damaged, possible hazard to occupants, limited entry only, (3) posted blue: major damage, safety of building questionable, entry prohibited, (4) posted red: major damage representing a severe hazard, in a state of incipient collapse, entry prohibited. Local governmental bodies should enact enabling ordinances prohibiting entry into buildings so posted.

A determination that a building must not be occupied can have severe impact on the owner or tenant. Because relatively large aftershocks often occur, weakened buildings possibly may be further damaged. A reinspection of all structures classified as unsafe to occupy or marginal in their first inspection must be required within one week. Reinspections should be more meticulous and complete. The reinspection team should be highly qualified and preferably be licensed structural engineers. A record of the reinspection must be filed with the agency in charge. Copies of these forms should be sent to police and fire departments and to participating state and federal disaster agencies.

REFERENCES:

Recommended Seismic Design Provisions for Buildings, Appendix "Emergency Post-Earthquake Inspection and Evaluation of Damage in Buildings," ATC-3, Applied Technology Council, Palo Alto, California (to be published).

A NONLINEAR SEISMIC DESIGN PROCEDURE FOR NUCLEAR FACILITIES

by

H. Kamil[I] and V. V. Bertero[II]

SYNOPSIS

A procedure is presented for an efficient, economic, and reliable earthquake resistant design for nuclear facilities. The main emphasis is on frame type structures, such as auxiliary or turbine buildings of a nuclear power plant complex. Reactor containment structures are also discussed. The design procedure for frame type structures consists of a step-by-step nonlinear, inelastic, optimum design approach, including proposed preliminary and final design techniques. Probabilistic methods for determining the reliability of designs so obtained are also reviewed.

INTRODUCTION

Safety and economy have become the primary considerations in the design of nuclear facilities. Different safety requirements may, however, apply to different structures and components in a nuclear power plant complex, depending upon the importance of the structure and the contained equipment, and the consequences of potential accidents related to that structure. In this context, the reactor containment structure (and the contained emergency cooling piping systems) are the most important and require special treatment in their analysis and design. Other structures, such as auxiliary buildings and turbine buildings, are relatively less important than containment structures from a safety point of view.

For the seismic design of a containment structure, it is therefore necessary that under a safety level earthquake, there should be no (or minimum) damage. The stresses should therefore remain well within the allowable limits, though it might result in uneconomical designs. For auxiliary, turbine, and other structures of a nuclear power plant complex, however, it is desirable to go into the nonlinear range so that a rational, economical, as well as reliable, design can be obtained. A seismic design procedure is presented here in view of the above overall considerations.

In general, the main objective of any designer is to obtain a design which should be economical, reliable, and serviceable. Recent advances in computer technology have lead to the development of sophisticated analysis procedures for complex structural systems. However, use of a sophisticated analysis procedure does not necessarily guarantee a design which would satisfy the necessary criteria of safety and serviceability. There are several other factors involved which would determine what kind of design is finally obtained. One of them is the desirability of a good and

---

I Dr. Hasan Kamil, Manager — Technical Development and Senior Project Engineer, Engineering Decision Analysis Company, Inc., 480 California Avenue, Palo Alto, California 94306

II Professor V. V. Bertero, Department of Civil Engineering, University of California, Berkeley, California 94720

efficient preliminary design. If the preliminary design of a structure is "poor," repeated analyses of such a design, regardless of how sophisticated the analysis procedure may be, would usually lead to an improved "poor" design. Another factor on which obtaining a good and efficient design would depend is the design concept used. These two factors would generally determine how the strengths and the stiffnesses of members are distributed through the whole structure, which in turn would determine the lateral story force (inertial force) distribution transmitted from bottom to top when the structure is subjected to a strong ground motion.

In addition, it is important that some kind of optimization procedure is used to be able to obtain the most economical design practically possible, which would at the same time satisfy all the desired design criteria. An approximate and informal optimization procedure may be used based on the judgment of the designer. On the other hand, if the designer is not very experienced, it may be desirable to use a formal optimization procedure such as Linear or Nonlinear Programming.

Finally, for a realistic estimation of the reliability of a design, it is desirable to use a combination of deterministic and probabilistic techniques. Simplified probabilistic approaches such as second-moment format may be employed for this purpose.

PROPOSED DESIGN PROCEDURE

The proposed design procedure is divided into two different parts, depending on the importance and the safety category of the structure and the structural system used. For auxiliary and turbine buildings, which are generally steel or concrete frame type structures, a nonlinear, inelastic, optimum design procedure is proposed, along with a simplified probabilistic approach to estimate the structural reliability of the final design. For the reactor containment structure, which usually consists of concrete shell or shear-wall systems, a linear, elastic design procedure is proposed, along with a simplified probabilistic approach to estimate the structural reliability.

FRAME TYPE AUXILIARY AND TURBINE STRUCTURES

A detailed description of a similar basic procedure developed by the authors, along with an example, was presented in References 1, 2, and 3. A very brief description of this procedure will therefore be presented here due to a shortage of space with details of the latest modifications only, where applicable.

In developing this proposed design method, an attempt is made to obtain the most economical (minimum weight) design practically possible. To this end, Linear Programming technique is utilized. Economic considerations also require that for a major dynamic loading (e.g., a major earthquake), the structure should be able to absorb and dissipate large amounts of energy through inelastic deformations. An inelastic model is therefore used here, so that the design is based on the limit state that actually controls it. A strong column-weak girder design concept is utilized so that all the large inelastic deformations are confined to girders only. This ensures that there would be no column failures resulting in disastrous structural failure, and also that there would be a more reasonable story load distribution through the height of the structure. In the absence of such a design concept, if a certain story yields under the action of a strong ground

motion, the story shear transmitted above that story would be equal to the capacity of that particular story and therefore the design of that story would govern the design of stories above it.

The proposed design procedure consists of a step-by-step computer-aided procedure which is basically carried out in the following major steps: (1) Preliminary Analysis; (2) Preliminary Design; (3) Analysis of Preliminary Design; (4) Final Optimum Design; (5) Analysis of Final Optimum Design; and (6) Determination of the Reliability of Final Optimum Design.

In the first step, after careful analysis of the data, serviceability and safety requirements are established and the corresponding design spectra from USNRC Regulatory Guide 1.60 are utilized. These linear elastic response spectra are then reduced to take into account the inelastic behavior corresponding to a properly selected pattern of values of ductility. Based on values of periods and mode shapes selected from tabulated values obtained from experimental and analytical investigations already carried out on similar frames, preliminary story shear forces are obtained using a mode superposition procedure. A step-by-step iterative procedure is used to achieve a proper combination of the values for the fundamental period, drift, damping, ductility, story shear forces, and seismic coefficient. When this is achieved, the values so obtained for the story shear forces are the ones used for the subsequent preliminary design of the structural members.

The preliminary design consists of a story-wise strong column-weak girder limit design using optimization to obtain first the sizes of the girders and then the sizes of the columns. The columns are designed with a larger factor of safety than the girders. This is done to account for the greater uncertainties involved in the design of columns, the probable effects of biaxial shear and bending, and possible increase in axial forces due to the other horizontal component as well as the vertical component of ground shaking. The girders are designed so that the weaknesses are uniform at each floor level as well as throughout the height of the building. This is required to avoid early yielding at one particular "critical region" of a girder, and, therefore, to reduce the possibility of a considerably higher rotation ductility demand in this region. Furthermore, in order for the application of modal superposition procedure and the use of a reduced response spectrum to provide satisfactory results, it is desirable that critical regions of the entire structure yield simultaneously. This preliminary design can be carried out by hand computations or through the use of a computer program developed for this purpose, and is based on elasto-plastic analysis using a single story subassemblage and including the P-Δ effects. Working load drift limitations can be imposed and an approximate cost minimization technique using linear programming can be applied (Ref. 1, 2, and 3).

The static response of the preliminary designed subassemblages and of the whole structure, and then the dynamic response of the whole structure are obtained using two nonlinear computer programs (Ref. 1, 2, and 3) based on an elasto-plastic moment-curvature relationship with linear strain-hardening. The inelastic rotations, which are assumed to take place at localized plastic hinges, are computed to provide a measure of the plastic rotation demand on the critical regions of the structure. The P-Δ effects and the influence of axial force on column yielding strength and flexural stiffness are also taken into account. Application of a nonlinear dynamic analysis program permits the evaluation of the response of the preliminary designed structure to different earthquake motion time-histories compatible with the design spectra.

From the outputs of the above two programs, maximum values as well as time-histories of the curvature, rotation, and displacement ductilities are obtained. If these ductility values and their variations agree closely with those preselected, and if the pattern of maximum shear forces obtained from the dynamic analysis as well as that of the shear capacities of each story obtained from the static analysis is close enough to the pattern of story shears used in the preliminary design, the values of this last set of shears are adjusted in accordance with those found from the two analyses, and they are then used for the final optimum design of the frame. If the agreement of one or more of the above parameters is poor, the results obtained in the preliminary analysis and design must be reviewed and modified until satisfactory agreement is achieved.

The final optimum design procedure is similar to that used for the preliminary design except that it is completely automated and uses more sophisticated story subassemblages and more formal linear programming technique.

Analyses of the structure to several different earthquake time-histories compatible with the NRC design response spectrum are then carried out using the nonlinear dynamic analysis computer program MULTY, developed by the senior author (Ref. 1 and 2). Dynamic response analyses of the designed structure to a set of different ground motion time-histories, covering as many characteristics as possible which can be critical to the behavior of the structure, are necessary because of the uncertainties involved in predicting the future earthquakes. Artifical time-histories compatible with the design spectra are generated using the computer program, SEQGEN, developed by the senior author and colleagues.

Finally, the reliability of the final optimum design is estimated by using simplified probabilistic methods. Probability of failure of each story is determined by considering it as a "parallel" or "fail-safe" type of system, and using the governing strong column-weak girder failure mechanism with the actual story shear applied at that story, already determined from the deterministic analysis above. Failure of the structure is assumed to result if any single story fails and the whole structure is therefore considered to be similar to a "series" or "weakest-link" type of system. An alternate procedure where a combined deterministic-cum-probabilistic approach is used is also being developed (Ref. 7). In this procedure, the deterministic and probabilistic techniques are used side-by-side when performing the nonlinear dynamic time-history analyses. Markov processes are used for the probabilistic part of the analyses.

The different steps of the basic methodology of this procedure are discussed in detail in References 1, 2, and 3. The procedure was applied to a 10-story, 3-bay unbraced frame (Ref. 1 and 2).

REACTOR CONTAINMENT STRUCTURE

The design of reactor containment structure is based on a linear, elastic approach. The preliminary design is usually already established on the basis of considerations other than seismic, such as radiation shielding requirements, protection against missile impact, etc. A linear dynamic seismic analysis is then performed using axi-symmetric or three-dimensional finite-elements Because the structural design of the containment is already established prior to seismic analysis, as mentioned above, and the seismic forces may not generally govern the design, it is not necessary to use any optimization procedure. The main objective is to check the adequacy of the structure for the

design seismic loading to determine if the seismic stresses are within the allowable limits. The reliability of the containment structure can then be estimated using probabilistic approaches, as described briefly in the next section.

RELIABILITY OF DESIGN

Reliability of a structure is not a physical, directly quantifiable property. The conventional way of measuring structural reliability is through the use of a "factor of safety." This can be useful to some extent for comparing the reliability of two very similar structural systems behaving in a very similar way under the action of very similar loads. However, for an absolute measure of reliability, this concept loses its usefulness. Probabilistic methods need to be used for this purpose.

Application of probabilistic methods in estimating the probability of failure of complex structural systems, such as frame type auxiliary and turbine buildings and reactor containment structures, becomes very difficult mainly because of the presence of a large number of possible failure modes as well as a large number of random variables, many of them dependent. Simplified approaches can be used to obtain an estimate of the reliability of a structural system, e. g., use of second-moment theory.

If L and R respectively denote the load and the corresponding structural resistance, the probability of structural failure can be written as

$$P_f = P(R \leq L)$$

The evaluation of such a probability requires the knowledge of probability distribution functions of R and L, which may sometimes become impractical and difficult to obtain. Second-moment theory can therefore be used to get a reasonable estimate of the probability of structural failure.

For the frame type structures, probability of failure of each story may be determined by considering it as a "parallel" or "fail-safe" type of subsystem and using the governing failure mechanism with the actual story shear applied at that story level, already determined from the deterministic analyses. Failure of the structure is assumed to result if any single story fails, and the complete structural system is considered to be similar to a "series" or "weakest link" type of system.

A containment structure can fail in a number of different modes and at different critical locations, e. g., cylinder (or hemisphere) in longitudinal direction at spring line, cylinder in hoop direction, and cylinder at base in longitudinal direction (possible yielding of reinforcing bars), etc., for a cylindrical containment structure with a hemispherical top. The structural resistances to failure at the same locations are also obtained. The failure of containment under seismic loading is then expressed as $P(F_{ST}/A)\ P(A)$, where F_{ST} indicates the structural failure due to the combination of overload and containment understrength, and A denotes the combined occurrence of gravity and semipermanent loads and a safety level earthquake. If the containment structure can fail in a number of different modes, $F_{ST1}, F_{ST2}, \cdots,$ these failure modes not necessarily being mutually exclusive, $P(F_{ST}/A) = \sum_M P(F_{SM}/A)$. The probability, $P(A)$, can be developed assuming, for example, that the occurrence of failure follows the law of Poisson arrivals. The value of $P(F_{ST}/A)$ can be developed mainly from structural considerations, using the possible failure modes.

An alternate and perhaps more sophisticated approach to determine the system reliability, e. g., of a frame type structure for auxiliary or turbine buildings, and at the same time determine the probabilistic-cum-deterministic response of the system, is to use the combined deterministic-cum-probabilistic approach proposed by the senior author in Reference 7. Along with the step-by-step deterministic time history dynamic analyses, Markov transition probability matrices are determined for each member at each time step, depending on the "condition" of that member at that instant. The "most probable stiffness matrix" is then determined and the procedure is continued for all the remaining time (load) steps, until the entire loading time history is applied to the structural system.

CONCLUSIONS

A seismic design procedure is described for nuclear facilities. For frame type auxiliary and turbine buildings, a nonlinear, inelastic, optimum design procedure is proposed, which consists of several steps including preliminary design, analysis of the preliminary design, final design with optimization, and the determination of the reliability of the final design using probabilistic methods. Most of the important factors affecting the design, viz. fundamental period, ductility factor, damping coefficient, seismic coefficient, story drift, etc. are included — thereby enabling the design procedure to exert far greater control over the seismic design than the conventional design procedures. References 1, 2, and 3 describe this procedure in considerable detail. The use of probabilistic methods provides a reasonable estimate of the reliability of the structural system for the design safety level earthquake. For the containment structure, it is proposed that the design be carried out in the linear, elastic range, and the reliability of the design is again estimated using probabilistic methods.

BIBLIOGRAPHY

1. H. Kamil, "Optimum Inelastic Design of Unbraced Multistory Frames Under Dynamic Loads," thesis presented to the University of California, Berkeley, California, 1972, in partial fullfillment of the requirements for the degree of Doctor of Philosophy.
2. V. V. Bertero and H. Kamil, "Nonlinear Seismic Design of Multistory Frames," Canadian Journal of Civil Engineering, National Research Council of Canada, Vol. 2, No. 4, December 1975.
3. H. Kamil and V. V. Bertero, "A Methodology for Efficient and Reliable Design of High-rise Structures Under Dynamic Loads," Proceedings, Fifth European Conference on Earthquake Engineering, Istanbul, Turkey, Sept. 1975.
4. F. Moses, "Reliability of Structural Systems," Journal of the Structural Division, American Society of Civil Engineers, Vol. 100, ST9, September 1974, pp. 1813-1820.
5. H. Kamil, R. L. Sharpe, and R. H. Scanlan, "Analysis of an Aircraft Impact on a Reactor Building," Third SMIRT Conference, London, Sept. 1975.
6. H. Kamil and V. V. Bertero, "Nonlinear Seismic Design of Multistory Frames," Second Canadian Earthquake Engineering Conference, Ontario, Canada, June 1975.
7. H. Kamil, "Computer-aided Deterministic-cum-probabilistic Approach to the Design of Structures Under Extreme Loading Conditions," Proceedings, Second National Symposium on Computerized Structural Analysis and Design, George Washington University, Washington, D. C., March 1976. (Also to be published in the Journal of Computers and Structures.)
8. Reliability Approach in Structural Engineering, Maruzen Company, Ltd., Tokyo, 1975.

DYNAMIC BEHAVIOR OF AN ELEVEN STORY MASONRY BUILDING

by

R.M. Stephen[I] and J.G. Bouwkamp[II]

SYNOPSIS

The results of a forced vibration study of an eleven story reinforced masonry structure are compared to a dynamic analysis. The experimental work determined the natural frequencies, mode shapes, and damping values. Considerable flexibility of the foundation was noted in the experimental studies. The analytical model was developed with both a fixed and flexible base. Experimental and analytical resonance data are compared.

INTRODUCTION

The design of multistory structures subjected to dynamic forces resulting from foundation motions require a consideration of both the characteristics of the ground motion and the dynamic properties of the structure. The availability of high speed digital computers and the sophistication of the idealization of structures and the computer model formulation of the structure have made available the elastic, and in certain structural systems, the inelastic response of structures when subjected to earthquakes. However, the accuracy of the results in large measure depend upon the computer model formulation of the structure and its foundation. In order to determine the accuracy of the calculated results and to accumulate a body of information on the dynamic properties of structures, especially when these structures have novel design features, a number of dynamic tests have been conducted on full-scale structures (1).

For the above reasons a dynamic test was performed on the Oak Center Towers, Oakland, California (2).

DESCRIPTION OF BUILDING

The Oak Center Towers is an eleven story structure located in Oakland, California. The 100 foot high building has an overall plan of 85 feet by 200 feet. The building is offset in the middle by approximately 16 feet so that it does not have a pure rectangular plan. It is constructed with reinforced concrete block shear walls and prefabricated prestressed concrete slab elements. The elevator shaft is located in the center south section of the structure with stairwells at either end. Figure 1 shows the east elevation of the building.

The building is designed as a housing development for the elderly and is therefore modular in concept. The building is serviced by two elevators in the center south section of the structure. Stairwells are located on either end of the building. Figure 2 shows a typical floor plan for the second through eleventh floors.

The vertical and horizontal load carrying systems are reinforced concrete masonry shear walls in both the transverse and longitudinal directions. These walls rise from the first floor and run up to the roof except in one section on the south end of the first floor where the dining

---

I Principal Development Engineer, University of California, Berkeley.
II Professor of Civil Engineering, University of California, Berkeley.

room is located. In this location the walls terminate at the second floor and a reinforced concrete frame system carries the loads to the foundations.

The foundations are in general spread footings under each of the walls from 4 feet to 6 feet in width and eighteen inches thick.

The compressive strength of the masonry unit is 3000 psi below the eighth floor and 2000 psi above the eighth floor. All of the cells in the masonry were grouted with 4000 psi hard rock concrete.

The transverse walls are made up of eight inch wide blocks from the first floor to the roof. The longitudinal walls, which basically run down each side of the corridor, are twelve inch wide block up to the fifth floor and eight inch block from the fifth floor to the roof.

The minimum reinforcement consisted of two number 4 bars at 24 inches on centers vertical and the same horizontal for the twelve inch block and in the eight inch block one number 4 bar at 24 inches on center, both vertically and horizontally. Special reinforcement is added at wall ends, corners and where two walls connect. This consisted mainly of number 8 bars up to the eighth floor then number 6 bars from the eighth to the tenth floors and number 5 bars from the tenth floor to the roof.

The floor system consists of precast prestressed planks 6 inches deep and 40 inches wide spanning between the transverse walls. A 2 inch lightweight concrete topping is placed over these planks.

EXPERIMENTAL PROGRAM

Forced vibrations were produced by two rotating-mass vibration generators or shaking machines mounted on the 11th floor of the building and oriented so as to induce the maximum forces in the East-West and North-South directions as shown in Figure 2. A complete description of the vibration generators is given elsewhere (1,3).

The transducers used to detect horizontal floor accelerations of the building were Statham Model A4 linear accelerometers, with a maximum rating of ± 0.25g. The electrical signals for all accelerometers were fed to amplifiers and then to a Honeywell Model 1858 Visicorder. For the translational motions the accelerometers were located near the center of the floor and oriented so as to pick up the appropriate East-West or North-South accelerations. For recording the torsional motion accelerometers were properly oriented near the north and south ends of the building. To determine the resonant frequencies of the building the accelerometers were located on the 11th floor. In addition vertical accelerations were taken at 6 locations on the 1st floor to determine the foundation motion. The mode shapes were evaluated from records taken at all of the floors including the roof.

MATHEMATICAL MODEL

A mathematical computer model of the Oak Center Tower Building was formulated to assess its dynamic characteristics. The model was formulated using both a rigid base and a flexible base. TABS, a general computer program developed by the Division of Structural Engineering and Structural Mechanics of the Department of Civil Engineering at the University of California, Berkeley, was used to calculate the frequencies and mode shapes of the building. A complete description of this program is given in reference (4).

The program considers the floors rigid in their own plane and to have zero transverse stiffness. All elements are assembled initially into planar frames and then transformed, using the previous assumption, to three degrees of freedom at the center of mass for each story level (2 translational, 1 rotational). Coupling between independent frames at common column lines is ignored. The basic model of the building was formulated as a system of independent frames and shear wall elements interconnected by floor diaphragms which were rigid in their own plane and fixed at the 1st floor level.

The story masses are obtained from the approximate dead loads per floor. These lumped weight values include the floor slabs and masonry walls for each floor level.

During the experimental phase of the work significant vertical motion was recorded at the first floor level in the building. Therefore as a second basic approach the model was allowed to have a flexible base.

Based on the measurements of the ground accelerations at the first floor of the building the following approach was used.

It was assumed that the accelerations measured were due primarily to first mode response. As such, a first mode shape was assumed and acceleration values at each mass point computed. These were used to calculate an effective overturning moment which when compared with the measured ground accelerations allowed an assessment of the base rotational and translational stiffness. An additional basement story was added to the structure with the stiffness values as determined above assigning to the elements as a means of modeling the rotational and translational flexibility.

RESULTS

In the forced vibration tests, two translational modes in the East-West and North-South directions were excited, as well as, the one torsional mode. Typical frequency response curves in the region of the resonant frequencies are shown in Figure 3. The typical vertical and horizontal modes shapes are shown in Figure 4. The resonant frequencies and damping factors evaluated from the experimental data along with the analytical results are summarized in Table 1.

CONCLUSIONS

In comparing the forced vibration as well as the analytical solution it is noted that there is reasonable agreement in the first two modes, however, this does not hold as true for the higher modes. The analysis indicated that in the first E-W mode there was a significant contribution of torsion in this mode. This is also noted in the forced vibration study where the first E-W mode and the first torsional mode (2.78 and 2.83 cps, respectively) were very close together.

The predominant feature which came out of the analytical solutions was the effect of the foundations on the response of the structure. The fundamental frequency was almost half for the flexible foundation as for the rigid foundation (2.45 versus 4.13 cps, respectively). The analysis of very rigid structures on flexible foundations must consider the soil-structure interaction phenomena or the solution could be as much as 100 percent off.

It is apparent that for structures where the in-plane stiffness of the floor system is less or comparable to the stiffness of the lateral load resisting system, the assumption that the floors are rigid in their

own plane does not seem to hold true.

This same response regarding the flexibility of the foundation and the in-plane bending of the floor system was also noted in some recent forced vibration studies carried out on a building in Sarajevo, Yugoslavia (5).

The damping values determined from the forced vibration studies varied from about 2 percent to almost 9 percent. The higher damping values could be due to the flexibility of the foundations and their contribution to the response of the building.

TABLE 1 COMPARISON OF RESONANT FREQUENCIES AND DAMPING RATIOS

EXCITATION	MODE							
	1				2			
	FORCED VIBRATION		ANALYSIS		FORCED VIBRATION		ANALYSIS	
	FREQ cps	DAMP %	FIXED BASE	FLEX BASE	FREQ cps	DAMP %	FIXED BASE	FLEX BASE
E-W	2.78	6.4	4.50	2.45	5.82	2.1	14.49	4.13
N-S	3.30	8.8	4.98	2.98	5.93	2.8	5.08	--
Torsional	2.83	2.6	--	--	--	-	--	--

ACKNOWLEDGMENT

The authors gratefully acknowledge the financial support provided by the National Science Foundation under Grant NSF GK-31883. They also wish to thank the owner, the Episcopal Homes Foundation, the Architect, Kennard and Silvers; and the contractors, Williams and Burrows and F.M. Taylor and Son, Inc., for their help and cooperation during the tests.

BIBLIOGRAPHY

1. Wiegel, R.L., Earthquake Engineering, Prentice-Hall, Inc., 1970.
2. Stephen, R.M., Hollings, J.P., Bouwkamp, J.G., Jurukovski, D., "Dynamic Properties of an Eleven Story Masonry Building", Earthquake Engineering Research Center, Report No. EERC 75-20, July 1975.
3. Hudson, D.E., "Synchronized Vibration Generators for Dynamic Tests of Full-Scale Structures", Earthquake Engineering Research Laboratory Report, California Institute of Technology, 1962.
4. Wilson, E.L., Dovey, H.H., "Static and Earthquake Analysis of Three-Dimensional Frame and Shear Wall Buildings", Earthquake Engineering Research Center, Report No. EERC 72-1, May 1972.
5. Petrovski, J., Jurukovski, D., Percinkov, S., "Forced Vibration Test of a 9 Story Building in Sarajevo, Constructed by the System 'Vranica'", Report DTL 75-4, IZIIS, University of Skopje - Yugoslavia, Skopje, May 1975.

FIG. 1 OAK CENTER TOWERS, OAKLAND, CALIFORNIA
(EAST ELEVATION)

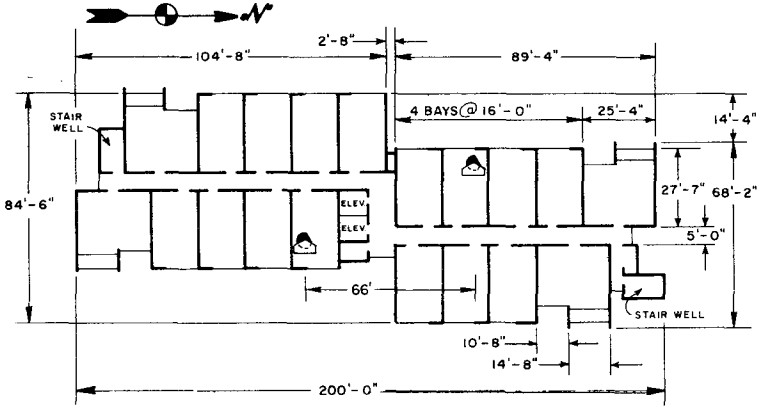

FIG. 2 TYPICAL FLOOR PLAN

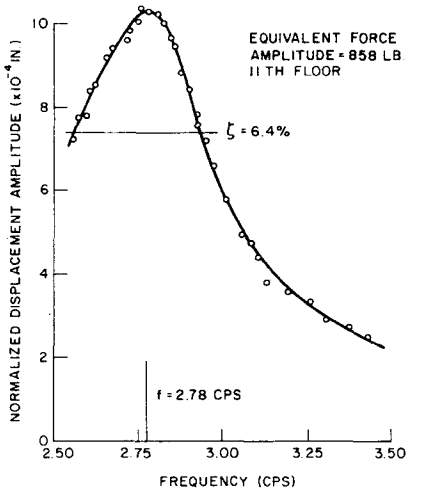

FIRST MODE EAST-WEST

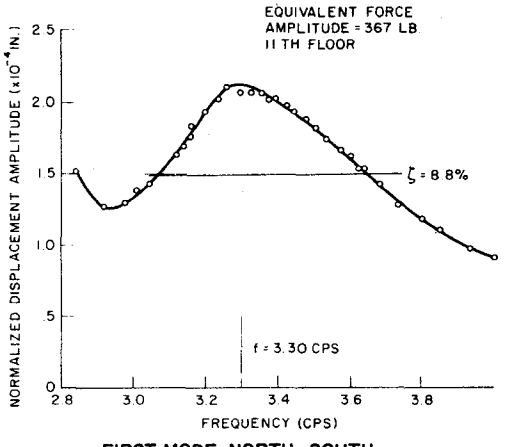

FIRST MODE NORTH-SOUTH

FIG. 3 TYPICAL FREQUENCY RESPONSE CURVES

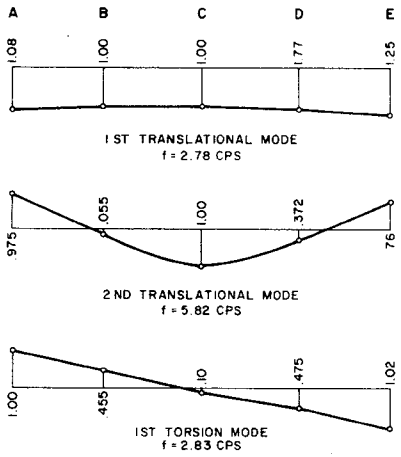

HORIZONTAL MODE SHAPES AT 11TH FLOOR, E-W

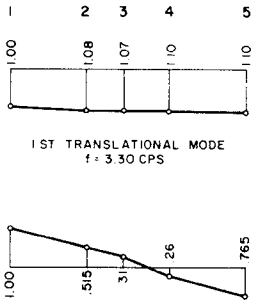

HORIZONTAL MODE SHAPES AT THE 11TH FLOOR, N-S

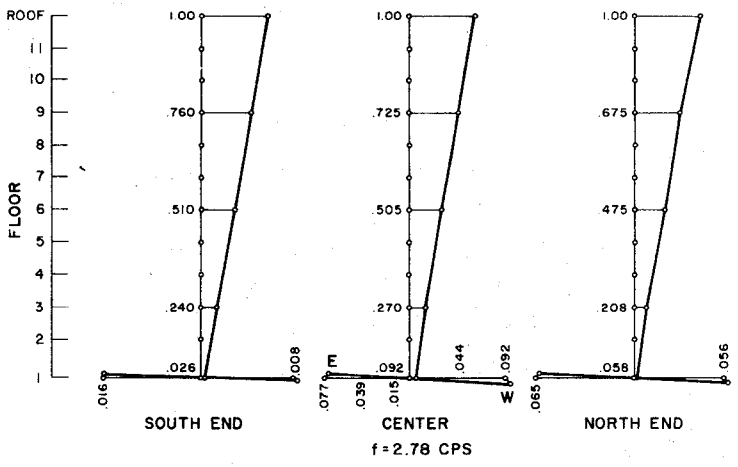

VERTICAL MODE SHAPES AT THREE SECTIONS OF BUILDING, TRANSLATIONAL FIRST MODE, E-W

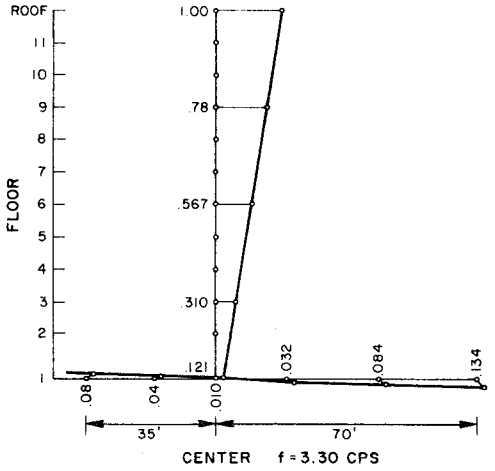

VERTICAL MODE SHAPES, TRANSLATIONAL FIRST MODE, N-S

FIG. 4 TYPICAL MODE SHAPES

Mathematical Modeling of a Steel Frame Structure

David T. Tang[1] and Ray W. Clough[2]

SYNOPSIS

By comparing the computed dynamic response with the performance of a three story steel frame structure observed during shaking table tests, three different mathematical models of the structure are evaluated. The testing was done in two phases: first with under-designed joint panel zones, and second after reinforcing the panel zones. The study demonstrates that a rationally formulated mathematical model can predict adequately both the linear and nonlinear seismic response of steel frames.

Introduction

Many analytical procedures for calculating the nonlinear dynamic response of structures have been developed in recent years. The accuracy of the results obtained with such programs depends, however, on the validity of the mathematical model chosen to represent the structure. Mathematical models often are derived from experimental studies of typical structural components and subassemblages; but their adequacy in depicting dynamic behavior can only be assessed by correlation with the results of tests on complete structures subjected to simulated earthquake motions. The Earthquake Simulator Facility at Berkeley was designed to provide this correlation capability, and results from tests of a three story steel building frame will be considered in this paper. The testing was done in two phases: during Phase I, the joint panel zones were deliberately underdesigned so that they would yield; during Phase II, 3/8 inch doubler plates were welded to each side of the panel zones so that yielding would be forced into the girder or column sections. Preliminary reports on these tests have appeared (1,2,3); subsequently two comprehensive reports were published on the experimental and analytical work, respectively (4,5). In this paper, three mathematical models used for data correlation are described and their relative efficiency is demonstrated.

Test Structure and Instrumentation

The test structure consists of two identical three story moment resistant steel frames, 17'-4" high by 12'-0" span (see Fig. 1), interconnected by rigid floor diaphragms. Columns and girders are W5x16 and W6x12; standard welded connections were provided for Phase I tests, and the doubler plates added for Phase II, as mentioned above. Concrete blocks weighing 8000 lbs were supported at each floor level in a way that did not alter the member stiffnesses. The column base plates were bolted to the shaking table through heavy steel footings to provide fixed end conditions. The dynamic performance of the frame was monitored by 67 instrumentation channels during Phase I, and by 85 channels during Phase II. Each channel was scanned 50 times per second and the signal recorded in digital form on a magnetic disc(6). Instrumentation included accelerometers and displacement gages at the floor levels, as well as strain and curvature transducers at selected column and girder locations; during Phase I, panel zone strains were measured by strain gages and displacement gages (see Figs. 2 and 3).

Test Results

During Phase I with the structure bolted to the laboratory floor, the first mode, free-vibration frequency and damping ratio were found to be 2.24 Hz

[1] Assistant Professor of Engineering and Applied Sciences, State University of New York at Buffalo, N. Y.

[2] Professor of Civil Engineering, University of California, Berkeley, Ca.

and 0.1% respectively; during Phase II with the structure mounted on the shaking table the corresponding quantities were 2.40 Hz and 0.5%. Four shaking table tests will be discussed here: Phase I tests EC100-I and EC400-I; Phase II tests EC400-II and EC900-II. All used the 1940 El Centro N-S record as the horizontal input signal. Table accelerograms for these tests are shown in Fig. 4; peak accelerations for the four cases were 0.16g, 0.53g, 0.25g and 0.57g respectively. The response was linear elastic during EC100-I and EC400-II; nonlinear strains were produced during the other two tests, as may be seen in Figs. 5 and 6 where the yield strain level (45.9 ksi) is indicated by the horizontal lines. The panel zone distortion ductility factor was found to be about 5 in test EC400-I. Maximum end rotation ductility factors during test EC900-II were 1.9 and 1.2 for columns and girders, respectively; permanent set was seen clearly at the girder ends, but only minimally at the column ends.

Mathematical Models and Data Correlation

For the purpose of calculating dynamic response results to compare with the test data, computer program DRAIN-2D(7) was used; both linear and nonlinear analyses were made with the same program, merely by setting the yield limit appropriately. The first mathematical model (designated Model A) included shear, axial and flexural deformations of columns and girders -- considering their clear span lengths; panel zones were treated as additional shear deformation elements. Masses were assumed lumped at story levels on the column lines, and mass-proportional damping was prescribed giving 0.5% critical in the first mode. The response to EC400-II was computed with this model; the third floor displacement result is shown in Fig. 8. The poor correlation with the observed data is due mainly to the first mode analytical frequency (2.44 Hz) being much higher than the apparent frequency observed during the test (2.25 Hz), even though it agrees well with the free vibration result (2.40 Hz). To demonstrate the source of the poor correlation, Model B was developed from Model A merely by using the center-to-center column lengths rather than clear span (Fig. 7B). The fundamental frequency provided by Model B is 2.24 Hz, and the response given by it is seen in Fig. 9 to correlate well with the observed result.

The third model, Model C, was developed from Model A by including the rotational flexibility of the shaking table (provided by two vertical springs). The spring stiffnesses were adjusted to provide the observed response frequencies (see Table I), otherwise the model was identical to Model A. Correlations of Model C results with observed data are shown in Figs. 10-13. Linear response to EC400-II, for both third story displacement and first floor girder moment are seen in Fig. 10 to correlate perfectly with the test data. The corresponding Phase I linear test (EC100-I) displacement correlation is shown in Fig. 11; to provide this good agreement the first mode damping was taken to be 1.5%. The same damping was used in the analysis of EC400-I, the Phase I nonlinear response, with results shown in Fig. 12. The panel zone yield moment of 170 k-in and 17% post-yield stiffness adopted for this analysis were taken from the experimental results (Fig. 5); dead load and residual stresses were neglected. The final correlation, for the Phase II nonlinear test (EC900-II), is shown in Fig. 13. In this analysis, the post-yield stiffness was set at 8% and 4% for the girders and columns, respectively, reflecting the rather significant yielding which took place. The correlation is generally very good. Note that the plot of girder end rotations compares the observed rotations at the two ends of the same member (not analysis vs. experiment) and shows the significant bias caused by dead load moments.

Conclusions

Based on these correlation studies, the following conclusions may be drawn on the mathematical modeling of steel frame structures.

1. The basic model may be derived from the mass and stiffness properties of the frame components, using clear span dimensions and treating the panel zone as an additional element.

2. It is essential to include the rotational flexibility of the shaking table in modeling the complete dynamic system.

3. Post yield behavior of the members must be specified reliably in both yield level and bilinear stiffness; predicting these from coupon test data may not be easy, due in part to the influence of dead load and residual strains.

4. Further tests will be needed to demonstrate model effectiveness for large nonlinear responses (ductility factors greater than two).

Acknowledgement

Financial support of the National Science Foundation in providing the earthquake simulator, and in funding the test program and data correlation is gratefully acknowledged.

REFERENCES

1. Clough, R. W., et al, "Earthquake Simulator Test of a Three Story Steel Frame Structure," Proc., 5WCEE, Italy, 1973.

2. Clough, R. W. and Tang, D., "Shaking Table Tests of a Steel Building Frame, A Progress Report," EERC Rep. No. 74-8, Univ. of Calif., Berkeley, 1974.

3. Clough, R. W. and Tang, D., "Seismic Response of a Steel Building Frame," Proc., U.S. Nat' Conf. on Earthq. Eng., Michigan, 1975.

4. Clough, R. W. and Tang, D., "Earthquake Simulator Study of a Steel Frame Structure, Vol. I-Experimental Results," EERC Rep. No. 75-6, Univ. of Calif., Berkeley, 1975.

5. Tang, D., "Earthquake Simulator Study of a Steel Frame Structure, Vol II-Analytical Results," EERC Rep. No. 75-36, Univ. of Calif., Berkeley, 1975.

6. Rea, D. and Penzien, J., "Structural Research Using an Earthquake Simulator," Proc., SEAOC, California, 1972.

7. Powell, G. H. and Kanaan, A., "General Purpose Computer Program for Inelastic Dynamic Response of Plane Structures," Proc., 5WCEE, Italy, 1973.

TABLE 1 MODEL PARAMETERS

Test Run	1st Mode frequency (Hz)	Vertical Spring Stiffness (kip/in)	1st Mode Damping (%)
EC400-II	2.312	212	0.5
EC100-I	2.155	212	1.5
EC400-I	2.155	212	1.5
EC900-II	2.279	193	0.5

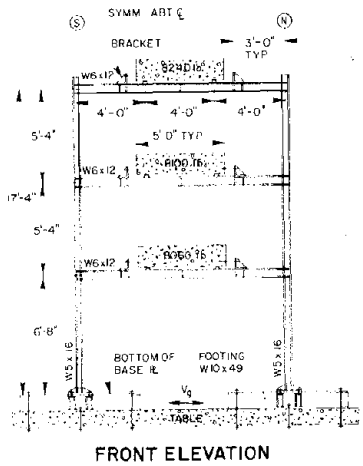

Fig. 1 The Test Structure

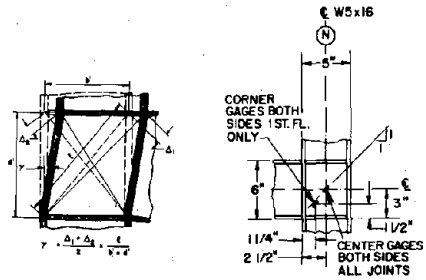

Fig. 2 Deformation Measurements (Phase I)

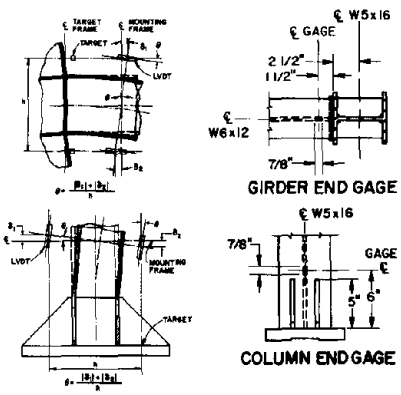

Fig. 3 Deformation Measurement (Phase II)

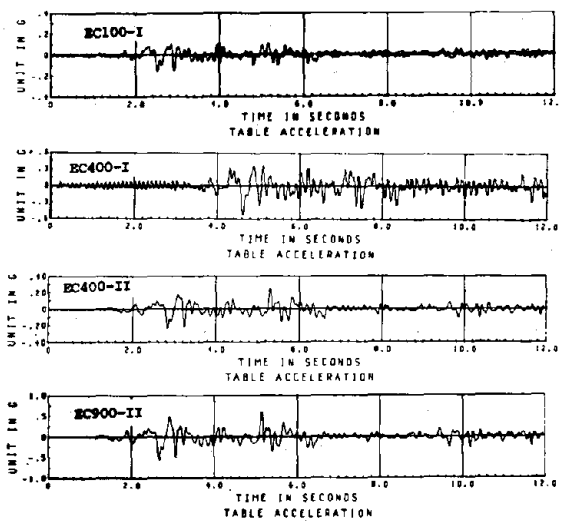

Fig. 4 Measured Table Accelerations

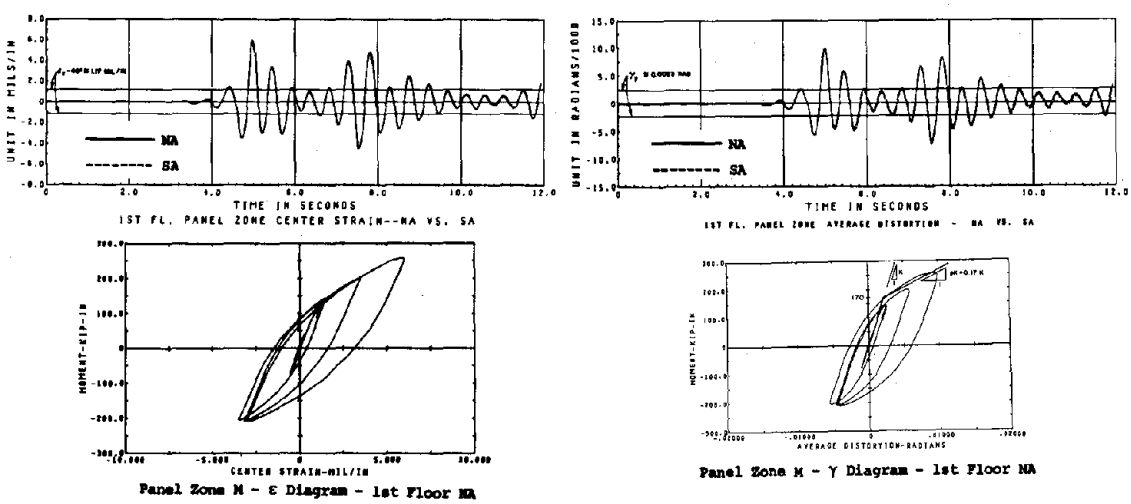

Fig. 5 Measured Nonlinear Structural Responses - EC400-I

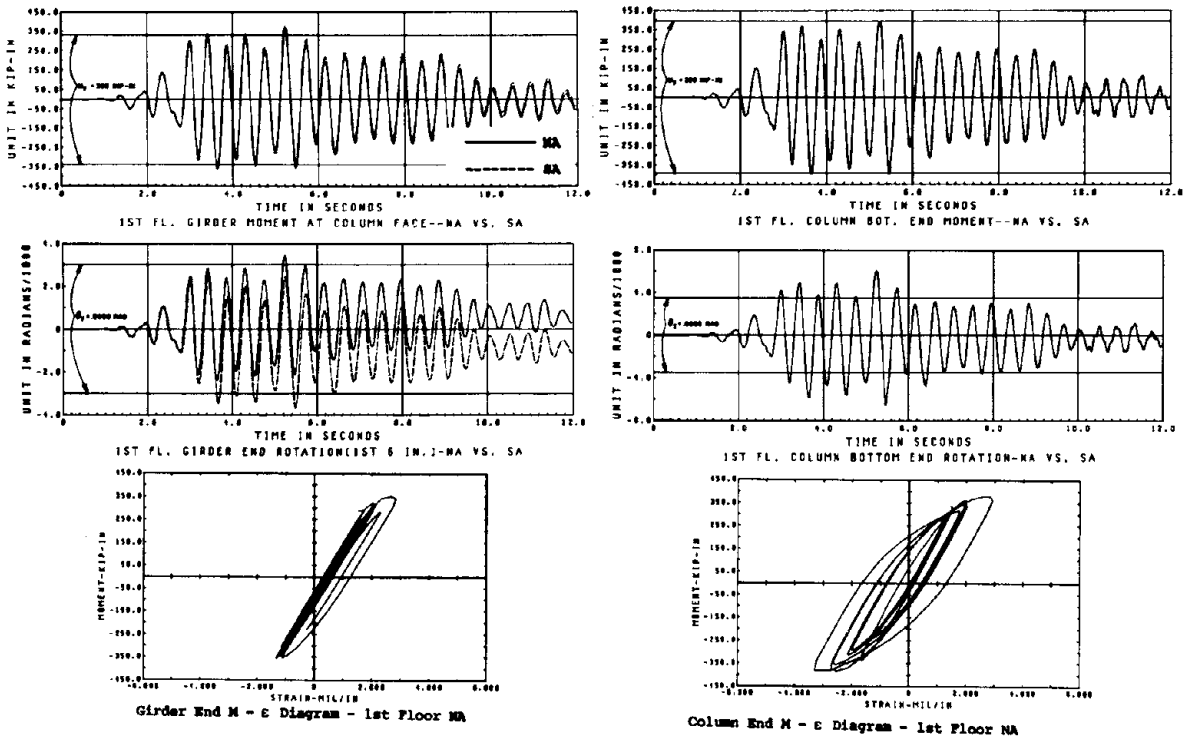

Fig. 6 Measured Nonlinear Structural Responses - EC900-II

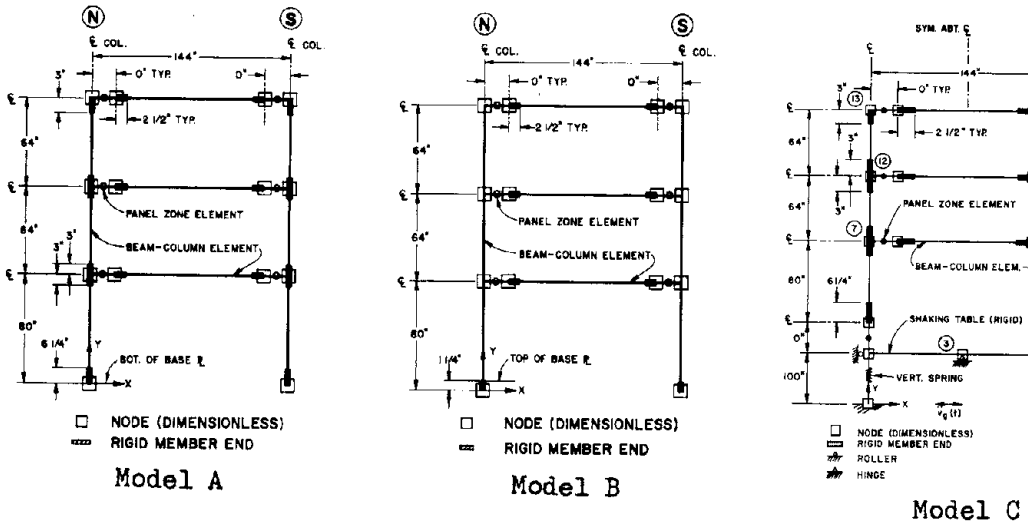

Fig. 7 Mathematical Models

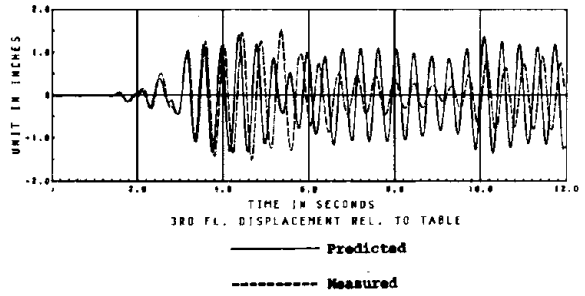

Fig. 8 Data Correlation by Model A (EC400-II)

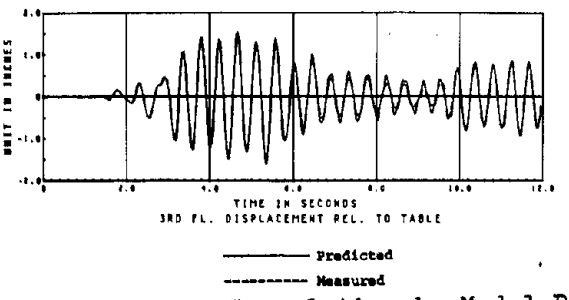

Fig. 9 Data Correlation by Model B (EC400-II)

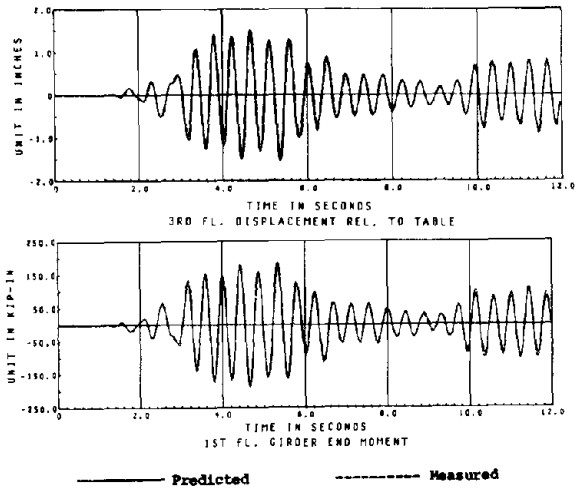

Fig. 10 Data Correlation by Model C (EC400-II)

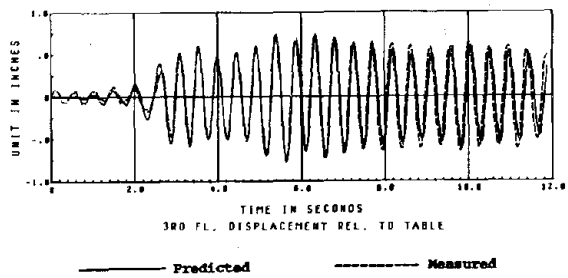

Fig. 11 Data Correlation by Model C (EC100-I)

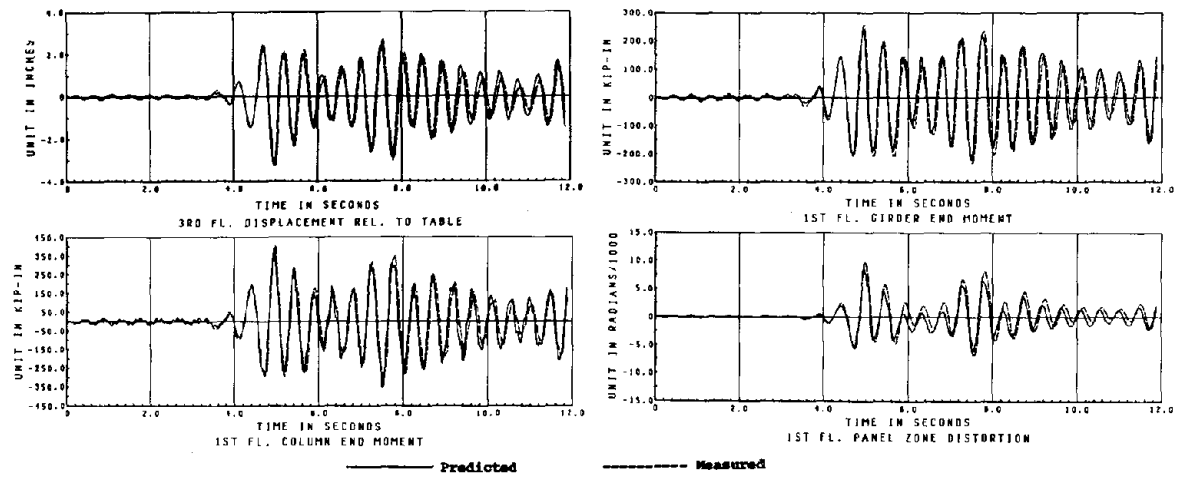

Fig. 12 Data Correlation by Model C (EC400-I)

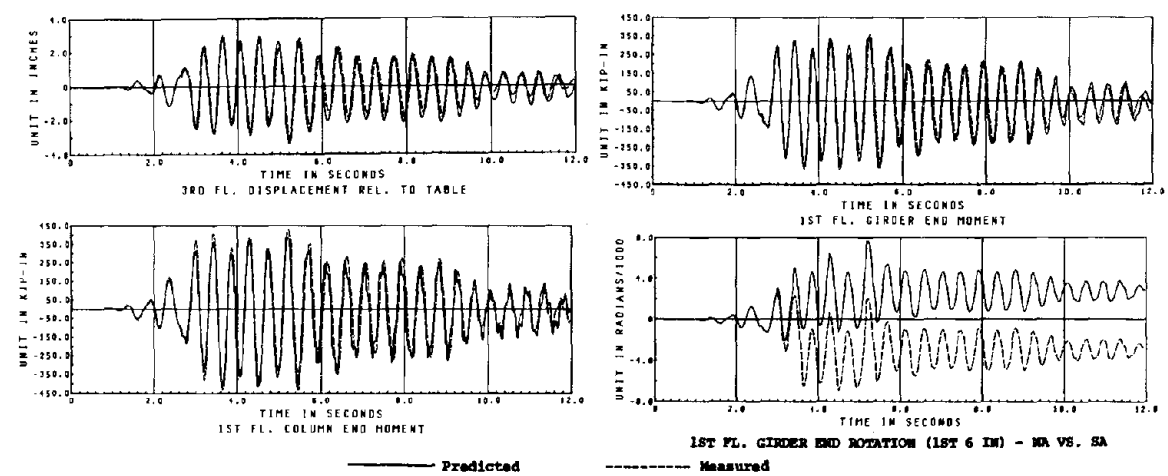

Fig. 13 Data Correlation by Model C (EC900-II)

EVALUATION OF CONTRIBUTION OF FLOOR SYSTEM TO DYNAMIC CHARACTERISTICS OF MOMENT-RESISTING SPACE FRAMES

by

Lincoln Edgar[I] and Vitelmo V. Bertero[II]

SYNOPSIS

Parametric, finite element analyses are used to study the contribution of beam-slab floor systems to the overall stiffness of moment-resisting frames, and to establish graphs of the influence of different floor parameters on the floor stiffness. The graphs are the basis of a practical and sufficiently accurate method for computing the contribution of the floor system to the lateral stiffness of a moment-resisting space frame. The proposed method was found to be more accurate than other methods currently used.

INTRODUCTION

The overall lateral stiffness of a moment-resisting frame is governed by the lateral and rotational stiffness of the columns, and the rotational stiffness of the floor system at its supports. The floor system contributes to the stiffness primarily by restraining the rotation of the columns at the floor levels. This type of restraint has a considerable influence on the overall frame stiffness which can usually be increased more efficiently by increasing the stiffness of the floor system rather than that of the columns. In general, a floor system of a moment-resisting frame building consists of a floor slab that is cast monolithically with the floor beams and thus becomes an integral part of the resisting frames. Studies have shown(1) that the lateral stiffness of such frames, which is an essential parameter in the determination of the dynamic characteristics of the structure, is very sensitive to the assumed participation of the floor slabs.

Several methods for estimating the floor slab's contribution to the lateral stiffness of buildings are presently used in the U.S. The ACI 318-71 Code(2) recommends the "equivalent frame method" whereby a three-dimensional slab-column system is represented by a series of two-dimensional frames which are then analyzed for vertical or horizontal loads acting in the plane of the frames. The frames consist of equivalent columns and beam-slab strips, bound laterally by the centerline of the panel on each side of the column centerlines. This method is difficult to use with most available computer programs, and of questionable accuracy when used to compute the lateral stiffness of buildings. Another approach is the effective slab width method whereby a building is modeled as a series of plane frames and the floor as equivalent beams. The floor beams and the effective width of the slab determine the stiffness of the uniaxial, prismatic equivalent beams. Several effective slab width ratios have been suggested, ranging from 0.50 of the half panel width on each side of the column centerline to values greater than unity. This method greatly simplifies the analysis but is open to serious questions as to its underlying assumptions and its accuracy in predicting building responses.

Objectives and Scope. - The objectives of the studies reported herein are: (1) to evaluate accurately the contribution of the main parameters affecting

---

[I]Graduate Student, University of California, Berkeley, Calif.
[II]Professor of Civil Engineering, University of California, Berkeley, Calif.

the stiffness of a floor system composed of a two-way slab supported on beams between the columns; (2) to develop a practical and reliable method to compute the contribution of such floors to the lateral stiffness of moment-resisting frames; and (3) to evaluate the adequacy and practicability of the method to compute the lateral stiffness of space frame structures. The floor systems consist of a slab of constant thickness, and beams with a 2:1 depth-to-width ratio (i.e., a constant relationship between the flexural and torsional stiffnesses of a beam is maintained). Homogeneous, isotropic, and elastic materials are also assumed. Different slab thicknesses, beam depths, bay aspect ratios and boundary conditions are considered in a parametric study of numerous floors to evaluate their influence on floor stiffness. These results are then used to develop a Stiffness Matrix Method (SMM) to model the stiffness of a composite beam-slab floor by a set of uniaxial members. The SMM is evaluated by using it to compute the lateral stiffness of several simple space frame structures and by comparing these results with those obtained using a finite element procedure and other currently used methods.

SUMMARY OF STUDIES CONDUCTED AND OF THEIR RESULTS

The investigation consisted of establishing an 8 x 8 stiffness matrix for each panel in a floor, based on two rotational degrees-of-freedom (DOF) at each support (Fig. 2). This was accomplished by calculating the moments needed to produce a unit rotation at one DOF while restraining the other DOF at the supports. The slab was modeled (Fig. 1) as a series of rectangular finite elements, where an LCCT9 element formed from four compatible triangles, is used to represent the bending behavior of the slab and a constant strain element with plane stress properties is used to represent its membrane behavior. The beams were modeled as uniaxial, prismatic members, connected by rigid links to the finite element nodes along the beams' centerline. The rigid links impose at the nodes the condition of plane sections in the beam remaining plane. Analytical tests confirmed this method's accuracy when used for slender, flexible floors, but it was found to lose accuracy as the beams' depth-to-span ratio increases and shear begins to dominate the behavior.

The influence of different combinations of the following parameters (Fig. 2) on the stiffness of a two-way slab floor were investigated: (1) the aspect ratio, L_1/L_2, where L_1 and L_2 are the panel span dimensions as indicated in Fig. 2; (2) the ratio of the slab thickness, d_s, to L_1; (3) the ratio of the flexural stiffness of the beam to that of a slab width bounded laterally by the centerline of the adjacent panel, if any, on each side of the beam, α; (4) the ratio of the torsional stiffness of the transverse (torsional) beam to the flexural stiffness of the flexural beam, β; (5) partial and full composite beam-slab action. Partial composite action is where the beams are symmetrical around the slab neutral axis and hence only vertical shears are transmitted between them. Full composite action was studied by introducing a beam-slab eccentricity due to having the tops of the beams and the slab coincide; (6) the different boundary conditions of the panel occurring in single-panel floors, and in corner, exterior and interior panels in multi-panel floors.

A total of 122 panels were analyzed, of which 46 were single-panel floors with partial composite action. The rest had full composite action of which 33 were single-panel floors, 14 were corner panels, 28 were interior panels, and 1 was an exterior panel. Table 1 gives some typical results describing the first line of the 8 x 8 stiffness matrix of a single-panel floor. The position of the neutral axis in floors with eccentric beams varies throughout the floor and is a function of the slab stiffness relative to that of

the beams and the coordinates of the point being considered in the floor. The neutral axis of the composite beam-slab floor is closer to the neutral axis of the beams at the edges of a panel and moves closer to that of the slab as it moves toward the center of the panel. The term, γ, defines the position of the neutral axis of the composite beam-slab section at the supports (Fig. 5). $(K_{11})_s$ is the first term of the floor's 8 x 8 stiffness matrix and $(K_{11})^r_B$, is the stiffness of the bare beams around a fictitious neutral axis defined by ξ (Fig. 5), so that:

$$(K_{11})^r_B = 4EI^r_B/L_1 + GJ_{CB}/L_2 \qquad (1)$$

and

$$I^r_B = \frac{BD^3}{12} + A\xi^2 \qquad (2)$$

The carry-over factors, CF_{ij}, shown in Table 1 are the off-diagonal terms of the floor stiffness matrix normalized with respect to $(K_{11})_s$. Figures 4 to 6 show typical trends of the important terms of the floor stiffnesses. It was found that the terms, γ, $(K_{11})_s/(K_{11})^r_B$, and CF_{13}, are primarily dependent on the values of L_1/L_2, α, and the boundary conditions, while CF_{15} is dependent on these three terms plus β. Furthermore, it was found that corner panel stiffnesses could be adequately estimated from results of single-panel floors, and exterior panel stiffnesses from results of interior panels. The slab participation, as reflected by $(K_{11})_s/(K_{11})^r_B$ (Fig. 4), is highest with shallow beams, but drops off quickly and the floor stiffness approaches that of the bare beams, $(K_{11})^r_B$, as α increases. The neutral axis of the floor (Fig. 5) also approaches that of the bare beams as α increases, but at a slower rate than the stiffness. The results show that while the coupling between DOF 1 and 3 is the most substantial, the coupling between DOF 1 and 5 should not be neglected, especially for cases with $\beta > 0.1$ and $L_1/L_2 > 1.0$. It was also found that coupling between panel support DOF along a diagonal or more than one panel length away is weak. Notice that the two-way action of the slab redistributes the moments between the floor beams. This is reflected in Fig. 6 where the values of CF_{13} are substantially smaller than 0.5 which is the value of the carry-over factor for prismatic members.

Stiffness Matrix Method and Its Applications. - The SMM was developed from the results of this investigation. In this method, the elastic stiffness of a beam-slab floor, Fig. 3, is estimated as the stiffness of equivalent uniaxial members, each with three DOF. The SMM does not identify a physical shape for these members; rather, it establishes a procedure by which the position of the neutral axis of the equivalent member in relation to the top of the slab and its member stiffness matrix can be computed directly from a set of graphs. The 3 x 3 member stiffness matrix has the form of:

$$[K]\ \text{member} = (K_{11})_s \begin{bmatrix} S_{11} & 0 & 0 \\ 0 & S_{22} & k_{23} \\ 0 & k_{23} & S_{22} \end{bmatrix} \qquad (3)$$

Each member stiffness matrix is added directly to obtain the structure's stiffness matrix which can then be used to analyze the building response. The effects of shear on the floor stiffness are already included in the terms of Eq. 3; hence, no other terms to model shear effects are necessary. The results obtained show that in the practical application of the SMM, it is sufficient to consider only edge members and interior members (Fig. 3). Figures 4 to 7 give the graphs necessary for computing the stiffness matrix of an edge member. The procedure is as follows: (1) With L_1 as the span length of the member and L_2 the transverse span, enter Fig. 5 to determine

γ, which identifies the position of the neutral axis with respect to the top of the slab, as well as ξ. This allows the determination of I_B^r and $(K_{11})_B^r$ based on Eqs. 1 and 2. (2) Enter Fig. 4 to determine the value of $(K_{11})_s/(K_{11})_B^r$ which is used to compute $(K_{11})_s$. (3) Enter Figs. 6 and 7 to determine k_{23} and S, where S is a term developed from the results of the investigation and used to determine the value of S_{11}, so that:

$$S_{11} = \frac{[(K_{11})_s] \text{ transverse member}}{[(K_{11})_s] \text{ member}} (S) \qquad (4)$$

And, finally

$$S_{22} = 1.0 - \frac{[(K_{11})_s S_{11}] \text{ transverse member}}{[(K_{11})_s] \text{ member}} \qquad (5)$$

It should be noted that in the calculations of edge members not framing into a corner support (e.g. member B'C') only half of the transverse beam (i.e. Beam BE in the example) is assumed to act in torsion with the flexural beam in the calculations of $(K_{11})_B^r$, β, S_{11} and S_{22}. The other half is assumed to act with the beam in the adjacent span. The stiffness matrix of the interior members is determined in a similar fashion. The member stiffness matrices are symmetric but differ from those for prismatic beams.

The accuracy and applicability of the SMM were evaluated by applying it to calculate the lateral stiffness, P/Δ, of 27 single-panel, single-story structures (Fig. 8) and of one single-story, 3 x 3 panel structure. The results were compared with those from analyses using a finite element method, the ACI equivalent frame method and an effective slab width method where the slab width was based on the requirements of section 8.7 of the ACI 318-71 Code. In each case, the lateral stiffness was defined as the force, P, necessary to produce a unit lateral displacement, Δ, of the top of the slab in the direction of P. The results, a sample of which is given in Table 2, show the equivalent frame method registering the largest deviation, 169%, from the finite element analysis, and especially, as the relative column-to-floor stiffness increases. This corresponds to a 39% deviation in the structure's period, which can lead to substantially different estimates of its dynamic responses. The equivalent frame method was also found to be inconsistent in that it overestimated or underestimated the lateral stiffness, depending on the individual case considered. The effective slab width method generally fared better than the equivalent frame, with a 13.8% maximum deviation from the results of the finite element analysis. However, this method is not based on reliable experimental or analytical studies, and the correlation of results from the effective slab width method with the finite element analysis was inconsistent and did not establish well defined trends. This suggests that the equivalent slab width could lead to much higher errors in estimating the lateral stiffness than the 13.8% deviation registered in this study. The SMM consistently estimated the lateral stiffness closer to the finite element analysis than the other two methods, with a maximum deviation of 6.1%, and maintained its accuracy even in cases where interpolation between the graphs was necessary. The graphs and the procedures of the SMM were found to be simple to apply in practice.

A trial-and-error procedure was used to compute an effective slab width, b_f, that would yield the same lateral stiffness of the single-panel, single-story structures analyzed, as estimated by the finite element method. The results, a sample of which is given in Table 3, show a wide range of values of b_f which vary with each of the parameters considered. This points out the difficulty of attempting to model the stiffness of a two-way floor system with an effective slab width method.

ACKNOWLEDGEMENT

Financial support by the National Science Foundation under Grants AEN-307732 A02 and ENV-76-01419 is gratefully acknowledged.

REFERENCES

1. Bertero, V., et al., "Seismic Analysis of the Charaima Building, Caraballeda, Venezuela," Rept. No. EERC 70-4, EERC, Univ. of Calif., Berk., 1970.
2. ACI Committee 318, Building Code Requirements for Reinforced Concrete (ACI 318-71), ACI, Detroit, 1971.

TABLE 1 TYPICAL RESULTS OF THE FIRST LINE OF THE 8 X 8 STIFFNESS MATRIX OF A FLOOR PANEL

L_1/L_2	α	β	d_s(in)	γ	$(K_{11})_S$ $\frac{K\text{-in}}{rad}$	$(K_{11})_S/(K_{11})^r_B$	CF_{12}	CF_{13}	CF_{14}	CF_{15}	CF_{16}	CF_{17}	CF_{18}
1.0 L_1=240"	3.0	.064	6.5	.39	684715	1.17	-.06	.35	.01	-.03	-.04	.02	-.01
			9.0	.35	1709489	1.15	-.06	.34	.01	-.03	-.03	.02	-.01
		.160	6.5	.40	736792	1.16	-.08	.34	.02	-.07	-.04	.03	-.01
	8.0	.064	6.5	.31	1625482	1.09	-.05	.35	.01	-.03	-.03	.02	--
0.5 L_1=120"	8.0	.064	6.5	.20	2750200	1.00	-.04	.33	.01	-.02	-.01	.01	-.02
2.0 L_1=240"	8.0	.064	6.5	.30	887192	1.22	-.06	.36	--	-.07	-.05	.04	--

TABLE 2 TYPICAL VALUES OF THE LATERAL STIFFNESS OF A SINGLE-PANEL, SINGLE-STORY STRUCTURE*

L_1/L_2	C(in)	α_{AB}	β_{AC}	d_s(in)	$\frac{P}{\Delta}$ (Fin. El)	Equivalent Fr.		Effective Slab Width		Stiff. Matrix Meth.	
						P/Δ	Diff %	P/Δ	Diff %	P/Δ	Diff %
1.0 L_1-240"	20	8.0	.064	6.5	349.6	393.3	-12.3	382.4	-9.4	357.3	-2.2
				9.0	488.8	485.0	0.8	520.5	-6.5	505.8	-3.5
			.160	6.5	353.0	390.6	-10.7	382.4	-8.3	359.5	-1.9
0.50 L_1=120"	25	0.4	.064	6.5	561.5	1512.8	-169.4	556.8	0.8	564.4	-0.5
0.75 L_1=180"	25	8.0	.064	6.5	1517.2	1967.3	-25.2	1748.4	-11.3	1656.0	-5.4
2.0 L_1=240"	20	8.0	.064	6.5	488.0	600.1	-23.0	555.3	-13.8	512.1	-4.9

* $\left(\frac{P}{\Delta}\right)$ in k/in., Diff % $= \frac{\left(\frac{P}{\Delta}\right)_{\text{Finite El.}} - \left(\frac{P}{\Delta}\right)_{\text{model}}}{(P/\Delta)_{\text{Finite El.}}} \times 100$

TABLE 3 EFFECTIVE WIDTH OF EQUIVALENT BEAMS

L_1/L_2	α_{AB}	β_{AC}	d_s(in)	b_f(in)	$\frac{b_f}{0.5L_2}$
1.0 L_1=240"	0.80	.064	6.5	25.0	.21
			9.0	29.8	.25
		.160	6.5	29.3	.24
	3.0	.064	6.5	17.6	.15
0.5 L_1=120"	3.0	.064	6.5	12.5	.10
2.0 L_1=240"	3.0	.064	6.5	17.1	.29

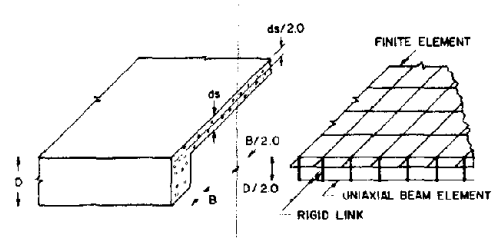

FIG. 1 FINITE ELEMENT MODEL OF A COMPOSITE BEAM-SLAB FLOOR

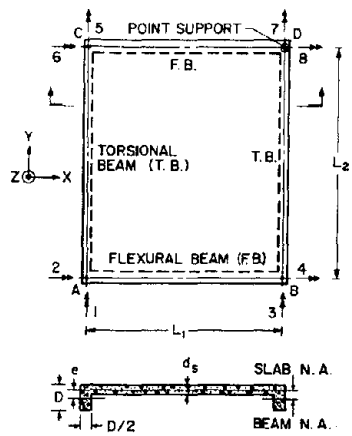

FIG. 2 DEGREES-OF-FREEDOM FOR A SINGLE-PANEL FLOOR

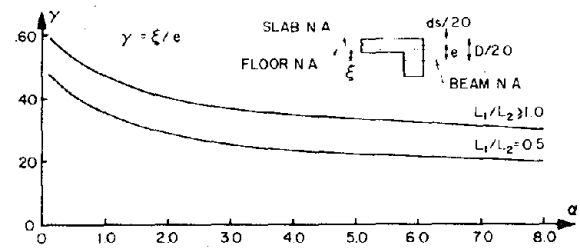

FIG. 5 γ VS. α FOR EDGE MEMBERS

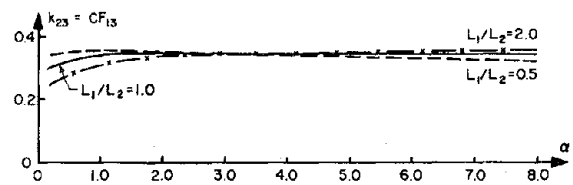

FIG. 6 k_{23} VS. α FOR EDGE MEMBERS

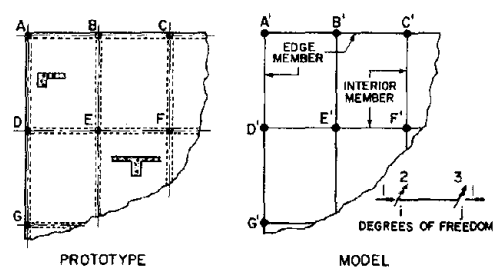

FIG. 3 MODELING OF STIFFNESS OF A BEAM-SLAB FLOOR BY SMM

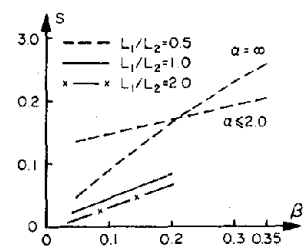

FIG. 7 S VS. β FOR EDGE MEMBERS

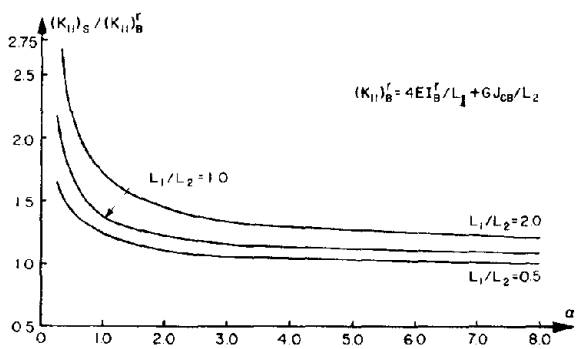

FIG. 4 $(K_{11})_s/(K_{11})^r_B$ VS. α FOR EDGE MEMBERS

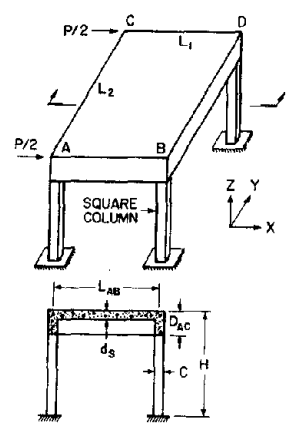

FIG. 8 SINGLE-STORY, SINGLE-PANEL FRAMED STRUCTURE

INELASTIC CYCLIC BEHAVIOR OF REINFORCED CONCRETE FLEXURAL MEMBERS

Bilgin Atalay[I] and Joseph Penzien[II]

SYNOPSIS

Presented is a mathematical model for predicting the force-deformation characteristics of reinforced concrete flexural members under inelastic cyclic conditions [1].

INTRODUCTION

Considering a reinforced concrete frame, the established philosophy of earthquake resistant design necessitates localized inelastic deformations occurring at certain overstressed regions designated as critical regions. Four series of tests have been conducted at the University of California, Berkeley [1,2,3,4] to study the flexural hysteretic behavior of critical regions under various combinations of internal force components controlling their behavior. The results of the series of tests reported in reference [1] in particular, permit the formulation of a mathematical model. The geometry and reinforcing details of a typical test specimen of this series is shown in Fig. 1.

INELASTIC HYSTERETIC BEHAVIOR

To formulate an appropriate mathematical model for reinforced concrete members subjected to cyclic inelastic deformations under combined moment, shear, and axial force, the lateral force-displacement behavior must be modelled realistically; i.e. one must be able to obtain the lateral force time history corresponding to a controlled lateral displacement time history.

Suppose for example, the lateral displacement time history of a member is that function shown in Fig. 2.a. The corresponding lateral force-displacement relation will be very similar to that shown by the solid line in Fig. 3. Knowing these two relations, the lateral force time history can be obtained as shown in Fig. 2.b.

In modelling the force-displacement relation of a member under constant axial load, one should first establish the so called "skeleton" curve. This curve is defined as the lateral force-displacement relation under separate but independent positive and negative monotonically increasing lateral displacements. Referring to Fig. 3, if the member under constant axial load is initially subjected to a positive monotonically increasing lateral displacement, the lateral load will increase "elastically" to point M, remain at essentially a constant value F_y under yielding conditions to point Q, and then will drop off along line QS showing a decrease in strength with increasing displacement beyond δ_N. This decrease is due primarily to crushing and spalling of the concrete cover on the compression sides of the member in the critical region. If instead the member under the same axial load had initially been subjected to a negative monotonically increasing lateral displacement, the lateral load would change along curve OM'Q' and then drop off with further increases in lateral displacement along line Q'S'. The force-displacement

[I]Research Assistant, University of California, Berkeley

[II]Professor of Structural Engineering, University of California, Berkeley

relations under these two monotonic conditions combine to form the basic skeleton curve S'Q'M'OMQS.

Let us now examine in more detail the force-displacement relation shown in Fig. 3 for cyclic loading. If initially, cyclic loading should take place at amplitudes in the range $-\delta_y < \delta < \delta_y$, the member will remain "elastic" and the corresponding force-displacement time history will be along line MM'. However as soon as the lateral displacement exceeds the yield level, hysteretic inelastic response follows with each subsequent cycle of deformation. In Fig. 3, the yield level is first exceeded at point M' with the displacement continuing to a value δ_1 as shown at point P'. The displacement then reverses and continues to δ_2 along curve P'MP (J = 1) which constitutes the first full half-cycle of deformation following initial yielding of the member. Again reversing the lateral displacement and continuing to δ_3 along curve PP'Q'R' (J = 2), the second full half-cycle of deformation is completed. Had this particular half-cycle terminated at point P' rather than R', continuing repeated cycles of deformation from δ_1 to δ_2 and back to δ_1 would produce stable hysteretic loops connecting points P and P'. Such stable behavior is experienced provided the absolute values of δ_1, δ_2, and all previous displacements have not exceeded δ_N and provided the shear stresses are relatively low. The third full half-cycle of deformation in Fig. 3 starts at point R', proceeds along curve J = 3 to point T, and then follows the skeleton curve to point R where the deflection equals δ_4. Note that at deflection δ_2 along this curve, the lateral force is somewhat reduced from the value F_y experienced on the previous half-cycle as represented by point P. Such a reduction at a fixed amplitude is experienced when the previous deformation time history has exceeded $\delta = \pm \delta_N$. This represents unstable hysteretic behavior which follows with each subsequent half-cycle as shown by curves J = 4,5,6,7 and 8. Note that quantities J, δ_J, t_J and F_J shown in Figs. 2, 3 and 4 refer to the number of inelastic half-cycles following initial yielding, the displacement at the initial point of the Jth inelastic half-cycle, time at the initial point of the Jth inelastic half-cycle, and the lateral force at the initial point of the Jth inelastic half-cycle, respectively.

Three important characteristics of inelastic cyclic behavior become apparent (1) the reduction in overall (or average) stiffness with increasing amplitudes of inelastic deformation beyond $\delta = \pm \delta_y$, (2) the reduction in lateral resistance at a fixed displacement with each repeated full half-cycle of inelastic deformation beyond $\delta = \pm \delta_N$, and (3) the shape of the hysteretic loops as influenced by certain member parameters and loading conditions. It is important when formulating an appropriate mathematical model that these characteristics be represented in a realistic manner. To be practical however this model must be easily adapted to numerical procedures. Therefore, a proper balance must be maintained between simplicity and accuracy.

FORM OF MATHEMATICAL MODEL

To formulate an appropriate force-deflection mathematical model, an analytical expression must be developed which will characterize the Jth inelastic half-cycle (J = 1,2,...) starting at time t_J. Since in applications, the extent of the Jth half is not known prior to its occurrence, this expression must be formulated knowing only the initial point (δ_J, F_J) representing $t = t_J$ and the previous force-deflection time history.

To accomplish this, a function $F_J(\delta)$ will be written as shown in Table 1 which passes through the known initial point (δ_J,F_J), designated here as point A, and an index point B whose location reflects the influence of the

member's force-deflection time history prior to $t = t_J$. The deflection at point B, designated as δ_J^M, is the maximum deflection which occurred prior to $t = t_J$ for half-cycles of increasing deflection and is the minimum deflection which occurred prior to $t = t_J$ for half-cycles of decreasing deflection; see Eq. (1).

TABLE 1: RELATIONS CONTROLLING THE Jth INELASTIC HALF-CYCLE

	HALF CYCLES OF INCREASING DEFLECTION, i.e. J=1,3,5,...1F INITIAL YIELD IN (-) DIRECTION, $F_1=-F_y$ J=2,4,6,...1F INITIAL YIELD IN (+) DIRECTION; $F_1=+F_y$	HALF CYCLES OF DECREASING DEFLECTION, i.e. J=2,4,6,...1F INITIAL YIELD IN (-) DIRECTION; $F_1=-F_y$ J=1,3,5,...1F INITIAL YIELD IN (+) DIRECTION: $F_1=+F_y$
δ_J^M † =	Max. $\{\delta(t)\}$; $0 < t < t_J$	Min. $\{\delta(t)\}$; $0 < t < t_J$ (1)
F_J^M † =	$F_J^P - \Delta F_{J-1} - \Delta F_J$	$F_J^P + \Delta F_{J-1} + \Delta F_J$ (2)
$F_J(\delta)$ =	$F_J+K_J(\delta-\delta_J)+A_J\cos\frac{\pi}{2}\left[\frac{2\delta-\delta_J^M-\delta_J}{\delta_J^M-\delta_J}\right] - B_J\left(\frac{1}{2}+\frac{1}{2}\cos\frac{\pi\delta}{\delta_{PJ}}\right)$; $\delta_{PJ} < 0$, $\delta_{PJ} \le \delta \le -\delta_{PJ}$	$F_J+K_J(\delta-\delta_J)-A_J\cos\frac{\pi}{2}\left[\frac{2\delta-\delta_J^M-\delta_J}{\delta_J^M-\delta_J}\right]+B_J\left(\frac{1}{2}+\frac{1}{2}\cos\frac{\pi\delta}{\delta_{PJ}}\right)$; $\delta_{PJ} > 0$, $-\delta_{PJ} \le \delta \le \delta_{PJ}$ (3)
	$F_J+K_J(\delta-\delta_J)+A_J\cos\frac{\pi}{2}\left[\frac{2\delta-\delta_J^M-\delta_J}{\delta_J^M-\delta_J}\right]$; $\delta_{PJ}<0$, $\delta\le\delta_{PJ}$, $\delta>-\delta_{PJ}$	$F_J+K_J(\delta-\delta_J)-A_J\cos\frac{\pi}{2}\left[\frac{2\delta-\delta_J^M-\delta_J}{\delta_J^M-\delta_J}\right]$; $\delta_{PJ}>0$, $\delta\le-\delta_{PJ}$, $\delta\ge\delta_{PJ}$ (4)
	$\delta_{PJ}>0$, $-\infty < \delta < \infty$	$\delta_{PJ}>0$, $-\infty < \delta < \infty$

† EXCEPT $\delta_1^M \equiv \delta_y$ & $F_1^M \equiv F_y$ if $F_1 = -F_y$

$\delta_1^M \equiv -\delta_y$ & $F_1^M \equiv -F_y$ if $F_1 = +F_y$

The lateral force at point B, designated as F_J^M, is given by Eq. (2) where F_J^P is equal to instantaneous lateral force which was present when $\delta(t)$ last reached the value δ_J^M as defined by Eq. (1) and where ΔF_{J-1} and ΔF_J are positive quantities representing resistance losses due to possible unstable hysteretic behavior during half-cycles J-1 and J, respectively. Each of these losses exist only if the deflection time-history during or prior to the half-cycle represented has exceeded + δ_N or - δ_N. The inelastic half-cycles for J = 1 through J = 8 in Fig. 3 are separated and shown again in Fig. 4. The initial point A, the index point B, and the terminal point C is shown for each half-cycle.

In formulating function $F_J(\delta)$, it is convenient to use the slope of the straight line passing through points A and B, i.e. $K_J \equiv (F_J^M - F_J)/(\delta_J^M - \delta_J)$, J=1,2,3,···. This function, with certain restrictions on its use, can be expressed by the approximate empirical Eqs. (3) and (4), Table 1. Quantities A_J and B_J appearing in Eqs. (3) and (4) are positive coefficients. Quantity δ_{PJ} appearing in Eq. (3) and in the conditional relations is that value of δ which yields a zero value for $F_J(\delta)$ using Eq. (4).

The first two terms on the right hand side of Eqs. (3) and (4) express the equation of the straight line passing through points A and B while the remaining two terms in Eq. (3) and the single remaining term in Eq. (4) represent the deviation of the function $F_J(\delta)$ from this straight line. The last term in Eq. (3) containing the coefficient B_J represents the pinched form of the hysteretic loop. Implicit in the form of this last term is the simplifying assumption that the pinched form is symmetric with respect

to $\delta = 0$. This assumption is, of course, not strictly true.

Function $F_J(\delta)$ as defined by Eqs. (3) and (4) can represent the entire Jth half-cycle only when it stays within certain bounds of the skeleton curve $F_S(\delta)$; i.e. the function $F_J(\delta)$ must never be extended across the skeleton curve for $|\delta| > \delta_y$. For example in Fig. 3, while half-cycles J = 4 through J = 8 can be represented entirely by Eqs. (3) and (4), half cycles J = 1 through J = 3 can only be partly represented by these equations. Function $F_J(\delta)$ as defined by Eqs. (3) and (4) represents half-cycles J = 1, J = 2, and J = 3 from their initial points to points M, P', and T, respectively. The remaining portions of these half-cycles, namely portions MP, P'Q'R', and TQR, must follow the skeleton curve . Mathematically this means that when $F_J(\delta)$ as defined by Eqs. (3) and (4) satisfies the condition

$$|F_J(\delta)| < |F_S(\delta)| \qquad \delta < -\delta_y \; ; \; \delta > \delta_y \; ; \; J = 1,2,... \tag{5}$$

it is applicable. However, when Eqs. (3) and (4) do not satisfy Eq. (5), it is not applicable in which case $F_S(\delta)$ should be used for $F_J(\delta)$. Obviously therefore, the skeleton curve must be represented in mathematical terms. Referring to Fig. 3, this relation can be expressed in the form

$$F_S(\delta) = \begin{cases} \dfrac{F_y}{\delta_y}\,\delta & -\delta_y \le \delta \le \delta_y \\ F_y & \delta_y \le \delta \le \delta_N \\ -F_y & -\delta_N \le \delta \le -\delta_y \\ F_y\left[1 - \beta_S\left(\dfrac{\delta_y}{\delta_N} - \dfrac{\delta_y}{\delta}\right)\right] & \delta \ge \delta_N \\ -F_y\left[1 - \beta_S\left(\dfrac{\delta_y}{\delta_N} + \dfrac{\delta_y}{\delta}\right)\right] & \delta \ge -\delta_N \end{cases} \tag{6}$$

where β_S is a positive scalar factor.

Parameters δ_N, β_S, ΔF_J, A_J, and B_J appearing in the above relations which formulate the overall mathematical model must be obtained from experimental evidence. Having their numerical values along with the numerical values for F_y and δ_y, the Jth inelastic half-cycle is completely defined. Once the Jth half-cycle is complete, its terminal point becomes the initial point for the J+1 half-cycle. One defines this half-cycle in exactly the same manner used for the Jth half-cycle. By this method, one can obtain the entire force-displacement time history.

EVALUATION OF PARAMETERS IN MATHEMATICAL MODEL

The parameters of the mathematical model presented in the previous section can be identified as F_y, δ_y, δ_N, β_S, ΔF_J, A_J, and B_J. Based on experimental data corresponding to a specimen with geometry and reinforcement detailing shown in Fig. 1, empirical relations have been formulated for their

numerical evaluation.

Factors F_y and δ_y - Numerical values for lateral force and displacement at initial yield, F_y and δ_y can normally be obtained through analytical methods of structural analysis.

Factor δ_N - The lateral displacement at initiation of loss of lateral resistance, δ_N can be evaluated using the empirical relation

$$\frac{\delta_y}{\delta_N} = 0.05 + 2.58\ \eta_o \tag{7}$$

where $\eta_o = N/bD\ f'_c$ is an axial compression index.

Factor β_S - Factor β_S is a measure of the loss of lateral resistance due to increasing lateral displacement, and as shown by experimental results, is a function of applied axial load, N, and transverse reinforcement spacing, s. Its value can be estimated using the empirical relation

$$\beta_S = 0.27 - 0.045\ \frac{d}{s} + \left(2.92 - 0.49\ \frac{d}{s}\right)\eta_o \tag{8}$$

Factor ΔF_J - For displacement amplitudes less than $\pm\ \delta_N$, there is no loss in resistance over a full half-cycle of deformation; therefore,

$$\Delta F_J = 0 \qquad \text{max.}\ \{|\delta(t)|\} \leq \delta_N \qquad 0 < t < t_J \tag{9}$$

For displacement amplitudes greater than $\pm\ \delta_N$ a loss in resistance does occur which can be approximated by the relation

$$\Delta F_J = [0.15\ \eta_o^2 + 0.002(3.33 - \frac{d}{s})]F_y \qquad \delta_M > \text{max.}\{|\delta(t)|\} > \delta_N \qquad 0 < t < t_J \tag{10}$$

Displacement δ_M is that value of δ beyond which the loss in resistance per full half-cycle ΔF_J becomes significantly larger than that given by Eq. (10).

Factors A_J and B_J - An analysis of experimental results shows that simple empirical relationships can be used in the estimation of factors A_J and B_J, namely:

$$\frac{A_J}{F_y} = -0.17 + (0.27 + 0.30\ \eta_o)\ \mu_J - (0.02 + 0.04\ \eta_o)\mu_J^2 \qquad \mu_J \geq 1 \tag{11}$$

and

$$\frac{B_J}{F_y} = \left(0.245 - 0.284\ \eta_o - 0.008\ \frac{d}{s}\right)\left(\mu_J - 1\right)^{1/2} \qquad \mu_J \geq 1 \tag{12}$$

The quantity μ_J appearing in Eqs. (11) and (12) is the cyclic lateral displacement ductility factor defined as:

$$\mu_J = \frac{|\delta_J^M - \delta_{J-1}^M|}{2\delta_y} \tag{13}$$

Factor B_J reflects the amount of "pinching", or the reduction of

instantaneous shear stiffness near zero lateral load. It is well established (see), for example [3]) that this reduction in stiffness is an inverse function of a/D, the moment arm-to-depth ratio. Since in the present experimental investigation only one a/D ratio (fairly high to prevent shear type failures) was used, the effect of this ratio is not apparent in Eq. (12); therefore, it is suggested that the quantity B_J/F_y be increased properly for decreasing values of a/D.

CONCLUDING STATEMENT

The mathematical model presented in the preceeding sections can be checked against the experimental test data using a specially developed computer program. An example lateral force-displacement relationship calculated through the use of the mathematical model is presented graphically in Fig. 5. Only the relationships corresponding to the first and last half cycles of lateral loading at a lateral displacement amplitude in the inelastic range are duplicated. The mathematical model reproduces satisfactorily the important response characteristics pertinent to inelastic cyclic behavior. As evidence of the simplicity of the mathematical model it is worth noting that the calculations needed to generate the lateral force-displacement diagrams for 6 specimens, each with a different combination of applied axial load and transverse reinforcement spacing and each containing about 40 half cycles of loading, required about 3 seconds of central processor time in the CDC-6400 computer.

ACKNOWLEDGMENT

The authors acknowledge the financial support provided by the National Science Foundation through Grant No. AEN73-07732 A02.

REFERENCES

[1] Atalay, B., and Penzien, J., "The Seismic Behavior of Critical Regions of Reinforced Concrete Components as Influenced by Moment, Shear, and Axial Force," EERC 75-19, Earthquake Engineering Research Center, University of California, Berkeley, 1975.

[2] Bertero, V. V., Bresler, B., and Liao, H., "Stiffness Degradation of Reinforced Concrete Structures Subjected to Reversed Actions," EERC 69-12, Earthquake Engineering Research Center, University of California, Berkeley, 1969.

[3] Mahin, S., Bertero, V. V., Rea, D., and Atalay, B., "Rate of Loading Effects on Uncracked and Repaired Reinforced Concrete Members," EERC 72-9, Earthquake Engineering Research Center, University of California, Berkeley, 1972.

[4] Celebi, M., and Penzien, J., "Experimental Investigation into the Seismic Behavior of Critical Regions of Reinforced Concrete Components as Influenced by Moment and Shear," EERC 73-4, Earthquake Engineering Research Center, University of California, Berkeley, 1973.

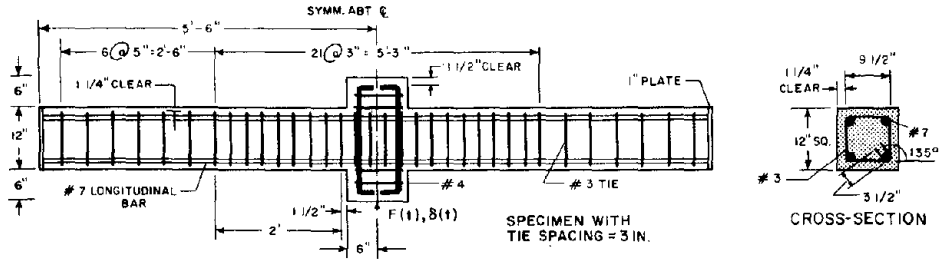

Fig. 1. Test Specimen Geometry and Reinforcement Details

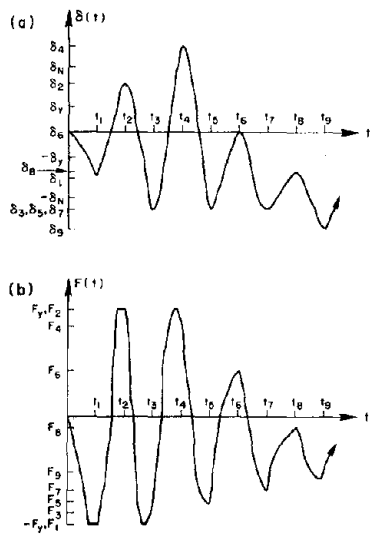

Fig. 2. Example Lateral Displacement-Time and Corresponding Lateral Force-Time Histories

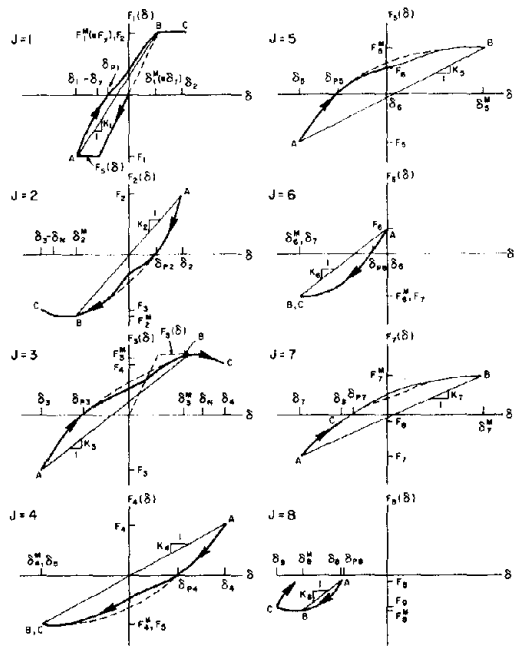

Fig. 4. Lateral Force-Displacement Relations for Inelastic Half Cycles of Loading

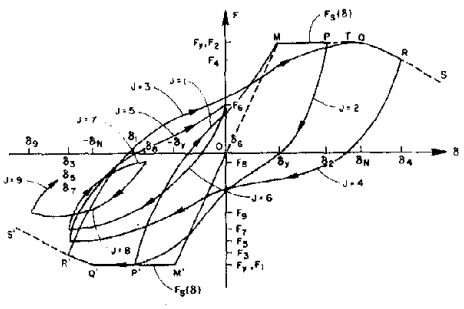

Fig. 3. Example Lateral Force-Displacement Relation

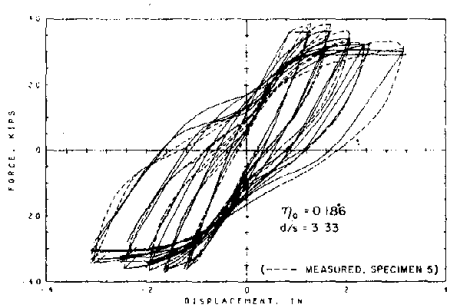

Fig. 5. Calculated Lateral Force-Displacement Relationship

CYCLIC SHEAR TESTS ON MASONRY PIERS

R. L. Mayes[I], Y. Omote[II], R. W. Clough[III]

ABSTRACT

The results of cyclic in plane shear tests on seventeen fixed-ended masonry piers are presented. The test set up is designed to simulate insofar as possible the boundary conditions the piers would experience in a perforated shear wall of a complete building. Each test specimen was a full-scale panel about 15 feet square consisting of two piers and a top and bottom spandrel. The panels were constructed from 6" wide x 8" high x 16" long hollow concrete block units. The variables included in the investigation were the quantity and distribution of reinforcement, the rate of load application, the vertical bearing stress and the effect of partial grouting. This paper discusses the effect of these parameters on the hysteresis envelopes and ductility of the piers.

I. Introduction

The test results presented herein demonstrate the cyclic behavior of concrete masonry piers subjected to the lateral loading. The variables included in the seventeen tests are the frequency of load application, the quantity and distribution of reinforcement, the vertical bearing stress and effect of partial grouting. The seventeen test specimen include eight sets of two identical panels. One of each pair is tested at an input displacement frequency of 0.02 cps (pseudo-static) and the other at 3 cps (dynamic). The other variables are listed in Table 1.

Only the characteristics of the load-deflection hysteresis envelopes are included in this paper, discussion of other parameters are included in references (1) and (2).

II. Test Specimen

The overall dimensions of the seventeen test specimen are the same and are shown in Figure 1. The piers with a height (5'-4") to width (2'-8") ratio of two were the elements of interest. The top and bottom spandrels were heavily reinforced in an attempt to prevent their failure, although this objective was not achieved in all cases.

The panels were constructed from standard two-core reinforcible hollow concrete blocks of nominal 6" wide x 8" high x 16" long dimensions. The core of each block was approximately 51.4 square inches with a ratio of net to gross area of 58%. Single units had an average gross compressive strength of 1714 psi (2944 psi net strength) with a range from 1340 psi to 2040 psi over five samples. The average tensile strength of the units was 267 psi with a range from 235 psi to 285 psi over five samples. The block test procedures followed the California Q-Block Quality Control Specification[3].

I Assistant Research Engineer, University of California, Berkeley
Principal, Computech, San Francisco
II Assistant Research Engineer, University of California, Berkeley
III Director, Earthquake Engineering Research Center, University of California, Berkeley

Tests 1, 2, 5, 6 and 9 to 12 had 2-#6 vertical re-bars in each jamb of the pier i.e. 0.92% reinforcement based on the gross cross sectional area. Tests 3 and 4 had 2-#4 vertical re-bars in each jamb of the piers - 0.41%. Tests 7 and 8 had 2-#6 vertical re-bars in each jamb and 3-#5 horizintal bars in each pier - 1.4% reinforcement. Tests 13 to 16 had a substantial amount of reinforcement, designed to ensure a flexural failure - 1.67%. In addition to the horizontal and vertical reinforcement, Tests 15 and 16 had steel plates inserted in the mortar joints at each of the three courses from the top and bottom of each pier. The plate used is shown in Figure 2. Test 17 was unreinforced.

III. Test Equipment and Procedure

The test equipment shown in Figure 3 permits lateral loads to be applied in the plane of the piers in a manner similar to that in which a floor diaphragm would load the piers during earthquake excitation. It consists of two, twenty-feet high, heavily-braced reaction frames to which a pair of hydraulic actuators are connected, a mechanism capable of applying vertical bearing loads similar to those experienced by the piers in an actual structure, and a concrete base on which the panel is constructed and bolted to the test floor.

The loading sequence of each panel consisted of 3 sinusoidal cycles of load applied at a specified actuator amplitude displacement and frequency. The actuator displacements generally followed the sequence 0.02", 0.04", 0.06", 0.08", 0.12", 0.16", 0.20", 0.25", 0.30", ---0.5", 0.6"----1.0"---1.5". After each set of 3 cycles of loading the walls were visually inspected and the crack pattern identified.

IV. Test Results and Discussion

A summary of the test results is listed in Table 1 and an example of a hysteresis loop and the mode of failure is shown in Figure 4 (for Test 3). Shear force indicators P_{u1}, P_{u2}, P_1, P_2 and P_3 and ductility indicators δ_1, δ_2, δ_3 and δ_4 listed in Table 1 are identified in Figure 4.

In the hysteresis envelopes plotted in Figures 5 to 8, there clearly are two distinct types of behavior. First those typified by Test 1 in Figure 5 where the hysteresis envelope reaches a maximum load and as the lateral displacement increases the load gradually decreases. Second those typified by Tests 11 and 15 in Figures 6 and 8 where the hysteresis envelope reaches a maximum load and as the lateral displacment increases this load is maintained until a certain displacement at which point the load decreases. This is somewhat similar to an elasto-plastic force deflection relationship. The first type of behavior is characterized by low values of the parameter $(\delta_1 + \delta_2)/2$ (about 1.5) and larger values of the parameter $(\delta_3 + \delta_4)/2$ (in the range of 2 to 6). The corresponding values for the second type of behavior are 2-5 and 4-10 respectively.

The effect of bearing stress on (Tests 1, 2, 5, 6, 9 and 10) the ductility of the piers is somewhat inconclusive. Evaluating the hysteresis envelopes of Figure 5 and the ductility indicators of Table 1, there is a trend towards a more ductile behavior as the bearing stress increases, however, this is offset by the fact that the piers with a bearing stress of 500 psi can only withstand a maximum lateral displacement of 0.5" as opposed to 1.0" for the 0 and 250 psi cases. If the maximum displacement

of 0.5" is not a limiting factor, then an increase in bearing stress could be considered to have a desirable effect on the ductility of the piers for the tests performed, however as the number of tests are limited and because this conflicts with the conclusion of other investigators[2] this indication obviously requires further investigation.

The effect of partial grouting on the ductility of the piers is also inconclusive. From the hysteresis envelopes of Figure 6, partial grouting produces a tendency towards an elasto-plastic type of force-deflection behavior and when compared to the fully grouted pseudo-static test (Test 1) the overall effect appears to be favorable. However, when compared to the fully grouted dynamic test the force-deflection curves are different and the fully grouted pier must be considered to have the more desirable ductile behavior[1]. In addition, both the partially grouted piers collapsed at a lateral displacement of 0.5" as opposed to 1.0" for the fully grouted walls. Because of the limited number of tests performed and the lack of any definite trend in the results, it is clear that further tests are required.

Horizontal reinforcement has a very desirable effect on the shear mode of failure (Tests 1, 2, 7 and 8). As seen from the hysteresis envelopes of Figure 7 and the ductility indicators of Table 1, horizontal reinforcement substantially increases the overall ductility of the piers, and the dynamic test shows a better performance than the pseudo-static test.

The performance of the flexural mode of failure was evaluated in Tests 3, 4 and 13-16 with the resulting hysteresis envelopes plotted in Figure 8. The basic difference between Tests 3, 4 and 13, 14 was the inclusion of horizontal reinforcement in Tests 13 and 14 to ensure that a pure flexural mode of failure was obtained. As expected, Tests 3 and 4 had characteristics of both the shear and flexural modes of failure, showing a more sudden drop in load carrying capacity at larger lateral displacements. Tests 13 and 14 show that the force deflection relationship of the flexural mode of failure tends towards elasto-plastic characteristics. The most significant result of this series of tests was the effect of joint reinforcement, (Figure 2), which was included in Tests 15 and 16. The addition of the horizontal plates substantially increased both sets of ductility indicators as well as the maximum displacement, that the piers could withstand, leading to an extremely desirable ductile behavior.

The main conclusion of this paper is that much more research is required on the shear strength of masonry piers. Trends of behavior were indicated but because the number of tests was small, definitive conclusions on many facets of the initial goals of the investigation could not be made. However, the following conclusions did emerge in the results obtained.

1) The inclusion of a sufficient amount of horizontal bar reinforcement significantly enhances the ductile behavior of piers failing primarily in the shear mode.

2) The inclusion of 1/8" plates in the toes of the piers produces extremely desirable ductile behavior for piers failing primarily in the flexural mode.

3) An increase in vertical bearing stress demonstrates a tendency towards a more ductile type of behavior for piers which fail mainly in

shear.

4) Partial grouting produces a tendency towards an elasto-plastic force-deflection relationship prior to failing in the shear mode. However, it is not clear whether or not this enhances the overall ductile behavior of the piers when compared to the behavior of fully grouted piers.

Acknowledgement

The authors wish to thank Mr. S. W. Chen, A. Agarwal, A. Shaban and J. Kubota for their help in performing the experimental work of this study.

References

(1) Mayes, R. L. Omote, Y., and Clough, R. W., "Cyclic Shear Tests on Masonry Piers, Part I - Test Results," EERC Report No. 76-8, Earthquake Engineering Research Center, University of California, Berkeley, May 1976.

(2) Mayes, R. L., Omote, Y. and Clough, R. W., "Cyclic Shear Tests on Masonry Piers, Part II - Analysis of Test Results," EERC Report No. 76-16, Earthquake Engineering Research Center, University of California, Berkeley, 1976.

(3) 1974 Masonry Codes and Specifications, Published by Masonry Industry Advancement Committee, California, 1974.

Table 1 Summary of the Test Results

TEST NO.	Frequency[1] (cps)	Bearing Stress[2] (psi)	Vertical Reinforcement[3]	Horizontal Reinforcement[4]	$\frac{P_{u1}+P_{u2}}{2}$; $\frac{\tau_{u1}+\tau_{u2}}{2}$ [5] (kips)	(psi)	$\frac{P_1+P_2}{2}$; $\frac{\tau_1+\tau_2}{2}$ [6] (kips)	(psi)	P_3 ; τ_3 [7] (kips)	(psi)	$\frac{\delta_1+\delta_2}{2}$ [8]	$\frac{d_1+d_4}{2}$ [9] (in)	$\frac{\delta_3+\delta_4}{2}$ [10]	$\frac{d_3+d_5}{2}$ [11] (in)	Max. Input Stroke of Actuator [12] (in)
1	0.02	250	2 - #6	--	26.0	135	24	125	20	104	1.55	.095	3.5	.065	1.0
2	3	250	2 - #6	--	33.2	173	31	161	28	146	1.55	.130	2.4	.095	1.0
3	0.02	125	2 - #4	--	27.3	142	26	135	21	109	1.9	.180	4.1	.105	1.0
4	3	125	2 - #4	--	26.0	135	22.8	119	18	94	1.8	.165	5.6	.085	1.0
5	0.02	0	2 - #6	--	20.5	107	18.5	96	15	78	1.55	.180	5.6	.075	1.0
6	3	0	2 - #6	--	25.5	133	21.7	113	19	99	1.85	.105	5.3	.070	1.0
7	0.02	250	2 - #6	1 - #5	40.7	212	39	203	33	172	1.5	.235	4.4	.123	0.7
8	3	250	2 - #6	1 - #5	48.6	252	44	229	33	172	1.45	.350	3.0	.180	1.0
9	0.02	500	2 - #6	--	29.5	154	28.7	149	24	125	2.1	.080	4.1	.060	0.45
10	3	500	2 - #6	--	34.1	178	32.7	170	28	146	2.8	.130	5.6	.055	0.5
11[13]	0.02	250	2 - #6	--	20.0	104 (132)	18.9	98 (124)	17	89 (113)	4.8	.120	6.5	.055	0.5
12[13]	3	250	2 - #6	--	21.8	114 (143)	20.6	107 (136)	18	94 (119)	5.1	.165	8.1	.048	0.55
13	0.02	125	2 - #4	3 - #7, 2 - #5	29.1	151	26.0	135	18	94	1.8	.215	5.2	.075	1.0
14	3	125	2 - #4	3 - #7, 2 - #5	28.8	150	24.0	125	19	99	3.1	.160	6.6	.080	0.9
15	0.02	125	2 - #6	3 - #7, 2 - #5R	35.2	183	33.6	175	23	120	2.5	.320	9.2	.090	1.5
16	3	125	2 - #4	3 - #7, 2 - #5R	36.7	189	32.4	169	22	115	3.4	.190	10.5	.090	1.5
17	3	250	--	--	23.7	123	20.7	108	17	89	1.6	--	--	--	0.7

Notes of Table

1. Frequency of the sinusoidally applied actuator displacement.
2. Bearing Stress based on the gross area (192 sq. in.).
3. Vertical reinforcement in each jamb of the piers.
4. Horizontal reinforcement as shown in Figure 2.3.
5. P_{u1} and P_{u2} are the peak shear loads in either direction, and defined in Figure 4.41. τ_{u1} and τ_{u2} are the corresponding shear stresses based on the gross area.
6. P_1 and P_2 are the average ultimate shear strengths as defined in Figure 4.41. τ_1 and τ_2 are the corresponding shear stresses based on the gross area.
7. P_3 is a working ultimate shear strength defined in Figure 4.41. τ_3 is the corresponding shear strength based on the gross area.
8. δ_1 and δ_4 are approximate ductility ratios associated with P_1 and P_2 and defined in Figure 4.41.
9. Average value of deflection associated with P_1 and defined in Figure 4.41.
10. δ_3 and δ_4 are ductility indicators associated with P_3 and defined in Figure 4.41.
11. Average value of deflection associated with P_3 and defined in Figure 4.41.
12. Maximum input displacement of activator.
13. Grouted at Re-bars only. Values in parentheses are stresses based on net area. (152 sq. in.).

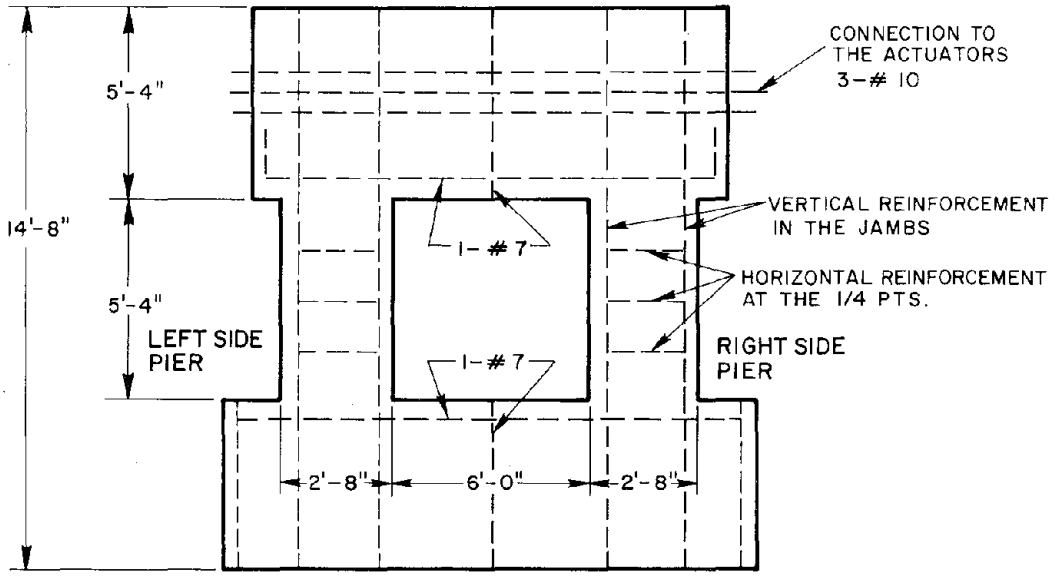

Fig. 1 Typical Double Pire Test Specimen

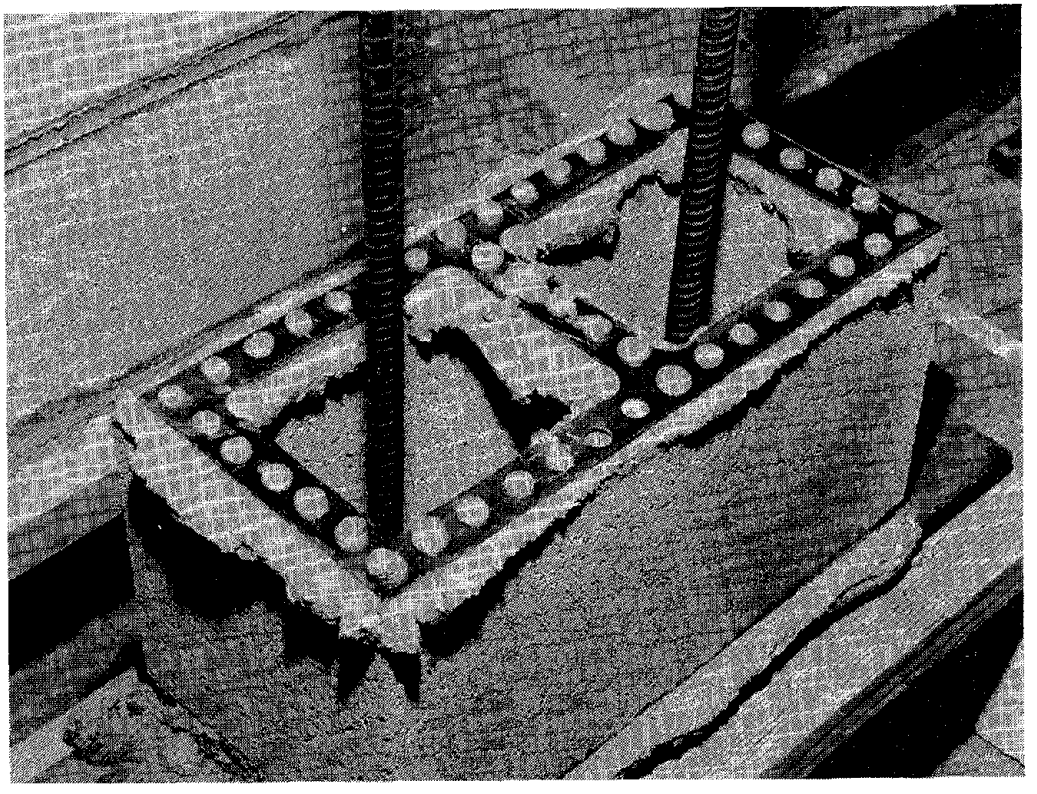

Fig. 2 1/8-in. Plate

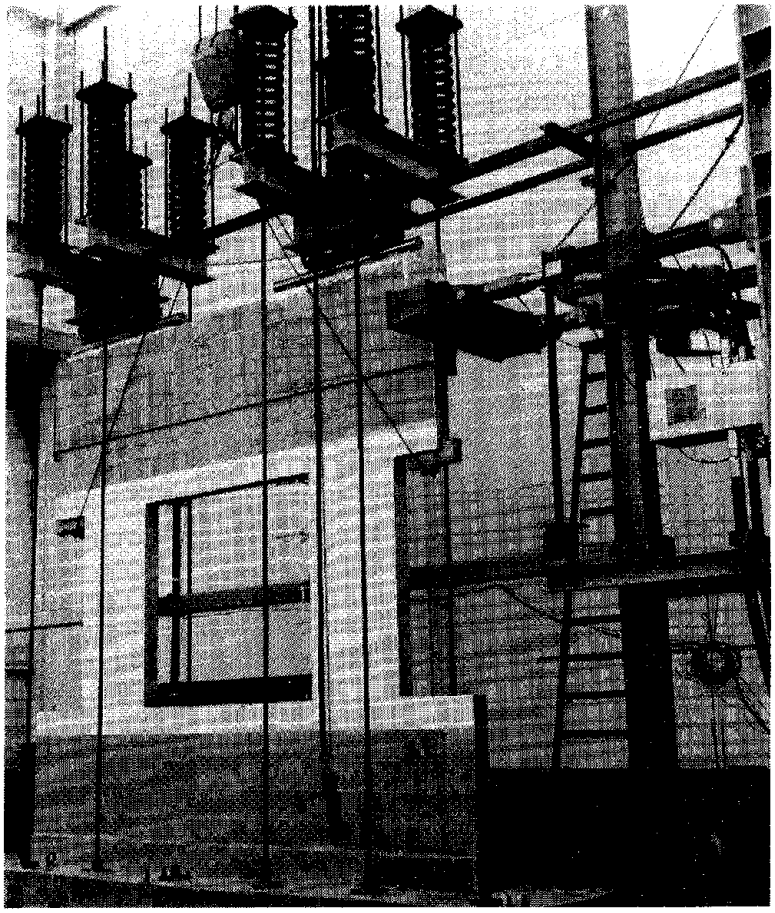

Fig. 3 Double Pier Test Set-up

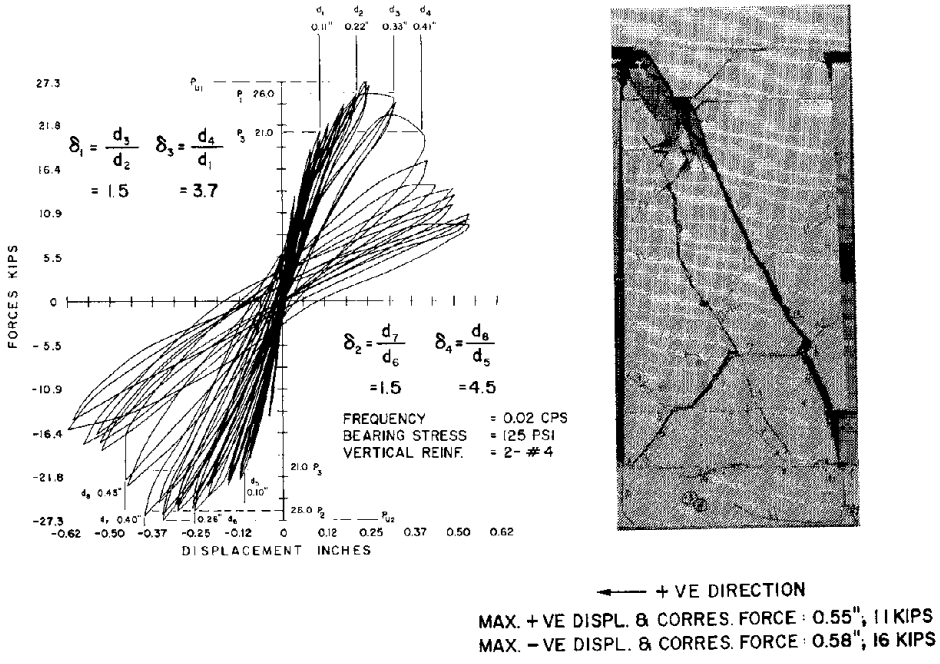

Fig. 4 Definition of Shear Strength and Ductility indicators

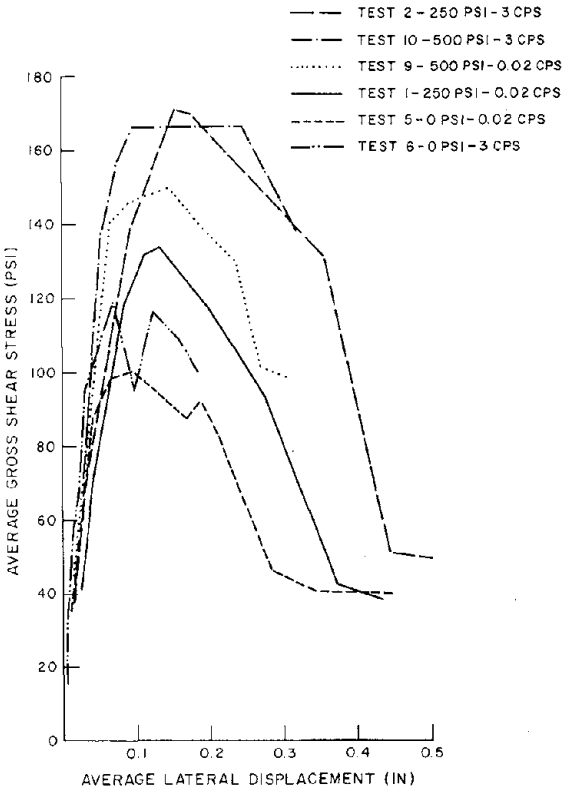

Fig. 5 Effect of Bearing Stress

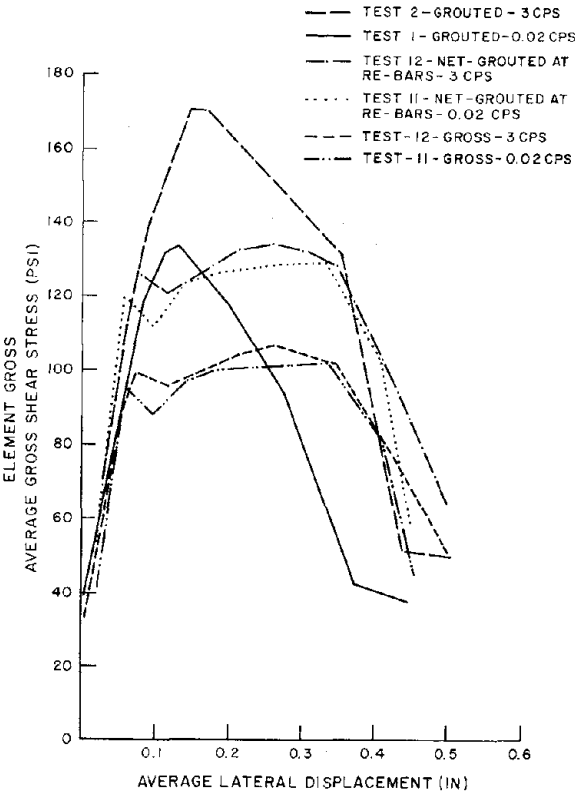

Fig. 6 Effect of Partial Grouting

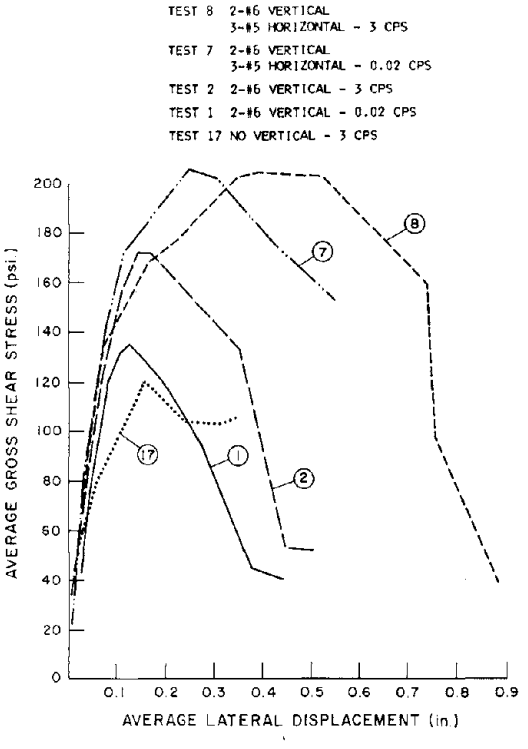

Fig. 7 Effect of Reinforcement

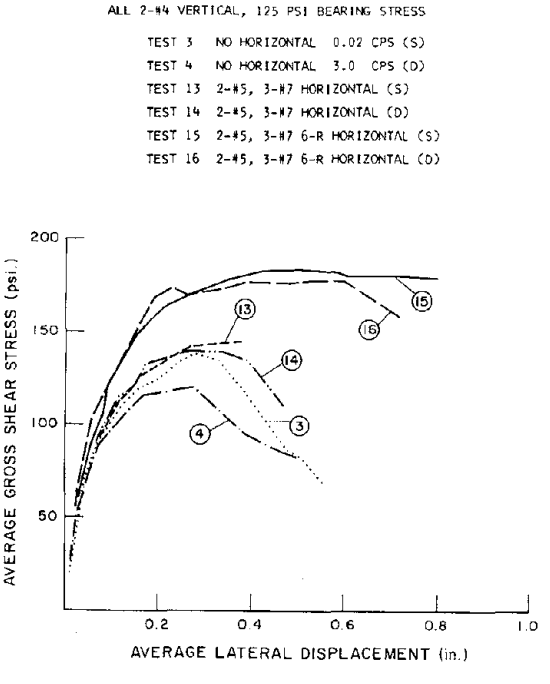

Fig. 8 Effect of Horiz-ntal Reinforcement

EFFECT OF TEST TECHNIQUE ON MASONRY SHEAR STRENGTH

Y. Omote[I], R. L. Mayes[II], R. W. Clough[III], S. W. Chen[IV]

ABSTRACT

The paper presents a comparison between the critical tensile strengths of concrete block masonry panels obtained by three different test techniques. The first two methods consist of simple diagonal tests on 32"x32" square panels. The test set up used in the third method was designed to simulate insofar as possible the boundary conditions the pier would experience in a perforated shear wall of a complete building. Each test specimen of the third method was a full scale panel about 15 feet square consisting of two piers and a top and bottom spandrel. Theoretical formulations are used in an attempt to correlate the experimental results. Good correlation of shear strength was achieved when an appropriate theoretical formula was used.

I. Introduction

One of the more important parameters required for the design of masonry structures is the shear strength of masonry walls. In order to determine the shear strength of masonry assemblages, a limited amount of both experimental and theoretical research has been performed. Many different test techniques have been used to investigate the shear strength of masonry assemblages and the diversity of methods has arisen because of the difficulty in simulating experimentally, the actual load and boundary conditions of a structural masonry component in a building.

The aim of this paper is first to survey the different types of test techniques; and the second to compare the results of the critical tensile strengths obtained by two different tests and the cyclic horizontal load tests recently performed at the Earthquake Engineering Research Center, University of California, Berkeley.

II. Test Techniques for Masonry Shear Strength

The rapid development of mechanical and electrical test equipment over recent years has lead to an increase in sophistication of apparatus available for use in experimental investigations. The scope and aim of many programs have consequently been broadened, resulting in the determination of more detailed and relevant information.

One of the first methods used in the determination of the shear strength of masonry walls was that shown in Figure 1(a). The external hold down force P_v was applied to resist the overturning moment of the panel. This method was used by Schneider[2], Scrivener et al.[3,4] and

---

I Assistant Research Engineer, University of California, Berkeley
II Assistant Research Engineer, University of California, Berkeley, Principal, Computech, San Francisco
III Director, Earthquake Engineering Research Center, University of California, Berkeley
IV Graduate Research Assistant, University of California, Berkeley

* These reference numbers correspond to the reference numbers published in EERC Report 75-21 (I)

in the test programs of the Structural Clay Products Research Foundation[5,6]. It also formed the basis of the standard racking tests described in ASTM E 72-61.

The above method was modified by Schneider[7] in a second series of tests performed in 1959, and the modified procedure was also utilized by Scrivener[8] in a series of three tests. Instead of using the external force to resist the overturning moment, an internal hold down anchor was used, as shown in Figure 1(b). Here the objection of the large external compressive stress applied by the overturning constraint at the edge of the panel is eliminated. However, since overturning resistance depends upon the development of bond between the jamb steel and the grout, a certain flexibility in the types and arrangement of jamb steel is lost, although a more realistic boundary condition is obtained.

Probably one of the most frequent techniques used to determine the relative shear strengths of walls is that shown in Figure 1(c). This method was used in the extensive program performed by Blume and Associates [9] and Degenkolb and Associates [II]. Borchelt[10] and Yokel and Fattal [III] also used the diagonal test method but added a compressive load as shown in Figure 1(d).

Schneider[11] in 1967 performed a series of tests on concrete masonry piers. The test set up he used is shown in Figure 1(e). The geometry of the system was maintained by the struts at the end of the openings and the axial and shear loads were applied by a system of jacks and tie rods.

Cyclic loading tests were performed by Williams[12], Meli[13] and Priestley and Bridgeman[14], utilizing the cantilever pier shown in Figure 1(f). Resistance to overturning moment was provided by whatever internal reinforcement was in the piers. This is a variation of the internal hold down method used by Scrivener and Schneider.

Recently, Mayes and Clough[15,IV] carried out an extensive test program which attempts to approximate as closely as possible the boundary conditions of the piers in a complete structure - Figure 1(g). Results of this test procedure are compared with results obtained by other methods in the present paper.

III. Test Program

The test arrangement depicted in Figure 1(g) was developed to carry out a major part of an experimental study of the earthquake behavior of masonry structures at the Earthquake Engineering Research Center. This test specimen was chosen because of the realistic manner in which the boundary conditions of the piers are simulated. Results of these experiments are reported in EERC Report No. 76-8 [V]. However, it was recognized that these results should be correlated with those obtained from a simple test procedure such as could be used in commercial test laboratories for obtaining the shear strength of masonry components. The method most commonly used to date is the diagonal compression test shown in Figure 1(c).

Some of the theoretical formulations associated with this test [9] assume that the compressive load P can be represented by a shear force of $P/\sqrt{2}$ applied on each side of the panel. To investigate the validity of

this assumption, a modified form of the test set-up was designed (Figure 3 which ensured that the components ($P/\sqrt{2}$) of the compressive force P were transferred to the panel as shear forces. In order to compare results obtained by the three different test procedures, test specimens of each type were constructed at the same with the same mortar and grout. In total eight sets of two identical double pier test specimen were constructed and for each set of large panels at least two "32 x 32" (81 cm x 81 cm) square shear panels were constructed. All test specimens were constructed from 6" (15.2 cm) wide x 8" (20.3 cm) high x 16" (40.6 cm) long hollow concrete block units. A short description of each test set up and a comparison of the results follows.

III-1. Diagonal Compression Tests

An overall view of the diagonal compression test set up is shown in Figure 2. Top and bottom shoes to apply the loading were fabricated from 1" (2-5 cm) thick steel angles to form a 90 degree bearing corner which transferred the vertical compressive force to the panel. A four million pound University Testing Machine applied the load at a rate of approximately 8000 pounds per minute until failure. The critical tensile strength σ_{tcr}, was calculated by two methods. The first employed a formula used by Blume[9] which was based on analytic and photoelastic studies performed by Frocht[24] on a homogeneous square panel.

$$\sigma_{tcr} = \sqrt{2.422\tau^2 + (\sigma_c/2)^2} - (\sigma_c/2 + 0.832\tau) \qquad -1.$$

where σ_c is the applied compressive stress and τ is the assumed shear stress. $\tau = P/\sqrt{2}A$. Here, P is the applied compressive load and A is the area of one side of the square - Figure 4. The second formula was used by Borchelt[10] and is based on the simple Mohr's circle approach

$$\sigma_{tcr} = \sqrt{\tau^2 + (\sigma_c/2)^2} - \sigma_c/2. \qquad -2.$$

III-2. Modified Diagonal Compression Test (Simple Shear Test)

In the initial stages of the test program the diagonal compressive test was the only simple test used to correlate results with the double pier tests. However, because certain theoretical formulations associated with the diagonal compression test[10] assumed that the vertical compressive load (P) had shear force components, $P/\sqrt{2}$, acting on each side of the panel, a modified test set up was developed to satisfy this assumed boundary condition. The test set up is shown in Figure 3 and is described in more detail in EERC Report No. 76-16[VI]. Because of the time required to develop the modified test set up, only one set of double piered test results has been used for correlation with these results. The critical tensile strength at failure was calculated by the formula developed by Borchelt[10]

III-3. Cyclic Shear Tests

Each test specimen was a full scale panel about 15 feet (4.6m) square consisting of a top and bottom spandrel and two piers as shown in Figure 5. The details of this test program are discussed in a paper presented at Session II-64 of this conference [IV]. A typical shear mode of failure in the piers is shown in Figure 6.

In order to estimate the critical tensile stress of the piers, a point of inflexion is assumed at the mid-height of the pier (Figure 7) and each pier is assumed to resist half of the applied shear load. The compressive load in each pier is modified by the axial forces induced by the overturning moment, acting on the panel, as shown in the Figure 7. The shear force across the width of the panel is assumed to have a parabolic distribution (18). With these assumptions the critical tensile strength of the double piers is calculated by the same formula used by Turnsek and Cacovic[18] which is based on a Mohrs Circle approach at the center of the pier, as follows

$$\sigma_{tcr} = \sqrt{(1.5\tau)^2 + (\sigma'_{c/2})^2} - \sigma'_{c/2} \qquad -3.$$

where τ is the average shear stress and σ'_c is the modified compressive stress.

IV. Discussion of Test Results

A comparison of the critical tensile strengths obtained from five sets of double pier tests with the corresponding critical tensile strengths obtained from both the diagonal and modified diagonal (simple shear) compression tests is shown in Figure 8. The critical tensile strengths obtained from the diagonal compression test are calculated from both Equations 1 and 2. Also included in the results are double piers that failed in a combination of the shear and flexural modes of failure.

For the simple diagonal compressive test the more exact formulation of Equation 1 gives the best correlation with the double pier results. The results obtained from Equation 2 are approximately 1·36 times greater than Equation 1 values, and therefore show corresponding poorer correlation. This indicates the inappropriatness in the theoretical model of the assumption that, the compressive load P can be considered to have shear force components $P/\sqrt{2}$. The only two pier results that can be used for correlation with the modified diagonal (simple shear) compressive test were from a double pier that failed in a combination of the shear and flexural modes. Before any conclusions can be drawn about the value of this method, further tests should be performed to correlate the results with double or single piers failing in the pure shear mode of failure.

Although this series of tests is limited in number it appears that a reasonable correlation exists between the critical tensile strengths obtained from the simple diagonal compressive test (Equation 1) and the more realistically loaded piers. In masonry research "reasonable correlation" is difficult to define because of the variability of the material. However, to further evaluate the test methods, it is the authors intention to continue determining the correlation between the results of the three test methods in an extensive (80) single pier test program. It is hoped that when completed the results can be used to recommend a more realistic test method for determining the allowable shear strength of masonry. At present the Uniform Building Code uses a proportion of the uniaxial compressive prism strength (f'_m) to estimate the shear strength of masonry.

Acknowledgement and References

The authors wish to thank Mr. A. Shaban, A. Agarwal, J. Kubota, and A. Anvar for their help in performing the experimental work of this study. References are available upon request from the authors.

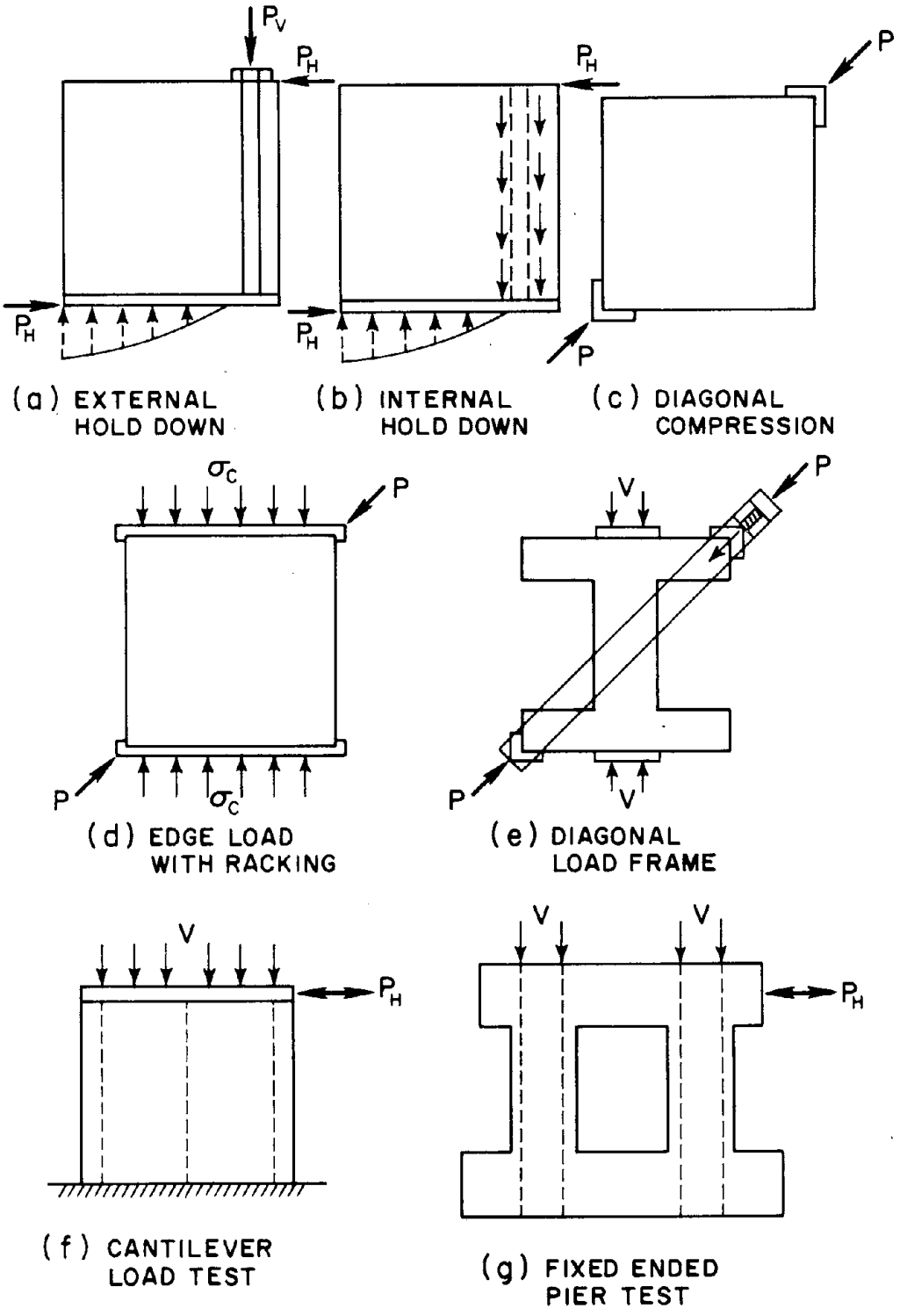

Fig. 1 Test Techniques on Masonry Shear Strength

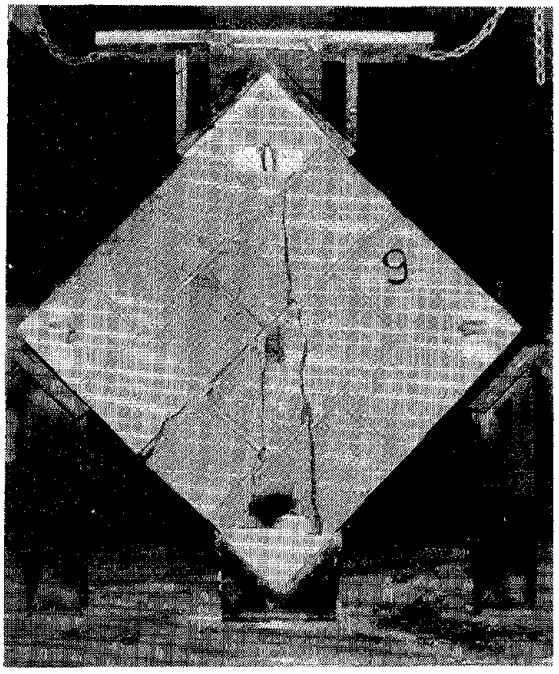

Fig. 2 Diagonal Compression Test

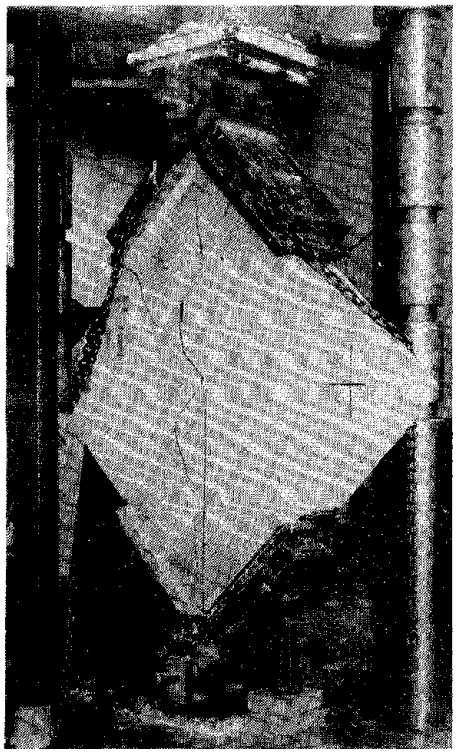

Fig. 3 Modified Diagonal Test

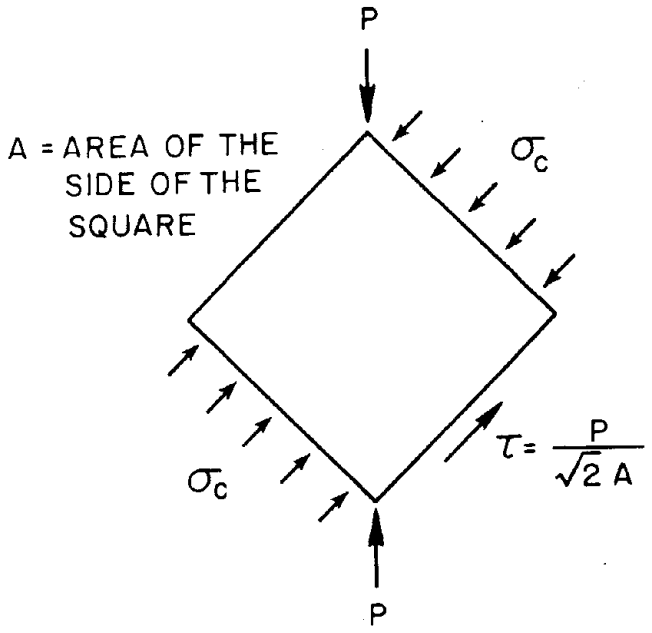

Fig. 4 Stress Distribution

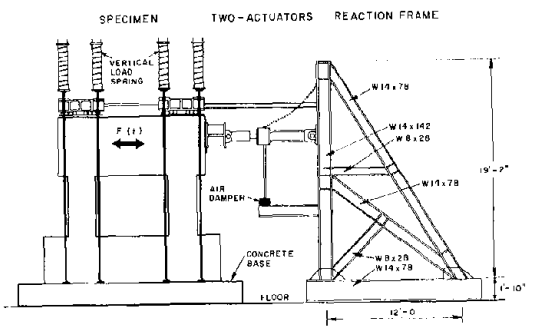

Fig. 5 Cyclic Shear Test

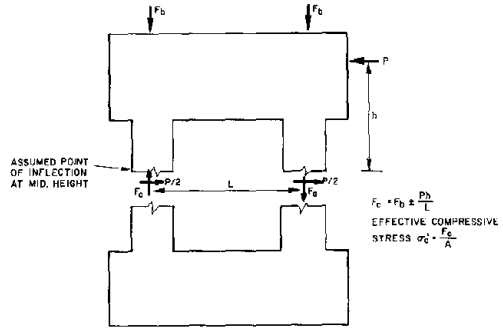

Fig. 7 Assumed Force Distribution in Double Pier

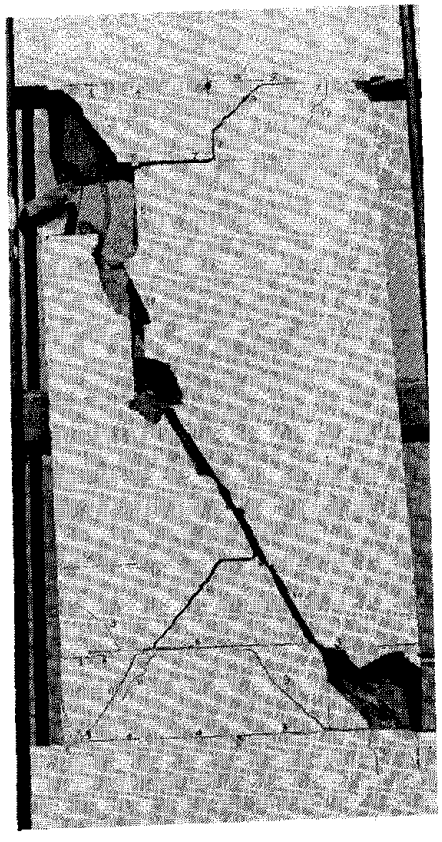

Fig. 6 Shear Mode of Failure on Pier

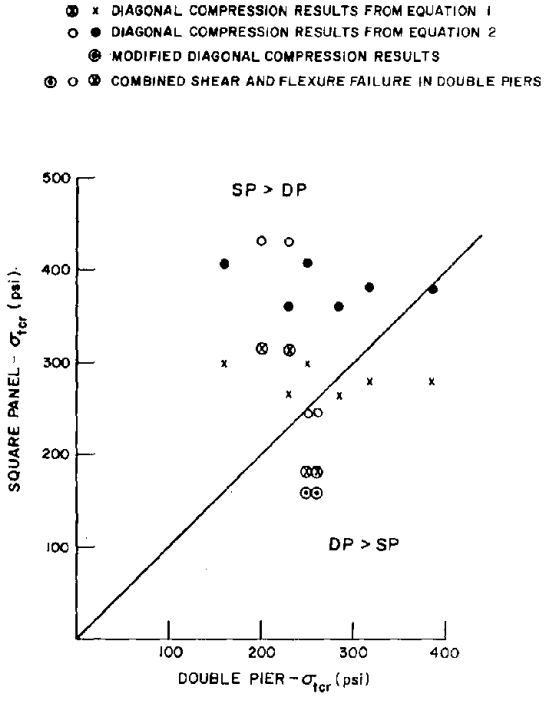

Fig. 8 Test Results of Critical Tensile Strength

TEST OF THE MODEL OF JOINT BETWEEN FLOORSLAB AND SHEAR WALLS OF A PRECAST MULTISTORY BUILDING MADE OR PRESTRESSED CONCRETE

by

B. Petrović[I] and J. Bouwkamp[II]

A full scale model of a floorslab spanned between two stiff shear walls by means of prestressed steel wires was tested in the Institute for Testing Materials of the S.R. Serbia in Belgrade with collaboration of the University of California Berkeley.

During the test, the shear walls were rotated by a hydraulic jack, and the angles of rotation and bending moments in the joints were measured and recorded. The alternating loading on the model increased in moderated steps untill the very large rotation of 23.10^{-3} was achieved. A large number of bending moment diagrams, as a function of the shear walls rotation were taken. The "Bending moment - Rotation" ($M - \phi$) diagrams obtained had a typical bilinear form with an expressive "S" skeleton curve. The change of stiffness corresponded to the opening of cracks between the floorslab and the shear walls and always appeared with the same rotation value. With opening of the cracks, the slope of the $M - \phi$ diagram decreased to 45% of its initial value. The decreasing branch of the $M - \phi$ diagram was always parallel to the increasing branch and the distance between these always reflected a constant value of M. Also, the "turning" points of the increasing and the decreasing branches corresponded to the same rotation of the joint namely $\phi = 2.10^{-3}$.

Areas under the hysteresis loops were constant and equal to 13% of the areas under the increasing part of the $M - \phi$ diagrams, i.e. dissipation of energy was constant to the very large rotations ($\phi = 20.10^{-3}$), and corresponded to approx. 2% from critical viscous damping.

Considering the experimental $M - \phi$ diagram the behaviour of the model was analyzed using the El Centro (E-W) ground acceleration record. Similarly the behaviour of two linear elastic models (using the experimental initial-phase stiffness values) with 2% and 0% of critical damping were analyzed. Spectral curves indicated the significantly improved behaviour of the system considering the actual observed $M - \phi$ relationship.The results pointed out the fact that amplification depends both on the form and the area of the hysteresis loop and, also, that the actual hysteretic behaviour can not be substituted correctly by a damped linear elastic system.

I Assoc.Prof.Institute for Testing of Materials of the S.R. Serbia, Belgrade

II Prof.University of California, Berkeley, California

ANALYSIS OF EARTHQUAKE EFFECTS ON PIPELINES

by

Graham H. Powell[I]

SYNOPSIS

A procedure for computing the seismic response of cross-country pipelines is described, with emphasis on above-ground lines. The procedure accounts for the effects of initial static loads, support nonlinearity, and out-of-phase ground motions at different points along the pipe. The idealization assumptions and theory are described, and the influence of certain parameters on the response is discussed.

INTRODUCTION

Cross-country pipelines in Artic regions are likely to be placed above ground over substantial portions of their length, because the soil deformations produced by buried lines may be unacceptably large. Analyses of earthquake effects on above-ground lines involve substantially different problems from those which arise in analyses of more conventional piping systems. In particular, the following two problems must be recognized.

(1) The pipeline must be firmly fixed to the ground by anchors at intervals along its length. Between anchors, however, it must be allowed to slide on its supports to avoid excessive restraint of movements due to thermal expansion. Hence, the pipe can also slide on its supports during an earthquake, with the result that the dynamic response is nonlinear and governed greatly by the properties of the supports. Linear dynamic analyses, of either response spectrum or time history type, are therefore not applicable.

(2) The pipeline extends long distances in plan, and hence different points on the structure will be subjected to different ground motions. In particular, the relative displacements between anchors may be substantial at any instant of time, producing a time-dependent effect similar to a thermal expansion. Hence, the analysis procedure must take account of out-of-phase support motions.

This paper describes a computational procedure and a computer program for the practical dynamic analysis of cross-country pipelines. The procedure is necessarily approximate, because of the many unknowns in the problem and because the costs for an "exact" analysis would be prohibitive. However, the important parameters affecting pipeline response are taken into account, and the procedure is believed to be of ample accuracy for use in pipeline design.

STRUCTURAL IDEALIZATION

The following assumptions are made to set up the structural model. (1) The pipe lies in a single plane (usually horizontal, but vertical if desired). (2) The pipe is elastic, but rests on inelastic supports. The pipe is idealized as a finite number of beam elements, with masses lumped at the nodes between elements. The supports are idealized as discrete nonlinear springs, to represent frictional resistance and the effects of displacement-limiting stops. (3) Displacements are assumed to be small in comparison with the plan dimensions of the system. (4) The system is prestressed by static loads

---

[I]Professor of Civil Engineering, University of California, Berkeley, California, U.S.A.

(gravity, thermal expansion and/or pressure) before the earthquake begins. This is important because initial loads on the supports substantially affect the subsequent dynamic response. (5) The ground motion is represented as a wave moving past the system with constant velocity.

The analysis can be applied to (a) above-ground configurations subjected to combined longitudinal and transverse ground motions; (b) above-ground configurations subjected to combined longitudinal and vertical motions (in which case the pipe may lift off the supports) and also (c) below-ground configurations subjected to longitudinal and transverse motions (in which case the nonlinear springs can represent longitudinal cohesive resistance as well as transverse soil stiffness). The procedures and computer program details have been described in reports to Alyeska Pipeline Service Company [1,2]. A similar procedure has been developed independently by Anderson and Johnston [3].

THEORY

There are three degrees of freedom at each node, namely rotation plus translations in each of the X and Y coordinate directions. The mass matrix is diagonal. At any instant of time, let:

(1) $\{r_a\}$, $\{\dot{r}_a\}$ and $\{\ddot{r}_a\}$ = vectors of nodal displacement, velocity and acceleration, respectively, with respect to a fixed coordinate system (i.e. absolute quantities).

(2) $\{r_g\}$, $\{\dot{r}_g\}$ and $\{\ddot{r}_g\}$ = vectors of displacement, velocity and acceleration, respectively, of the ground immediately beneath the corresponding node.

(3) $\{r_r\}$, $\{\dot{r}_r\}$ and $\{\ddot{r}_r\}$ = vectors of nodal displacement, velocity and acceleration, respectively, relative to the ground. That is

$$\{r_r\} = \{r_a\} - \{r_g\} \tag{1}$$

with similar equations for $\{\dot{r}\}$ and $\{\ddot{r}\}$.

(4) $[M]$ = diagonal mass matrix, assumed to be constant.

(5) $\{F_m\}$ = vector of inertia forces on the nodes, given by

$$\{dF_m\} = [M]\ \{d\ddot{r}_a\} \tag{2}$$

(6) $[K_p]$ = static structure stiffness matrix for the pipe alone, which is constant because the pipe is elastic and displacements are small.

(7) $\{F_p\}$ = vector of nodal forces due to deformation of the pipe alone, given by

$$\{dF_p\} = [K_p]\ \{dr_a\} \tag{3}$$

(8) $[K_s]$ = tangent static stiffness matrix for the support elements only, which varies because the supports are nonlinear.

(9) $\{dF_s\}$ = increment of nodal forces due to support deformations, given by

$$\{dF_s\} = [K_s]\ \{dr_r\} \tag{4}$$

(10) $[K]$ = tangent static stiffness matrix for complete structure, given by

$$[K] = [K_p] + [K_s] \tag{5}$$

(11) $[C]$ = tangent viscous damping matrix, assumed to be given by

$$[C] = \alpha\ [M] + \beta\ [K] \tag{6}$$

(12) $\{dF_c\}$ = increment of nodal forces due to viscous damping effects, assumed to be given by

$$\{dF_c\} = [C]\{d\dot{r}_r\} \quad (7)$$

Over a time interval dt, the following dynamic equilibrium equation must be satisfied.

$$\{dF_m\} + \{dF_c\} + \{dF_p\} + \{dF_s\} = \{0\} \quad (8)$$

Hence, from Eqs. 2, 3, 4 and 7

$$[M]\{d\ddot{r}_a\} + [C]\{d\dot{r}_r\} + [K_p]\{dr_a\} + [K_s]\{dr_r\} = \{0\} \quad (9)$$

and hence from Eqs. 1 and 5

$$[M]\{d\ddot{r}_r\} + [C]\{d\dot{r}_r\} + [K]\{dr_r\} = -[M]\{d\ddot{r}_g\} - [K_p]\{dr_g\} \quad (10)$$

Eq. 10 can be integrated by step-by-step methods. Equilibrium violations produced in any step because of the finite step size are compensated for by applying an out-of-balance force correction in the succeeding step. The procedure is identical to that used in the DRAIN-2D general purpose computer program for earthquake response of plane inelastic structures [4,5], and is not repeated here.

Two different ground acceleration records may be specified, one representing longitudinal motion of the ground and the second representing transverse motion. The ground displacement records are obtained by double integration within the computer program. Each ground motion is assumed to propagate past the pipeline as a wave with straight wavefront and constant velocity. Any two points on the ground therefore experience the same motions, but these motions are out of phase by the length of time required for the wave to travel between the points.

FACTORS AFFECTING RESPONSE

A typical segment of a large diameter cross-country pipeline will extend approximately 600m between points of "rigid" anchorage to the ground, and will have shallow bends in plan to prevent excessive stresses developing due to restraint of thermal expansion. The pipe will rest on supports at intervals, and will be free to slide laterally on the supports. The amount of lateral movement will be restricted by stops at certain supports, to prevent excessive displacements during an earthquake. Because the operating temperature of the pipe will exceed the construction temperature, the pipe will typically be tending to move outwards at the bends, while being restrained by friction forces. These initial stress effects in the structure have a substantial effect on the subsequent dynamic dynamic response.

Because the anchors are substantial distances apart in plan, it can be expected that the ground displacements will differ at adjacent anchors during an earthquake, possibly by substantial amounts. This relative anchor movement may have a substantial influence on the earthquake response. In particular, if the anchors are assumed to be rigid and infinitely strong, then the computed anchor reactions may be very high, and anchors designed to resist these reactions may have to be massive structures. In fact, however, no anchor can be completely rigid. Also, it may be a sound design procedure to design the anchors to have limited strength, sufficiently large to prevent movement under thermal and pressure loadings, but such as to allow slip during an earthquake. Analyses have shown that substantial reductions in pipe stresses and forces on the pipe stops can be produced by allowing anchor slip, with required slip distances of the order of 15 cm for severe earthquakes.

In order to understand the computed response, it is important to recognize that the X and Y ground motions exert substantially different influences on

on the structure, as follows.

For the case of zero initial stresses in the structure, the Y motions (i.e. transverse to the pipe) exert a relatively small effect on the pipe. This is because the pipe is flexible transversely, and is supported at close intervals on supports which can transmit only small forces to the pipe and which absorb substantial amounts of energy. The effects of Y motion alone in this situation are therefore small. Also, these effects do not change much as the wave propagation velocity changes, because the pipe is flexible and is insensitive to relative support displacements.

For the case with initial stresses, the effect of Y direction shaking is primarily to relieve the stresses produced by frictional restraint of thermal expansion. That is, the pipe tends to move outward, to the position it would adopt if there were no friction. In this case, there is a tendency for the pipe to contact the stops, and the stress changes may be more substantial than for the case with zero initial forces. However, these stress changes tend to relieve the initial stresses.

The effects of X ground motions (i.e. along the pipe) are quite different from those of Y motions. If the pipe were rigidly anchored and the supports all were to move in phase, the stresses produced by the X motions would be small. However, if there are differences between the X displacements at the anchors, then effects similar to those of thermal expansion are produced (except that they are dynamic). The anchor movements in this case tend to produce substantial outward and inward movements of the pipe at the bends, and may produce substantial stop loads and pipe stresses. The effect is more severe for anchors which are rigid than for anchors in which some of the relative ground displacement can be accommodated by anchor slip.

Space does not allow a more detailed discussion of results in this paper.

CONCLUSION

The procedure described in this paper is believed to provide a sound approach for determining the effects of earthquakes on cross-country pipelines. The procedure takes account of the most important parameters affecting the pipeline response, yet is sufficiently simple and efficient for practical use. In the author's opinion, it is doubtful whether any significantly greater accuracy would be obtained for design purposes by using a more refined analysis (for example, accounting for three dimensional effects, inelastic behavior of the pipe, etc.).

ACKNOWLEDGMENT

The development work described in this paper was supported by Alyeska Pipeline Service Co.

REFERENCES

1. Powell, G.H., "DRAIN-PIPE Program User's Guide," Consultant's Report to Alyeska Pipeline Service Co., 1972.

2. Powell, G.H., "Earthquake Response of Above-Ground Piping Configurations," Consultant's Report to Alyeska Pipeline Service Co., 1972.

3. Anderson, J.C. and Johnston, S.B., "Seismic Behavior of Above-Ground Oil Pipelines," Intl. Jrl. of Earthquake Engin. and Struct. Dynamics, Vol. 3, 319-336 (1975).

4. Kanaan, A.E. and Powell, G.H., "General Purpose Computer Program for Inelastic Dynamic Response of Plane Structures," Report No. EERC 73-6, Earthquake Engineering Research Center, University of Caifornia, Berkeley, April 1973.

5. Powell, G.H., "DRAIN-2D User's Guide," Report No. EERC 73-22, Earthquake Engineering Research Center, University of California, Berkeley, October 1973.

PANEL ON DESIGN AND ENGINEERING DECISIONS: FAILURE CRITERIA (LIMIT STATES)

by V. Bertero[1] and B. Bresler[1]

INTRODUCTION

Aseismic design is only one aspect of the design process. In this process, the designer must establish functional and environmental demand conditions on a building and acceptable levels of performance under these conditions. In terms of aseismic design, this requirement calls for establishing critical design earthquake or earthquakes and corresponding acceptable levels of performance or failure criteria. Usually, this problem is stated in terms of establishing design loads and their critical combinations and in terms of permissible limits of structural response under these loading conditions.

The establishment of appropriate loadings and their critical combinations requires decisions as to failure criteria and is the most difficult problem in the design process. One of the major difficulties in establishing such loadings and combinations is the uncertainty associated with predicting future ground motions and that associated with the complex behavior of soil-building systems under severe ground motions. An additional problem is caused by socio-economic requirements for greatest safety at a least reasonable cost. In order to optimize a design or to maximize utility [1], an estimate of economic losses resulting from failure is required. The term failure as used herein is synonymous with "inadmissible limit states" and includes all modes of undesirable behavior, from damage to cosmetic appearance to collapse, which may render buildings unfit for use [1].

OBJECTIVES AND SCOPE. - Other contributions to the Panel on Design and Engineering Decisions will deal with problems of optimization, consequences of failure, and codes. Therefore, the main objective of this paper is to discuss the failure criteria (inadmissible limit states) which

---

1. Professor of Civil Engineering, University of California, Berkeley, U.S.A.

should be considered in aseismic design of buildings. After discussing the principal failure criteria (serviceability and ultimate limit states) presently used in design, results from surveys and analyses of building damage during recent earthquakes are briefly reviewed. These recent observations indicate that an additional category of limit states related to damage which cannot be properly assigned to either serviceability failure or inadmissible ultimate limit states is needed. A discussion of damageability criteria and possible forms of damageability indices is included. Observations of damage in recent earthquakes have clearly indicated that a significant number of existing buildings are hazardous and may suffer varying degrees of damage even under moderate earthquakes. The cumulative effects of aging and other sources of possible distress--such as extreme climatic environment, wind, and fire--must therefore be considered in designing new buildings and in evaluating hazards in existing buildings.

DESIGN BASED ON LIMIT STATES

DEFINITION OF LIMIT STATES. - All structures must be designed to sustain safely all loads and deformations liable to occur during construction and in use, and to have adequate durability during its service life. A structure, or a part of a structure, is rendered unfit for use when it reaches a particular state, called a "limit state," in which it ceases to fulfill the function or to satisfy the conditions for which it was designed [2]. To define the different limit states, it is necessary to identify the various events that might lead to some cost of "disutility" to the occupant, owner, or designer. The different limit states are presently grouped as either serviceability or ultimate limit states. The events normally considered in limit state design and the applications of limit state philosophy to practical design methods are discussed in Refs. 2, 3, and 4. The format used in formulating the limit state design philosophy encourages the use of probabilistic methods where sufficient statistical information is available [3,4]. Because of uncertainties involved in defining the design earthquake, as well as the structural parameters controlling the mechanical behavior of a building, a

probabilistically formulated limit state design philosophy is well-suited for developing aseismic design methods. A logical approach to the aseismic design of a structure is that of comprehensive design.

COMPREHENSIVE DESIGN. - Sawyer [5] discussed a comprehensive design procedure in which the resistance of the structure to the various failure stages is correlated with the probability of the corresponding excitations, so that the total cost, including the first cost and the expected losses from all the limit stages, is minimized. Failure of a structure under increasing loads generally occurs in successively more severe stages under successively less probable levels of load. To illustrate this point, the relationship shown in Fig. 1 shows the failure stages versus a monotonically increasing pseudo-static load for a typical statically indeterminate reinforced concrete building. Due to the variability of loss for a given load (or the variability of load for a given loss), the relationship shown in Fig. 1 should be considered as representing mean values of the random variables involved. The full redistribution, as shown in Fig. 2, can, in some cases, involve large variances [6].

In comprehensive design, identification of the potential modes of failure requires prediction of the mechanical behavior of a structure at each significant level of critical combinations of all possible excitations to which the structure may be subjected. Because it is usually not possible to consider real behavior under the actual critical excitations to which the structure may be subjected, it is common to base structural design on idealized conceptions of mechanical behavior under a simplified set of excitations. The sources, treatment, and effects of the different types of excitations which may be exerted on structures are summarized in Fig. 3 [7]. The sequence of actions to which a structure may be subjected often consists of unpredictable fluctuations in the magnitude, direction and/or position of each of the individual excitations. The only characteristics that may be estimated accurately are the extreme values between which each of these actions will oscillate. These types of actions have been classified in Fig. 3 as generalized or variable-repeated excitations.

The particular phenomena associated with variable-repeated excitations are classified as long-endurance fatigue, low-cycle fatigue, and incremental collapse. Long-endurance fatigue is a critical consideration only in special structures. A review of results regarding low-cycle fatigue, which is associated with repeated-reversible actions, indicates that the real danger of these actions is not fracture of the structural material, but deterioration of the stiffness, particularly in the case of reinforced concrete [7]. Incremental collapse is associated with progressive development of excessive deflections which occur under the cyclic applications of different combinations of peak actions. Because deterioration of stiffness can lead to an undesirable increase in deformations, in examining actual generalized excitations, the effects of alternating excitations cannot be treated independently, as is usually done, from those caused by excitation patterns leading to incremental deformations [7].

CURRENT FAILURE CRITERIA IN ASEISMIC DESIGN

GENERAL GOALS AND CURRENT PRACTICE. - The general philosophy of earthquake resistant design for buildings other than essential facilities has been well-established and proposed to: (1) prevent nonstructural damage in minor earthquake ground shakings which may frequently occur in the service life of the structure, (2) prevent structural damage and minimize nonstructural damage in moderate earthquake shakings which may occasionally occur, and (3) avoid collapse or serious damage in major earthquake ground shakings which may rarely occur. This philosophy is in complete accordance with the concept of comprehensive design. Current design methodologies, however, fall short of realizing the objectives of this general philosophy. Application of the comprehensive design approach to aseismic design would entail replacing the load and load probability scales by the seismic excitation intensity and intensity probability scales, respectively (Figs. 1 and 2). Practical application of this approach is, however, considerably more complex because of difficulties involved in assessing the relationship between loss and seismic excitation. According to the concept of comprehensive design, the ideal design is

that which results in the minimum total cost, including possible losses, for all limit states. However, this ideal is not an immediate practical possibility in actual design. No practical design method has yet been developed that satisfies simultaneously all the requirements imposed by the different limit states. In practice, the most critical limit state is used as the basis for proportioning members in the preliminary design; all other main limit states should then be checked through a comprehensive analysis. The advantages of developing a design method based on two failure stages have been discussed by Sawyer [5], and a design method based on two behavior criteria (collapse and loss of serviceability) and on four optimizing criteria has been developed [8]. Application of this method to the aseismic design of ductile moment-resisting frames seems feasible and practical [9].

Because current design practice in regions of high seismic risk focusses on collapse of the main structure as the controlling limit state, the resulting design must be checked for serviceability requirements under normal loading conditions. Examination of building damage resulting from recent severe seismic ground shaking reveals that although buildings were far from reaching the collapse limit state, the degree of nonstructural damage was so great as to constitute failure. Therefore, it is desirable to introduce a new group of limit states based on damageability. Before discussing this need in more detail, the failure criteria used in present aseismic design practice should be considered.

SERVICEABILITY REQUIREMENTS. - Although the conditions leading to serviceability limit states under normal loading have been defined in general terms [2], specific quantitative limits have not been adequately determined. More practical and consistent quantifications are needed for determining failure stages of structural and nonstructural components under all types of service excitations. For example, it has been recommended that the maximum tolerable drift index for walls be limited to 0.002 [10]. On the other hand, in the case of seismic loads, the 1976 Uniform Building Code (UBC) specifies a maximum index of 0.005. Since seismic forces specified in this code apply to designs at service

load levels; the UBC value for seismic drift appears to be unconservative when compared to that suggested in Ref. 10.

In quantifying the serviceability limit states for seismic excitations, it is necessary to determine the building's function and the level of excitation intensity under which the facility should remain serviceable. In the case of essential facilities, these should not only be safe, but they should be functional for emergency purposes even after the occurrence of the maximum credible excitations expected during the service life of the building. Some quantitative limits for serviceability requirements for essential facilities are shown in Table 1. Although the seismic design forces for the different codes considered in this table are not strictly comparable, the significant differences between these specified tolerable drift indices indicate the need for more thoroughly investigating the degree of damage constituting failure and corresponding tolerable drift criteria.

ULTIMATE OR SAFETY REQUIREMENTS. - Analysis of the causes leading to ultimate failure of the building reveals that this can be induced by different failure mechanisms acting independently or in combination. Some of these limit states appear to be extremely critical under pseudo-static loads, while they may be negligible under dynamic loads. Under a sustained pseudo-static overload, for example, the limit state caused by transformation of the structure into a mechanism leads to instability of the whole structure; this is usually not so under dynamic loading. Actually, present aseismic design methods are based on the assumption that large displacements (large ductility) develop after the structure is transformed into a mechanism. The distinction between pseudo-static and dynamic effects also applies in the case of ultimate limit state caused by deformation instability.

Failures under Generalized Dynamic Excitations. - Collapse of a structure can occur as a consequence of "low-cycle fatigue" or "incremental deformations" under excitation intensities lower than those required to induce instantaneous collapse if these excitations are considered as monotonically increasing. As pointed out in Refs. 1 and 7, cumulative damage resulting from a long, strong ground motion, a short main shock followed by a

succession of aftershocks, or a combination of the main shock and another consequential event or environmental exposure such as fire, can lead to either one of the above two phenomena and therefore merits considerably more attention that it has received.

Yamada and Kawamura [11] have discussed an ultimate aseismic design philosophy of reinforced concrete based on low-cycle fatigue. This type of failure is very sensitive to detailing and quality control of materials and workmanship used in construction. If errors in design or construction, or lack of quality control of materials and of workmanship are eliminated, then application of adequate seismic design provisions with possible further improvements [12], will result in structural designs in which low-cycle fatigue would not control the design. By detailing the expected critical regions of different structural members according to recently proposed seismic code provisions, the energy absorption and energy dissipation capacity developed under cyclic reversals of deformation will be so large as to resist the energy input of even the toughest of credible seismic motions. Even under the most severe ground motions recorded, the number of reversals that can occur between opposite peak deformations having the maximum intensity is not usually large enough to be of serious concern [12]. It should also be noted that under full reversals of symmetrically yielding and strain-hardening or strain-softening structures, the P-Δ effect is cancelled out (Fig. 4).

Studies carried out at Berkeley [13] have shown that one case where low-cycle fatigue could control the design involves members that are used as structural dampers to dissipate energy. One typical example of such a case is that involving coupling girders in coupled wall systems [13]. However, failure of these members does not necessarily lead to complete structural failure. Since these elements act as safety fuses between two different structural resistant systems, their failure would lead to a change in the dynamic characteristics of the system rather than to a brittle failure of the complete system.

A schematic illustration of the incremental collapse, denoted as "crawling collapse," is shown in Fig. 5. Recent studies [14] have shown that this type of failure can control the aseismic design of structure, particularly at sites near the source of seismic ground motions containing severe, long acceleration pulses. For example, the study of the response of a multistory steel frame, optimally designed using a nonlinear method, to seismic ground motions derived from those recorded during the 1971 San Fernando earthquake shows that the frame will collapse due to the type of incremental deformations illustrated by the first story displacement time-history response of Fig. 6. The danger of incremental collapse is aggravated by the high probability that several aftershocks of intensities and dynamic characteristics comparable to that of the main shock will occur. As Newmark and Rosenblueth [1] have pointed out, it is not unusual for a structure which is able to withstand a major shock with visible damage, to collapse during an aftershock.

Although the P-Δ effect is not a factor in failures due to low-cycle fatigue, it is of paramount importance in failures of an incremental collapse type. As a structure is deflected away from its original vertical equilibrium position, the increment in sidesway deflection under repetition of the same acceleration pulse will increase since the structure's available net yielding resistance against lateral inertial forces is considerably reduced by the P-Δ effect (Fig. 5). Accumulation of these increasing incremental deflections can lead to an instability phenomenon under a working load combination (gravity forces plus wind or minor earthquake). Figure 5 indicates that structural instability under working loads may be prevented or delayed by a reduction in the maximum tolerable story drift, by an increase in the yielding strength against lateral forces, or by a combination of these two possibilities. It should be noted, however, that the only advantage in increasing the initial stiffness without either modifying the yielding strength or maximum tolerable story drift will be a small increase in the energy absorption and energy dissipation capacity. Such an increase is illustrated in Fig. 7(a). This figure also indicates that an increase in initial stiffness without a reduction in tolerable story drift will

lead to a considerable increase in ductility demands, and, therefore, greater structural damage. A reduction in the acceptable story displacement ductility will generally lower the danger of instability because such a reduction implies an increase in the required yielding strength of the structure which in turn usually requires a corresponding increase in the initial stiffness. The end result is a story drift at yielding equal to or less than that corresponding to a structure with a lower yielding strength, and a considerably smaller story drift at ultimate condition.

The behavior depicted in Fig. 5 suggests the approximate design method, illustrated in Fig. 7, for preventing or delaying the deformation instability under working load levels. The method is based on the assumption that maximum tolerable story drift, Δ_s^{MAX}, and story shear due to lateral working loads, S_s^W, are known. The total axial force acting on a story during severe seismic shaking is also assumed to be known since it depends only on the gravity forces acting above that story, P_s^G. Two different examples of possible inelastic behavior are considered in Fig. 7. If the mechanism deformation is of a perfectly plastic type, it will be sufficient to draw a line, BO', parallel to OA through point B [Fig. 7(a)]. If the mechanism deformation of the structural system is developed with some strain-hardening, it will be necessary first to locate point B'. Then drawing B'O' with a slope equal to the expected rate of strain hardening, intersection O' will give the mechanism yielding strength required, S_s^Y, as shown in Fig. 7(b). Comparison of Figs. 7(a) and 7(b) illustrates the advantage of having a structural system whose mechanism deforms with some strain hardening.

Experimental results [15] have shown that requirements for preventing instability of structural members depends on the desired level of ductililty. The larger the tolerable ductility, the more stringent the requirements should be. Under loading reversals, when the ductility value exceeds a certain limit, there is a sudden drop in resistance against instability, particularly in the case of reinforced concrete structures.

DAMAGEABILITY LIMIT STATES

LESSONS LEARNED FROM RECENT EARTHQUAKE DAMAGES. - Review of recent earthquake damage reveals that many buildings which did not collapse had to be either completely or partially demolished due to the high amount of nonstructural and structural damage which constituted failure. Numerous buildings whose structural systems did not undergo any significant structural damage, suffered such damage to nonstructural components as to render the entire building unfit for use. As previously pointed out, most present aseismic design methods focus on collapse (ultimate strength and displacement ductility) of the main structural system as the essential limit state. The main problem in applying such methods is in establishing the proper displacement ductility value. Selection of just one value cannot ensure that a structure will be safe and economical or that damage will remain within acceptable limits in all cases.

Although it is generally recognized that the most important single cause of damage is deformation, the types of deformations primarily responsible for damage to nonstructural components remain unclear. It has been argued that while lateral displacement ductility factors generally provide a good indication of structural damage, they do not adequately reflect damage to nonstructural elements [16]. Nonstructural damage is more dependent on the relative displacements (interstory drift) than on the overall lateral displacements. Aseismic design methods must incorporate drift (damage) control in addition to lateral displacement ductility as design constraints. Story drifts and drift ductility factors may also be useful in providing information on the distribution of structural damage, although conventionally computed story drifts are unreliable indicators of potential structural or nonstructural damage to multistory buildings. In some structures, a substantial portion of horizontal displacements results from axial deformations in columns. Story drifts due to these deformations are not usually a source of damage [Fig. 8(a)]. A better index of both structural and nonstructural damage, particularly for frames tightly infilled

with partitions, is the tangential story drift index R. As schematically indicated in Fig. 8(b), this index is used to measure the shearing distortion within a story. For the displacement components shown in Fig. 8(c), the average tangential drift index is equal to $R = (u_3 - u_1)/H + (u_6 + u_8 - u_2 - u_4)/2L$.

Glogau [17] discussed the different types of deformations that could cause damage to nonstructural elements as well as formulated different damage control strategies. Broad damage mitigation strategies have also been discussed by Kost and associates [18].

DAMAGEABILITY. - Establishment of a proper failure criterion based on damageability requires development of a methodology for damageability as an inadmissible limit state under extreme (potentially catastrophic) environmental hazards of the whole building rather than that of the bare structure. Similar to other failure criteria for aseismic design, damageability limit states depend on the type of ground motions being generated. Not only should the intensity of these excitations be considered, but their general dynamic characteristics and their combinations with loads resulting from gravity forces and environmental effects should be accounted for. Damageability limit states can be considered as a category that bridges the gap between serviceability and safety against collapse. Although the primary causes of damageability with which we will be concerned are due to significant overexcitations (large deformational behavior of structural and nonstructural components), effects of service excitations on damageability should not be ruled out. Inadmissible limit states are usually described in terms of limiting the levels of structural response, e.g. maximum displacement, crack width, forces and moments. Although such structural responses may be related to the risk of life-loss, injury, and to economic losses resulting from damage, the relationship of structural response to damage and to socio-economic losses has not been clearly established. To facilitate the establishment of such a relationship, it is proposed to define indices of damageability for a given load or environment exposure history which can be used as an indicator of a limit state condition.

DAMAGEABILITY CRITERIA. - In considering damageability, three general types of damage must be distinguished: (1) local damage - limited to one or several typical elements; (2) global damage - overall damage in a particular event related to the total building; and (3) cumulative damage - overall damage resulting from a series of events, such as strong earthquakes followed by a series of aftershocks, or by other consequential or independent events such as fire, or some other combination of normal and catastrophic events.

Physical damage to both structural and nonstructural components is related to structural response characteristics. Recent advances in methods of structural analysis for complex nonlinear behavior under a variety of dynamic load conditions as well as under fire [19-21] and other environmental exposures provide a basis for investigating damageability. One problem encountered in these investigations involves the proper modeling of nonstructural components to study their interaction with structural models. Because there are no reliable data on the actual mechanical behavior of these components, it will be necessary to study the type and amount of deformation and/or forces that are required to produce different levels of damage in masonry, wood panels, gypsum boards, glazed openings, equipment, etc. Another difficulty in realistically assessing structural response and potential damage in existing structures subjected to earthquake is in properly evaluating the current state of the building at the time of the earthquake. Such evaluation involves considering the effects of (1) previous exposure to climatic environment (thermal changes or shrinkage), causing a state of residual stress or distress, and deterioration in structures due to aging and corrosion; (2) degradation in strength and stiffness caused by previous exposure to high winds, fires and/or earthquakes; (3) other disturbances or movements of the foundation; and (4) changes in strength and stiffness due to alterations, repair, or strengthening. Because any one of these conditions can significantly alter structural response, one of the problems that must be included in the study of damageability is the effect of variations in load and environmental histories, and the residual conditions in the structure (residual stress, cracking,

corrosion, and other changes in stiffness or strength of the materials). Once the "present state" of a building has been properly assessed, and the mechanical (or mathematical) model is clearly described in terms of the intensity and characteristics of the ground motion, the response of a building (structural and nonstructural components) can be determined. A general evaluation framework, which is based on a sequence of basic procedures starting with the simplest models and employing more complex models as needed to achieve desired reliability, has been formulated [22]. This procedure is referred to as "screening."

Several procedures for evaluating earthquake safety of existing buildings were proposed following the 1971 San Fernando earthquake and have since been incorporated into practice [23]. These methods fall into two general categories. The first includes procedures which may be found in mandatory regulations, the second, proposals which focus on methodology and are published as technical reports or papers. These methods do not, however, address the problem of global or cumulative damage, nor do they provide a means for including nonstructural damage in an overall assessment of damageability.

DAMAGEABILITY INDICES. - An index of local damageability, D_i, for a given element i in a building exposed to a specified load or environmental exposure is defined here as the ratio of building response demand for this element (d_i) to its corresponding resistance capacity (c_i) that is, $D_i = d_i/c_i$, where capacity c_i is the limit value for building response without damage. Both structural and nonstructural elements should be considered in evaluating damageability index D_i. For the design of new buildings, values of d_i and c_i must consider randomness in loading demand as well as in "as built" condition determined by quality control during construction. With properly defined values of d_i and c_i, damage will occur when $D_i > 1$; when $D_i < 1$, no local damage should occur, and in this case, D_i should be assigned a value of zero.

Overall or global damageability index D_g may be defined as the sum of nonzero values of D_i, including structural and nonstructural components which might be damaged in a particular event of extreme

exposure. Values of D_i must be weighted by an appropriate importance (life hazard, cost, etc.) factor, p_i, as $D_g = \sum_n p_i D_i$. The sum is taken over n damageable elements, including both structural and nonstructural components. Index D_g should be normalized to $\overline{D}_g$ in order to use the latter for comparing two buildings or two alternate designs of the same building. Several possible ways to accomplish this normalization should be explored. For example, $\overline{D}_g$ may be defined as $\overline{D}_g = D_g/\sum_n p_i$, or more appropriately as $\overline{D}_g = D_g/\sum_m p_i$, where n is the number of damageable elements, m is the total number of elements (both damageable and nondamageable), and $\sum_m p_i$ reflects some overall current value of a building.

The cumulative damageability index, D_c, may be defined as the sum of nonzero values of $p_i D_i$, including structural and nonstructural components which might be damaged as a result of a specified sequence of events, for example, fire exposure, repair of fire damage, strong earthquake, with specified strong aftershocks. Such factors can be taken into account in evaluating local damageability by introducing service history influence coefficients n_i (for demand) and χ_i (for capacity), which are also influenced by the randomness of these influences. Then $D_i' = n_i d_i/\chi_i c_i$, where D_i' is the current nonzero local damageability index which accounts for the assumed service history of a building. If N is the number of damageable components in such a case, then $D_c = \sum_N p_i D_i'$. Normalized value $\overline{D}_c$ can then be expressed as $\overline{D}_c = D_c/\sum_m p_i$. For old buildings, evaluation of the damageability index is further complicated by the significant influence that the service history of a building may have on the values of both demand and capacity (either increasing or decreasing these values), due to such factors as aging, change in use or occupancy or in socio-economic conditions (which would affect p_i values), structural and nonstructural modifications, fire damage and repair, corrosion, etc. The same problems exist for new buildings, due to the uncertainties associated with predicting future earthquakes. Then $D_g' = \sum_n p_i' D_i'$ and $D_c' = \sum_N p_i' D_i'$, where p_i' is the current importance factor (which may differ from the factor p_i used in the original design). Normalized values of $\overline{D}_g'$ and $\overline{D}_c'$ for existing buildings can be defined

similarly to $\overline{D}_g$ and $\overline{D}_c$ values for new buildings. The larger the value of $\overline{D}$ or $\overline{D}'$, the greater the overall damageability index of a building. When $\overline{D}$ or $\overline{D}'$ exceeds some specified limit value, the damageability risk is too great and the building should either be redesigned or strengthened, or demolished.

DAMAGEABILITY AS FAILURE CRITERION. - The general philosophy of developing a method and criteria for assessing damageability has been presented, but the methodology for evaluating the different damageability indices are still undergoing development [23]. One of the main problems encountered in developing such methodology is in defining reliable procedures for calculating the values of d_i, c_i, p_i, η_i, χ_i, and p_i'. Quantification of damageability limit states will require extensive investigation of the mechanical behavior of nonstructural elements, or, what Kost et. al. [18] have termed, EFS (enclosure, finish, and service systems) components. With the findings from such studies, it will be possible to develop a conceptual model for analyzing the dynamic behavior of entire soil-structure systems. Implementation of the model in damageability limit state studies will enable guidelines for assessing failure criteria in aseismic design to be formulated.

ACKNOWLEDGEMENTS

This paper is based on studies conducted under the sponsorship of the National Science Foundation.

REFERENCES

1. Newmark, N. M. and Rosenblueth, E., Fundamental Earthquake Engineering, Prentice-Hall, Inc., 1971.

2. International Recommendations for the Design and Construction of Concrete Structures, 2nd ed., FIP 6th Congress, Prague, 1970.

3. "Limit States Design," Proceedings of Intl. Conf. on Planning and Design of Tall Buildings, ASCE Tech. Comm. 26, Lehigh Univ., Aug. 1972.

4. Stevens, L. K., "Limit State Philosophy and Application," Proceedings of Austral. and N.Z. Conf. on Planning and Design of Tall Buildings, Sydney, 1973.

5. Sawyer, H. A., Jr., "Comprehensive Design of Reinforced Concrete Frames by Plasticity Factors," 9th Planning Session of CED Symp.: Hyperstatique, Ankara, September 1964.

6. Tichy, M. and Vorlicek, N., "Flexural Mechanics of Reinforced Concrete Frames by Plasticity," Proceedings of Intl. Symp. on Flex. Mechs of Reinforced Concrete, ACI SP-12, Miami, November 1964.

7. Bertero, V. V., "Research Needs in Limit Design of Reinforced Concrete Structures," Report No. EERC 71-4, University of California, Berkeley, 1971.

8. Cohn, M. and Parimi, , "Inelasticity and Nonlinearity in Structural Concrete," Study No. 8, Solid Mechanics Division, University of Waterloo, Ontario, 1973,.

9. Bertero, V. V., "Nonlinear Seismic Design of Multistory Frames," ACI-IMCYC Fall Conference, Mexico City, October 1976.

10. "Allowable Deflections," Proceedings, Journal of the ACI, ACI Comm. 435, Vol. 65, No. 6, June 1968.

11. Yamada, M. and Kawamura, H., "Resonance-Fatigue Characteristics for Evaluation of the Ultimate Aseismic Capacity of Structures," 6WCEE, New Delhi, January 1977.

12. Bertero, V. V. and Popov, E. P., "Hysteretic Behavior of Ductile Moment-resisting Reinforced Concrete Frame Components," Report No. EERC 75-16, University of California, Berkeley, 1975.

13. Mahin, S. A. and Bertero, V. V., "Nonlinear Seismic Response of a Coupled Wall System," Jnl. of the Struc. Div., ASCE, Vol. 102, No. ST9, September 1976.

14. Bertero. V. V., "Establishment of Design Earthquakes - Evaluation of Present Methods," ISESE, St. Louis, August 1976.

15. Bertero, V. V., et al., "Seismic Design Implications of Hysteretic Behavior of Reinforced Concrete Structural Walls," 6WCEE, New Delhi, January 1977.

16. Mahin, S. and Bertero, V., "Problems in Establishing and Predicting Ductility in Aseismic Design," ISESE, St. Louis, August 1976.

17. Glogau, O. A., "Damage Control in New Zealand Public Buildings through Separation of Nonstructural Components," 6WCEE, New Delhi, January 1977.

18. Kost, et al., "The Interaction of Building Components during Seismic Action," 6WCEE, New Delhi, January 1977.

19. Becker, J.M. and Bresler, B., "Reinforced Concrete Frames in Fire Environments," Jnl. of the Struc. Div. of ASCE, Vol. 103, No. ST1, January 1977, pp. 211-224.

20. Bresler, B., "Response of Reinforced Concrete Frames to Fire," Prelim. Report of the 10th Cong. of the IABSE, 1976.

21. Bresler, B., et al., "Limit State Behavior of Reinforced Concrete Frames in Fire Environments," Proceedings of the Regional Conference on Tall Buildings, Hong Kong, September 1976.

22. Okada, T. and Bresler, B., "Strength and Ductility Evaluation of Existing Low-rise Reinforced Concrete Buildings - Screending Method," Report No. EERC 76-1, University of California, Berkeley, 1976.

23. Bresler, B., and Axley, J., "Rehabilitation of an Existing Building: A Case Study," Report No. EERC 76-25, University of California, Berkeley, 1976.

TABLE 1 LATERAL INTERSTORY DRIFT INDEX LIMITATIONS FOR ESSENTIAL FACILITIES

U.S. VETERAN ADMINISTRATION HOSPITALS[1]	1976 UBC[2]	NEW ATC-3 PROPOSAL[1]	MEXICO FEDERAL DISTRICT[1]	NEW ZEALAND[1]
0.0078 0.0026[a]	0.005 0.01[b]	0.01	0.05	0.006[c] 0.01[d]

(1) Maximum value considering inelastic deformations.

(2) Maximum value based on code prescribed forces at service level.

(a) For glazed openings.

(b) Equipment must remain in place and be functional.

(c) When nonstructural components are not separated from the structure.

(d) When nonstructural components are separated from the structure.

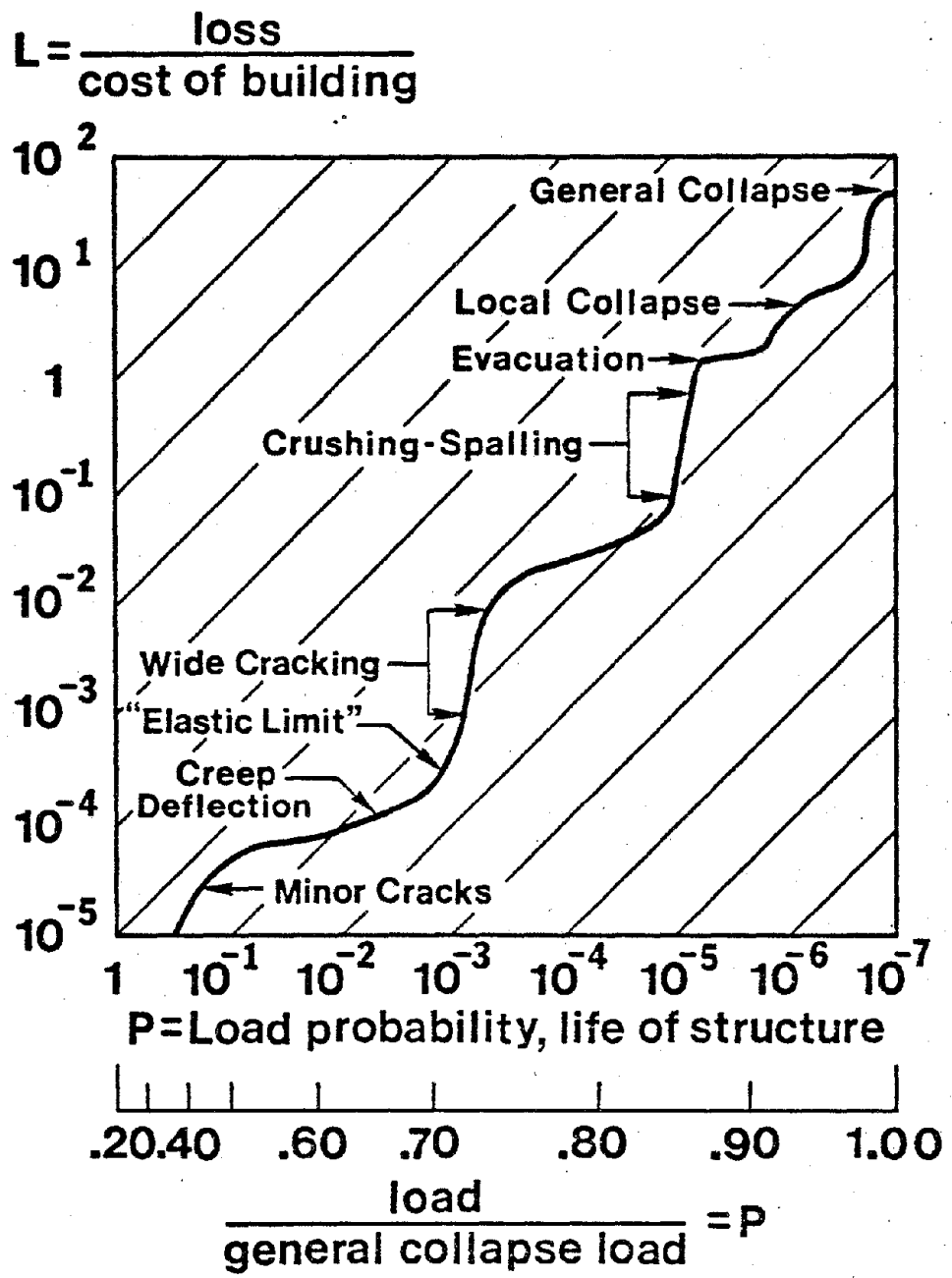

FIGURE 1 ASSESSMENT OF MEAN LOSSES VS. LOAD PROBABILITIES DURING THE LIFE OF STRUCTURE [5]

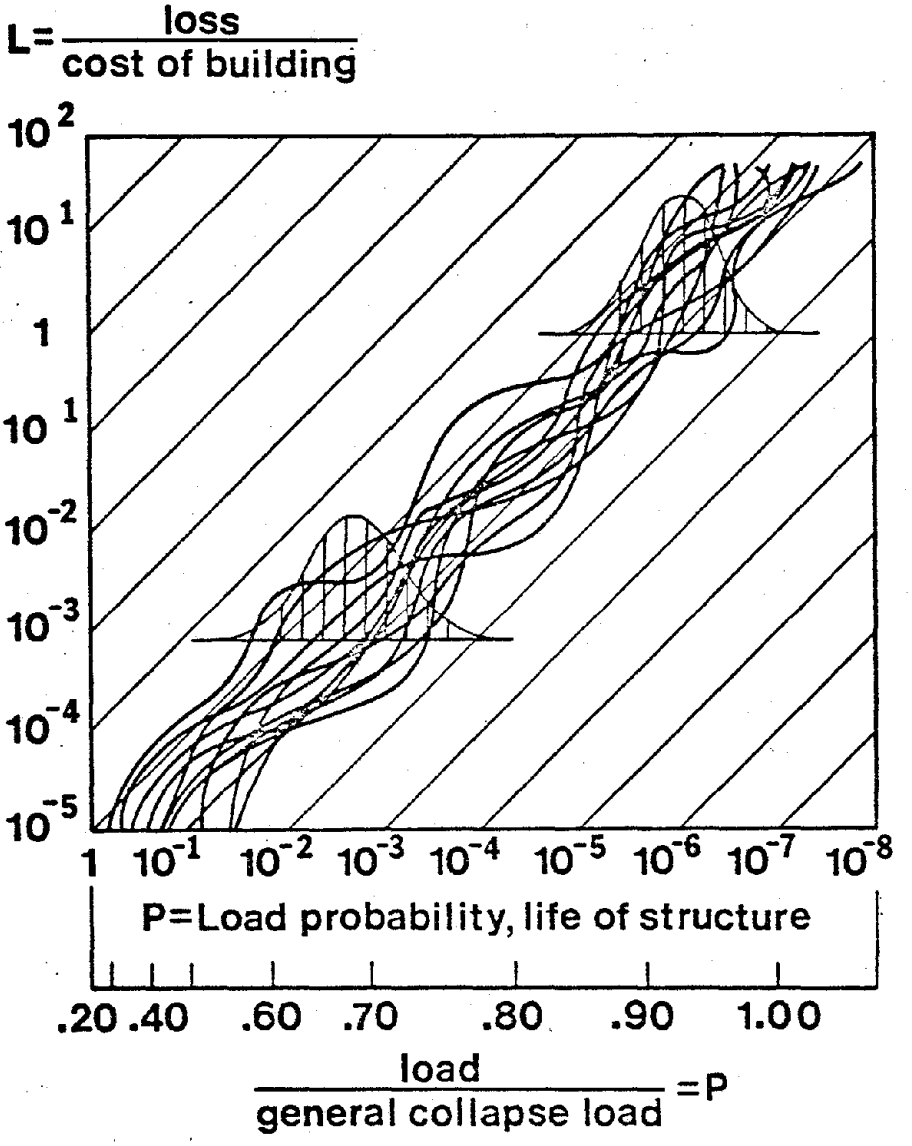

FIGURE 2 DISTRIBUTION OF LOSSES VS. LOAD PROBABILITIES DURING THE LIFE OF STRUCTURE [6]

SOURCES TREATMENT AND EFFECTS OF EXCITATIONS ON STRUCTURES

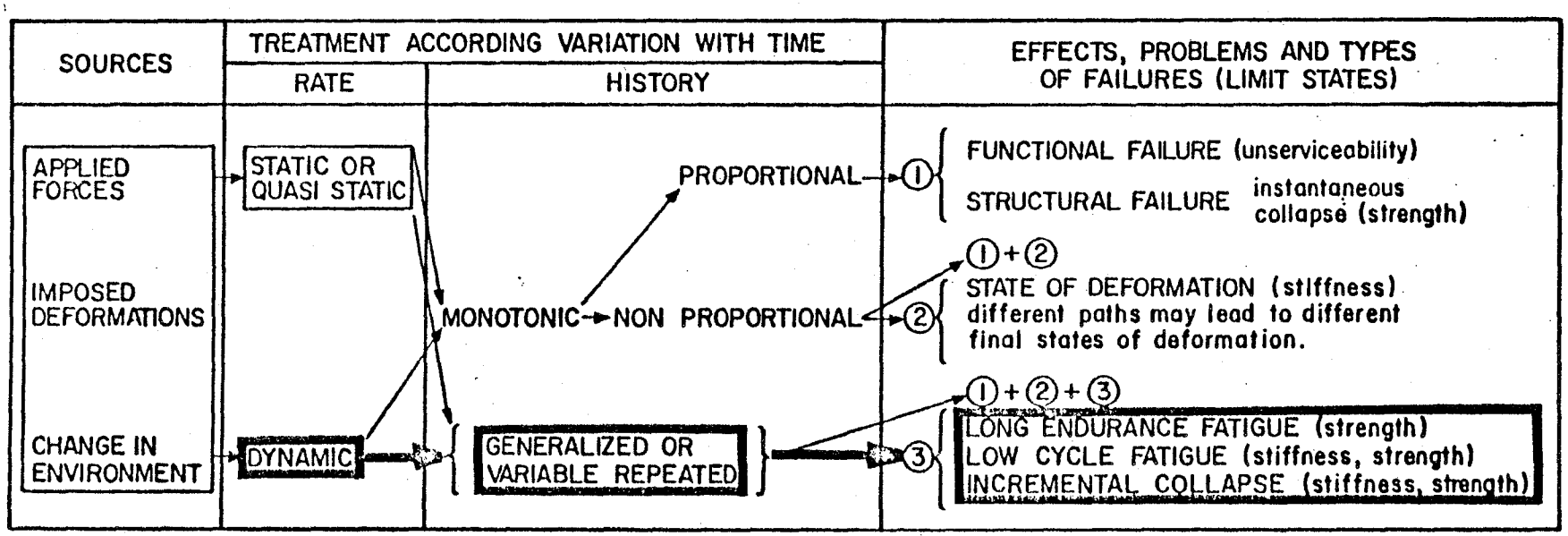

FIGURE 3 SOURCES, TREATMENT, AND EFFECTS OF EXCITATIONS ON STRUCTURES

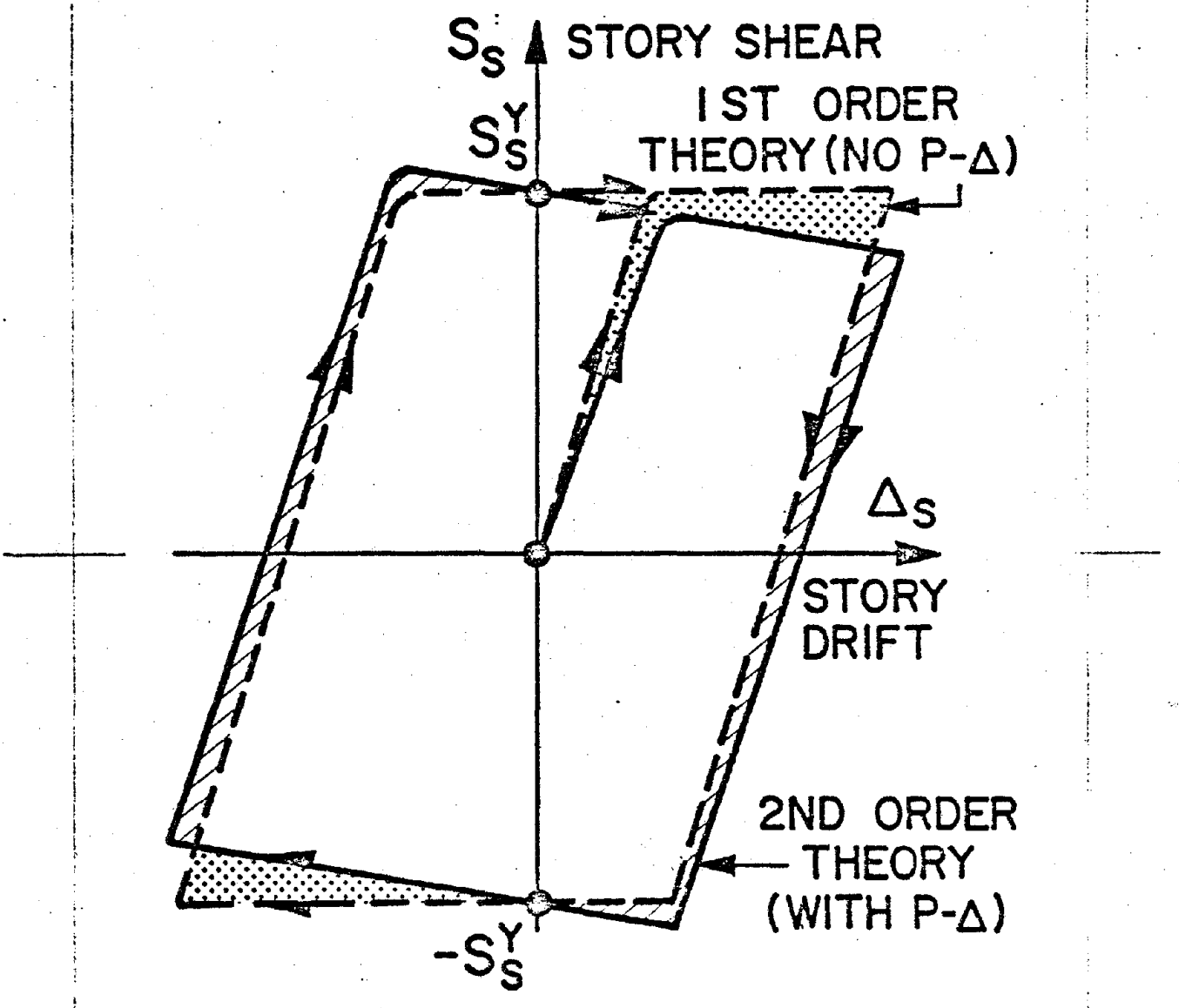

FIGURE 4 EFFECT OF P-Δ ON LOW-CYCLE FATIGUE

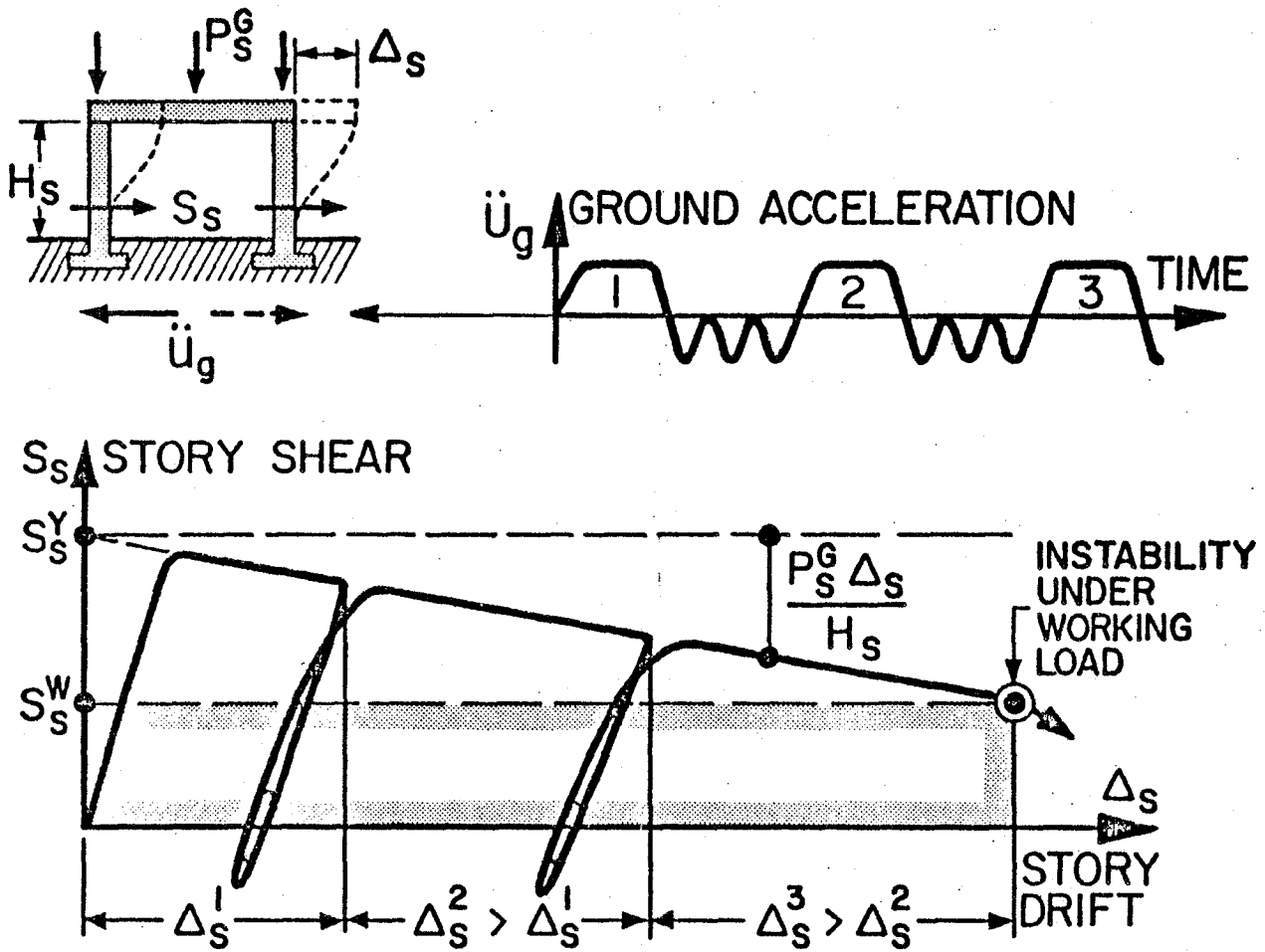

FIGURE 5 INCREMENTAL COLLAPSE

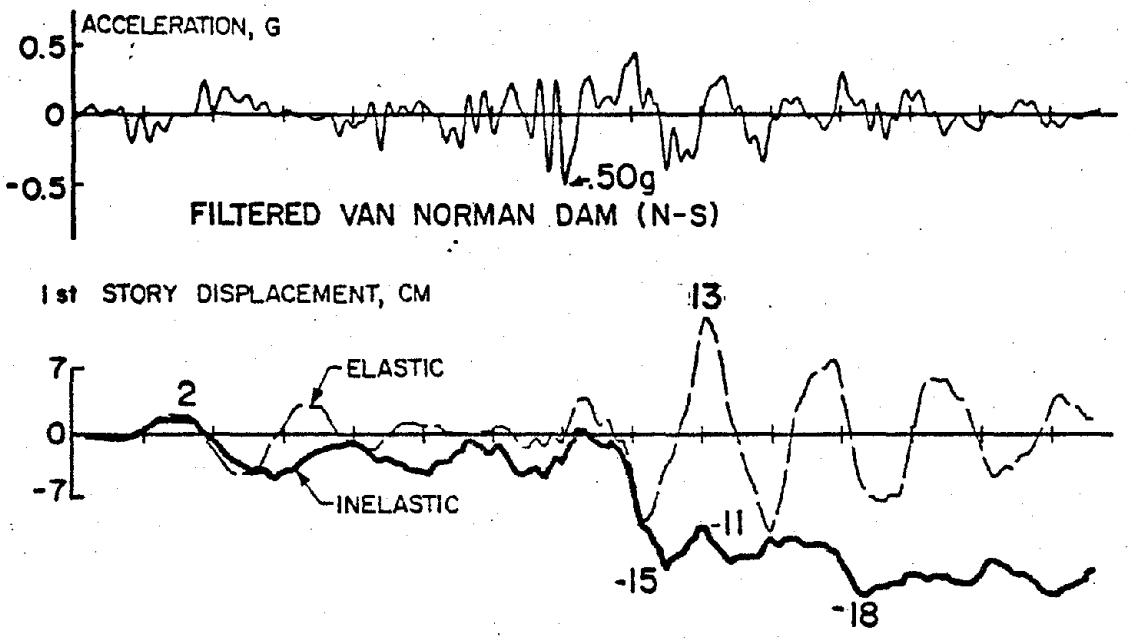

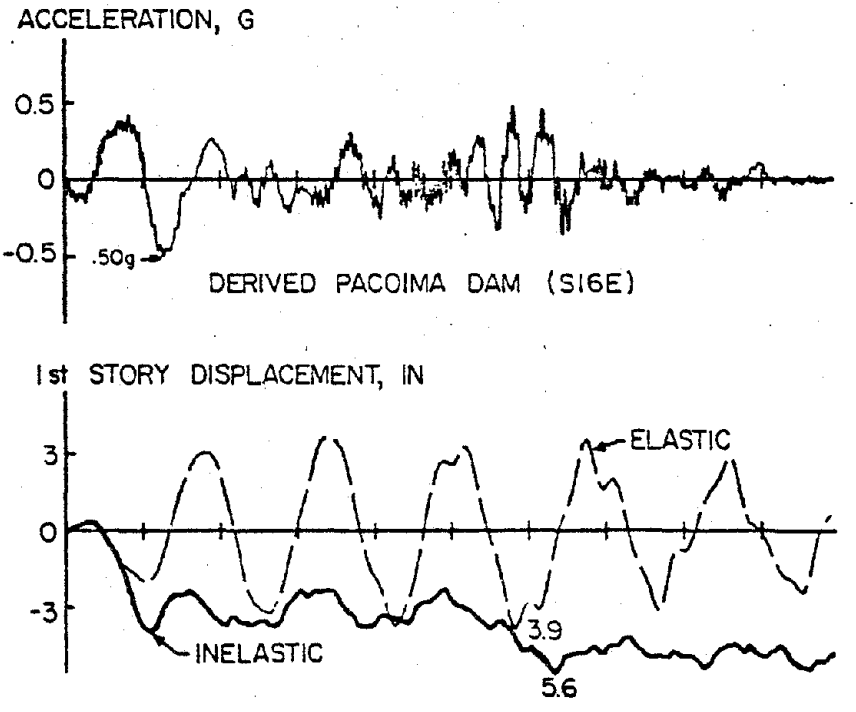

FIGURE 6 FIRST-STORY DISPLACEMENT TIME-HISTORY RESPONSE [14]

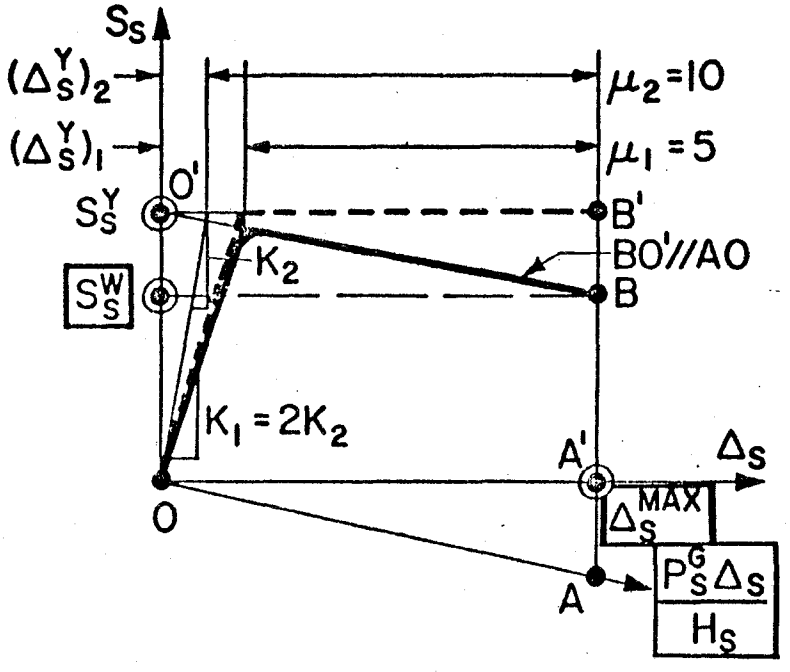

(a) ELASTIC-PERFECTLY PLASTIC BEHAVIOR

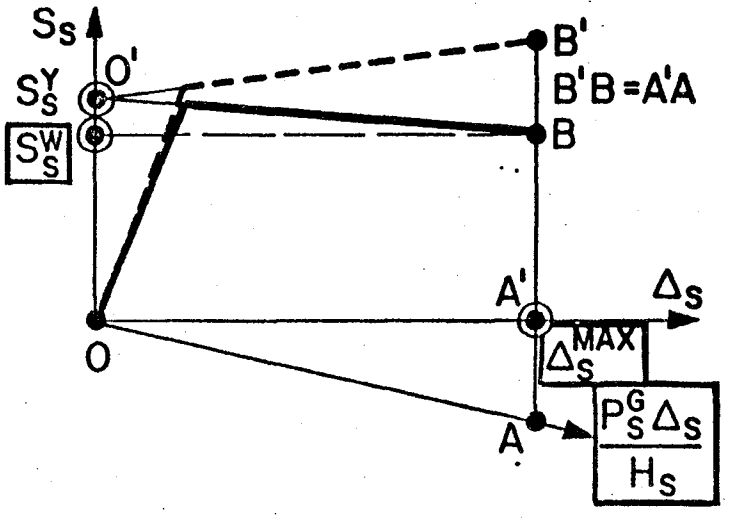

(b) STRAIN-HARDENING BEHAVIOR

FIGURE 7 DETERMINATION OF REQUIRED YIELDING STRENGTH TO AVOID INSTABILITY DUE TO P-Δ

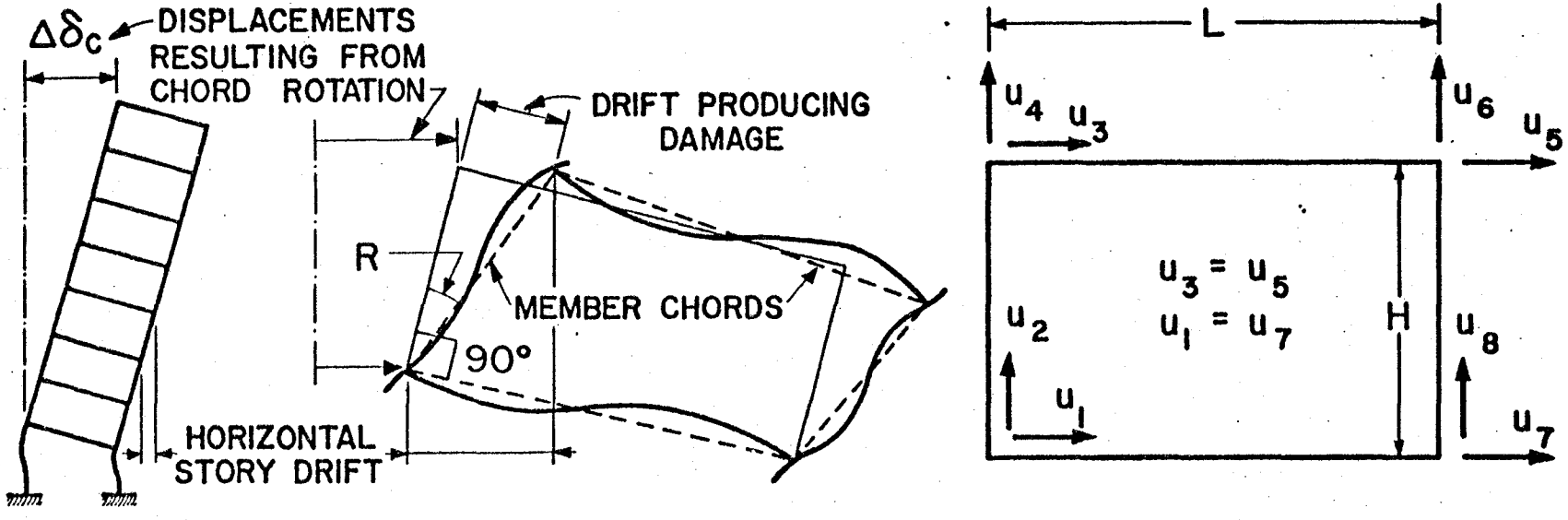

(a) DRIFTS DUE TO AXIAL FORCES IN FIRST STORY COLUMNS

(b) DRIFT DUE TO STORY DEFORMATION

(c) DISPLACEMENT COMPONENTS FOR COMPUTING R

FIGURE 8 STORY DRIFT

Dynamic Tests on Structures

(Theme Report)

by

Joseph Penzien[I]

SYNOPSIS

Presented is a brief report on the thirty papers assigned to TOPIC 9 - DYNAMIC TESTS ON STRUCTURES. While some coverage is given in these papers to experimental techniques, including certain recommendations for improvements, they generally concentrate on the interpretation of dynamic test results in terms of structural performance under seismic conditions. The tests were performed on real buildings, test buildings, building frames, water tanks, chimneys, dams, and a suspension bridge. Some general overall observations are made regarding the content of these papers and certain recommendations are given for future testing.

OBJECTIVE

The main objective of conducting dynamic tests on structures is to improve and verify mathematical modelling which is intended to realistically represent prototype behavior under seismic conditions. Therefore, such tests must concentrate on obtaining dynamic response characteristics of complete structure-foundation systems, including force-deformation, energy absorption, and failure characteristics. Ultimately, the objective of performing dynamic tests on structures is to improve seismic resistant designs and, through analyses, to verify that adequate levels of safety have been provided.

EXPERIMENTAL TECHNIQUES

Various types of dynamic excitation were used in the test programs reported including ambient ground motions, microtremors, wind, impact, mechanical vibration, hydraulic actuator forces, shaking table motions, and strong seismic ground motions; thus, the dynamic forces imposed varied greatly in their time-history characteristics, spatial distributions, and intensities. Dynamic force-deformation characteristics were obtained through standard measurements of force, displacement, velocity, acceleration, and strain which, when combined with visual observations, provided the means for determining failure characteristics. Correlation of test results with analytical predictions were made using well-known methods of dynamic analysis. Recently developed Fast Fourier Transform techniques aided greatly in this effort.

The on-line system described in paper No. 1* represents a significant new development in controlling dynamic testing. When testing with hydraulic actuators using displacement electronic control, this system allows the displacement command signals to be consistent with the test structure's response to a prescribed earthquake excitation; thus, the command signals are coupled to the actual force-deformation characteristics of the structure being tested. While this on-line system has been applied to only a single actuator case, its use could be extended to multi-actuator applications.

I Professor of Structural Engineering, University of California, Berkeley.

* See Listing of Pages

As pointed out in paper No. 2, a need exists for developing improved measurement techniques for dynamic testing. Laser displacement measurements, photogrammetry, and telemetry were techniques mentioned which could assist in this development. Whatever techniques are used, it is important to know the possible quantitative errors present in experimental results. As pointed out in paper No. 3, regression analyses can be used for this purpose.

TEST RESULTS

A. REAL BUILDINGS

1. General - Papers Nos. 4 and 5 present results of dynamic tests performed on numerous buildings in Japan. Without identifying specific buildings, quantitative results showing dynamic response characteristics for different classes of buildings and foundation conditions are given.

Using test data from vibration measurements on many high-rise buildings under ambient, forced vibration, and actual earthquake conditions, the authors of paper No. 4 obtained natural periods of vibration and equivalent damping ratios for translational and torsional modes by applying Fourier analysis techniques to the motions measured at numerous floor levels. Although these results have wide scatter, the general trends show the damping ratio to be inversely proportional to period of vibration (except in the long period range) and to be considerably less for the fundamental mode than for higher modes. The approximate relationship between fundamental period T_1 and its damping ratio h was found to be $h = 0.04/T_1$ and $h = 0.02/T_1$ for soft and hard soil conditions, respectively. It was concluded by the authors that for analysis purposes the mechanism of equivalent viscous damping for buildings should be coupled to a mechanism representing foundation damping under rocking conditions. Combining these two mechanisms, their analytical results correlated well with experimental results.

In paper No. 5, the authors present the results of vibration tests carried out on 18 tall buildings to obtain periods of vibration and equivalent damping ratios and they present similar results obtained by analyzing the measured response of 11 tall buildings during earthquakes. The vibration tests showed the relationship between fundamental period T_1 and number of stories N to be approximately $0.06N<T_1<0.10N$ and $0.03N<T_1<0.06N$ for steel frame buildings and for reinforced concrete and reinforced concrete-steel composite frame buildings, respectively. On the average, the second and third periods of vibration were related to the fundamental period as given by $T_2 = 0.33T_1$ and $T_3 = 0.19T_1$, respectively, for all construction types. The fundamental torsional period T_T was found equal to $0.8T_1$ on the average but in some cases it was found to be nearly equal to T_1. The damping ratios for the modes in general were found to be in the ranges $.005<h<.020$ and $.015<h<.060$ for steel frame buildings and for reinforced concrete and reinforced concrete-steel composite frame buildings, respectively. From the results obtained for the 11 buildings subjected to earthquake excitations, it was found that the fundamental periods had increased by about 13 percent over their corresponding values obtained from vibration tests. These longer periods due to the higher response (10 - 50 times) produced by earthquake excitation over the response developed by mechanical excitation, indicate that buildings generally act as nonlinear softening systems.

2. Oak Center Towers Building - Paper No. 6 presents the results of forced vibration tests carried out on the Oak Center Towers, an eleven-story reinforced masonry building located in Oakland, California. It is constructed with reinforced concrete block shear walls and prefabricated prestressed concrete slab

floor elements. The foundation consists of spread footings under each shear wall. Mode shapes, frequencies, and damping ratios were obtained from the test results. All of these quantities were significantly affected by foundation and in-plane floor flexibilities. The fundamental transverse frequency (2.78 cps) was found to be nearly equal to the fundamental torsional frequency (2.83 cps) showing considerable coupling between these two modes. The damping ratios in the various modes examined were in the range 2 to 9 percent depending upon the relative importance of foundation damping. Consistent with this observation, damping was much higher in the fundamental transverse mode than in the second transverse mode. Analytical predictions of shapes and frequencies for the first and second modes correlated well with experimental results but large discrepancies were found in these same correlations for higher modes.

3. Millikan Library Building - Paper No. 7 presents the results of forced vibration tests carried out on the Millikan Library, a nine-story reinforced concrete building located on the campus of the California Institute of Technology in Pasadena, California. During the tests, closely spaced three-dimensional measurements of the motions on many floors were recorded along with selected strain measurements. This extensive set of measurements permitted a close examination of the deformation patterns produced; thus, providing valuable information on the type and amount of interaction between the various structural elements, e.g., between frames and shear walls, between structural and nonstructural systems, and between building and foundation. The shear walls were observed to act much like Euler beams with shearing deformations included and the foundation was observed to contribute significantly to the flexibility of the overall structural system (4 and 25 percent of the roof translation in a fundamental mode were produced by translation and rotation of the basement slab, respectively).

4. Ralph M. Parsons Building - Paper No. 7 also presents the results of forced vibration tests carried out on the Ralph M. Parsons Company World Headquarters building, a twelve-story steel frame building located in Pasadena, California. Like the Oak Center Towers building, the test results show strong interference or coupling between translational and torsional modes. The authors indicate that such coupling could produce stresses 75% higher in outer columns than would be produced with purely uncoupled translational motion and they properly question whether or not codes adequately provide for such a possibility. Similar to many buildings, the Ralph M. Parsons building responds with large interaction between structural and nonstructural systems under small-amplitude test conditions. It was found that this interaction appreciably increased the frequencies of the first three translational modes in the N-S direction. As pointed out by the authors, this strong interaction would undoubtedly be greatly lessened under large-amplitude seismic conditions, i.e., the building would act as a nonlinear softening system. The damping ratios for the various modes were found to be in the range 2.5 to 6.5 percent of critical; thus, showing considerable scatter and influence from the interaction of structural and nonstructural systems.

5. Jet Propulsion Laboratory Building 180 - Paper No. 8 presents the results of forced vibration tests carried out over a period of 12 years on Building 180 of the Jet Propulsion Laboratory, Pasadena, California, a nine-story steel frame structure supported on continuous strip footings. The results obtained reveal the variable nature of the building's dynamic characteristics over that period due to changes in mass and stiffness distributions. Using natural frequencies measured upon completion of the steel frame and the corresponding frequencies measured later upon completion of the building and considering mass changes due to the addition of materials (concrete to columns, fireproofing of girders and trusses, air conditioning, windows, facing, etc.), it was determined that the building's

overall stiffness had increased over this final phase of construction by factors of 1.75 and 1.45 in the N-S and E-W directions respectively; thus showing the large influence of the nonstructural system on overall stiffness. Later during the San Fernando, California, earthquake of 1971, measurements of the building's response indicate that these same overall stiffnesses decreased during the earlier part of the motion by factors of 1.69 and 1.51, respectively, showing nonlinear softening behavior. Subsequent repair resulted in the building regaining some of its stiffness lost during the earthquake. All of the above changes in stiffness emphasize the difficulties in arriving at realistic mathematical models for buildings.

B. TEST BUILDINGS

1. Reinforced Concrete Frame Buildings - Results of vibration tests on a full-scale four-story reinforced concrete test building having no nonstructural elements located at the Nevada Test Site of the U. S. Energy Research and Development Administration are reported in paper No. 9. Using a large mechanical vibrator capable of producing force amplitudes up to 5,500 kg at frequencies greater than 1.6 H_z, amplitudes of response were developed sufficiently large to produce major damage, i.e., spalling of concrete on columns and yielding of reinforcing steel. Initially, nondestructive tests were performed, exciting 4 translational modes in the elastic range. Next, by exciting the structure at its lowest mode frequency, a destructive test causing major damage was performed. Finally, post-destructive tests at force amplitudes comparable to the nondestructive tests were carried out. During the initial nondestructive tests, the period of the lowest mode increased about 25 percent from low to high amplitude conditions and the corresponding damping ratio increased from 1.25 to 1.75 percent of critical; thus, showing a slightly nonlinear softening system. This same fundamental mode showed an increase in period by 60-70 percent with a corresponding increase in damping ratio to 4 percent of critical from the non-destructive to post-destructive state. During the destructive test, the fundamental mode period increased from 0.52 seconds in the elastic range to 0.90 seconds in the range of major damage with corresponding changes in the damping ratio from 2.2 to 5.5 percent of critical.

Paper No. 10 presents the results of static and shaking table tests on a 1:3 scale model of a rectangular five-story reinforced concrete building having 4 rigid frames in each horizontal direction with precast concrete floors. This building was tested in a bare state, i.e., without any nonstructural elements. Four successive static monotonic loadings were applied at the fifth floor level (1) an initial loading in the elastic range, (2) a loading following shaking table tests which produced micro-cracking, (3) a loading following shaking table tests which produced major cracking, and (4) a loading following shaking table tests which produced major damage in the vicinity of beam-column joints. Stiffness degradation by a factor of 3.8 was noted from the initial elastic loading to the final loading prior to reaching a collapse state. In the shaking table tests, damping ratios were found to range from less than 1% in the uncracked condition to a maximum of about 3.5% for amplitudes of response near failure. Undoubtedly, these damping ratios would have been much higher had typical nonstructural elements been added to the building. Consistent with observed reductions in stiffness, large increases in the natural periods were measured. Failure characteristics were noted by observing the development of major cracking in the vicinity of the beam-column joints.

Using the results of shaking table tests on a 1:3 scale model of a five-story prefabricated reinforced concrete building, the authors of paper No. 11 made comparisons with the results obtained analytically using a mathematical model which

assumed rigid floors in their own plane. This assumption was shown to be incorrect and that floor flexibility greatly influenced the distribution of lateral shear to the transverse frames. In fact it was shown that for this structure a central frame would carry 1.5 to 2 times the load it would be required to carry if the floors were indeed rigid in their own plane.

2. Small Brick Buildings - In paper No. 12, a tilting platform 8½ ft x 8½ ft was used to test the lateral resistance of 9 pairs of brick structures 4 ft x 6 ft x 31 in. high, one brick thick, laid in 1:5 lime-sand mortar, sand, mud, and no mortar at all. A 1350 lb roof slab rested on foam rubber on the walls. The table was then mounted on wheels and pulsed horizontally to attempt to relate building-strength under repetitive pulses to strength under static tilt. Building performance under static tilt was quite consistent while performance under pulse loading showed wide scatter. The two kinds of tests produced similar patterns of failure in the mortared buildings; however, the unmortared buildings were more vulnerable to the pulse type excitation.

C. TEST FRAMES

1. Reinforced Concrete Frames - The results of hydraulic actuator displacement control tests simulating earthquake conditions on 4 one-story reinforced concrete frames having different natural periods of vibration are given in paper No. 1. Using a mathematical model based on the authors' fully defined hysteretic stress-strain relationship for concrete and the Ramberg-Osgood stress-strain relationship for reinforcing steel, good correlations were obtained between analytical predictions and experimental results.

2. Reinforced Concrete Shear Wall-Frame Structures - Paper No. 13 presents the results of shaking table tests on (1) a pair of three-story one-bay reinforced concrete frames, and (2) a similar pair of frames built monolithically with a three-story slender shear wall. Scaled earthquake motions in one horizontal direction were applied with the intensity of the first test run (for 3 specimens) being roughly comparable to the intensity of a design earthquake. The intensities of motion were doubled with each successive test run until failure of the specimen occurred. The test results show that reinforced concrete frame structures (with or without shear walls) can withstand very intense earthquake motions provided they are carefully designed to prevent diagonal shear failures, anchorage failures, and brittle compressive failures. Thus, it is important that columns have a sufficient web reinforcement to develop the maximum possible shear controlled by end moment capacities and that the exterior columns be designed to carry the additional axial forces caused by overturning effect without brittle compressive failure or tensile fracture of the reinforcement.

3. Infilled Reinforced Concrete Frames - Results of shaking table tests on 8 models consisting of two parallel 1:4 scale three-story brick infilled reinforced concrete frames are presented in paper No. 14. These models differed only in geometry of door and window openings and in bracing around openings which consisted of vertical and horizontal lintels. A concrete block was supported at the top of each specimen to simulate building weight and vertical prestressing cables were used to reproduce axial stresses in the frame columns. Each specimen was subjected to seismic excitations of sufficient numbers, intensities, and durations to simulate the lifetime seismic environment of the prototype structure. The test results showed that good performance can be achieved provided favorable interaction between frames and infill walls is developed through proper confinement around openings. Such confinement can be obtained using both vertical and horizontal reinforced lintels carried through and connected to beams and columns of the frame,

respectively. Using finite element modelling, the authors found good correlation between analytical predictions and experimental results, even for response into the cracking stage.

4. Reinforced Concrete Frames With Partition Walls - Subjecting 1:6 scale, one-bay, three-story, reinforced concrete frame models, with and without partition walls, to free vibration and harmonic base excitation, the author of paper No. 15 found that partition walls appreciably affect dynamic response. Therefore, their stiffnesses should be considered in mathematical modelling of the complete structural system.

5. Steel Frames - The results of cyclic loading tests on single rectangular steel rigid frames having various kinds of bracings are presented in paper No. 16. Subjecting the two columns of each frame to constant loads, pairs of self-equilibrating loads are alternately applied diagonally across the frame producing the desired cyclic loading. The elasto-plastic behavior of each frame, including post-yield buckling of bracings, is measured and correlated with analytical predictions. Examining high-strain fatigue life shows it to be relatively shorter for braced frames over unbraced frames.

Paper No. 17 presents the results of tests carried out on one-story, single-bay steel rigid frames having joints of different types. It was pointed out that if the zones of plastic deformation should include joint welds, the failure of the frame will often be caused by early fracture in the welds; thus greatly reducing the ductility of the overall system. To avoid such failures, it was shown that tapered sections near the joint forcing the plastic zones of deformation away from welds were effective. However it was shown that when using tapered sections, proper strength and ductility is achieved only when premature local buckling in flanges and webs and overall buckling of columns are presented. The importance of providing adequate strength and ductility in design is emphasized.

The results of monotonic unidirectional static loading of spatial one-story mild-steel frames are given in paper No. 18. Due to the nonsymmetrical arrangements of 3 pipe columns, eccentricities were present which caused torsion and translation in two horizontal directions to occur. Such results are simply a reminder that proper consideration should be given to the effects of eccentricities on dynamic response. As pointed out in paper No. 19, consideration should also be given to the influence of interconnecting members on the combined stiffness of parallel plane frames.

D. WATER TANKS

The seismic performance of a water tower, consisting of an inverted truncated shell supported concentrically on a cylindrical column, is discussed in paper No. 20. Tests were performed to study the sloshing problem and its influence on fluid pressures and stresses in the conical shell. The total coupled seismic response of the fluid-tower system with a critical volume of water is examined at amplitudes of response up to failure. Clearly, the dynamics of the fluid system greatly affects overall tower response under seismic conditions and therefore should be considered realistically in design, not only in sizing of structural elements but also in the earlier selection of overall tank geometry.

E. CHIMNEYS

Results of an analysis of the seismic behavior of the chimney of the TVA 1200 MW fossil steam generating power plant, Unit 3, at Paradise, Kentucky, are presented

in paper No. 21. This chimney consists of two tapered concentric cylindrical shells having no significant structural inter-connections. Time-histories of tip deflection, base shear, and overturning moment were obtained by modal analysis using various values for damping ratios and using the N-S component of the 1940 El Centro, California, earthquake as input. Also using a refined quadrilateral plate element modelling, stress distributions around flue openings were obtained. It is clear that such analyses which are straightforward, would be very useful if carried out during the design phase. The first three mode shapes and frequencies of the chimney were measured and were found to agree well with the results of analysis.

F. DAMS

Paper No. 22 describes a field test program being conducted by the Italian National Board for Electric Power to obtain the dynamic characteristics of the most important Italian dams. Using mechanical vibrators, shapes, frequencies, and damping ratios for at least four modes are measured and, by placing a vibrator at discrete locations on the crest, transfer functions between force input (maximum amplitude 10 tons; frequency range 2-15 H_z) at each point and velocity response at discrete locations are obtained. These transfer functions are then correlated with those of a finite element model with the intent of verifying and improving mathematical modelling. Damping ratios were found in the range 1 to 3 percent for arch dams and in the range 4 to 8 percent for gravity dams with no noticeable variation with mode number. Reservoir-dam interaction has been found to be important and is still being investigated.

The results of forced vibration tests on 2 earth-fill and 2 rock-fill dams in Yugoslavia are given in paper No. 23. Measured mode shapes, frequencies, and damping ratios are used to develop realistic mathematical models for low amplitude response. Dam-foundation interaction and, in some cases, reservoir-dam interaction were found important and should be included in mathematical modelling. Damping ratios were found to be highly variable in the range 2 to 9 percent.

G. SUSPENSION BRIDGE

Mode shapes, frequencies, and damping ratios for the Lion's Gate Suspension Bridge in Vancouver, Canada, as measured under ambient and impact loading conditions, are presented in paper No. 24. Using both continuum and discrete mathematical models, excellent agreement between measured and calculated frequencies for vertical modes and the lowest horizontal mode was obtained. Some difficulty was experienced however in obtaining good correlation for torsional modes, apparently due to inaccurate evaluations of the bridge girder's torsional stiffness. The measured low-amplitude damping ratios varied greatly over the range 0.3 to 1.6 percent.

OVERVIEW OF TEST PROGRAMS

A. GENERAL

As stated previously, the main objective of conducting dynamic tests on structures is to improve and verify mathematical modelling which is intended to realistically represent prototype behavior under seismic conditions. Consistent with this objective, dynamic tests have been carried out on small, medium-, and full-scale components, assemblages, and complete structural systems using various types of excitation.

B. SMALL-SCALE TESTS

Obviously for economic reasons, the use of small-scale models for dynamic testing should be encouraged whenever the results obtained permit, either directly or indirectly through analysis, realistic predictions to be made of prototype performance under seismic conditions. Such is the case when modelling structural systems which are designed to remain essentially elastic during strong motion earthquakes. Prototype response can be predicted directly from the test results in this case provided similitude conditions as discussed in papers Nos. 25 and 26 are met and provided realistic boundary and loading conditions are maintained. These latter conditions can be maintained effectively through the use of modern electronically controlled shaking tables of the type described in paper No. 27 on which models, including boundary elements (e.g., a three-dimensional dam including portions of foundation and abutments), are mounted.

Since gravity and seismic forces scale differently, a centrifuge can be used to modify the effective gravity forces; thus, bringing into agreement the associated similitude conditions. The small-scale simple oscillator models made of different materials and the nine-story large-panel dwelling models described in paper No. 28 were tested within a centrifuge for this purpose and were subjected to simulated seismic excitations. This particular investigation was carried out to study the influence of foundation conditions on response. It was found, as in other investigations, that both damping and fundamental period of vibration increased substantially when changing from hard to soft foundation conditions.

Examples of structural types designed to remain essentially elastic during strong motion earthquakes are arch and arch-gravity dams as described in paper No. 29. Optical techniques were used extensively in this investigation to measure mode shapes, frequencies and dynamic stress distributions.

The use of small-scale models for testing into the inelastic range is very limited due to extreme difficulties in interpreting prototype behavior from the test results. Paper No. 26 discusses the basic principles which must be adhered to when modelling in the inelastic range. These principles require the development of new modelling materials with specified properties which, in many cases, are very difficult to produce. Therefore, it is impossible to assess the future success of small-scale testing into the inelastic range of response. Undoubtedly, it will be quite limited, thus greater emphasis should be placed on medium and full-scale testing.

C. MEDIUM-SCALE TESTS

One approach to mathematical modelling of prototype structural systems is to combine sub-element models representing individual structural components and/or assemblages into global models representing complete systems. Therefore, much dynamic testing has been carried out on medium-scale structural elements and assemblages for this purpose. Once the force-deformation and failure characteristics of these sub-elements have been defined in terms of loading and structural parameters, these same characteristics are supposedly fully defined for the global models. Unfortunately, in some cases, extrapolation of medium-scale test data to the prototype structure is questionable. Further, realistic representations of the many complex interactions (e.g., between frames and walls, frames and floors, super-structure and foundation, structural and nonstructural systems) in the prototype model are still very uncertain. Although this approach to modelling prototype structures through medium-scale testing has many deficiencies, it must continue due to the severe limitations of small-scale testing and the high cost

of full-scale testing. To implement this approach, the development of effective and efficient three-dimensional nonlinear dynamic analysis procedures must continue as well.

D. FULL-SCALE TESTS

Establishing mathematical models for prototype structures through testing of full-scale structures has the distinct advantage that the uncertainties involved in extrapolating dynamic characteristics from one scale to another are removed. If these full-scale structures are only test structures, the validity of using the test results directly in characterizing prototype structures depends on the degree to which the test structures actually represent real structures. For example, if a full-scale building is tested without a nonstructural system (fire proofing, partitions, windows, facings, etc.), its dynamic characteristics can be very different from the prototype structure it represents. Therefore, when testing full-scale structures, it is desirable that they be constructed exactly like real complete structures and that they be placed on similar foundations. Further, to obtain maximum information on true seismic performance, it is desirable that the tests be carried out with realistic loadings producing response well into the inelastic range. To fully meet these conditions, the tests would obviously have to be performed under actual earthquake conditions similar to the design earthquake. This suggests that limited numbers of real buildings in regions of high seismicity should be fully instrumented to measure their dynamic response characteristics during future earthquakes.

Due to the long return period for high magnitude earthquakes, most dynamic tests on real structures have been carried out using mechanical vibration or ambient ground motions as the source of excitation. Unfortunately, due to the low-amplitudes of response produced, the results obtained have limited value. Certainly they cannot provide information on force-deformation characteristics into the inelastic range or information on failure characteristics. They do however provide valuable information which can be used to improve or validate mathematical modelling in the low amplitude range.

In the past, most dynamic tests under forced vibration and ambient conditions have been performed on high-rise buildings. The information obtained usually consists of mode shapes, frequencies, and damping ratios; the latter being highly variable with structural type, foundation condition, and amplitude of response. In view of the vast amount of such information already collected, it would seem desirable to concentrate future testing on unusual high-rise buildings and that they be instrumented fully so that in addition to obtaining mode shapes, frequencies, and damping ratios, quantitative data will also be obtained on deformation patterns and interaction effects, e.g., interactions between structure and foundation, frames and walls, frames and floors, and structural and nonstructural systems. Further, it is suggested that these tests be carried out during various stages of construction and, later, after the occurrence of each earthquake of significant intensity. Should an important building be subjected to internal fire, forced vibration tests as described in paper No. 30 can be used to indicate possible damage incurred.

In addition to testing unusual high-rise buildings, future forced vibration tests should also be carried out on selected low-rise buildings of various types, including industrial buildings. Similar tests should be carried out on other structural types, e.g., freeway bridge structures, nuclear power reactor structures, industrial plant facilities, dams, etc.

Recognizing the limitations of low-amplitude dynamic tests on structures, it is clear that an effort should be made to test large-scale complete structures, closely simulating real structures, under conditions producing high amplitude response similar to that produced by high intensity earthquake motions. Therefore, further consideration should be given to the development and use of large-scale testing facilities.

CONCLUDING REMARK

An attempt has been made in this brief report on TOPIC 9 - DYNAMIC TESTS ON STRUCTURES to summarize the significant test results contained in the 30 papers listed below and to present some general observations with recommendations for future testing. Undoubtedly, due to lack of time and space, inadequate reporting has been made on many of the papers. For this possible shortcoming, the present author expresses his sincere apologies.

LISTING OF PAPERS

1. Okada, T., and Seki, M., "A Simulation of Earthquake Response of Reinforced Concrete Buildings".

2. Ward, H. S., "Experimental Techniques and Results for Dynamic Tests on Structures and Soils".

3. Hiromatsu, T., "Regression Analysis on Resonance Curves of Forced Vibration Tests and Its Error Estimation Due to Microtremors".

4. Kobayashi, H., and Sugiyama, N., "Viscous Damping of Structures Related to Foundation Conditions".

5. Ohta, T., Adachi, N., Uchiyama, S., Niwa, M., and Takahashi, K., "Results of Vibration Tests on Tall Buildings and Their Earthquake Response".

6. Stephen, R. M., and Bouwkamp, J. G., "Dynamic Behavior of An Eleven Story Masonry Building".

7. Foutch, D. A., and Jennings, P. C., "Dynamic Tests of Full-Scale Structures".

8. Foutch, D. A., and Housner, G. W., "Observed Changes in the Natural Periods of Vibration of A Nine Story Steel Frame Building".

9. Chen, C. K., Czarnecki, R. M., and Scholl, R. E., "Vibration Tests of a 4-Story Concrete Structure".

10. Mihai, C., Diaconu, D., Manolovici, M., Marinescu, ST., Cirlan, ST., Iticovici, M., Amariei, D., and Soroceanu, I., "On the Static and Seismic Behavior of A Structural Model of An Industrial Storied Hall".

11. Negoita, A., Missir, I., and Schärf, F., "Seismic Analysis of Multistory Prefabricated Framed Structures".

12. Munski, K. D., and Keightley, W. O., "Tilting Platform for Measuring Earthquake Resistance of Small Buildings".

13. Otani, S., "Earthquake Tests of Shear Wall-Frame Structures to Failure".

14. Ravara, A., Mayorga, A., and Carvalho, C., "Seismic Tests of Infilled Reinforced Concrete Frames".

15. Mirabal, Y. M., "The Influence of Partition Walls on The Rigidity of Frame Structures".

16. Yamada, M., Tsuji, B., and Nakanishi, S., "Elasto-Plastic Behavior of Braced Frames Under Cyclic Horizontal Loading".

17. Korchynsky, I. L., and Aliev, G. A., "Behavior of Structures During Earthquakes Beyond the Limits of the Elastic Stage".

18. Focardi, F., "Experiments on the Spatial Behavior of Plastic Frames".

19. Basak, A. K., and Gupta, Y. P., "Experimental Determination of Lateral Stiffness Characteristics of Space Framed Three Dimensional Steel Structures".

20. Diaconu, D., Manolovici, M., Iticovici, M., Marinescu, S., Carlan, S., and Soroceanu, I., "Seismic Response of Elevated Water-Towers, With Tronconic Tanks and Central Tube, Taking Into Account the Water Swinging Effect".

21. Yang, T.Y., Kayser, K. W., and Shiau, L. C., "Theoretical and Experimental Studies of Earthquake Response of A Chimney". Refer paper No. 45, theme 3-263.

22. Calciati, F., Castoldi, A., Fanelli, M., and Mazzieri, C., "In Situ Tests for the Determination of the Dynamic Characteristics of Some Italian Dams".

23. Paskalov, T. A., Petrovski, J. T., Jurukovski, D. V., and Taskovski, B. M., "Forced Vibration Full-Scale Tests on Earth-Fill and Rock-Fill Dams."

24. Rainer, J. H., and Van Selst, A., "Dynamic Properties of a Suspension Bridge".

25. Monahenico, D. V., "Principles of Physical Modelling of Structures Resistant to Earthquakes".

26. Bostjancic, J., "Model Materials Suitable for Dynamic Tests of Models in the Plastic Range".

27. Diaz, J. A., and del Valle, E.,"Dynamics Laboratory of The National University of Mexico".

28. Aliev, G. A., "Influence of Properties and Stressed State of Foundation Soils on Absorption and Diffusion of Energy of Seismic Vibrations".

29. Belogorodsky, B. A., Malyshev, L. K., and Panteleev, A. A., "The Solution of Seismic Stability Problems on Small-Scale Models by Optic Methods".

30. Srinivasulu, P., Lakshmanan, N., and Vaidyanathan, C. V., "Assessment of A Multistoreyed Building by Vibration Tests".

EERC 67-1 "Feasibility Study Large-Scale Earthquake Simulator Facility," by J. Penzien, J. G. Bouwkamp, R. W. Clough and D. Rea - 1967 (PB 187 905)

EERC 68-1 Unassigned

EERC 68-2 "Inelastic Behavior of Beam-to-Column Subassemblages Under Repeated Loading," by V. V. Bertero - 1968 (PB 184 888)

EERC 68-3 "A Graphical Method for Solving the Wave Reflection-Refraction Problem," by H. D. McNiven and Y. Mengi 1968 (PB 187 943)

EERC 68-4 "Dynamic Properties of McKinley School Buildings," by D. Rea, J. G. Bouwkamp and R. W. Clough - 1968 (PB 187 902)

EERC 68-5 "Characteristics of Rock Motions During Earthquakes," by H. B. Seed, I. M. Idriss and F. W. Kiefer - 1968 (PB 188 338)

EERC 69-1 "Earthquake Engineering Research at Berkeley," - 1969 (PB 187 906)

EERC 69-2 "Nonlinear Seismic Response of Earth Structures," by M. Dibaj and J. Penzien - 1969 (PB 187 904)

EERC 69-3 "Probabilistic Study of the Behavior of Structures During Earthquakes," by P. Ruiz and J. Penzien - 1969 (PB 187 886)

EERC 69-4 "Numerical Solution of Boundary Value Problems in Structural Mechanics by Reduction to an Initial Value Formulation," by N. Distefano and J. Schujman - 1969 (PB 187 942)

EERC 69-5 "Dynamic Programming and the Solution of the Biharmonic Equation," by N. Distefano - 1969 (PB 187 941)

Note: Numbers in parenthesis are Accession Numbers assigned by the National Technical Information Service. Copies of these reports may be ordered from the National Technical Information Service, 5285 Port Royal Road, Springfield, Virginia, 22161. Accession Numbers should be quoted on orders for the reports (PB --- ---) and remittance must accompany each order. (Foreign orders, add $2.50 extra for mailing charges.) Those reports without this information listed are not yet available from NTIS. Upon request, EERC will mail inquirers this information when it becomes available to us.

EERC 69-6 "Stochastic Analysis of Offshore Tower Structures," by A. K. Malhotra and J. Penzien - 1969 (PB 187 903)

EERC 69-7 "Rock Motion Accelerograms for High Magnitude Earthquakes," by H. B. Seed and I. M. Idriss - 1969 (PB 187 940)

EERC 69-8 "Structural Dynamics Testing Facilities at the University of California, Berkeley," by R. M. Stephen, J. G. Bouwkamp, R. W. Clough and J. Penzien - 1969 (PB 189 111)

EERC 69-9 "Seismic Response of Soil Deposits Underlain by Sloping Rock Boundaries," by H. Dezfulian and H. B. Seed - 1969 (PB 189 114)

EERC 69-10 "Dynamic Stress Analysis of Axisymmetric Structures under Arbitrary Loading," by S. Ghosh and E. L. Wilson - 1969 (PB 189 026)

EERC 69-11 "Seismic Behavior of Multistory Frames Designed by Different Philosophies," by J. C. Anderson and V. V. Bertero - 1969 (PB 190 662)

EERC 69-12 "Stiffness Degradation of Reinforcing Concrete Structures Subjected to Reversed Actions," by V. V. Bertero, B. Bresler and H. Ming Liao - 1969 (PB 202 942)

EERC 69-13 "Response of Non-Uniform Soil Deposits to Travel Seismic Waves," by H. Dezfulian and H. B. Seed - 1969 (PB 191 023)

EERC 69-14 "Damping Capacity of a Model Steel Structure," by D. Rea, R. W. Clough and J. G. Bouwkamp - 1969 (PB 190 663)

EERC 69-15 "Influence of Local Soil Conditions on Building Damage Potential during Earthquakes," by H. B. Seed and I. M. Idriss - 1969 (PB 191 036)

EERC 69-16 "The Behavior of Sands under Seismic Loading Conditions," by M. L. Silver and H. B. Seed - 1969 (AD 714 982)

EERC 70-1 "Earthquake Response of Concrete Gravity Dams," by A. K. Chopra - 1970 (AD 709 640)

EERC 70-2 "Relationships between Soil Conditions and Building Damage in the Caracas Earthquake of July 29, 1967," by H. B. Seed, I. M. Idriss and H. Dezfulian - 1970 (PB 195 762)

EERC 70-3 "Cyclic Loading of Full Size Steel Connections," by E. P. Popov and R. M. Stephen - 1970 (PB 213 545)

EERC 70-4 "Seismic Analysis of the Charaima Building, Caraballeda, Venezuela," by Subcommittee of the SEAONC Research Committee: V. V. Bertero, P. F. Fratessa, S. A. Mahin, J. H. Sexton, A. C. Scordelis, E. L. Wilson, L. A. Wyllie, H. B. Seed and J. Penzien, Chairman - 1970 (PB 201 455)

EERC 70-5 "A Computer Program for Earthquake Analysis of Dams," by A. K. Chopra and P. Chakrabarti - 1970 (AD 723 994)

EERC 70-6 "The Propagation of Love Waves across Non-Horizontally Layered Structures," by J. Lysmer and L. A. Drake - 1970 (PB 197 896)

EERC 70-7 "Influence of Base Rock Characteristics on Ground Response," by J. Lysmer, H. B. Seed and P. B. Schnabel - 1970 (PB 197 897)

EERC 70-8 "Applicability of Laboratory Test Procedures for Measuring Soil Liquefaction Characteristics under Cyclic Loading," by H. B. Seed and W. H. Peacock - 1970 (PB 198 016)

EERC 70-9 "A Simplified Procedure for Evaluating Soil Liquefaction Potential," by H. B. Seed and I. M. Idriss - 1970 (PB 198 009)

EERC 70-10 "Soil Moduli and Damping Factors for Dynamic Response Analysis," by H. B. Seed and I. M. Idriss - 1970 (PB 197 869)

EERC 71-1 "Koyna Earthquake and the Performance of Koyna Dam," by A. K. Chopra and P. Chakrabarti - 1971 (AD 731 496)

EERC 71-2 "Preliminary In-Situ Measurements of Anelastic Absorption in Soils Using a Prototype Earthquake Simulator," by R. D. Borcherdt and P. W. Rodgers - 1971 (PB 201 454)

EERC 71-3 "Static and Dynamic Analysis of Inelastic Frame Structures," by F. L. Porter and G. H. Powell - 1971 (PB 210 135)

EERC 71-4 "Research Needs in Limit Design of Reinforced Concrete Structures," by V. V. Bertero - 1971 (PB 202 943)

EERC 71-5 "Dynamic Behavior of a High-Rise Diagonally Braced Steel Building," by D. Rea, A. A. Shah and J. G. Bouwkamp - 1971 (PB 203 584)

EERC 71-6 "Dynamic Stress Analysis of Porous Elastic Solids Saturated with Compressible Fluids," by J. Ghaboussi and E. L. Wilson - 1971 (PB 211 396)

EERC 71-7 "Inelastic Behavior of Steel Beam-to-Column Subassemblages," by H. Krawinkler, V. V. Bertero and E. P. Popov - 1971 (PB 211 335)

EERC 71-8 "Modification of Seismograph Records for Effects of Local Soil Conditions," by P. Schnabel, H. B. Seed and J. Lysmer - 1971 (PB 214 450)

EERC 72-1 "Static and Earthquake Analysis of Three Dimensional Frame and Shear Wall Buildings," by E. L. Wilson and H. H. Dovey - 1972 (PB 212 904)

EERC 72-2 "Accelerations in Rock for Earthquakes in the Western United States," by P. B. Schnabel and H. B. Seed - 1972 (PB 213 100)

EERC 72-3 "Elastic-Plastic Earthquake Response of Soil-Building Systems," by T. Minami - 1972 (PB 214 868)

EERC 72-4 "Stochastic Inelastic Response of Offshore Towers to Strong Motion Earthquakes," by M. K. Kaul - 1972 (PB 215 713)

EERC 72-5 "Cyclic Behavior of Three Reinforced Concrete Flexural Members with High Shear," by E. P. Popov, V. V. Bertero and H. Krawinkler - 1972 (PB 214 555)

EERC 72-6 "Earthquake Response of Gravity Dams Including Reservoir Interaction Effects," by P. Chakrabarti and A. K. Chopra - 1972 (AD 762 330)

EERC 72-7 "Dynamic Properties on Pine Flat Dam," by D. Rea, C. Y. Liaw and A. K. Chopra - 1972 (AD 763 928)

EERC 72-8 "Three Dimensional Analysis of Building Systems," by E. L. Wilson and H. H. Dovey - 1972 (PB 222 438)

EERC 72-9 "Rate of Loading Effects on Uncracked and Repaired Reinforced Concrete Members," by S. Mahin, V. V. Bertero, D. Rea and M. Atalay - 1972 (PB 224 520)

EERC 72-10 "Computer Program for Static and Dynamic Analysis of Linear Structural Systems," by E. L. Wilson, K.-J. Bathe, J. E. Peterson and H. H. Dovey - 1972 (PB 220 437)

EERC 72-11 "Literature Survey - Seismic Effects on Highway Bridges," by T. Iwasaki, J. Penzien and R. W. Clough - 1972 (PB 215 613)

EERC 72-12 "SHAKE-A Computer Program for Earthquake Response Analysis of Horizontally Layered Sites," by P. B. Schnabel and J. Lysmer - 1972 (PB 220 207)

EERC 73-1 "Optimal Seismic Design of Multistory Frames," by V. V. Bertero and H. Kamil - 1973

EERC 73-2 "Analysis of the Slides in the San Fernando Dams during the Earthquake of February 9, 1971," by H. B. Seed, K. L. Lee, I. M. Idriss and F. Makdisi - 1973 (PB 223 402)

EERC 73-3 "Computer Aided Ultimate Load Design of Unbraced Multistory Steel Frames," by M. B. El-Hafez and G. H. Powell - 1973

EERC 73-4 "Experimental Investigation into the Seismic Behavior of Critical Regions of Reinforced Concrete Components as Influenced by Moment and Shear," by M. Celebi and J. Penzien - 1973 (PB 215 884)

EERC 73-5 "Hysteretic Behavior of Epoxy-Repaired Reinforced Concrete Beams," by M. Celebi and J. Penzien - 1973

EERC 73-6 "General Purpose Computer Program for Inelastic Dynamic Response of Plane Structures," by A. Kanaan and G. H. Powell - 1973 (PB 221 260)

EERC 73-7 "A Computer Program for Earthquake Analysis of Gravity Dams Including Reservoir Interaction," by P. Chakrabarti and A. K. Chopra - 1973 (AD 766 271)

EERC 73-8 "Behavior of Reinforced Concrete Deep Beam-Column Subassemblages under Cyclic Loads," by O. Kustu and J. G. Bouwkamp - 1973

EERC 73-9 "Earthquake Analysis of Structure-Foundation Systems," by A. K. Vaish and A. K. Chopra - 1973 (AD 766 272)

EERC 73-10 "Deconvolution of Seismic Response for Linear Systems," by R. B. Reimer - 1973 (PB 227 179)

EERC 73-11 "SAP IV: A Structural Analysis Program for Static and Dynamic Response of Linear Systems," by K.-J. Bathe, E. L. Wilson and F. E. Peterson - 1973 (PB 221 967)

EERC 73-12 "Analytical Investigations of the Seismic Response of Long, Multiple Span Highway Bridges," by W. S. Tseng and J. Penzien - 1973 (PB 227 816)

EERC 73-13 "Earthquake Analysis of Multi-Story Buildings Including Foundation Interaction," by A. K. Chopra and J. A. Gutierrez - 1973 (PB 222 970)

EERC 73-14 "ADAP: A Computer Program for Static and Dynamic Analysis of Arch Dams," by R. W. Clough, J. M. Raphael and S. Majtahedi - 1973 (PB 223 763)

EERC 73-15 "Cyclic Plastic Analysis of Structural Steel Joints," by R. B. Pinkney and R. W. Clough - 1973 (PB 226 843)

EERC 73-16 "QUAD-4: A Computer Program for Evaluating the Seismic Response of Soil Structures by Variable Damping Finite Element Procedures," by I. M. Idriss, J. Lysmer, R. Hwang and H. B. Seed - 1973 (PB 229 424)

EERC 73-17 "Dynamic Behavior of a Multi-Story Pyramid Shaped Building," by R. M. Stephen and J. G. Bouwkamp - 1973

EERC 73-18 "Effect of Different Types of Reinforcing on Seismic Behavior of Short Concrete Columns," by V. V. Bertero, J. Hollings, O. Kustu, R. M. Stephen and J. G. Bouwkamp - 1973

EERC 73-19 "Olive View Medical Center Material Studies, Phase I," by B. Bresler and V. V. Bertero - 1973 (PB 235 986)

EERC 73-20 "Linear and Nonlinear Seismic Analysis Computer Programs for Long Multiple-Span Highway Bridges," by W. S. Tseng and J. Penzien - 1973

EERC 73-21 "Constitutive Models for Cyclic Plastic Deformation of Engineering Materials," by J. M. Kelly and P. P. Gillis - 1973 (PB 226 024)

EERC 73-22 "DRAIN - 2D User's Guide," by G. H. Powell - 1973 (PB 227 016)

EERC 73-23 "Earthquake Engineering at Berkeley - 1973" - 1973 (PB 226 033)

EERC 73-24 Unassigned

EERC 73-25 "Earthquake Response of Axisymmetric Tower Structures Surrounded by Water," by C. Y. Liaw and A. K. Chopra - 1973 (AD 773 052)

EERC 73-26 "Investigation of the Failures of the Olive View Stairtowers during the San Fernando Earthquake and Their Implications in Seismic Design," by V. V. Bertero and R. G. Collins - 1973 (PB 235 106)

EERC 73-27 "Further Studies on Seismic Behavior of Steel Beam-Column Subassemblages," by V. V. Bertero, H. Krawinkler and E. P. Popov - 1973 (PB 234 172)

EERC 74-1 "Seismic Risk Analysis," by C. S. Oliveira - 1974 (PB 235 920)

EERC 74-2 "Settlement and Liquefaction of Sands under Multi-Directional Shaking," by R. Pyke, C. K. Chan and H. B. Seed - 1974

EERC 74-3 "Optimum Design of Earthquake Resistant Shear Buildings," by D. Ray, K. S. Pister and A. K. Chopra - 1974 (PB 231 172)

EERC 74-4 "LUSH - A Computer Program for Complex Response Analysis of Soil-Structure Systems," by J. Lysmer, T. Udaka, H. B. Seed and R. Hwang - 1974 (PB 236 796)

EERC 74-5 "Sensitivity Analysis for Hysteretic Dynamic Systems: Applications to Earthquake Engineering," by D. Ray - 1974 (PB 233 213)

EERC 74-6 "Soil-Structure Interaction Analyses for Evaluating Seismic Response," by H. B. Seed, J. Lysmer and R. Hwang - 1974 (PB 236 519)

EERC 74-7 Unassigned

EERC 74-8 "Shaking Table Tests of a Steel Frame - A Progress Report," by R. W. Clough and D. Tang - 1974

EERC 74-9 "Hysteretic Behavior of Reinforced Concrete Flexural Members with Special Web Reinforcement," by V. V. Bertero, E. P. Popov and T. Y. Wang - 1974 (PB 236 797)

EERC 74-10 "Applications of Reliability-Based, Global Cost Optimization to Design of Earthquake Resistant Structures," by E. Vitiello and K. S. Pister - 1974 (PB 237 231)

EERC 74-11 "Liquefaction of Gravelly Soils under Cyclic Loading Conditions," by R. T. Wong, H. B. Seed and C. K. Chan - 1974

EERC 74-12 "Site-Dependent Spectra for Earthquake-Resistant Design," by H. B. Seed, C. Ugas and J. Lysmer - 1974

EERC 74-13 "Earthquake Simulator Study of a Reinforced Concrete Frame," by P. Hidalgo and R. W. Clough - 1974 (PB 241 944)

EERC 74-14 "Nonlinear Earthquake Response of Concrete Gravity Dams," by N. Pal - 1974 (AD/A006583)

EERC 74-15 "Modeling and Identification in Nonlinear Structural Dynamics, I - One Degree of Freedom Models," by N. Distefano and A. Rath - 1974 (PB 241 548)

EERC 75-1 "Determination of Seismic Design Criteria for the Dumbarton Bridge Replacement Structure, Vol. I: Description, Theory and Analytical Modeling of Bridge and Parameters," by F. Baron and S.-H. Pang - 1975

EERC 75-2 "Determination of Seismic Design Criteria for the Dumbarton Bridge Replacement Structure, Vol. 2: Numerical Studies and Establishment of Seismic Design Criteria," by F. Baron and S.-H. Pang - 1975

EERC 75-3 "Seismic Risk Analysis for a Site and a Metropolitan Area," by C. S. Oliveira - 1975

EERC 75-4 "Analytical Investigations of Seismic Response of Short, Single or Multiple-Span Highway Bridges," by Ma-chi Chen and J. Penzien - 1975 (PB 241 454)

EERC 75-5 "An Evaluation of Some Methods for Predicting Seismic Behavior of Reinforced Concrete Buildings," by Stephen A. Mahin and V. V. Bertero - 1975

EERC 75-6 "Earthquake Simulator Study of a Steel Frame Structure, Vol. I: Experimental Results," by R. W. Clough and David T. Tang - 1975 (PB 243 981)

EERC 75-7 "Dynamic Properties of San Bernardino Intake Tower," by Dixon Rea, C.-Y. Liaw, and Anil K. Chopra - 1975 (AD/A008406)

EERC 75-8 "Seismic Studies of the Articulation for the Dumbarton Bridge Replacement Structure, Vol. I: Description, Theory and Analytical Modeling of Bridge Components," by F. Baron and R. E. Hamati - 1975

EERC 75-9 "Seismic Studies of the Articulation for the Dumbarton Bridge Replacement Structure, Vol. 2: Numerical Studies of Steel and Concrete Girder Alternates," by F. Baron and R. E. Hamati - 1975

EERC 75-10 "Static and Dynamic Analysis of Nonlinear Structures," by Digambar P. Mondkar and Graham H. Powell - 1975 (PB 242 434)

EERC 75-11 "Hysteretic Behavior of Steel Columns," by E. P. Popov, V. V. Bertero and S. Chandramouli - 1975

EERC 75-12 "Earthquake Engineering Research Center Library Printed Catalog" - 1975 (PB 243 711)

EERC 75-13 "Three Dimensional Analysis of Building Systems," Extended Version, by E. L. Wilson, J. P. Hollings and H. H. Dovey - 1975 (PB 243 989)

EERC 75-14 "Determination of Soil Liquefaction Characteristics by Large-Scale Laboratory Tests," by Pedro De Alba, Clarence K. Chan and H. Bolton Seed - 1975

EERC 75-15 "A Literature Survey - Compressive, Tensile, Bond and Shear Strength of Masonry," by Ronald L. Mayes and Ray W. Clough - 1975

EERC 75-16 "Hysteretic Behavior of Ductile Moment Resisting Reinforced Concrete Frame Components," by V. V. Bertero and E. P. Popov - 1975

EERC 75-17 "Relationships Between Maximum Acceleration, Maximum Velocity, Distance from Source, Local Site Conditions for Moderately Strong Earthquakes," by H. Bolton Seed, Ramesh Murarka, John Lysmer and I. M. Idriss - 1975

EERC 75-18 "The Effects of Method of Sample Preparation on the Cyclic Stress-Strain Behavior of Sands," by J. Paul Mulilis, Clarence K. Chan and H. Bolton Seed - 1975

EERC 75-19 "The Seismic Behavior of Critical Regions of Reinforced Concrete Components as Influenced by Moment, Shear and Axial Force," by B. Atalay and J. Penzien - 1975

EERC 75-20 "Dynamic Properties of an Eleven Story Masonry Building," by R. M. Stephen, J. P. Hollings, J. G. Bouwkamp and D. Jurukovski - 1975

EERC 75-21 "State-of-the-Art in Seismic Shear Strength of Masonry - An Evaluation and Review," by Ronald L. Mayes and Ray W. Clough - 1975

EERC 75-22 "Frequency Dependencies Stiffness Matrices for Viscoelastic Half-Plane Foundations," by Anil K. Chopra, P. Chakrabarti and Gautam Dasgupta - 1975

EERC 75-23 "Hysteretic Behavior of Reinforced Concrete Framed Walls," by T. Y. Wong, V. V. Bertero and E. P. Popov - 1975

EERC 75-24 "Testing Facility for Subassemblages of Frame-Wall Structural Systems," by V. V. Bertero, E. P. Popov and T. Endo - 1975

EERC 75-25 "Influence of Seismic History of the Liquefaction Characteristics of Sands," by H. Bolton Seed, Kenji Mori and Clarence K. Chan - 1975

EERC 75-26 "The Generation and Dissipation of Pore Water Pressures during Soil Liquefaction," by H. Bolton Seed, Phillippe P. Martin and John Lysmer - 1975

EERC 75-27 "Identification of Research Needs for Improving a Seismic Design of Building Structures," by V. V. Bertero - 1975

EERC 75-28 "Evaluation of Soil Liquefaction Potential during Earthquakes," by H. Bolton Seed, I. Arango and Clarence K. Chan 1975

EERC 75-29 "Representation of Irregular Stress Time Histories by Equivalent Uniform Stress Series in Liquefaction Analyses," by H. Bolton Seed, I. M. Idriss, F. Makdisi and N. Banerjee 1975

EERC 75-30 "FLUSH - A Computer Program for Approximate 3-D Analysis of Soil-Structure Interaction Problems," by J. Lysmer, T. Udaka, C.-F. Tsai and H. B. Seed - 1975

EERC 75-31 "ALUSH - A Computer Program for Seismic Response Analysis of Axisymmetric Soil-Structure Systems," by E. Berger, J. Lysmer and H. B. Seed - 1975

EERC 75-32 "TRIP and TRAVEL - Computer Programs for Soil-Structure Interaction Analysis with Horizontally Travelling Waves," by T. Udaka, J. Lysmer and H. B. Seed - 1975

EERC 75-33 "Predicting the Performance of Structures in Regions of High Seismicity," by Joseph Penzien - 1975

EERC 75-34 "Efficient Finite Element Analysis of Seismic Structure - Soil - Direction," by J. Lysmer, H. Bolton Seed, T. Udaka, R. N. Hwang and C.-F. Tsai - 1975

EERC 75-35 "The Dynamic Behavior of a First Story Girder of a Three-Story Steel Frame Subjected to Earthquake Loading," by Ray W. Clough and Lap-Yan Li - 1975

EERC 75-36 "Earthquake Simulator Study of a Steel Frame Structure, Volume II - Analytical Results," by David T. Tang - 1975

EERC 75-37 "ANSR-I General Purpose Computer Program for Analysis of Non-Linear Structure Response," by Digambar P. Mondkar and Graham H. Powell - 1975

EERC 75-38 "Nonlinear Response Spectra for Probabilistic Seismic Design and Damage Assessment of Reinforced Concrete Structures," by Masaya Murakami and Joseph Penzien - 1975

EERC 75-39 "Study of a Method of Feasible Directions for Optimal Elastic Design of Framed Structures Subjected to Earthquake Loading," by N. D. Walker and K. S. Pister - 1975

EERC 75-40 "An Alternative Representation of the Elastic-Viscoelastic Analogy," by Gautam Dasgupta and Jerome L. Sackman - 1975

EERC 75-41 "Effect of Multi-Directional Shaking on Liquefaction of Sands," by H. Bolton Seed, Robert Pyke and Geoffrey R. Martin - 1975

EERC 76-1 "Strength and Ductility Evaluation of Existing Low-Rise Reinforced Concrete Buildings - Screening Method," by Tsuneo Okada and Boris Bresler - 1976 (PB 257 906)

EERC 76-2 "Experimental and Analytical Studies on the Hysteretic Behavior of Reinforced Concrete Rectangular and T-Beams," by Shao-Yeh Marshall Ma, Egor P. Popov and Vitelmo V. Bertero - 1976 (PB 260 843)

EERC 76-3 "Dynamic Behavior of a Multistory Triangular-Shaped Building," by J. Petrovski, R. M. Stephen, E. Gartenbaum and J. G. Bouwkamp - 1976

EERC 76-4 "Earthquake Induced Deformations of Earth Dams," by Norman Serff and H. Bolton Seed - 1976

EERC 76-5 "Analysis and Design of Tube-Type Tall Building Structures," by H. de Clercq and G. H. Powell - 1976 (PB 252 220)

EERC 76-6 "Time and Frequency Domain Analysis of Three-Dimensional Ground Motions, San Fernando Earthquake," by Tetsuo Kubo and Joseph Penzien - 1976 (PB 260 556)

EERC 76-7 "Expected Performance of Uniform Building Code Design Masonry Structures," by R. L. Mayes, Y. Omote, S. W. Chen and R. W. Clough - 1976

EERC 76-8 "Cyclic Shear Tests on Concrete Masonry Piers, Part I - Test Results," by R. L. Mayes, Y. Omote and R. W. Clough 1976 (PB 264 424)

EERC 76-9 "A Substructure Method for Earthquake Analysis of Structure - Soil Interaction," by Jorge Alberto Gutierrez and Anil K. Chopra - 1976 (PB 257 783)

EERC 76-10 "Stabilization of Potentially Liquefiable Sand Deposits using Gravel Drain Systems," by H. Bolton Seed and John R. Booker - 1976 (PB 258 820)

EERC 76-11 "Influence of Design and Analysis Assumptions on Computed Inelastic Response of Moderately Tall Frames," by G. H. Powell and D. G. Row - 1976

EERC 76-12 "Sensitivity Analysis for Hysteretic Dynamic Systems: Theory and Applications," by D. Ray, K. S. Pister and E. Polak - 1976 (PB 262 859)

EERC 76-13 "Coupled Lateral Torsional Response of Buildings to Ground Shaking," by Christopher L. Kan and Anil K. Chopra - 1976

EERC 76-14 "Seismic Analyses of the Banco de America," by V. V. Bertero, S. A. Mahin, and J. A. Hollings - 1976

EERC 76-15 "Reinforced Concrete Frame 2: Seismic Testing and Analytical Correlation," by Ray W. Clough and Jawahar Gidwani - 1976 (PB 261 323)

EERC 76-16 "Cyclic Shear Tests on Masonry Piers, Part II - Analysis of Test Results," by R. L. Mayes, Y. Omote and R. W. Clough 1976

EERC 76-17 "Structural Steel Bracing Systems: Behavior Under Cyclic Loading," by E. P. Popov, K. Takanashi and C. W. Roeder 1976 (PB 260 715)

EERC 76-18 "Experimental Model Studies on Seismic Response of High Curved Overcrossings," by David Williams and William G. Godden - 1976

EERC 76-19 "Effects of Non-Uniform Seismic Disturbances on the Dumbarton Bridge Replacement Structure," by Frank Baron and Raymond E. Hamati - 1976

EERC 76-20 "Investigation of the Inelastic Characteristics of a Single Story Steel Structure using System Identification and Shaking Table Experiments," by Vernon C. Matzen and Hugh D. McNiven 1976 (PB 258 453)

EERC 76-21 "Capacity of Columns with Splice Imperfections," by E. P. Popov, R. M. Stephen and R. Philbrick - 1976 (PB 260 378)

EERC 76-22 "Response of the Olive View Hospital Main Building during the San Fernando Earthquake," by Stephen A. Mahin, Robert Collins, Anil K. Chopra and Vitelmo V. Bertero - 1976

EERC 76-23 "A Study on the Major Factors Influencing the Strength of Masonry Prisms," by N. M. Mostaghel, R. L. Mayes, R. W. Clough and S. W. Chen - 1976

EERC 76-24 "GADFLEA - A Computer Program for the Analysis of Pore Pressure Generation and Dissipation during Cyclic or Earthquake Loading," by J. R. Booker, M. S. Rahman and H. Bolton Seed - 1976 (PB 263 947)

EERC 76-25 "Rehabilitation of an Existing Building: A Case Study," by B. Bresler and J. Axley - 1976

EERC 76-26 "Correlative Investigations on Theoretical and Experimental Dynamic Behavior of a Model Bridge Structure," by Kazuhiko Kawashima and Joseph Penzien - 1976 (PB 263 388)

EERC 76-27 "Earthquake Response of Coupled Shear Wall Buildings," by Thirawat Srichatrapimuk - 1976

EERC 76-28 "Tensile Capacity of Partial Penetration Welds," by Egor P. Popov and Roy M. Stephen - 1976 (PB 262 899)

EERC 76-29 "Analysis and Design of Numerical Integration Methods in Structural Dynamics," by Hans M. Hilber - 1976 (PB 264 410)

EERC 76-30 "Contribution of a Floor System to the Dynamic Characteristics of Reinforced Concrete Buildings," by L. J. Edgar and V. V. Bertero -1976

EERC 76-31 "The Effects of Seismic Disturbances on the Golden Gate Bridge," by Frank Baron, Metin Arikan and Raymond E. Hamati - 1976

EERC 76-32 "Infilled Frames in Earthquake Resistant Construction," by R. E. Klinger and V. V. Bertero - 1976

UCB/EERC-77/01 "PLUSH - A Computer Program for Probabilistic Finite Element Analysis of Seismic Soil-Structure Interaction," by Miguel P. Romo Organista, John Lysmer and H. Bolton Seed - 1977

UCB/EERC-77/02 "Soil-Structure Interaction Effects at the Humboldt Bay Power Plant in the Ferndale Earthquake of June 7, 1975," by J. E. Valera, H. Bolton Seed, C. F. Tsai and J. Lysmer 1977

UCB/EERC-77/03 "Influence of Sample Disturbance on Sand Response to Cyclic Loading," by Kenji Mori, H. Bolton Seed and Clarence K. Chan - 1977

UCB/EERC-77/04 "Seismological Studies of Strong Motion Records," by Jafar Shoja-Taheri - 1977

UCB/EERC-77/05 "Testing Facility for Coupled-Shear Walls," by Lee Li-Hyung, Vitelmo V. Bertero and Egor P. Popov - 1977

UCB/EERC-77/06 "Developing Methodologies for Evaluating the Earthquake Safety of Existing Buildings," No. 1 - B. Bresler; No. 2 - T. Okada and D. Zisling; No. 3 - T. Okada and B. Bresler; No. 4 - V. Bertero and B. Bresler - 1977

UCB/EERC-77/07 "A Literature Survey - Transverse Strength of Masonry Walls," by Y. Omote, R.L. Mayes, S.W. Chen and R.W. Clough 1977

UCB/EERC-77/08 "DRAIN-TABS - A Computer Program for Inelastic Earthquake Response of Three Dimensional Buildings," by R. Guendelman-Israel and G.H. Powell - 1977

UCB/EERC-77/09 "SUBWALL - A Special Purpose Finite Element Computer Program for Practical Elastic Analysis and Design of Structural Walls with Substructure Option," by Dao Quang Le, Hans Petersson and Egor P. Popov - 1977

UCB/EERC-77/10 "Experimental Evaluation of Seismic Design Methods for Broad Cylindrical Tanks," by Douglas P. Clough - 1977

UCB/EERC-77/11 "Earthquake Engineering Research at Berkeley - 1976."